AD661287

Distribution of this document is unlimited. It may be released to the Clearinghouse, Department of Commerce, for sale to the general public.

121

EOSCIENCES OPERATIONS

TEXAS INSTRUMENTS
INCORPORATED
SCIENCE SERVICES DIVISION
100 EXCHANGE PARK NORTH
P. O. BOX 35084 · DALLAS, TEXAS

ARPA Order No. 292, Amendment 7
ARPA Project Code No. 8100

NOISE STUDY

By
George D. Hair, James H. Funk
and Research Staff

Special Report No. X
15 November 1964

Project Manager
R. R. Guidroz

Telephone

Dallas, Texas
Area Code 214
Fleetwood 7-5411
Extension 447

Contractor: Texas Instruments Incorporated
Date of Contract: 15 May 1961
Contract Expiration Date: 15 November 1964

Contract No. AF 19(604)-8517

TABLE OF CONTENTS

LIST OF ILLUSTRATIONS

LIST OF ILLUSTRATIONS (CONT'D)

SECTION I

SUMMARY AND CONCLUSIONS

Worldwide seismic noise levels and characteristics for 1963 are discussed in this report. Data for evaluation includes absolute power density spectra and contour maps of average worldwide microseismic activity.

Relative power density spectra were computed from 1963 data from Worldwide Standard Stations. Slopes of the least-mean-square line through the power density points were computed and a pattern of slope changes appeared at a frequency of 1.0 cps. A uniform worldwide pattern of slopes was observed between 1 cps and 2 cps. This suggests two separate sources generating microseisms above and below 1 cps, respectively, and that the spectra above 1 cps are independent of storms, fronts, etc.

The spectra for frequencies less than 1.0 cps show greater seasonal variations. These were concluded to be mostly meteorological in origin.

Monthly contour maps of average noise show that noise is seasonally variable and that it is attenuated at continental structures.

SECTION II

POWER DENSITY SPECTRA

A. PROCEDURE

Power density spectra were computed using short-period instruments from selected Worldwide Standard Stations. The data were obtained from the Coast and Geodetic Survey on 70 mm film clips. These were chosen over the 35 mm film clips because of the larger image size and better reproduction quality.

To assure that the same method of determining input data was used throughout the program, one person made all data reductions. The selected noise sample was projected approximately ten times the original gram size on a large wall-mounted grid.

The availability of film largely determined the samples chosen. Effort was concentrated on the first six months of 1963 when it became apparent that film for the latter months of the year would not be available.

The noise samples were objectively chosen to be representative of the recording period. An attempt was made to eliminate extremely high cultural noise if it was present only during part of the recording period.

As far as was practical, the horizontal instruments were sampled at the same time that the corresponding vertical sample was chosen. Any exceptions were caused by poor optics in the original gram, missing grams or reduced quality of reproduction.

Several samples were taken from the same station at different times of the same day to show the repeatibility of the method. Refer to the following spectra in Appendix A:

Station	Code	Component	Date
Nurmijarvi, Finland	NUR	N, E	15 January
Quetta, W. Pakistan	QUE	Z	24 January

Four samples were taken on different days in the same month to show variations at a station during the month. Refer to the following:

Station	Code	Component	Date
Valentia, Ireland	VAL	Z	15 Jan., 18 Jan.
Kevo, Finland	KEV	Z	5 March, 13 March

Station	Code	Component	Date
Valentia, Ireland	VAL	Z	2 April, 3 April
Anpu, Taiwan	ANP	Z	14 April, 28 April

Twenty spectra were computed from one station to show seasonal variations. Valentia, Ireland (VAL) was chosen as the station because of film availability and the quality of recordings.

A total number of 151 absolute power density spectra were computed from data recorded during nine months in 1963.

B. METHOD

The method used in the determination of absolute power density spectra was the technique developed by Texas Instruments for use with film data. The previously used polarity technique[1] was improved by the following:

- Film traces were differentiated before infinite clipping to pre-emphasize the high frequency energy, and
- Compensation was made for station response.

The flow diagram (Figure II-1) and the data example (Figure II-2) illustrate the individual operations involved in the method and their proper sequence.

The polarity technique applies only to time series having a Gaussian distribution of amplitudes. The sampling rate on the 1960 short-period data was four times per second or a sampling interval of 0.25 seconds. For the 1963 study, it was found that in most cases 300 seconds of noise gave good results with a sampling rate of eight times per second or a sampling interval of 0.125 seconds. Figure II-3 compares the sampling rate and results using data from (a) 1960 and (b) 1963.

1. Film Measurements

The noise samples were projected from film strips and a time sample of 300 seconds was traced. The tracings were sampled at intervals of 0.125 seconds, yielding 2400 digital samples each. A sample was recorded as +1 if the amplitude at that point was greater than that at the preceding sample point and -1 if less. This corresponds to differentiating the trace, then clipping at the +1 and -1 levels. The +1's were then punched

[1] Semiannual Technical Report No. III, Contract AF 19(604)-8517, 31 October 1962.

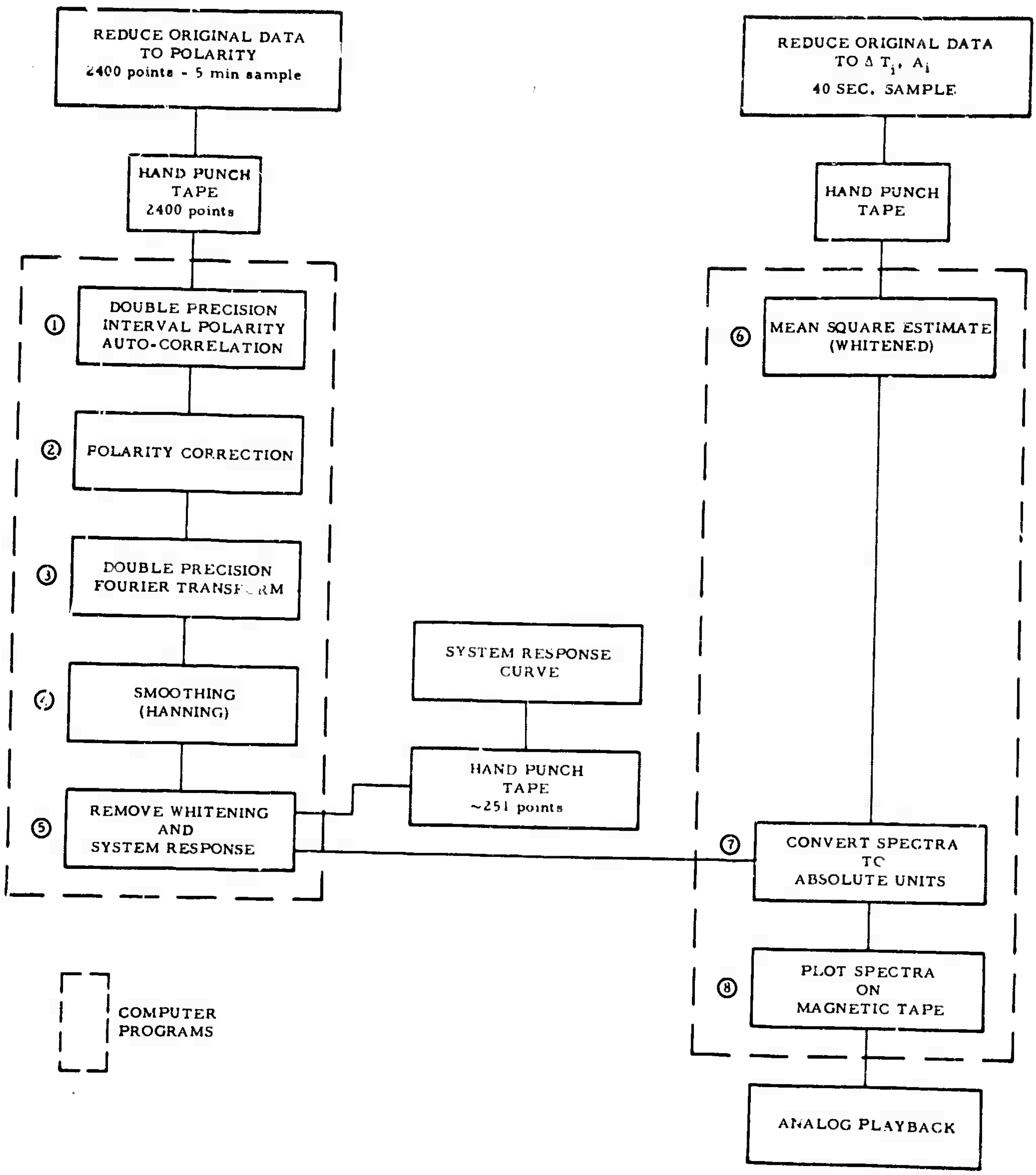

Figure II-1. Flow Diagram for Obtaining Absolute Power Density Spectra by Polarity Method

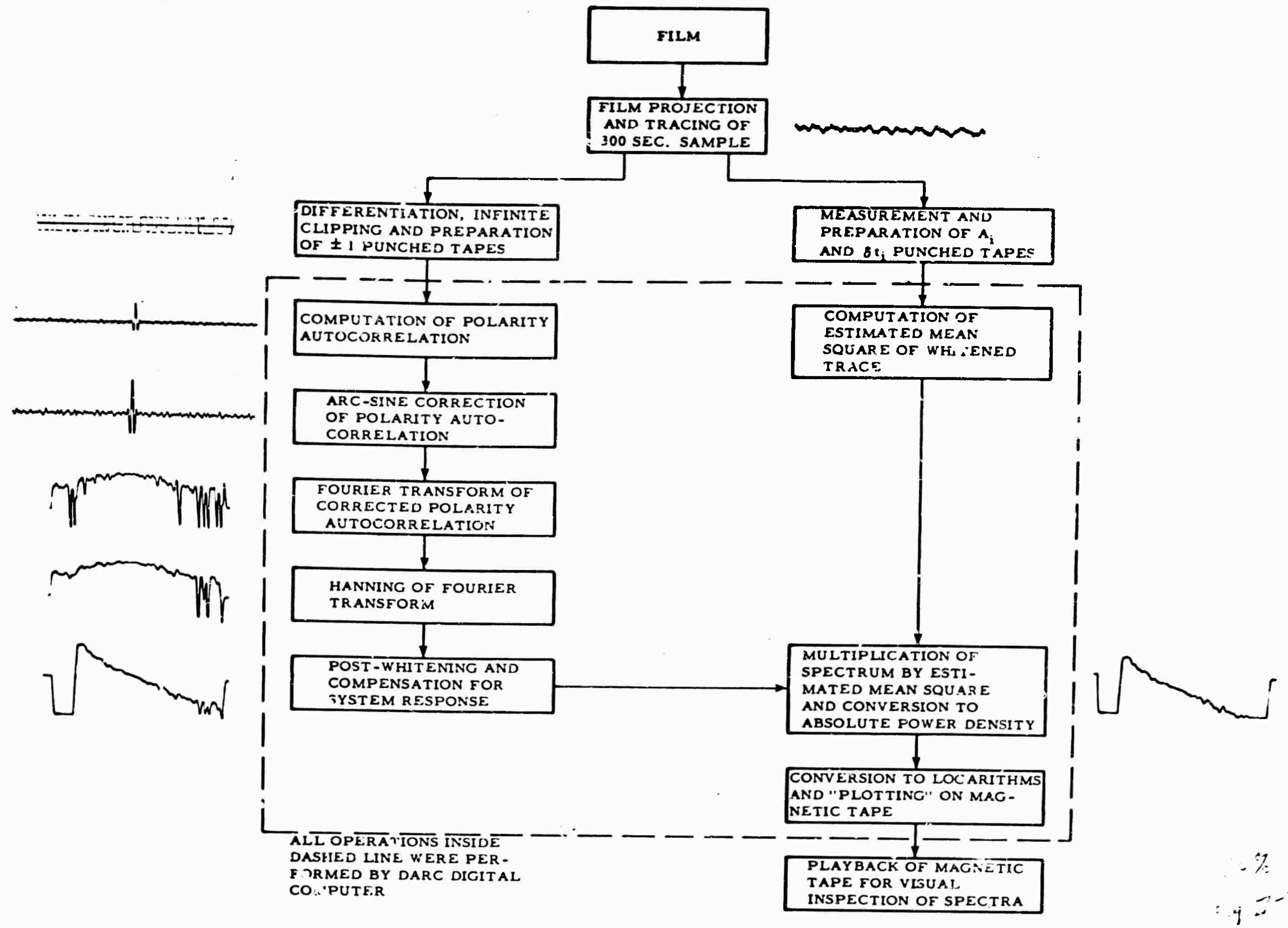

Figure II-2. Data Example for Obtaining Absolute Power Density Spectra by Polarity Method

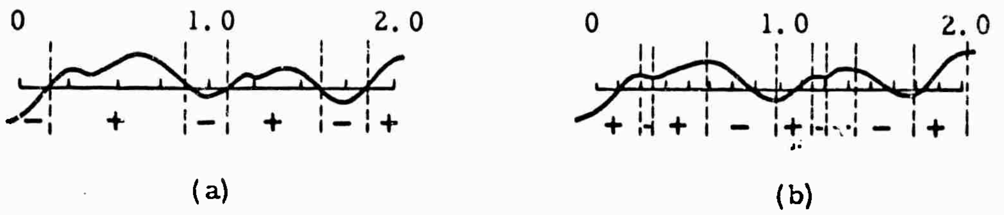

Figure II-3. Sampling Rate for Power Density Spectra Data (a) 1960; (b) 1963

on paper tape suitable for input to the DARC computer for computation of relative power density spectra.

Another set of measurements was made on a selected 40-second section of each tracing for the purpose of estimating the mean square of the differentiated trace. See paragraph 6 for a discussion of the mean-square estimate. These measurements consisted of measuring the amplitude of the trace (relative to any base line parallel to the axis of the film) at each relative maxima and minima, and measuring the time intervals between successive relative maxima and minima. For example, if the total number of maxima and minima in the 40-second sample was N, then N amplitude and N-1 time-interval measurements were made. These measurements were also punched on paper tape suitable for computer input.

2. Pre-Whitening by Differentiation

Past experience with the noise recorded by the Worldwide Stations has shown that the power spectra (before allowance for system response) generally fall off rather rapidly with increasing frequency. Since the polarity technique gives highest fidelity when the spectra are roughly "white," the performance of any operation tending to whiten the noise before infinite clipping would improve the spectral estimates. One such operation is differentiation, which corresponds to a 6 db/octave multiplication of the power spectrum. With digitized data, differentiation may be approximated by subtracting the previous sample from a given sample. Symbolically, the operation is

$$\Delta t \, g'(t) = g(t) - g(t - \Delta t)$$

This operation is equivalent to convolution with a two-point (+1, -1) operator whose power response is $2(1 - \cos 2\pi f \Delta t)$.

3. Computation and Correction of Polarity Autocorrelations

The polarity autocorrelations were computed as

$$\phi(k\Delta t) = \sum_{n=1}^{2400-k} h(n\Delta t)\, h(n\Delta t + k\Delta t) \quad \text{for } k = 0, 1, 2, \ldots\ldots, 250$$

where $h(n\Delta t)$ is either +1 or -1, and $\Delta t = 0.125$ second.

The autocorrelations were then "arc-sine corrected" to obtain estimates of the autocorrelations that would have been obtained if the data had been fully quantized. This correction is

$$\phi'(k\Delta t) = \sin\left[\frac{\pi}{2}\,\frac{\phi(k\Delta t)}{\phi(0)}\right] \quad \text{for } k = 0, 1, 2, \ldots\ldots, 250.$$

The theory of polarity autocorrelations and the arc-sine correction has been fully presented in a previous report[2] and thus will not be repeated here.

4. Computation of Relative Power Density Spectra

The corrected polarity autocorrelations were Fourier transformed as follows:

$$\Phi(j\Delta f) = \sum_{k=-250}^{250} \phi'(k\Delta t) \cos\left[2\pi(j\Delta f)(k\Delta t)\right] \Delta t$$

$j = 0, 1, 2, \ldots\ldots, 125$, where $\Delta f = \dfrac{1}{500\Delta t}$.

These Fourier transforms were then Hanned by convolving with a three-point (1/4, 1/2, 1/4) operator to obtain the smoothed power density spectra. These spectra are relative spectra only, since the $\phi'(k\Delta t)$ are normalized autocorrelation functions.

5. Post-Whitening and Compensation for System Response

These two operations were performed simultaneously for reasons of computer efficiency and precision. Since the power response of the whitening operation is $2(1 - \cos 2\pi f\Delta t)$, post-whitening to remove this effect consists of dividing the spectrum by $2(1 - \cos 2\pi f\Delta t)$. Compensation for system response consists of dividing the spectra by $H^2(f)$ where $H(f)$ is the amplitude response of the system. Amplitude response was obtained

---

[2] Ibid

from U. S. Department of Commerce bulletin "Instrumentation of the World-Wide Seismograph System," Figure II-4. This system response includes all effects of the recording apparatus (seismometers, galvanometers, etc.) and relates absolute ground motion to film trace deflection.

6. Mean Square Estimation

To obtain absolute power density spectra from the relative power density spectra obtained with normalized autocorrelations, it is necessary to multiply each by the mean square of the corresponding time function. Using polarity data, we have no way of computing the mean square; however, we may obtain a good estimate of the mean square of each whitened trace. We approximate the unwhitened film trace between successive relative maxima and minima by half cycles of cosine functions of appropriate amplitudes and frequencies. This approximation is illustrated by the $g_i(t)$ in the diagram below:

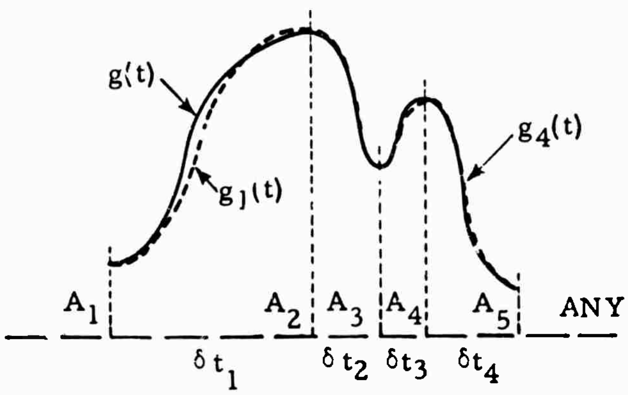

Then $g_i(t) = \dfrac{A_i + A_{i+1}}{2} + \dfrac{A_i - A_{i+1}}{2} \cos\left(\pi \dfrac{t}{\delta t_i}\right)$ for the interval δt_i.

Differentiating $g_i(t)$ we obtain

$$g'_i(t) = \frac{A_{i+1} - A_i}{2} \frac{\pi}{\delta t_i} \sin\left(\pi \frac{t}{\delta t_i}\right) \text{ for the interval } \delta t_i.$$

Then the mean square of $g'(t)$ may be estimated as

$$\text{E.M.S.} = \frac{1}{\sum_i \delta t_i} \sum_i \int_{t=0}^{\delta t_i} \left| g'_i(t) \right|^2 dt$$

$$\text{E.M.S.} = \frac{1}{\sum_i \delta t_i} \sum_i \frac{(A_{i+1} - A_i)^2 \pi^2}{4\delta t_i^2} \int_{t=0}^{\delta t_i} \sin^2\left(\pi \frac{t}{\delta t_i}\right) dt$$

$$\text{E.M.S.} = \frac{1}{\sum_i \delta t_i} \sum_i \frac{\pi^2 (A_{i+1} - A_i)^2}{8\delta t_i}$$

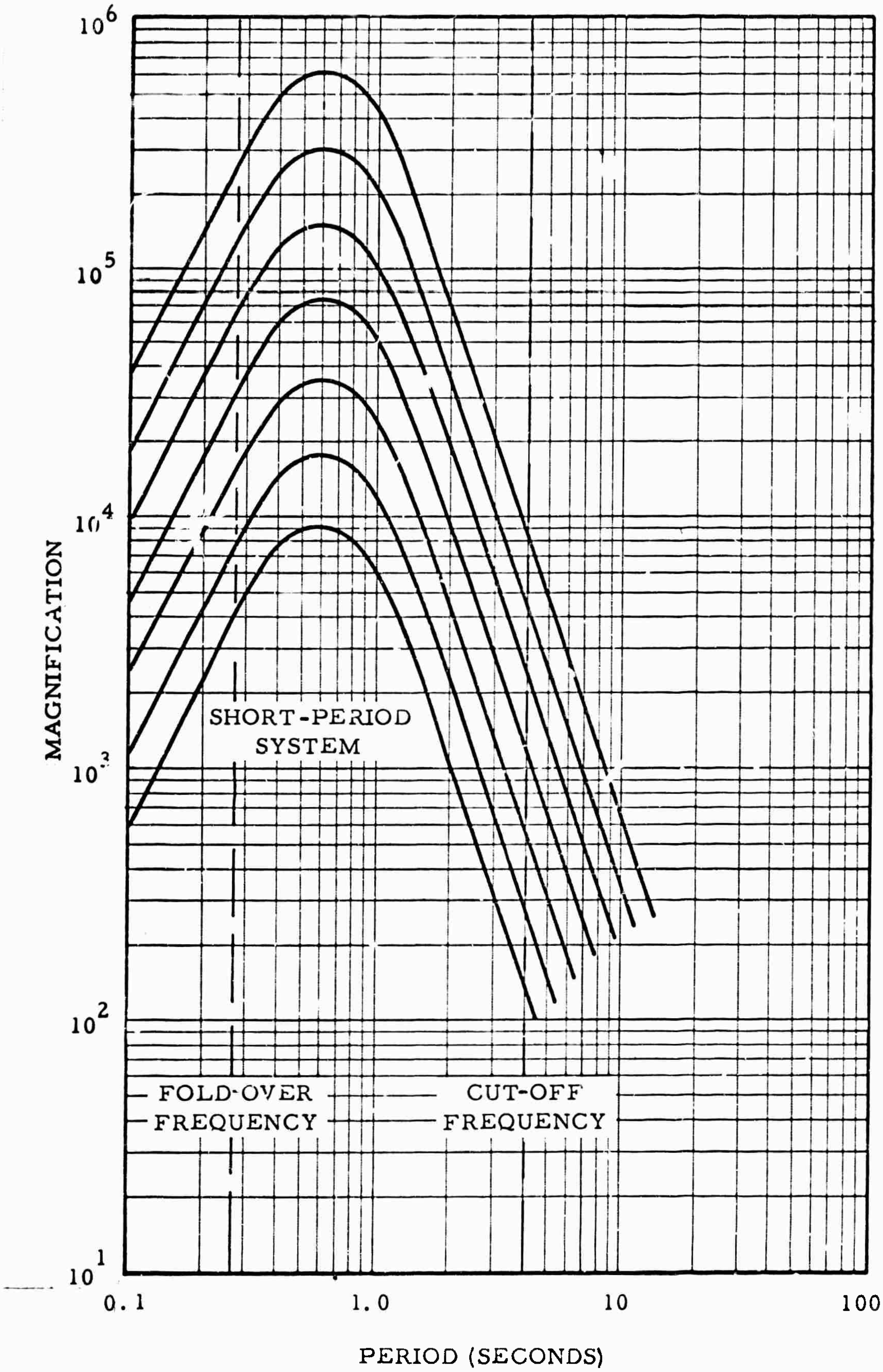

Figure II-4. Frequency Response of the USC&GS World-Wide Standard Short Period Seismograph System

The A_i and δt_i measurements were made directly from the film as described in paragraph 1. These measurements were input to DARC, and estimated mean squares for each whitened noise sample were computed using the formula just derived.

7. Conversion of Relative Spectra to Absolute Spectra

Absolute power density spectra were obtained by multiplication of the relative power density spectra, previously corrected for whitening and system response, by their respective mean-square estimates, and by a constant. This constant contains such scaling factors as:

- Magnification factor involved in projecting film and measuring A_i's
- Variations in gain from that gain at which the system response was calibrated, and
- Computer scale factors introduced in data processing.

8. Presentation of Spectra

The logarithm of each point of each absolute power density spectrum was written on magnetic tape by the DARC computer in a special configuration. This configuration was such as to provide a plot of the logarithm of the power density function versus linear frequency by playback of the magnetic tape through a digital-to-analog converter and oscillograph.

SECTION III

EVALUATION OF POWER DENSITY SPECTRA

The power density spectra, computed on a worldwide basis and converted to absolute values, lends itself to a study of the noise of the world.

The spectra plots are located in Appendix A. In each case, the slope of the plots were determined by the least mean square method. It is interesting to note the change in slope on the plots in the range of 1.0 cps. This slope change is interpreted to suggest that two source mechanisms are causing the noise above and below 1.0 cps. The same change in slope was observed by Vinnik and Pruchkina (1964).

Several comparisons were made between the slopes obtained from the spectra plots. The first is the number of stations whose spectral slope (frequency 1.0 cps or greater) falls within each slope increment of 10 db/octave (Figure III-1). It was noted that 84.1 percent of the slopes' values fall within the range of 10-40 db/octave and that of these 48.8 percent fall within the range of 20-30 db/octave. This worldwide uniformity in noise between the periods of 0.5 sec to 1.0 sec suggests a constant universal noise.

Several theories have been advanced thus far as to the reason for the presence of microseisms throughout the world. Iyer (1962) suggests that the earth itself is filled with noise. Other causes from cultural noise to sea storms have been investigated. The problem lends itself for further study.

The power density spectra plots yield an increase in slope between 0.25 cps to 1.0 cps. This spectral range corresponds with the theory that microseisms in the 2-6 sec period range receive their energy from pressure fronts.

A comparison was made between the slopes of the spectra plots and the station distance from large bodies of water. Station geologic structures were also taken into consideration (refer to Figures III-2 and III-3). As can be seen from Figure III-2, the noise present in the 3 sec period range levels off at a distance of around 300 miles from the shore. The high frequency spectra (Figure III-3) drops off much more rapidly although it apparently levels off at about 300 miles also. There is no apparent relationship of these noise spectra with the geologic environment near the recording stations.

The results from the seasonal study at Valentia, Ireland show that the seasonal change in the spectra around 1.0 cps and above is less than that below 1.0 cps.

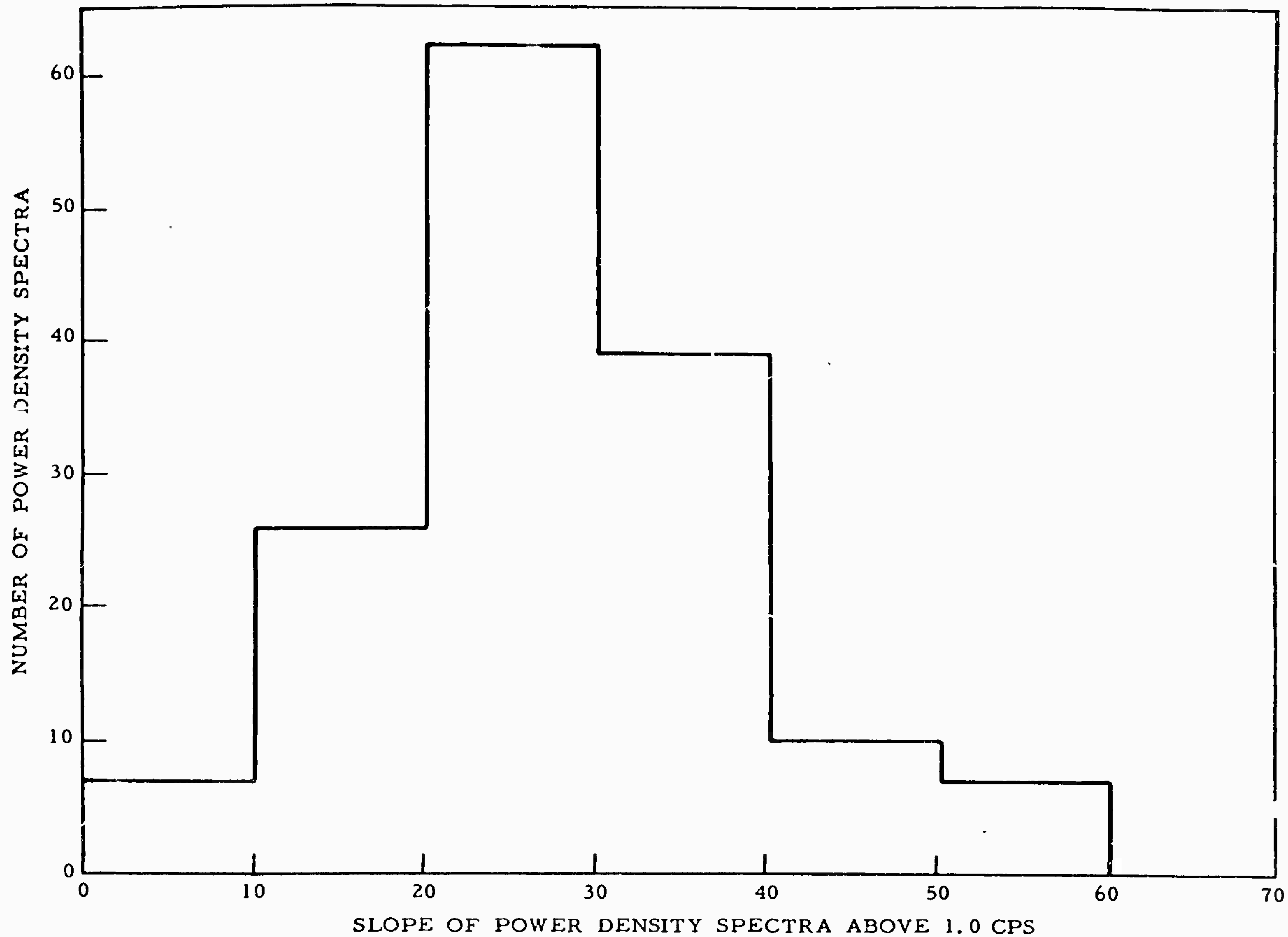

Figure III-1. Comparison of Spectra Slopes at Frequency of 1.0 CPS or Greater

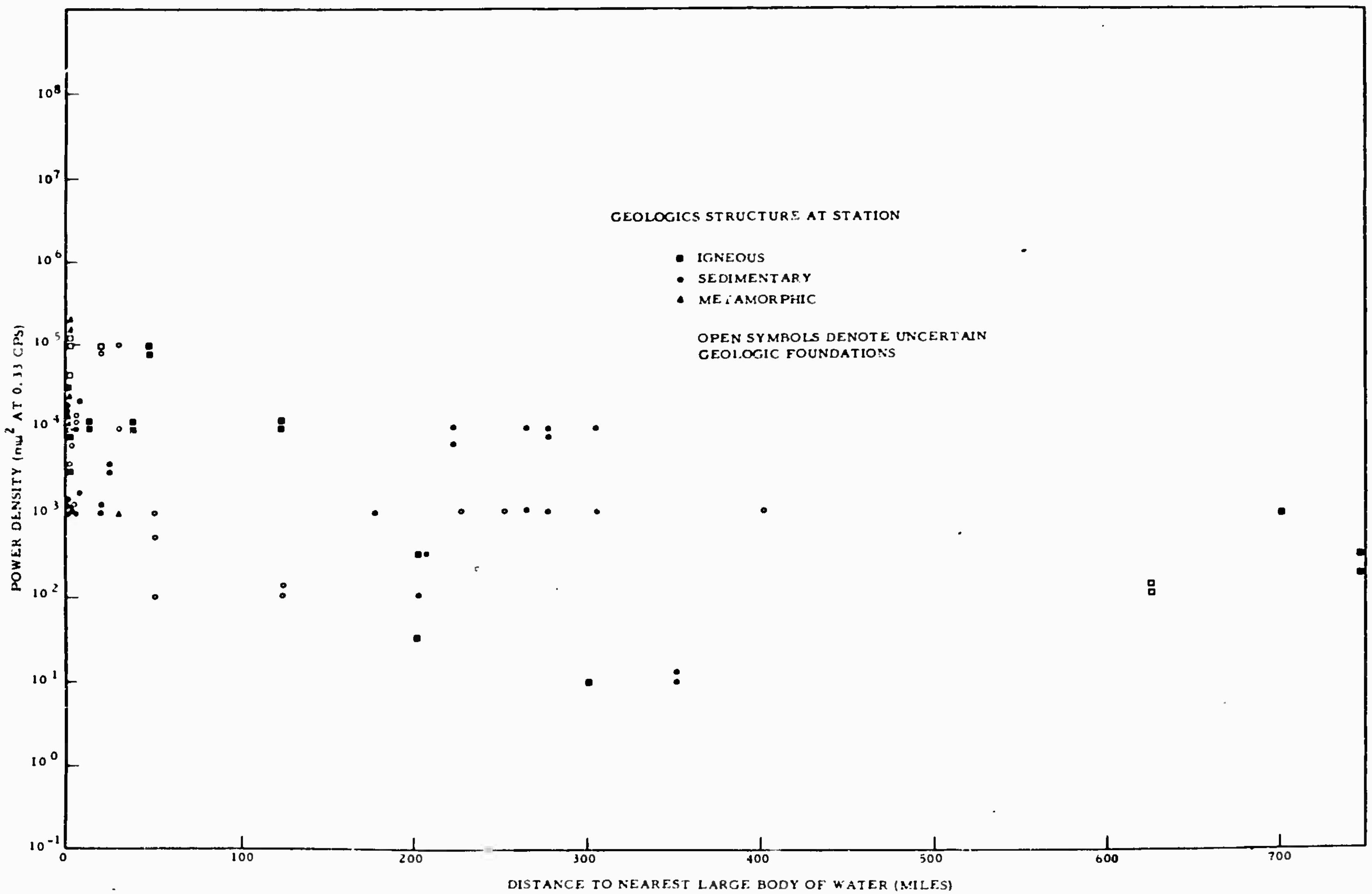

Figure III-2. Power Density (Frequency = 0.33 cps) vs Distance of Station From Large Body of Water

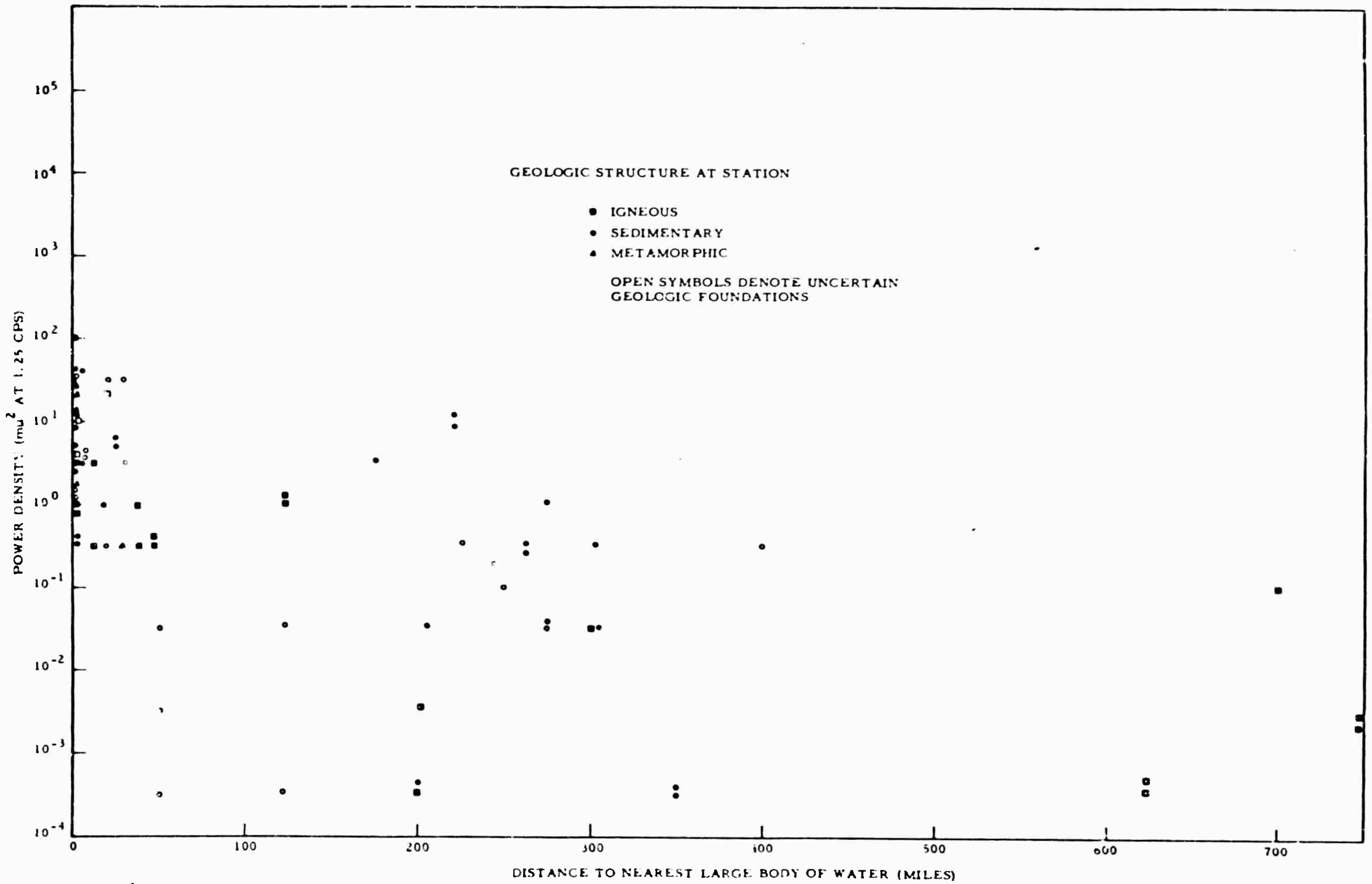

Figure III-3. Power Density (Frequency = 1.25 cps) vs Distance of Station From Large Body of Water

SECTION IV

VISUAL NOISE MEASUREMENTS

In addition to the noise power density spectra study, measurements and companions of average microseismic levels on a worldwide basis were made. Visual noise measurements were made at selected stations in order that noise levels could be compared. To improve station distribution, 35 mm records from the Canadian Network were obtained and used along with Worldwide Standard Station records.

Measurements of period and amplitude of the average maximum short-period and long-period noise on the respective instruments were made at each station. A comparison was made between one measurement each day, one measurement every other day, one measurement every third day and one measurement every fifth day at several stations. It was decided that ten measurements each month could be made and not significantly affect the average maximum measurements.

The measurements were taken at the same time at each station, within limits. Anomalous data, e.g., long-period noise on short-period instruments, were eliminated by limiting the measurements to noise in the 0.5 to 2.0 sec period range as the short-period instruments and the 3.0 to 8.0 sec period range on the long-period instruments.

The measurements were converted to ground motion using the approximate response curves (Figure IV-1 - USC&GS Standard Stations; Figure IV-2 - Canadian Network Stations) and averaged for each month.

Contour maps of the average maximum noise for each month were constructed. These maps are contained in Appendix B. Only nine months of the year were included as data for July, August and September were not available when data reduction was terminated.

To assure consisten[illegible] measuring techniques, the measurements were made by one person, and one analyst was responsible for data reduction and the preparing of the maps.

Several large areas of the world have sparse data available for this study. An attempt has been made to subjectively qualify the maps. Solid lines indicate adequate control points and dashed lines indicate a lack of control points.

As can be seen from the maps, the noise level increases during the winter months and, as was expected, the noise level was attenuated at continental structures.

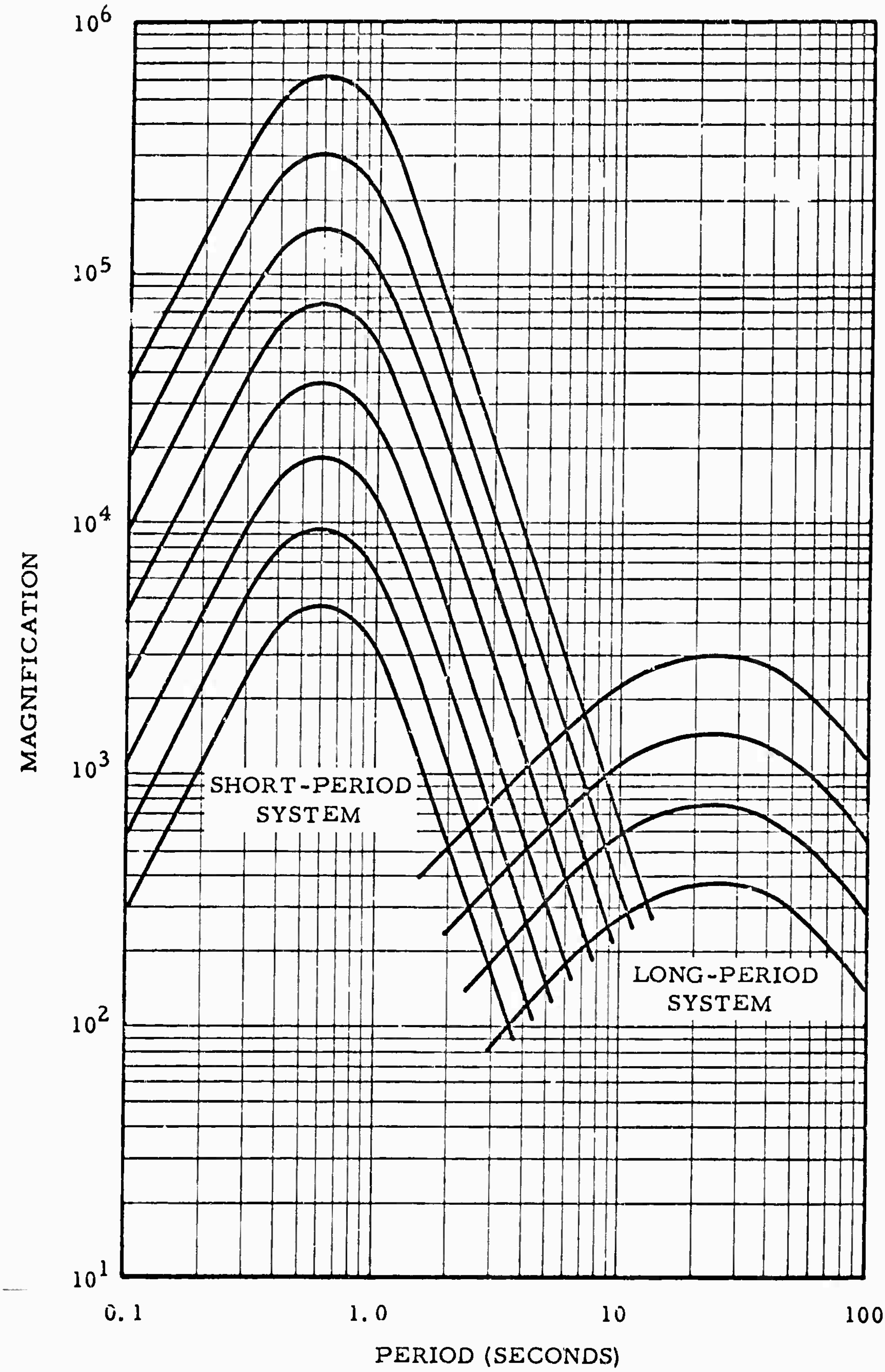

Figure IV-1. Frequency Response of the USC&GS World-Wide Standard Seismograph Systems

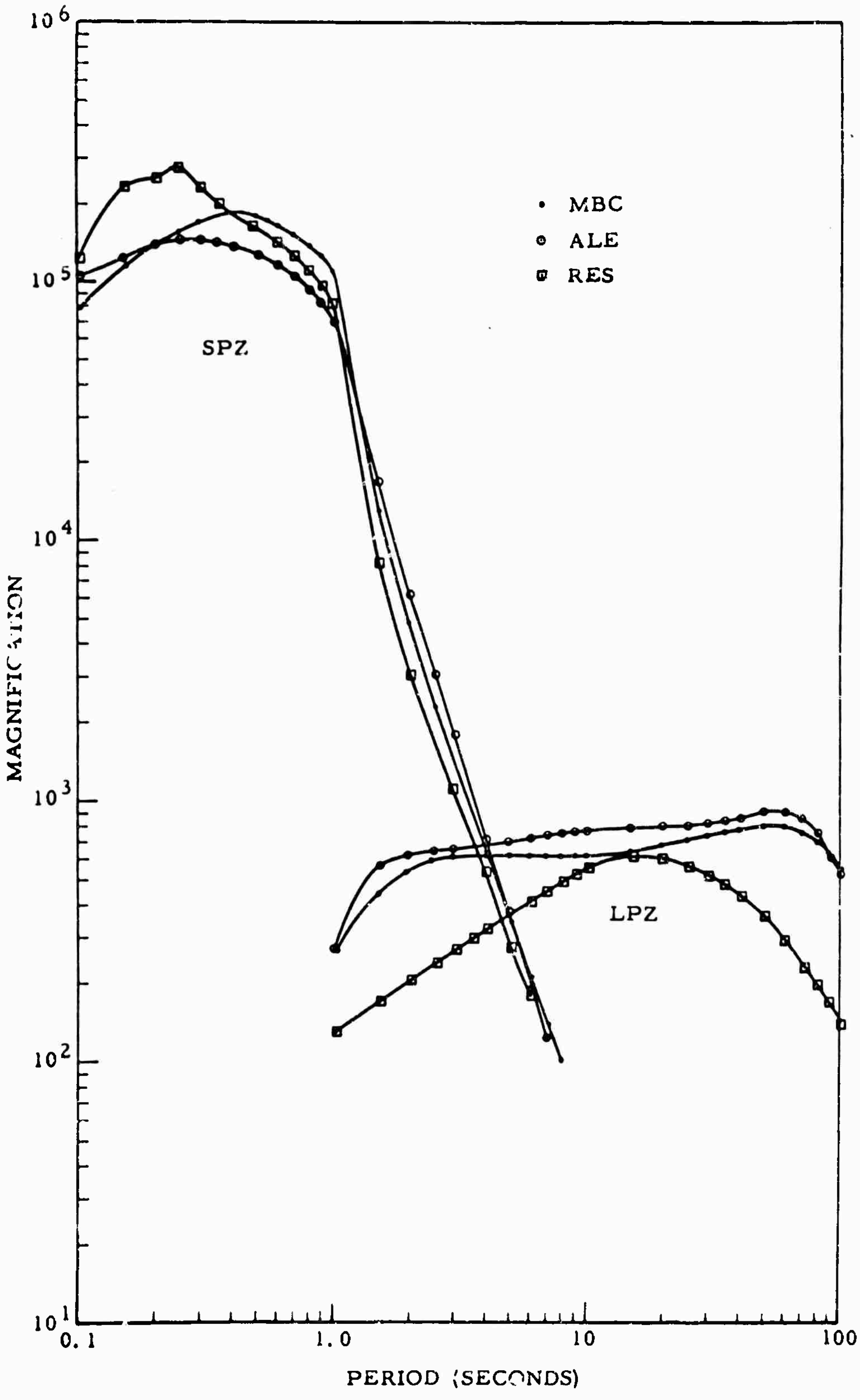

Figure IV-2. Frequency Response of the Canadian Network Seismograph Systems (Vertical Components)

Microseisms studies are needed in conjunction with seismicity studies to obtain a better understanding of the noise that can be expected at various stations around the world. This noise can be used to calculate the theoretical limits of perceptibility for each station.

Microseisms studies should also add to the knowledge of seasonal variations at the stations studied. This information could aid in determining what stations, if any, should change their gains to cope with these variations.

The 1963 microseisms study yielded the following results as to the gain and noise at the stations studied.

List of Stations with Cultural Noise Limiting the Gain

Addis Ababa, Ethiopia
Ann Arbor, Michigan
Athens, Greece
Baguio, Philippines
Bogota, Colombia
Helwan, Egypt
Hong Kong
La Paz, Bolivia
Lubbock, Texas
Malaga, Spain
Minneapolis, Minnesota
Quito, Ecuador
Rabaul, New Britain
Stuttgart, West Germany

List of Stations with Noise in the 4-8 Second Range on SP Instruments

Albuquerque, New Mexico
Blacksburg, Virginia
Bulawayo, Southern Rhodesia
Chiengmai, Thailand
Golden, Colorado
Kipapa, Hawaii
Kongsberg, Norway
State College, Pennsylvania
South Pole, Antarctica
Tasmanian University, Tasmania
Tucson, Arizona

List of Stations Where Gains Could Be Raised

Chiengmai, Thailand (LP only)
Hong Kong
Nairobi, Kenya (only if better photographic technique employed)
New Delhi, India

Any further work in this area should include more stations as they become available and, if no World Standard Stations are available for areas such as Eastern South America and Western Africa, reliably calibrated non-Standard station data should be used.

The overall quality of the film reproductions used in this study varied widely from excellent to, in a few cases, unuseable. The reasons

t' at some records were unuseable could, in some cases, be attributed to p · reproductions while others were due to poor original grams. In addition, n. y stations had excessive trace width which made accurate measurements of low noise levels difficult.

The most common problem of the World Standard Network records, as a whole, is excessive drift on the long-period horizontal instruments, possibly caused by inadequately insulated vaults.

SECTION V

RECOMMENDATIONS

1. Noise background studies are greatly improved if a technique of obtaining power density spectra is used.

2. Continued worldwide effort should include gathering of meteorological information to aid in the interpretation of spectra.

3. Any additional effort to investigate worldwide microseisms should have as a prime objective the association of spectra and observations with existing theories of microseisms origin.

4. Additional theoretical and practical work should be associated to explain constant microseismic background apparently not associated with storms, fronts, etc.

APPENDIX A

ABSOLUTE POWER DENSITY SPECTRA

APPENDIX A

ABSOLUTE POWER DENSITY SPECTRA

This appendix contains absolute power density spectra obtained from the 1963 data. The station abbreviations are listed with the location of each station in Table A-1. The spectra are presented in Figures A-1a through A-1f. The list of stations used and the dates of the records are presented in Tables A-2a through A-2f for the associated spectral illustrations.

TABLE A-1

STATION ABBREVIATIONS

STATION	LOCATION	STATION	LOCATION
AAE	Addis Ababa, Ethiopia	KIP	Kipapa, Hawaii
ADE	Adelaide, S. Australia	KON	Kongsberg, Norway
AFI	Afiamalu, W. Samoa	LON	Longmire, Washington
ALQ	Albuquerque, New Mexico	MAL	Malaga, Spain
ANP	Anpu, Taiwan	MAN	Manila, Philippines
ATU	Athens, Greece	MDS	Madison, Wisconsin
BAG	Baguio, Philippines	MUN	Mundaring, W. Australia
BKS	Berkeley, California	NAI	Nairobi, Kenya
BLA	Blacksburg, Virginia	NUR	Nurmijarvi, Finland
BUL	Bulawayo, S. Rhodesia	PLM	Palomar, California
CCG	Camp Century, Greenland	PMG	Port Moresby, New Guinea
CHG	Chiengmai, Thailand	PRE	Pretoria, S. Africa
CMC	Copper Mine, Canada	PTO	Porto, Portugal
COP	Copenhagen, Denmark	QUE	Quetta, W. Pakistan
COR	Corvallis, Oregon	SCP	State College, Pennsylvania
GDH	Godhavn, Greenland	SEO	Seoul, S. Korea
GOL	Golden, Colorado	SHL	Shillong, India
GSC	Goldstone, California	SPA	South Pole, Antarctica
GUA	Guam, Mariana Islands	TOL	Toledo, Spain
HUR	Honiara, Solomon Islands	VAL	Valentia, Ireland
IST	Istanbul, Turkey	WES	Weston, Massachusetts
KEV	Kevo, Finland	WIN	Windhoek, S. Africa

TABLE A-2a

ABSOLUTE POWER DENSITY SPECTRA LOCATED IN FIGURE A-la

STATION	DATE	COMPONENT	GAIN(K)
AAE	16 January	SPZ	25
ADE	15 January	SPZ	25
ADE	15 January	SPN	25
ADE	15 January	SPE	25
ADE	16 April	SPZ	25
AFI	16 January	SPZ	12.5
ALQ	7 January	SPZ	200
ALQ	19 April	SPZ	400
ALQ	19 April	SPN	400
ALQ	19 April	SPE	400
ANP	14 April	SPZ	6.25
ANP	28 April	SPZ	6.25
ANP	28 April	SPN	6.25
ANP	28 April	SPE	6.25
ATU	16 January	SPZ	12.5
ATU	19 April	SPZ	12.5
ATU	19 April	SPN	12.5
ATU	19 April	SPE	12.5
BAG	21 January	SPZ	25
BAG	21 January	SPN	25
BAG	21 January	SPE	25
BAG	19 April	SPZ	25
BAG	19 April	SPN	25
BAG	19 April	SPE	25
BKS	10 January	SPZ	25

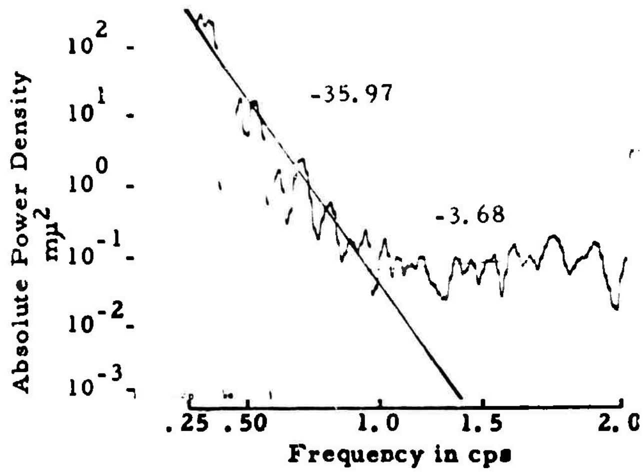

AAE
SPZ

16 JAN.
25 K

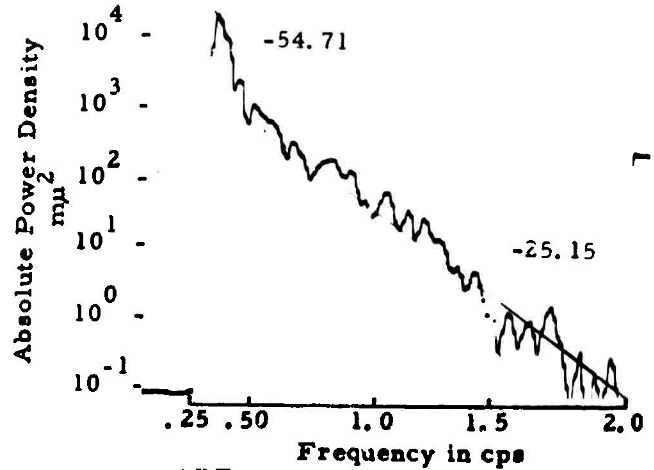

ADE
SPE

15 JAN.
25 K

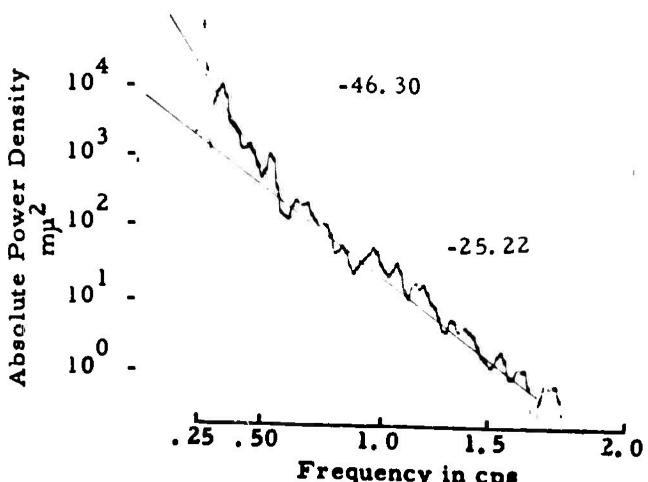

ADE
SPZ

15 JAN.
25 K

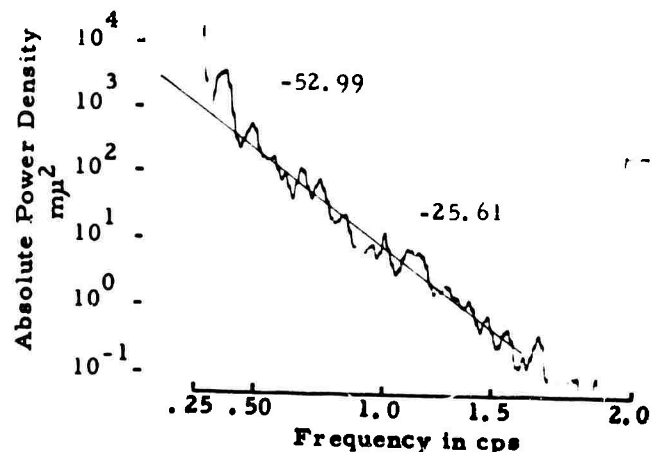

ADE
SPZ

16 APR.
25 K

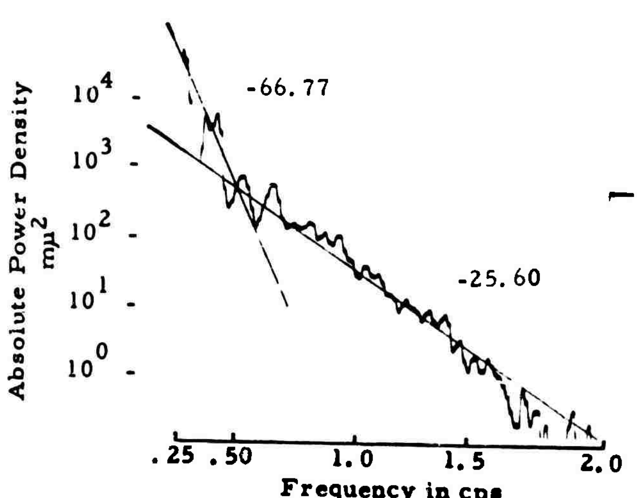

ADE
SPN

15 JAN.
25 K

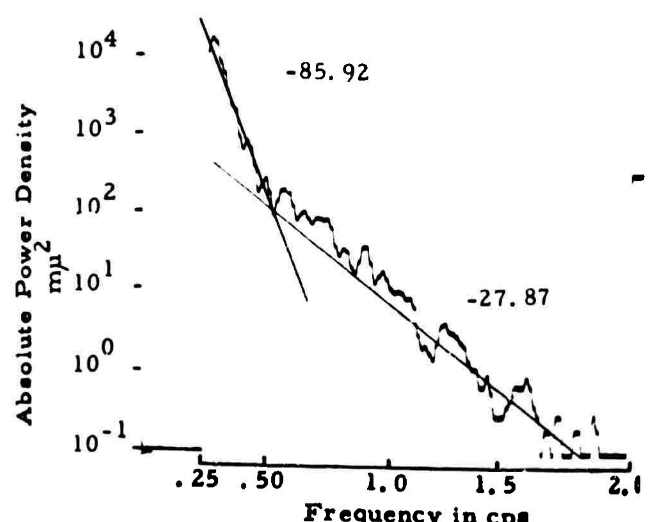

AFI
SPZ

16 JAN.
12.5 K

A

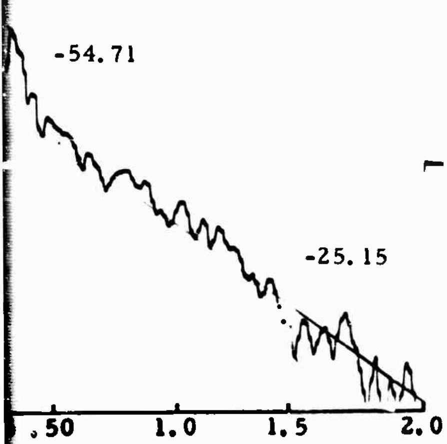

DE 15 JAN.
E 25 K

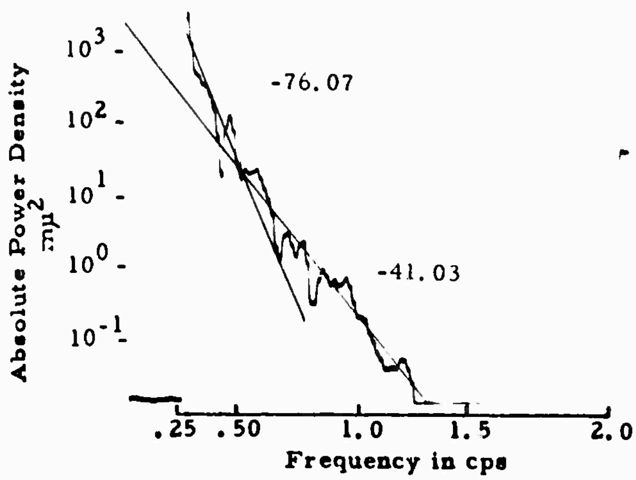

ALQ 7 JAN.
SPZ 200 K

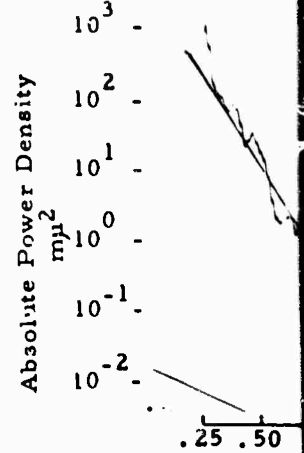

ALQ
SPE

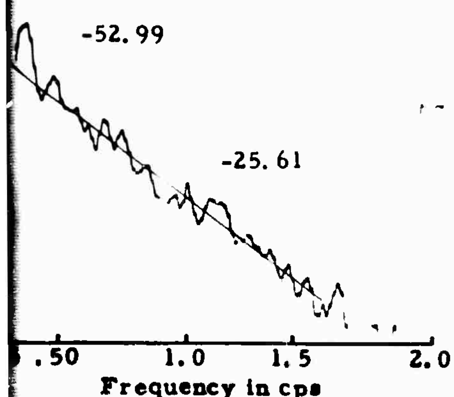

DE 16 APR.
PZ 25 K

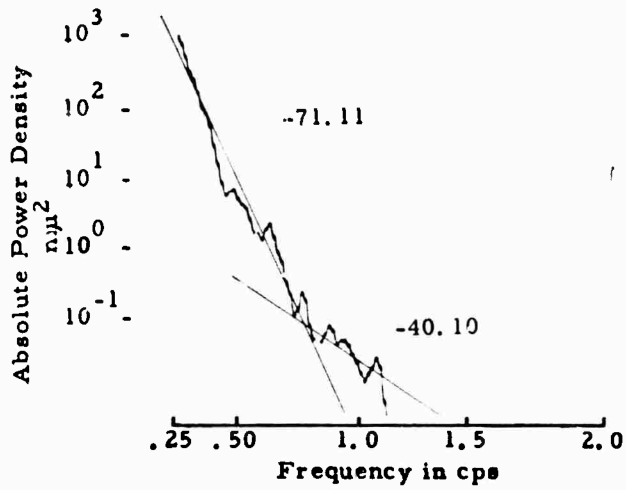

ALQ 19 APR.
SPZ 400 K

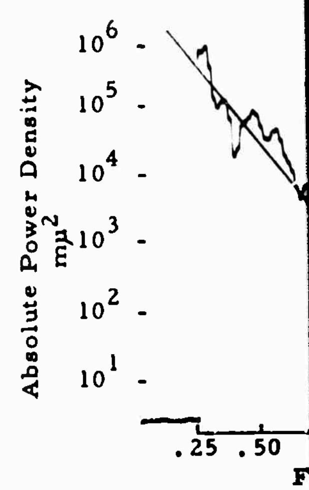

ANP
SPZ

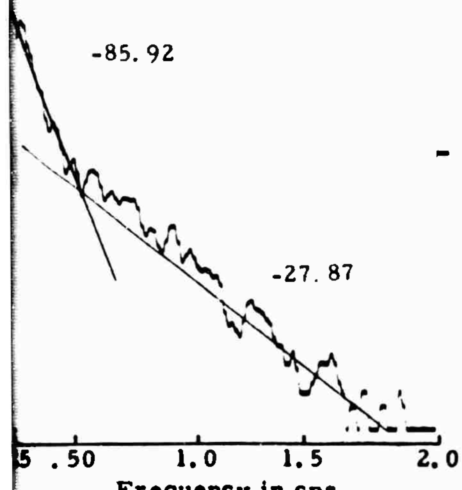

TI 16 JAN.
PZ 12.5 K

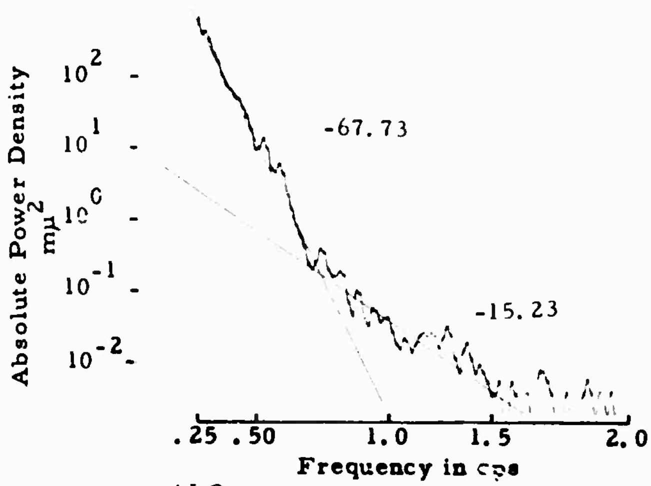

ALQ 19 APR.
SPN 400 K

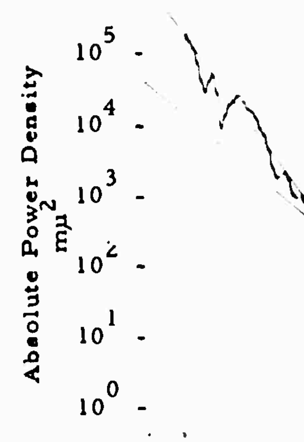

ANP
SPZ

B

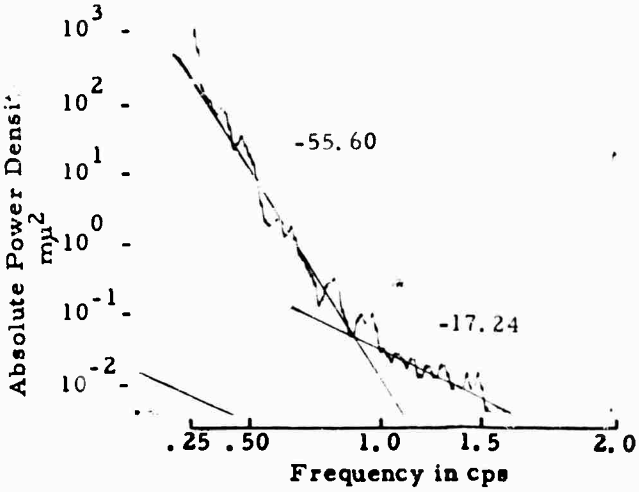

ALQ 19 APR.
SPE 400 K

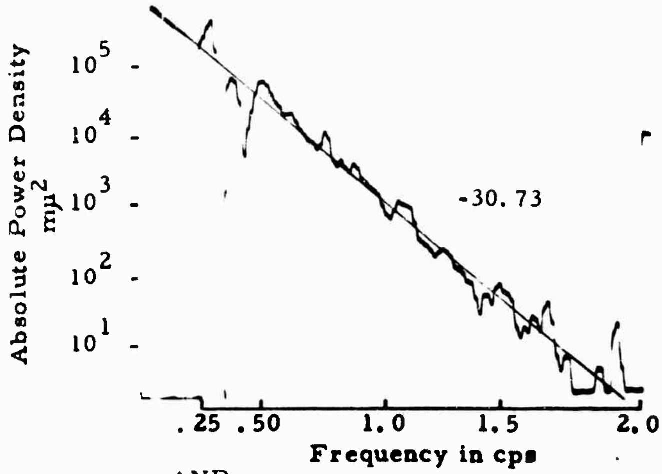

ANP 28 APR.
SPN 6.25 K

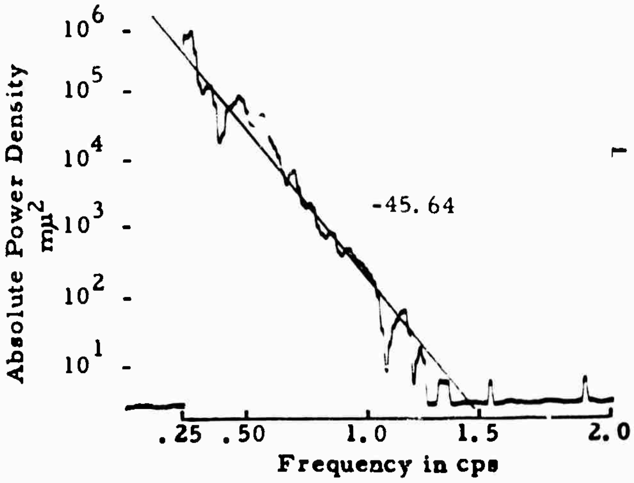

ANP 14 APR.
SPZ 6.25 K

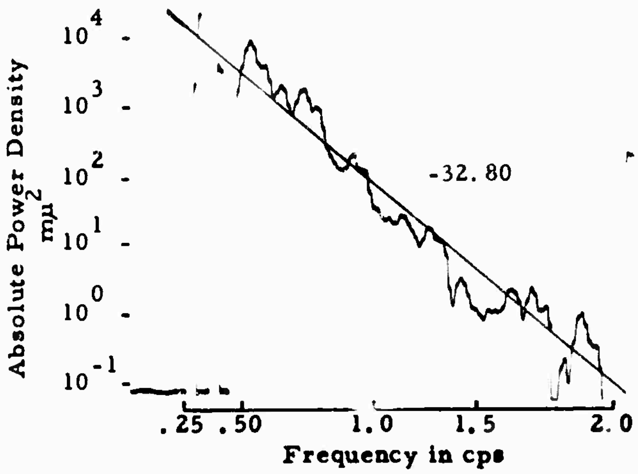

ANP 28 APR.
SPE 6.25 K

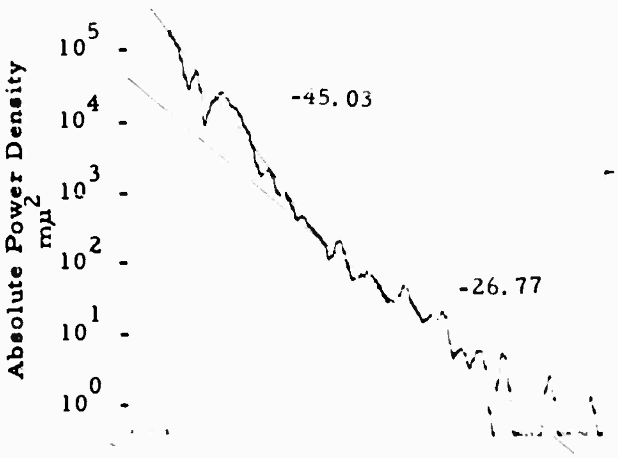

ANP 28 APR.
SPZ 6.25 K

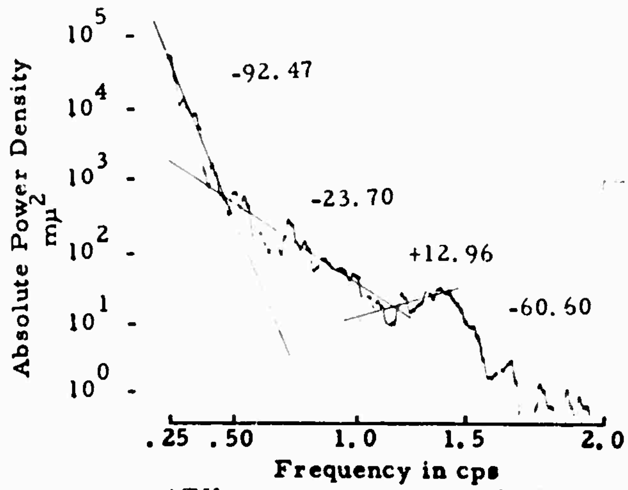

ATU 16 JAN.
SPZ 12.5 K

c

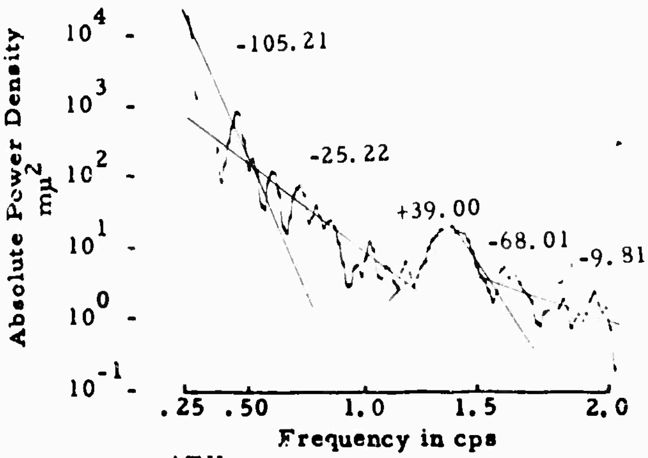

ATU 19 APR.
SPZ 12.5 K

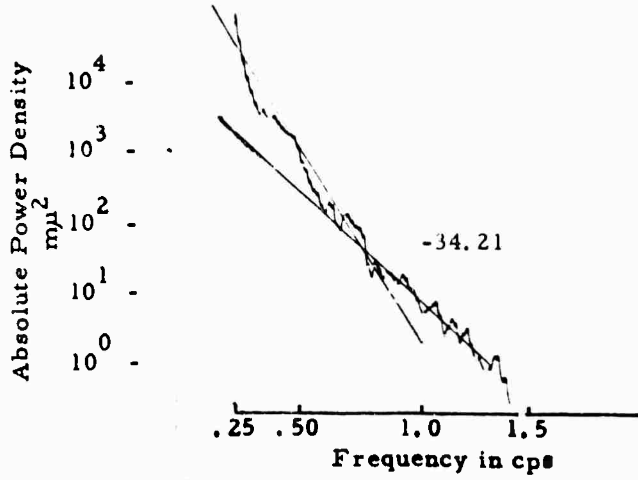

BAG 21 JAN.
SPZ 25 K

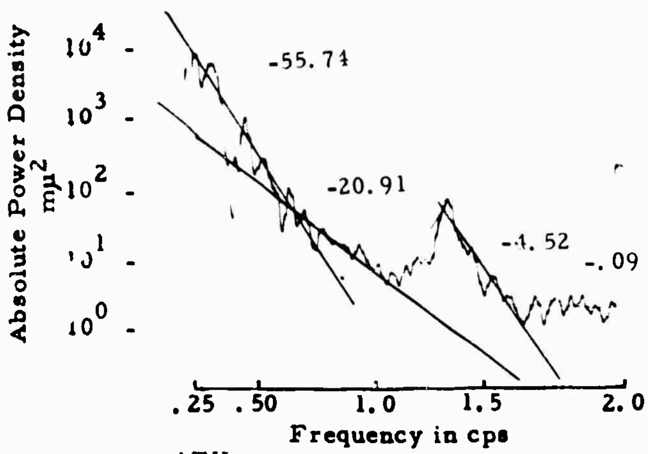

ATU 19 APR.
SPN 12.5 K

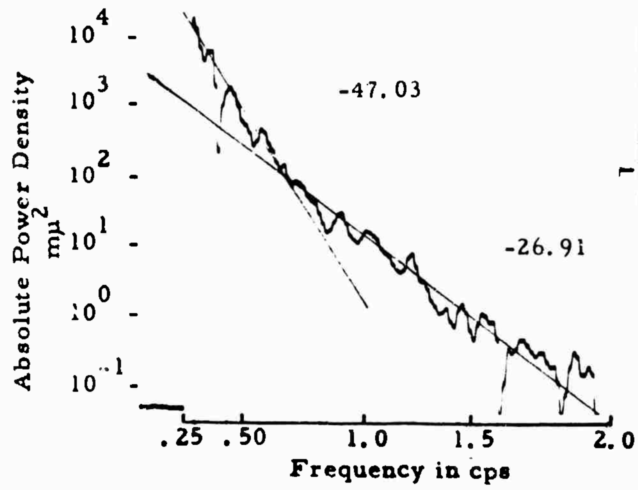

BAG 21 JAN.
SPN 25 K

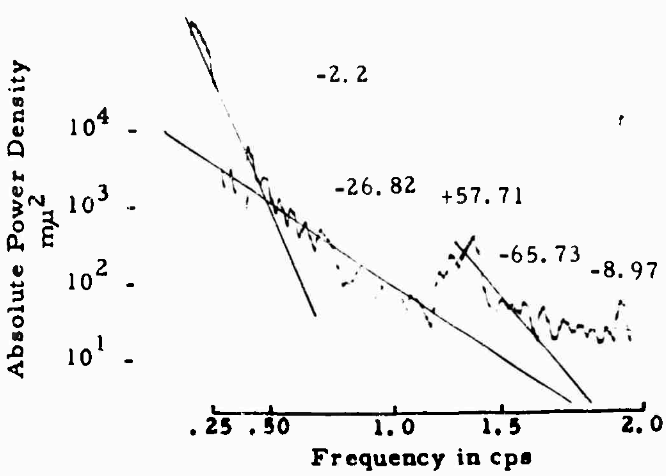

ATU 19 APR.
SPE 12.5 K

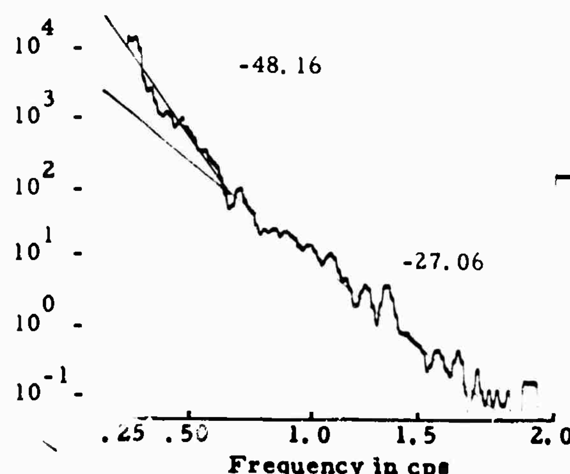

BAG 21 JAN.
SPE 25 K

D

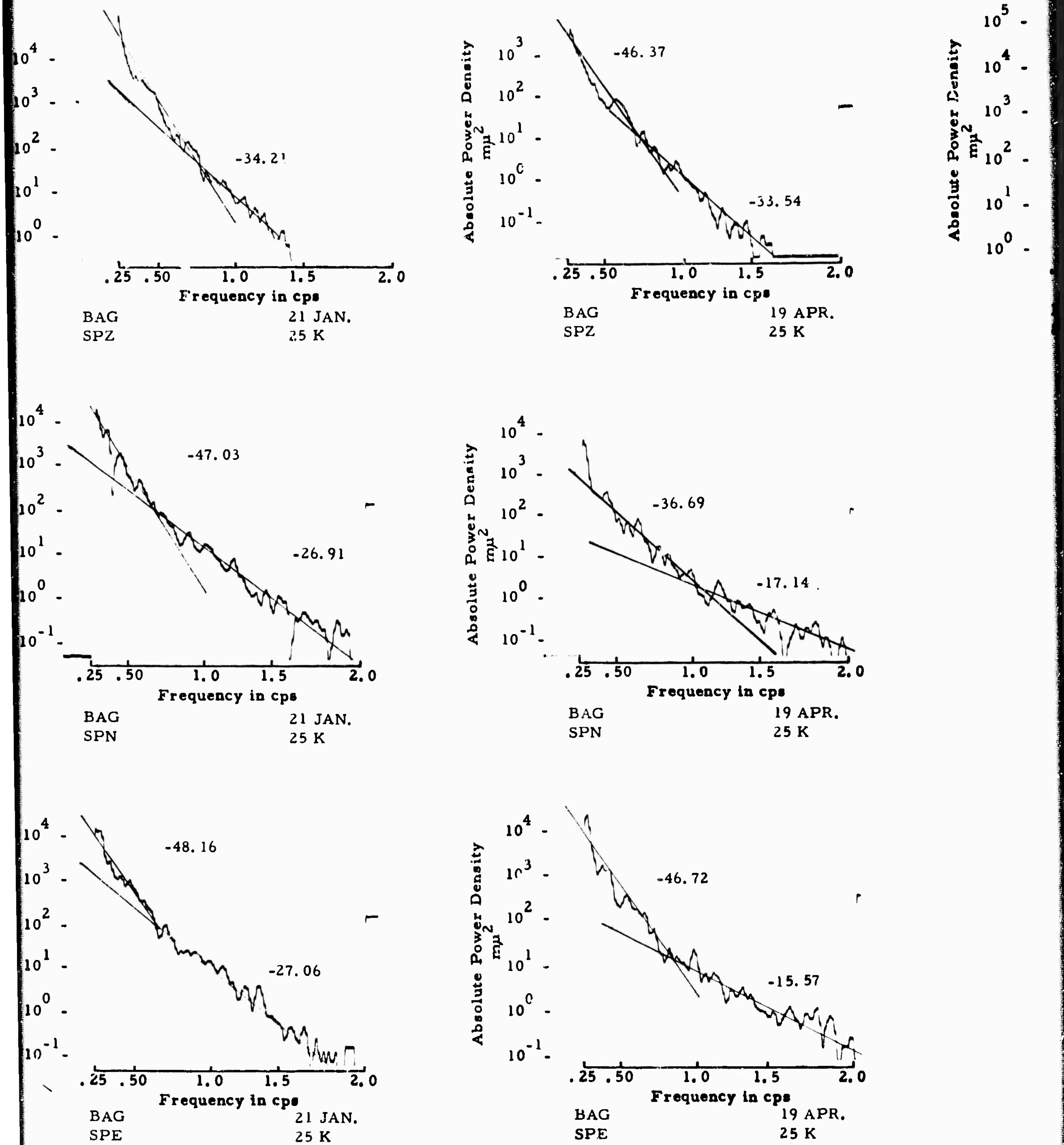

Figure A-1a. Absolute Power Density Spectra Obta

E

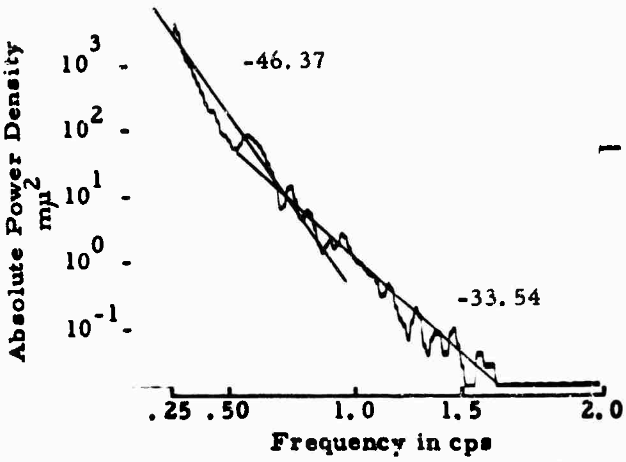

BAG 19 APR.
SPZ 25 K

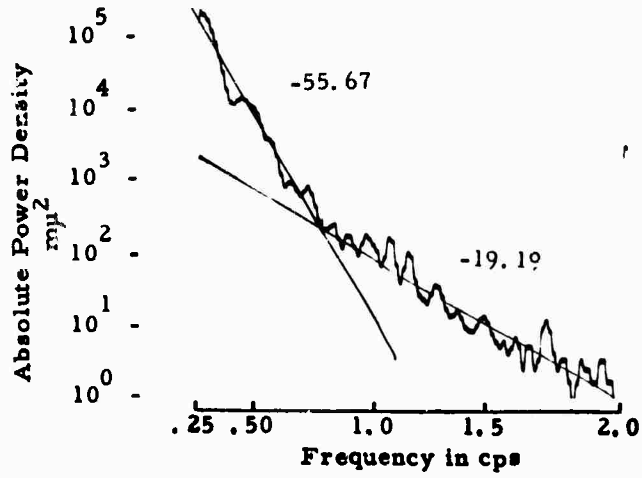

BKS 10 JAN.
SPZ 25 K

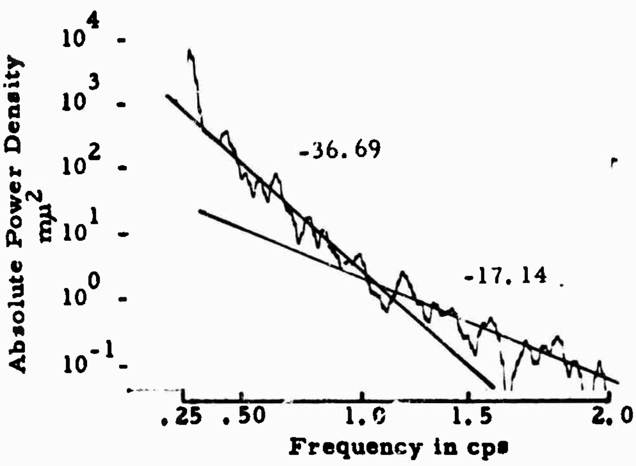

BAG 19 APR.
SPN 25 K

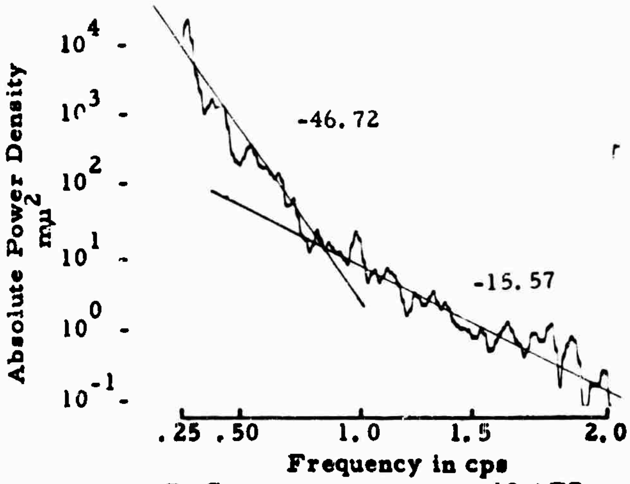

BAG 19 APR.
SPE 25 K

Figure A-1a. Absolute Power Density Spectra Obtained From 1963 Data

TABLE A-2b

ABSOLUTE POWER DENSITY SPECTRA LOCATED IN FIGURE A-1b

STATION	DATE	COMPONENT	GAIN(K)
BKS	19 April	SPZ	25
BKS	19 April	SPN	25
BKS	19 April	SPE	25
BLA	14 January	SPZ	50
BLA	10 April	SPZ	25
BUL	15 April	SPZ	100
CCG	7 April	SPZ	100
CHG	18 March	SPZ	400
CHG	7 June	SPZ	400
CHG	7 June	SPN	400
CHG	7 June	SPE	400
CMC	1 May	SPZ	200
CMC	1 May	SPN	200
CMC	1 May	SPE	200
COP	15 January	SPZ	12.5
COP	19 April	SPZ	12.5
COR	5 January	SPZ	25
COR	1 April	SPZ	25
GDH	16 January	SPZ	12.5
GOL	16 January	SPZ	400
GOL	5 April	SPZ	400
GSC	3 April	SPZ	200
GUA	26 May	SPZ	6.25
GUA	26 May	SPN	6.25
GUA	26 May	SPE	6.25
HNR	16 January	SPZ	12.5
HNR	16 January	SPN	12.5

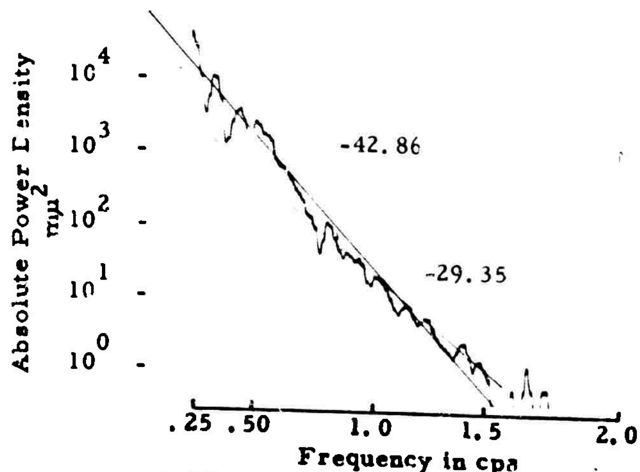

BKS 19 APR.
SPZ 25 K

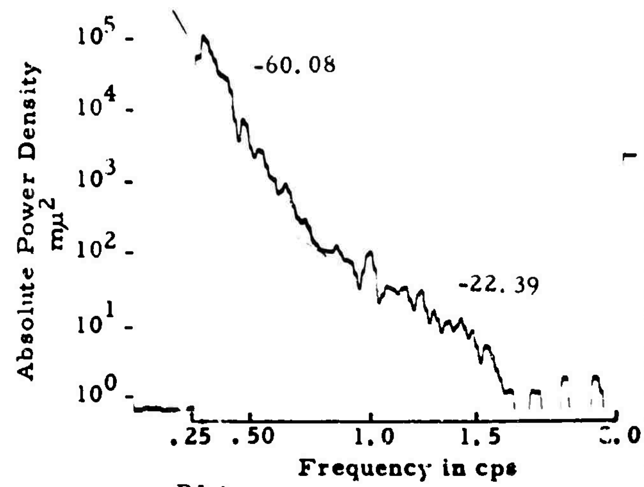

BLA 14 JAN.
SPZ 50 K

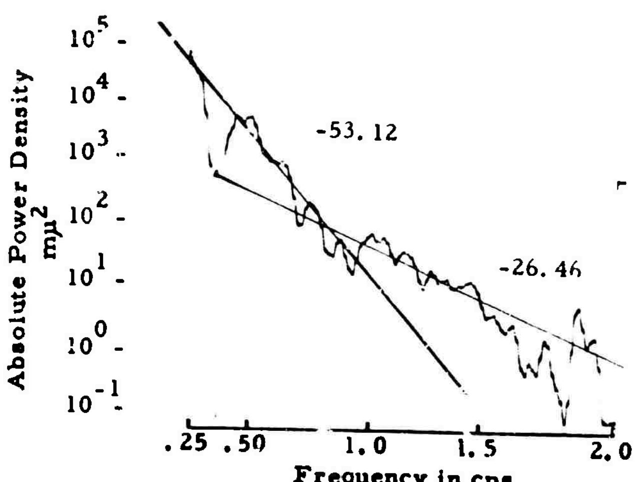

BKS 19 APR.
SPN 25 K

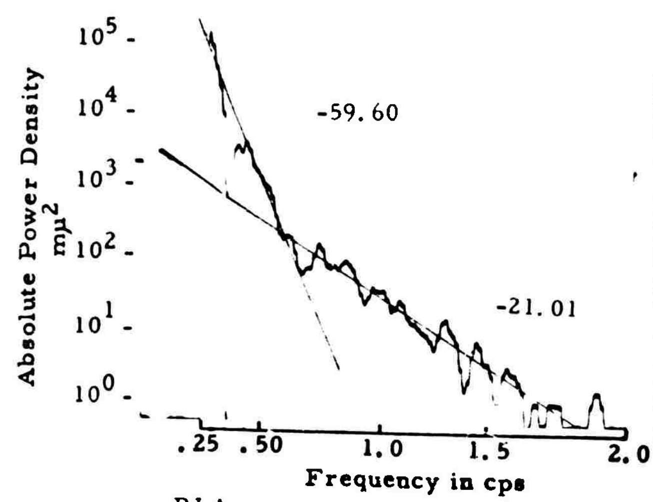

BLA 10 APR.
SPZ 25 K

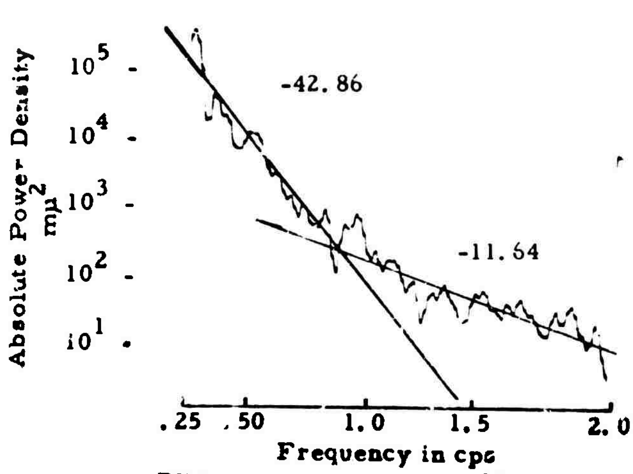

BKS 19 APR.
SPE 25 K

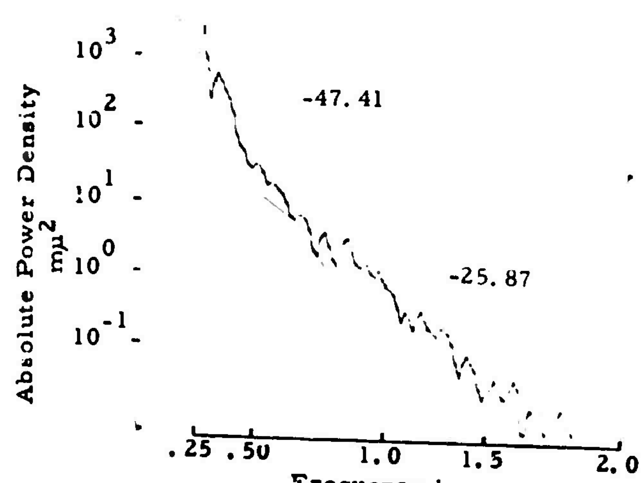

'IL 15 APR.
SPZ 100 K

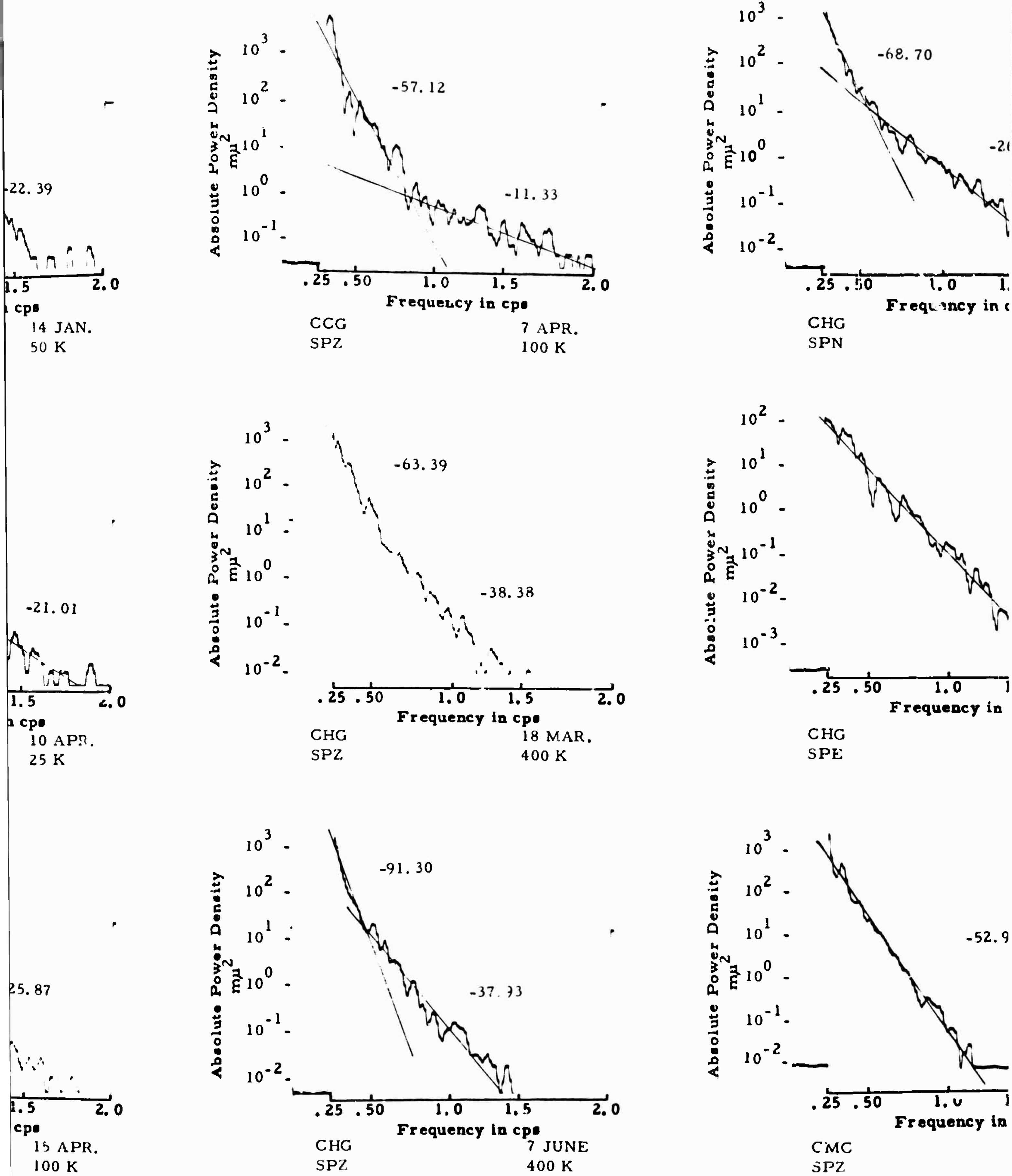
-22.39
1.5
2.0
cps
14 JAN.
50 K
Absolute Power Density
$m\mu^2$
-57.12
-11.33
.25 .50 1.0 1.5 2.0
Frequency in cps
CCG
SPZ
7 APR.
100 K
-68.70
CHG
SPN
-21.01
10 APR.
25 K
-63.39
-38.38
CHG
SPZ
18 MAR.
400 K
CHG
SPE
25.87
15 APR.
100 K
-91.30
-37.93
CHG
SPZ
7 JUNE
400 K
-52.9
CMC
SPZ

B

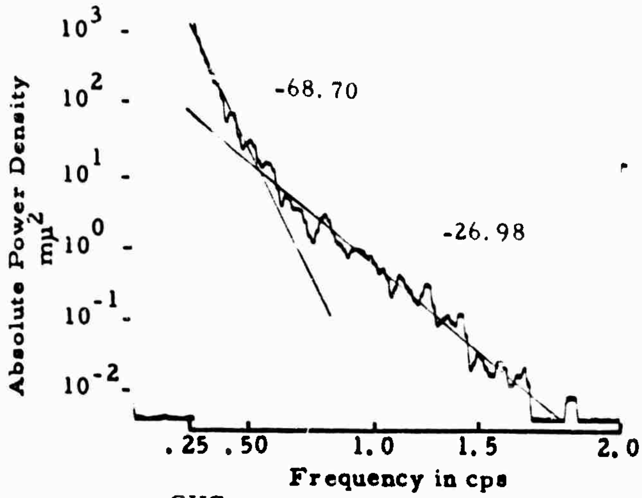

CHG
SPN

7 JUNE
400 K

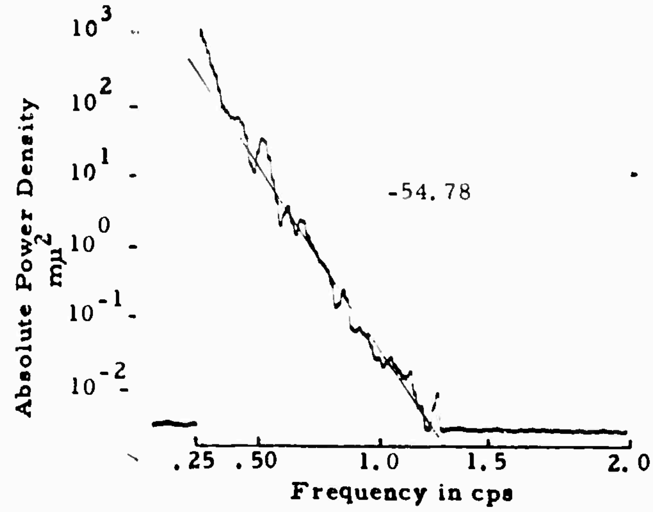

CMC
SPN

1 MAY
200 K

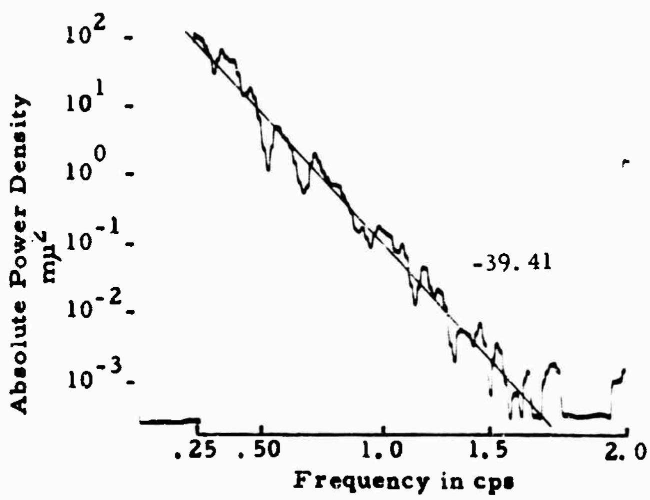

CHG
SPE

7 JUNE
400 K

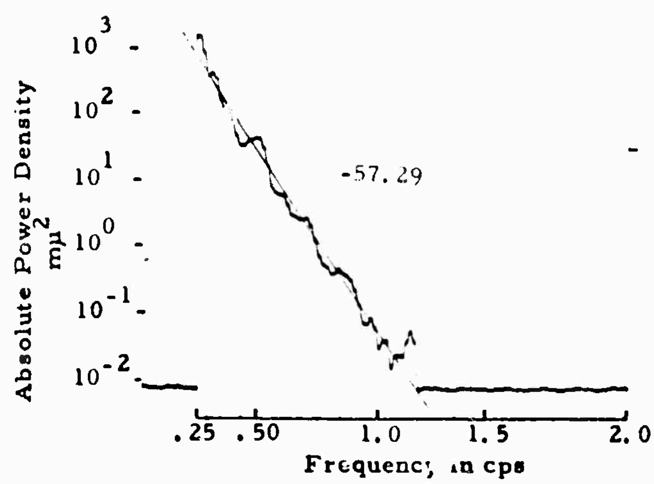

CMC
SPE

1 MAY
200 K

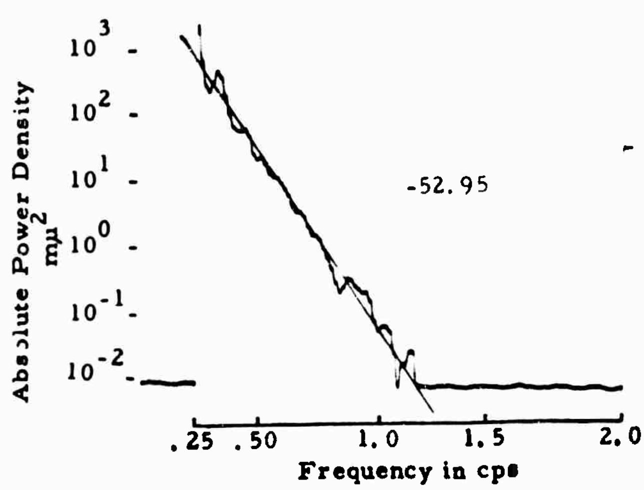

CMC
SPZ

1 MAY
200 K

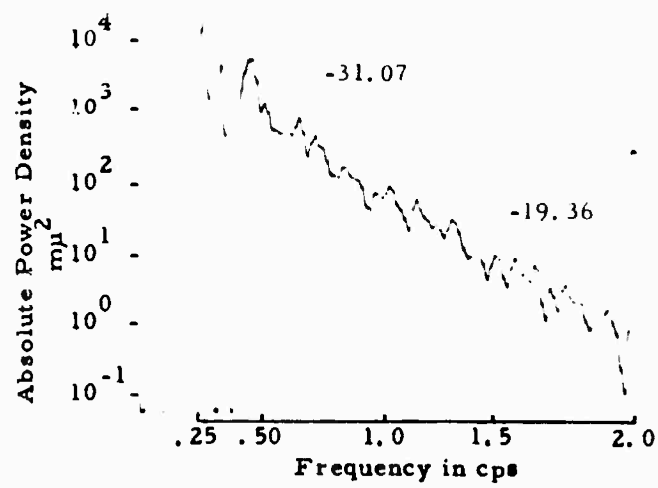

COP
SPZ

15 JAN.
12.5 K

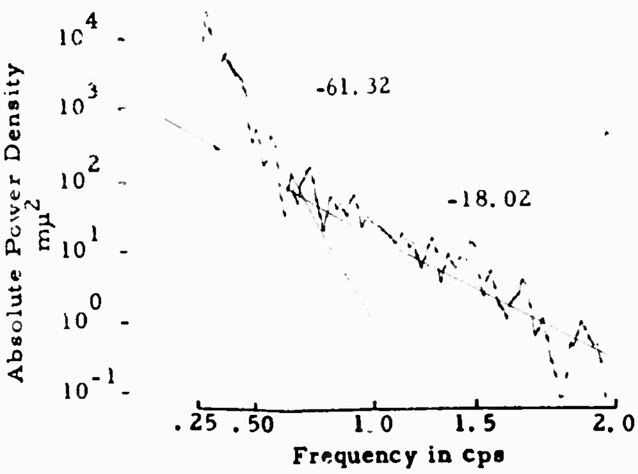

COP 19 APR.
SPZ 12.5 K

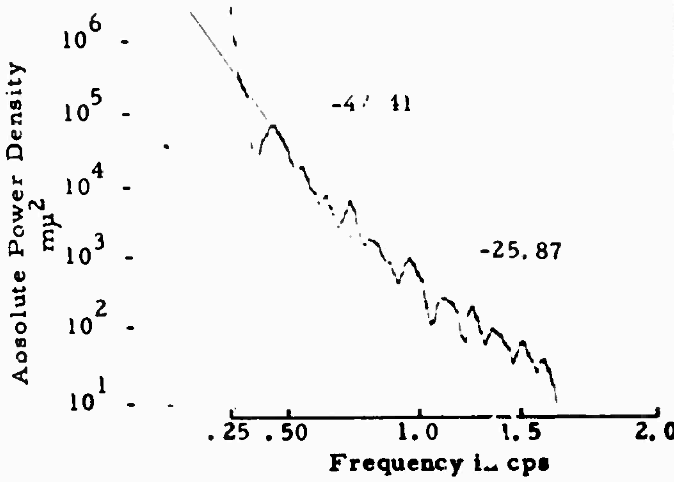

GDH 16 JAN.
SPZ 12.5 K

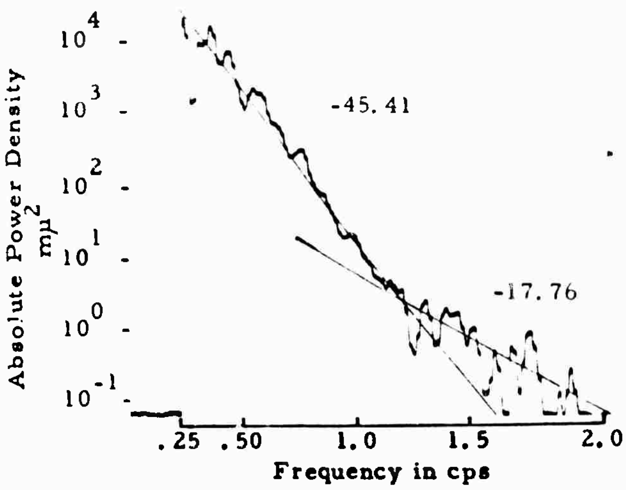

COR 5 JAN.
SPZ 25 K

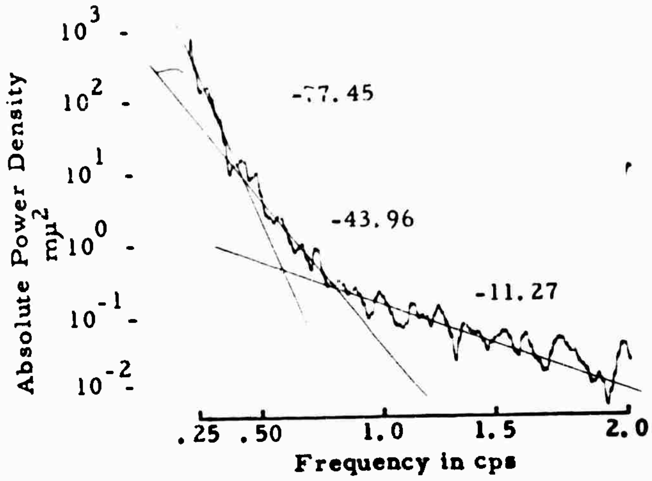

GOL 16 JAN.
SPZ 400 K

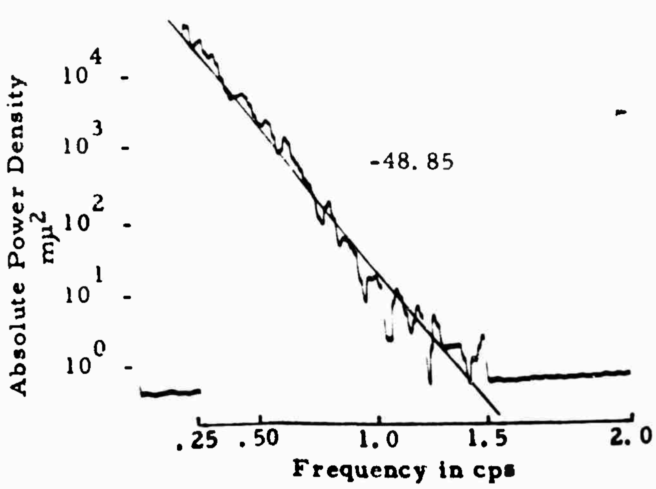

COR 1 APR.
SPZ 25 K

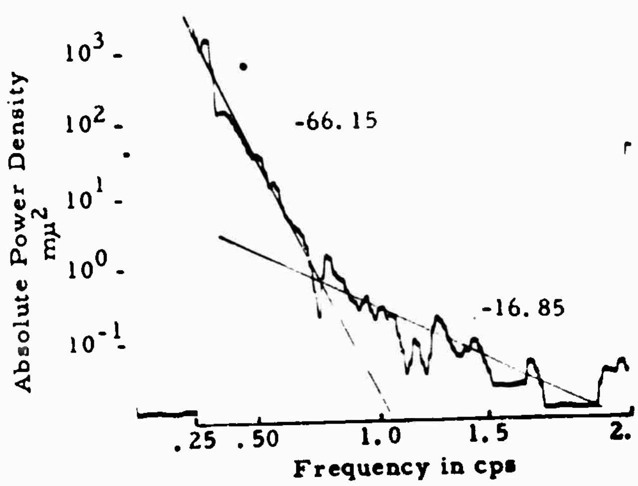

GOL 5 APR.
SPZ 400 K

D

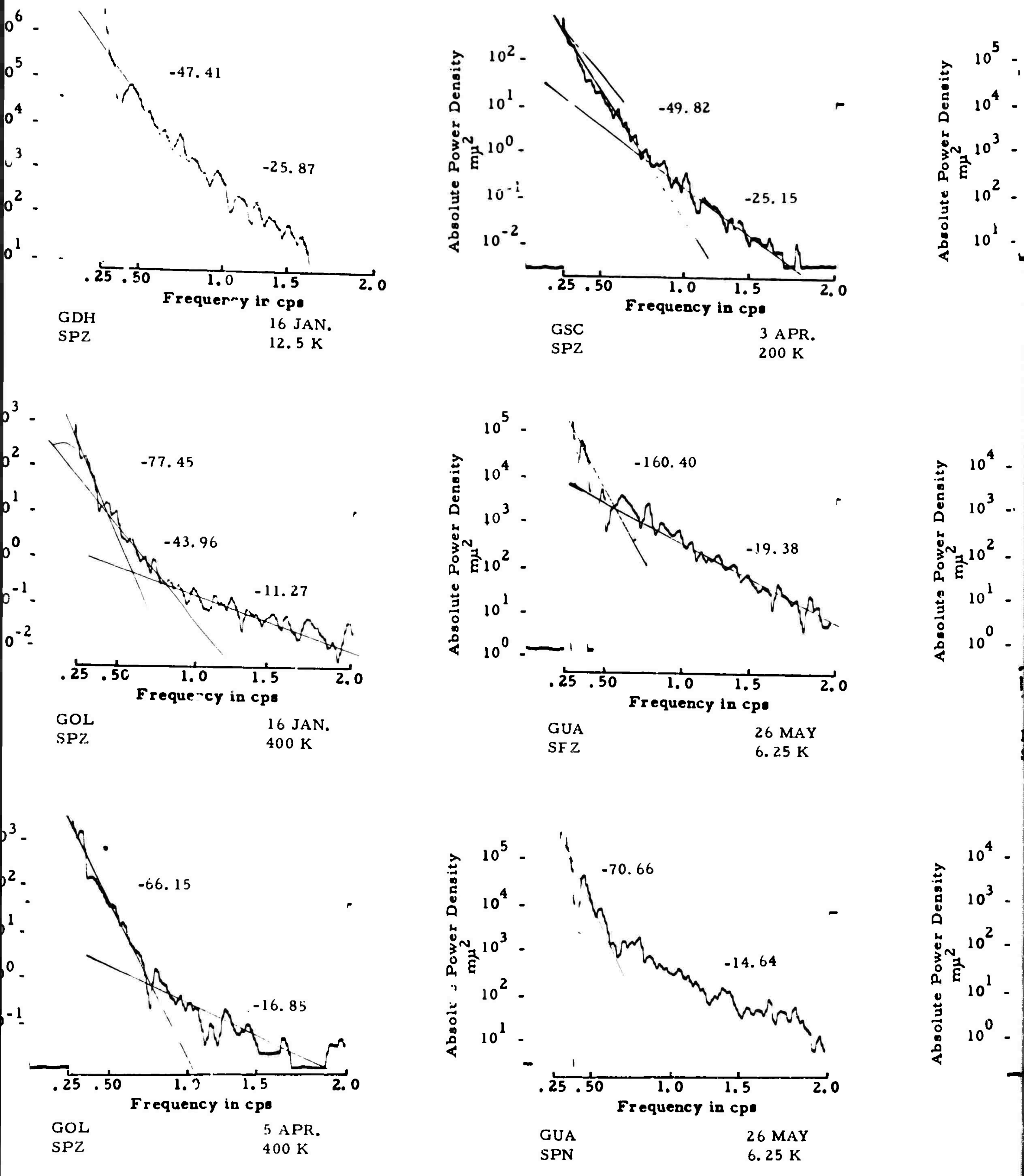

Figure A-1b. Absolute Power Density Spect

E

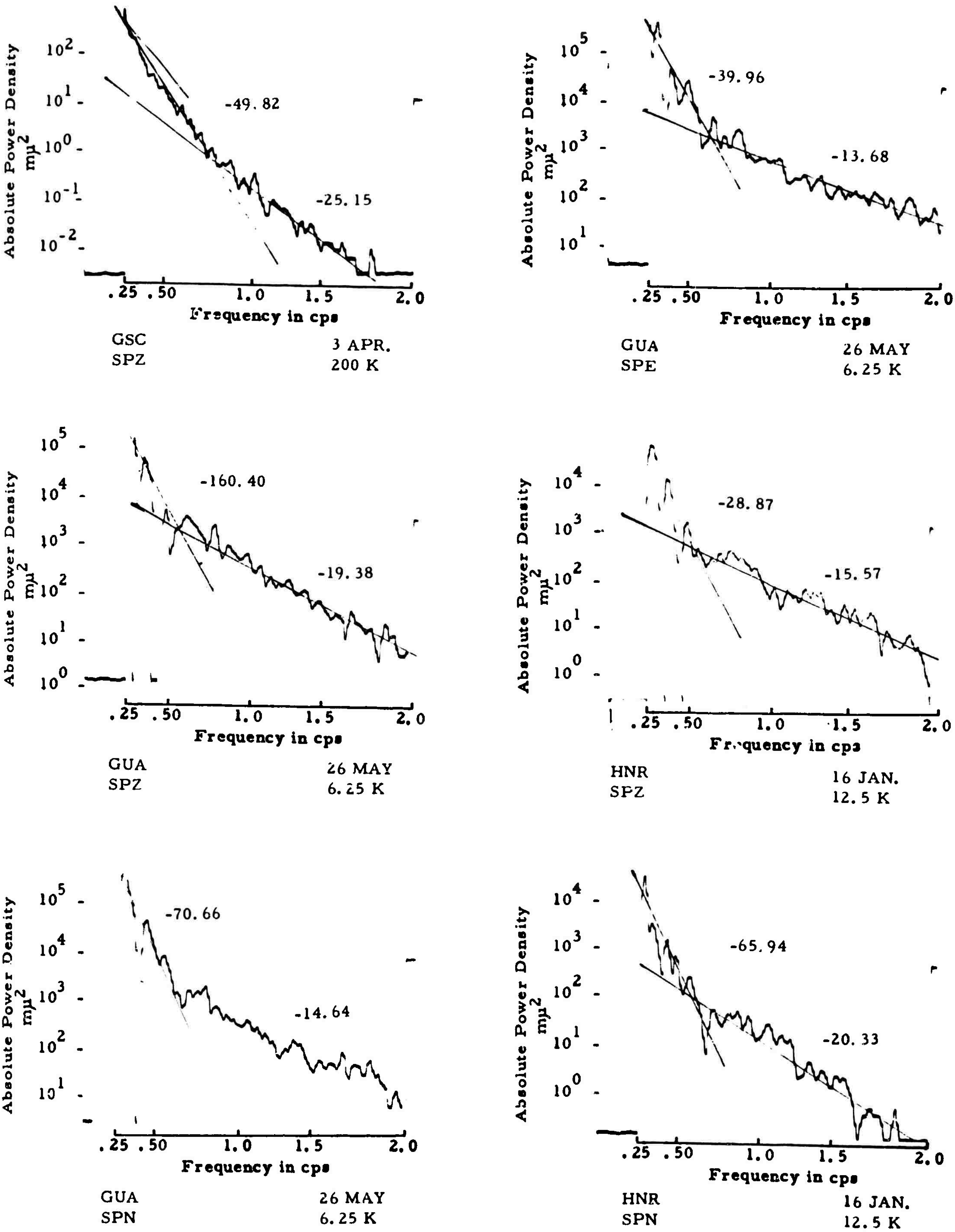

Figure A-1b. Absolute Power Density Spectra Obtained From 1963 Data

TABLE A-2c

ABSOLUTE POWER DENSITY SPECTRA LOCATED IN FIGURE A-1c

STATION	DATE	COMPONENT	GAIN(K)
HNR	4 March	SPZ	12.5
IST	2 January	SPZ	25
IST	19 January	SPZ	25
IST	20 April	SPZ	25
IST	20 April	SPN	25
IST	20 April	SPE	25
KEV	12 January	SPZ	25
KEV	5 March	SPZ	25
KEV	13 March	SPZ	25
KIP	16 January	SPZ	12.5
KIP	15 April	SPZ	12.5
KIP	15 April	SPN	12.5
KIP	15 April	SPE	12.5
KON	7 April	SPZ	50
KON	7 April	SPN	50
KON	7 April	SPE	50
LON	7 January	SPZ	100
LON	5 April	SPZ	100
MAL	7 April	SPZ	50
MAN	15 January	SPZ	12.5
MAN	15 January	SPN	12.5
MAN	15 January	SPE	12.5
MAN	20 April	SPZ	12.5
MAN	20 April	SPN	12.5
MAN	20 April	SPE	12.5

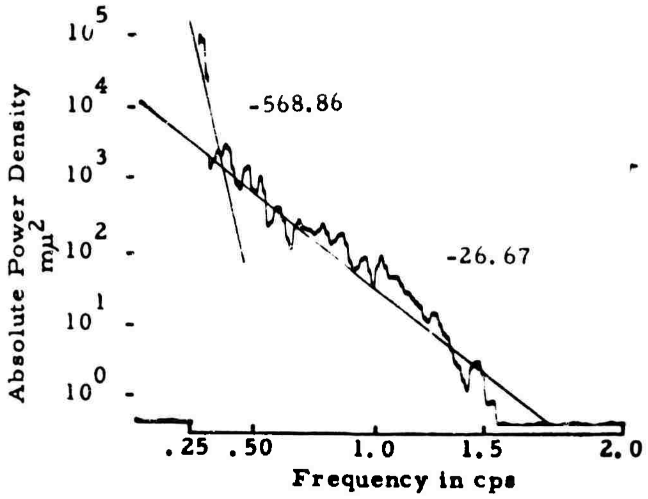

HNR 4 MAR.
SPZ 12.5 K

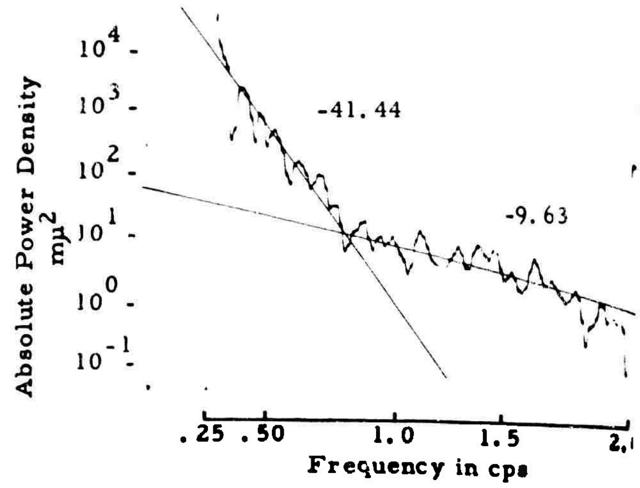

IST 20 APR.
SPZ 25 K

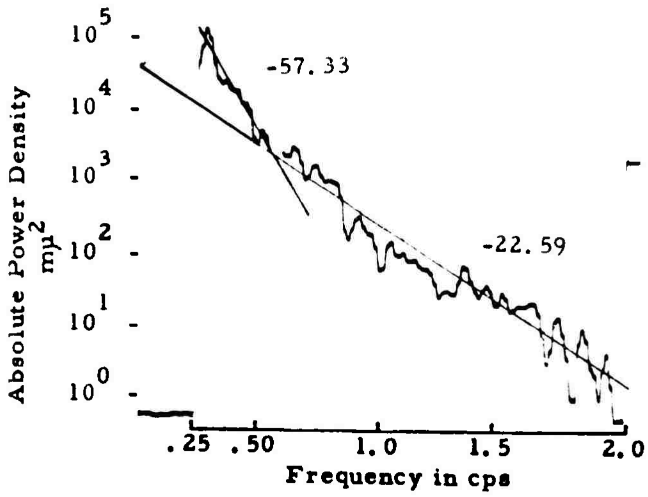

IST 2 JAN.
SPZ 25 K

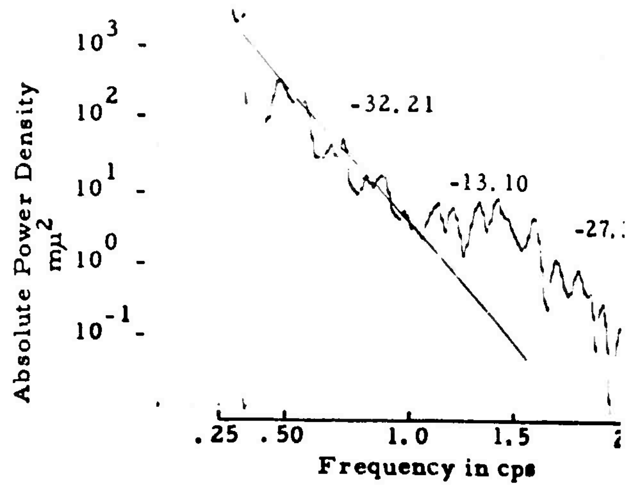

IST 20 APR.
SPN 25 K

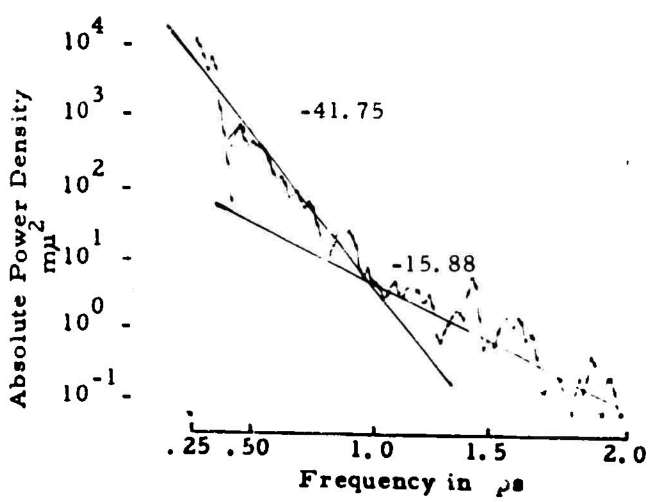

IST 19 JAN.
SPZ 25 K

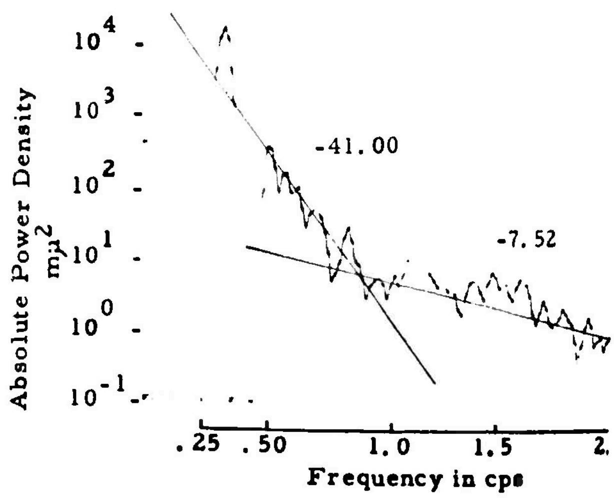

IST 20 APR.
SPE 25 K

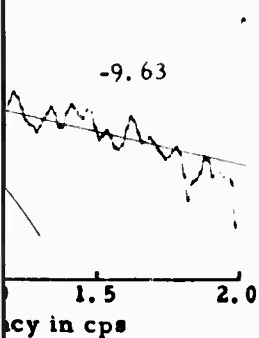

20 APR.
25 K

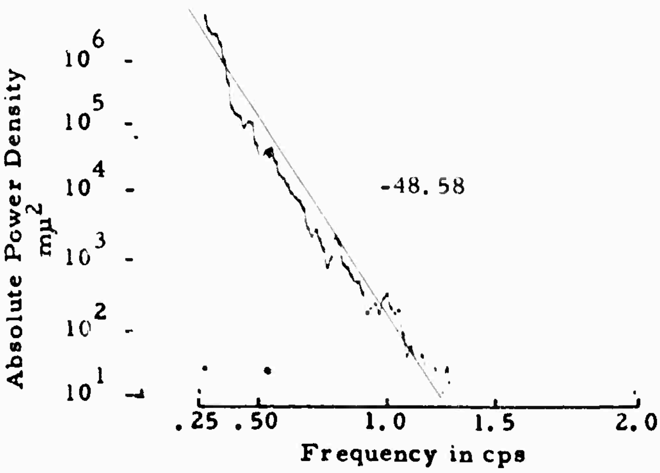

KEV
SPZ

12 JAN.
25 K

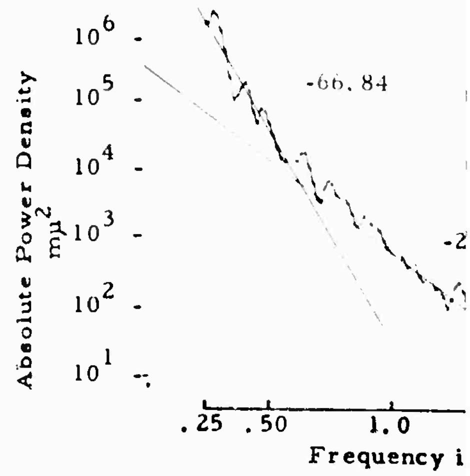

KIP
SPZ

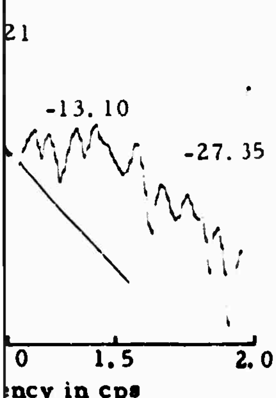

20 APR.
25 K

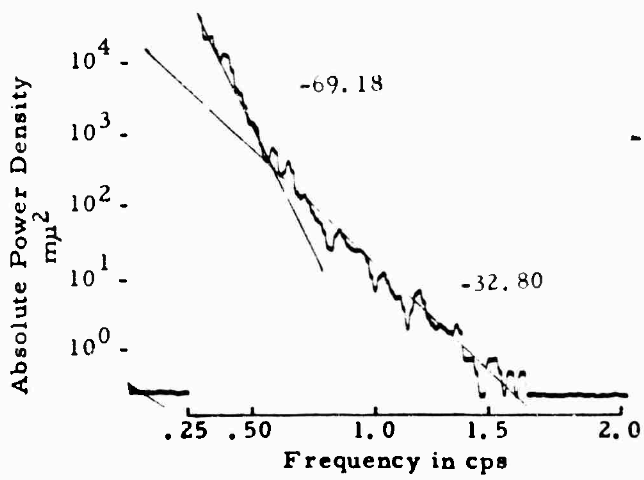

KEV
SPZ

5 MAR.
25 K

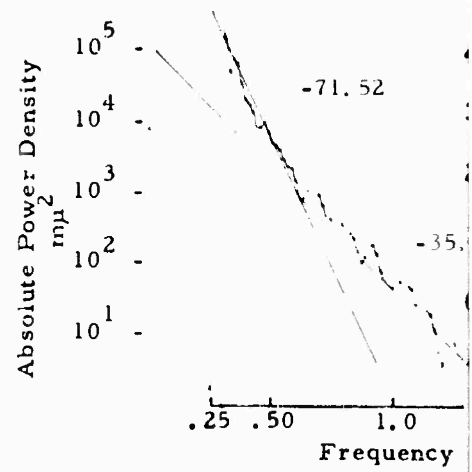

KIP
SPZ

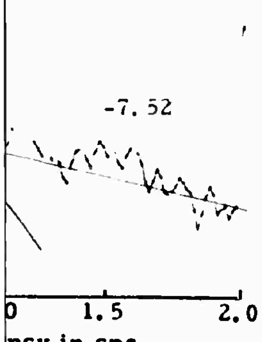

20 APR.
25 K

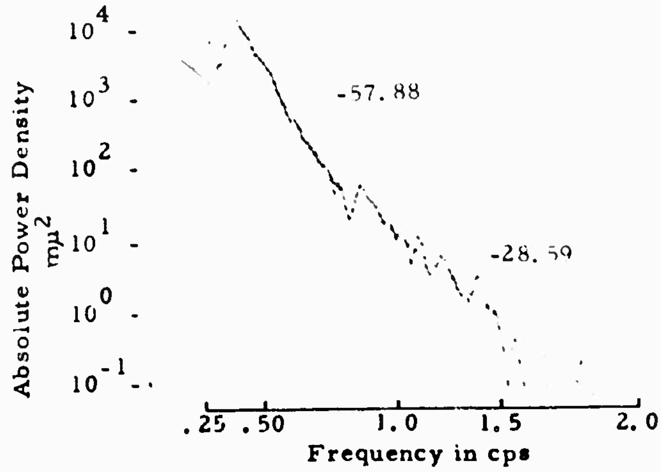

KEV
SPZ

13 MAR.
25 K

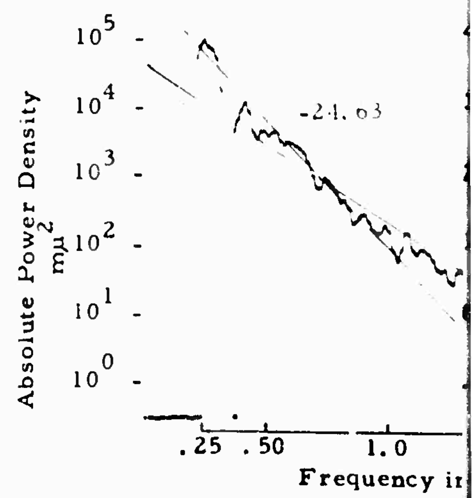

KIP
SPN

B

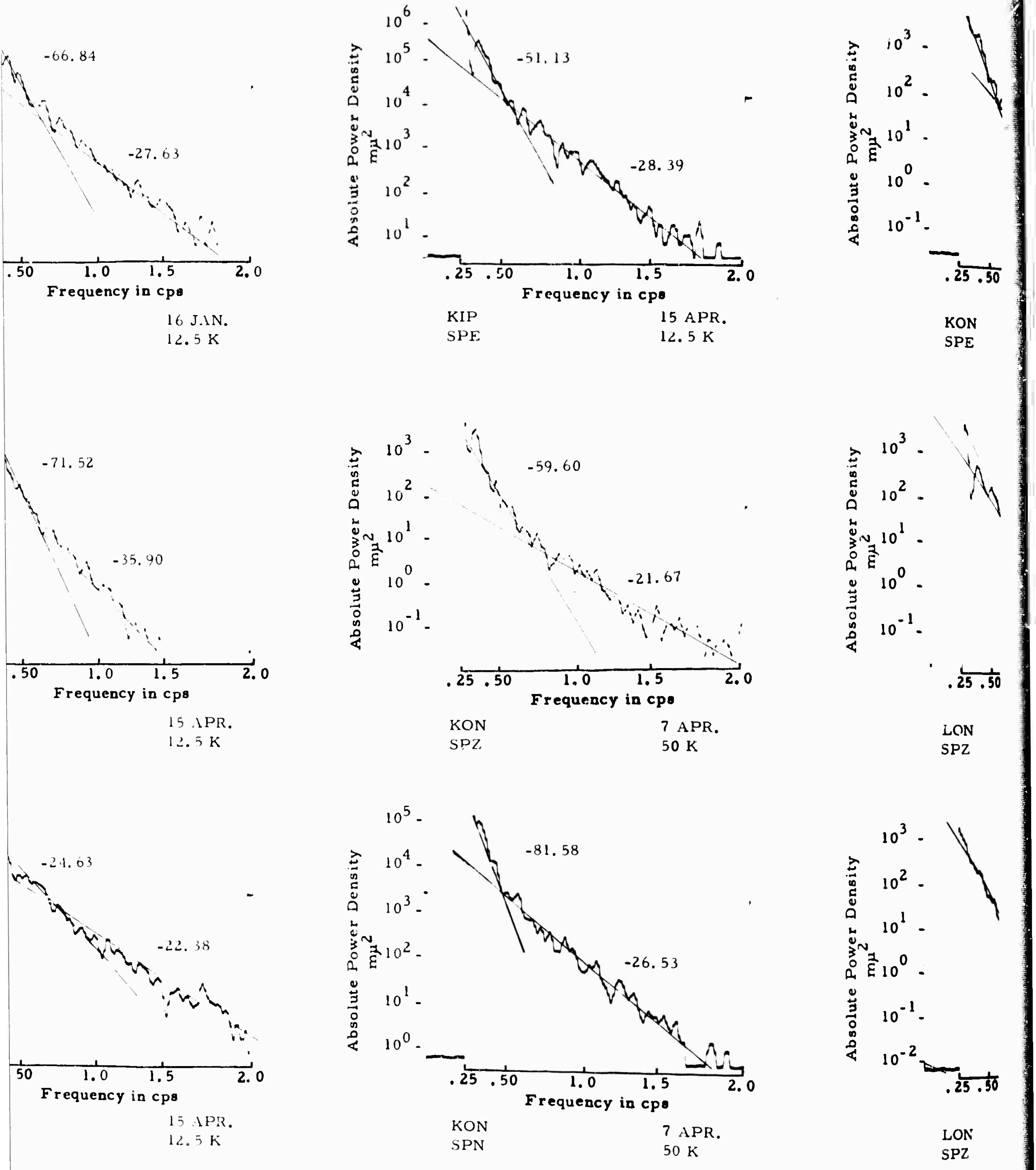
-66.84
-27.63
.50 1.0 1.5 2.0
Frequency in cps
16 JAN.
12.5 K
Absolute Power Density
$m\mu^2$
10^6 10^5 10^4 10^3 10^2 10^1
-51.13
-28.39
.25 .50 1.0 1.5 2.0
Frequency in cps
KIP
SPE
15 APR.
12.5 K
Absolute Power Density
$m\mu^2$
10^3 10^2 10^1 10^0 10^{-1}
.25 .50
KON
SPE
-71.52
-35.90
.50 1.0 1.5 2.0
Frequency in cps
15 APR.
12.5 K
Absolute Power Density
$m\mu^2$
10^3 10^2 10^1 10^0 10^{-1}
-59.60
-21.67
.25 .50 1.0 1.5 2.0
Frequency in cps
KON
SPZ
7 APR.
50 K
Absolute Power Density
$m\mu^2$
10^3 10^2 10^1 10^0 10^{-1}
.25 .50
LON
SPZ
-24.63
-22.38
50 1.0 1.5 2.0
Frequency in cps
15 APR.
12.5 K
Absolute Power Density
$m\mu^2$
10^5 10^4 10^3 10^2 10^1 10^0
-81.58
-26.53
.25 .50 1.0 1.5 2.0
Frequency in cps
KON
SPN
7 APR.
50 K
Absolute Power Density
$m\mu^2$
10^3 10^2 10^1 10^0 10^{-1} 10^{-2}
.25 .50
LON
SPZ

C

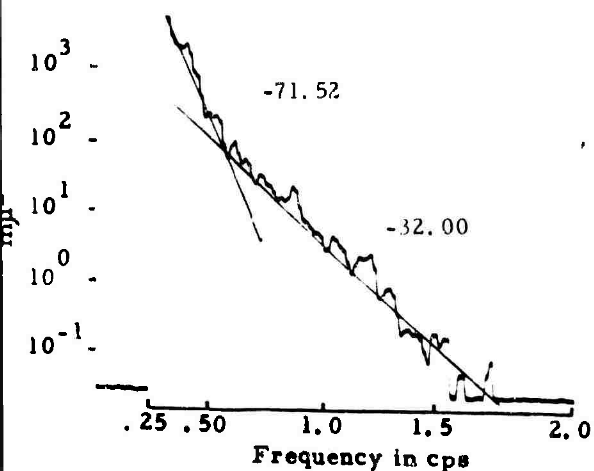

KON SPE — 7 APR. 50 K

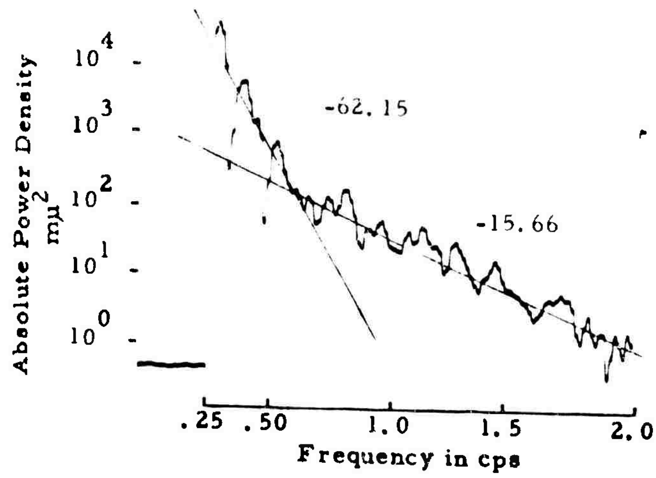

MAL SPZ — 7 APR. 50 K

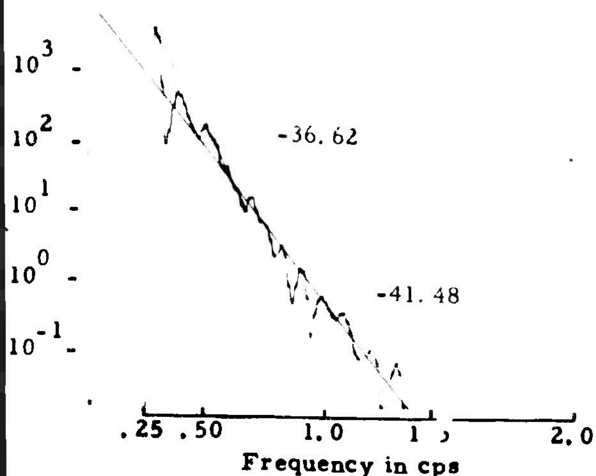

LON SPZ — 7 JAN. 100 K

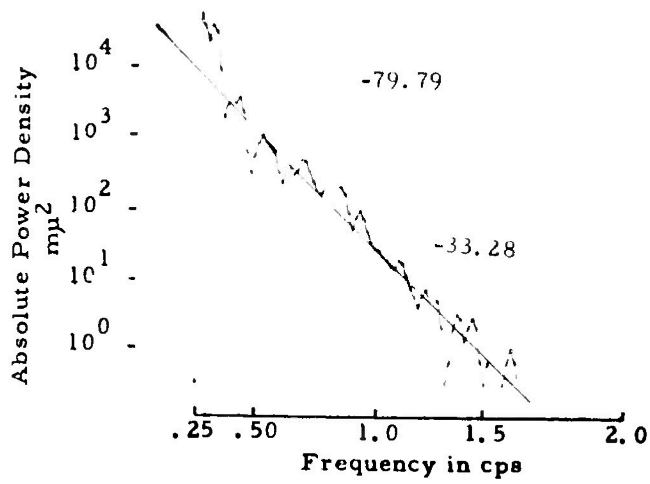

MAN SPZ — 15 JAN. 12.5 K

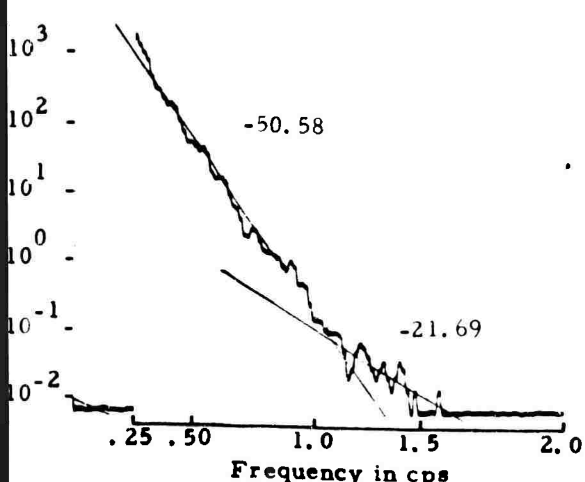

LON SPZ — 5 APR. 100 K

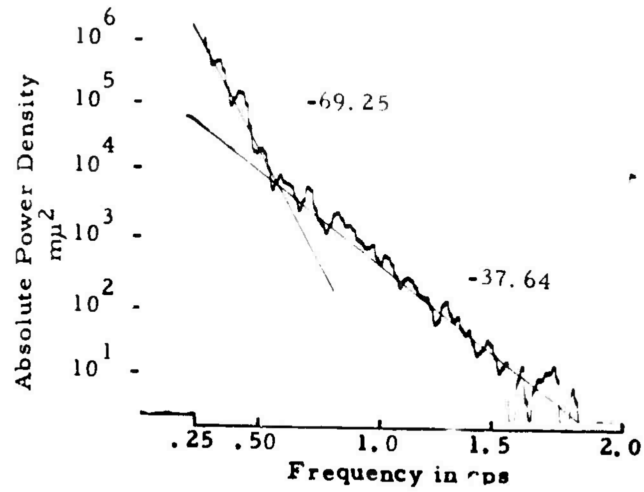

MAN SPN — 15 JAN. 12.5 K

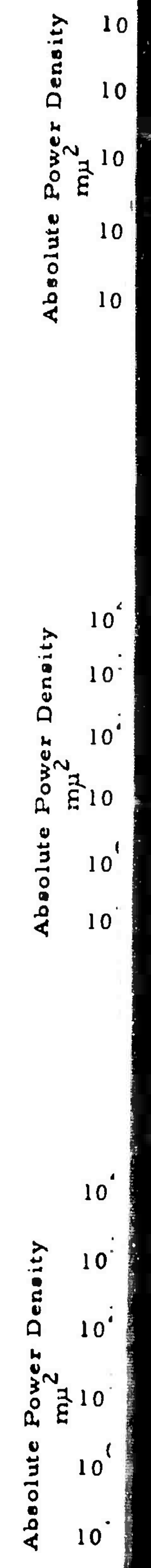

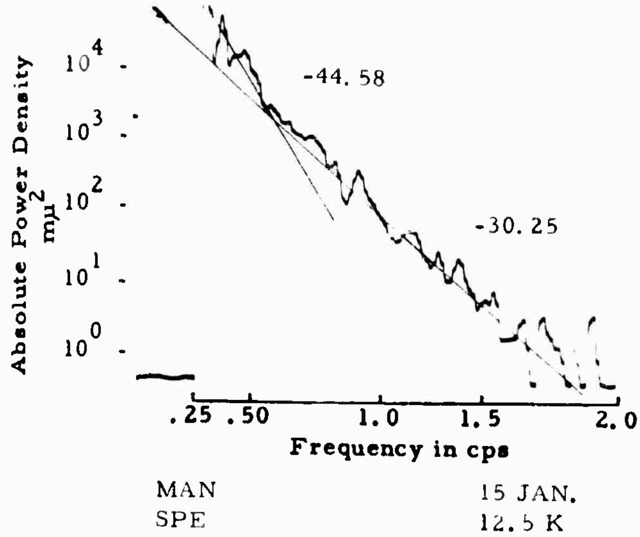

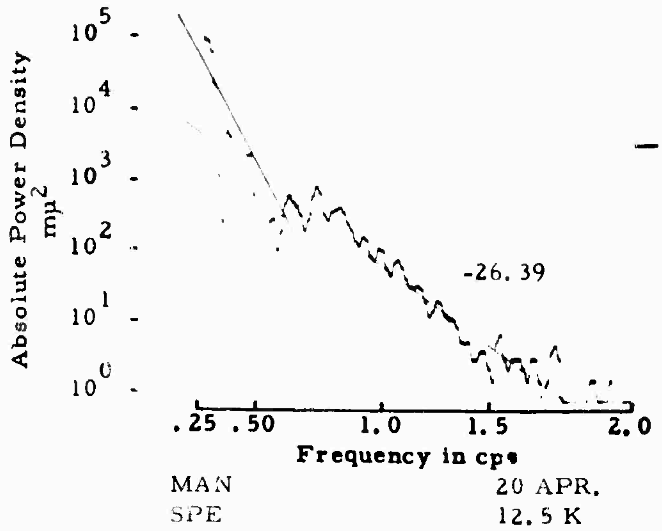

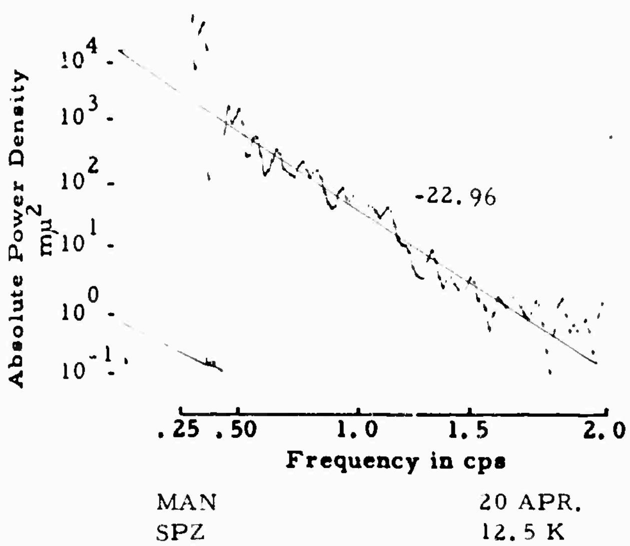

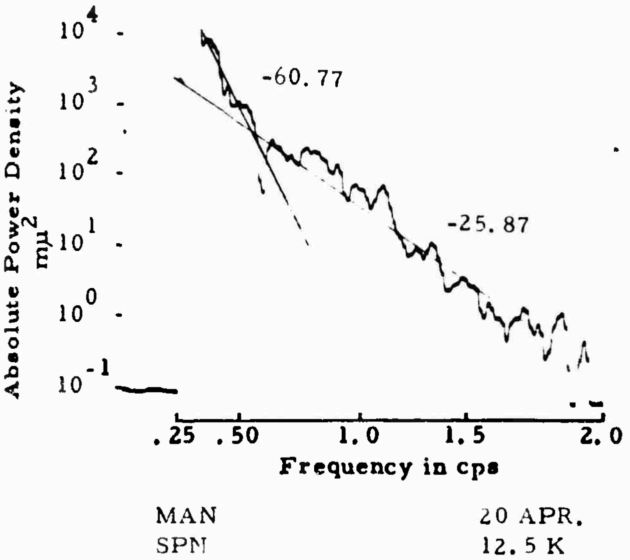

Figure A-1c. Absolute Power Density Spectra Obtained From 1963 Data

E

TABLE A-2d

ABSOLUTE POWER DENSITY SPECTRA LOCATED IN FIGURE A-1d

STATION	DATE	COMPONENT	GAIN(K)
MAN	3 June	SPZ	12.5
MAN	3 June	SPN	12.5
MAN	3 June	SPZ	12.5
MDS	18 January	SPZ	100
MUN	18 January	SPZ	25
MUN	18 January	SPN	25
MUN	18 January	SPE	25
MUN	5 April	SPZ	25
NAI	30 June	SPZ	50
NAI	30 June	SPN	100
NAI	30 June	SPZ	100
NUR	15 January	SPZ	25
NUR	15 January	SPN	25
NUR	15 January	SPE	25
NUR	15 January	SPN	25
NUR	15 January	SPE	25
NUR	19 April	SPZ	25
NUR	19 April	SPN	25
NUR	19 April	SPE	25
FLM	4 January	SPZ	50
PMG	15 January	SPZ	50
PMG	19 April	SPZ	50
PMG	19 April	SPN	50
PMG	19 April	SPE	50
PMG	19 April	SPE	50
PRE	7 January	SPZ	50
PRE	6 April	SPZ	50

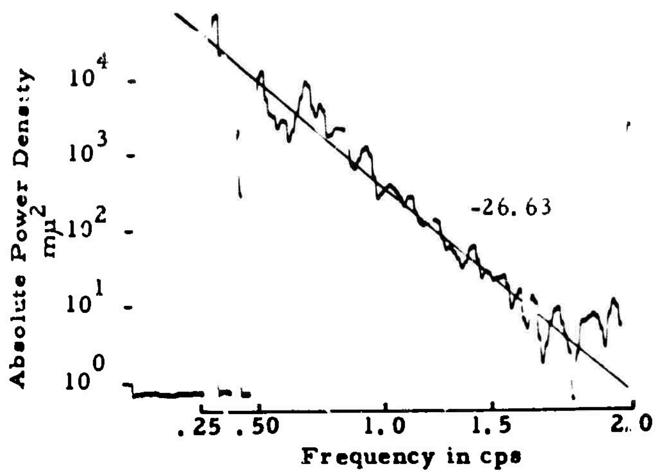

MAN 3 JUNE
SPZ 12.5 K

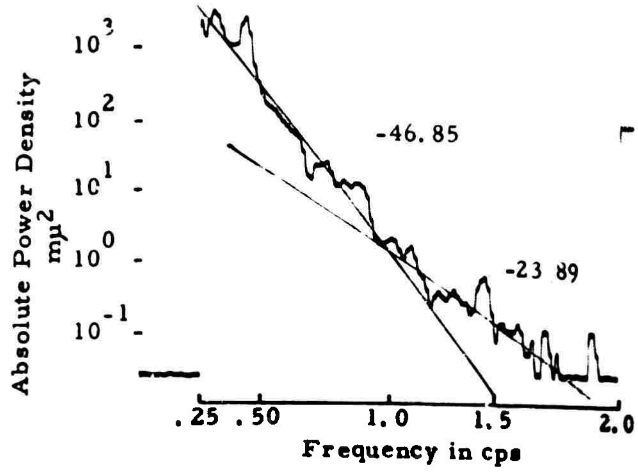

MDS 18 JAN.
SPZ 100 K

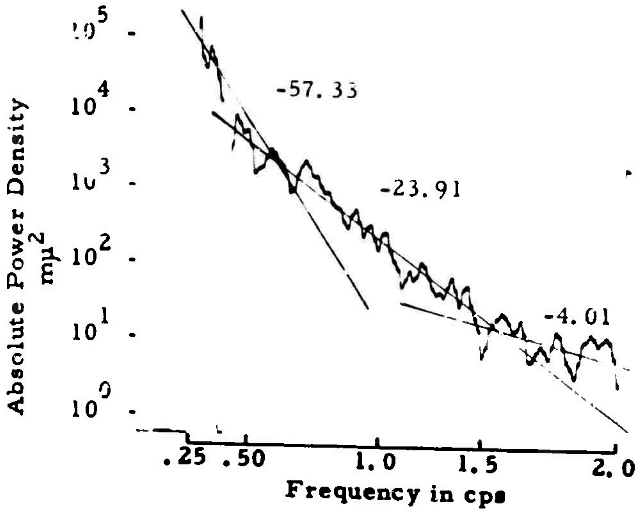

MAN 3 JUNE
SPN 12.5 K

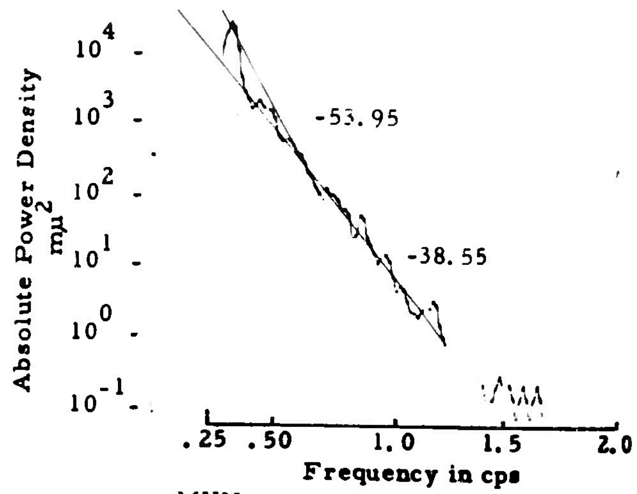

MUN 18 JAN.
SPZ 25 K

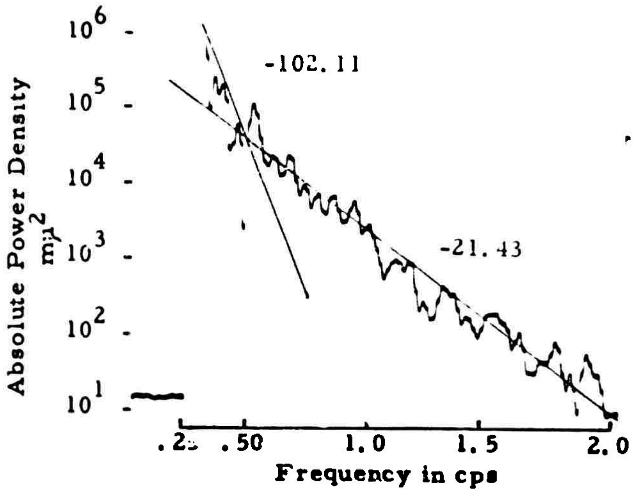

MAN 3 JUNE
SPE 12.5 K

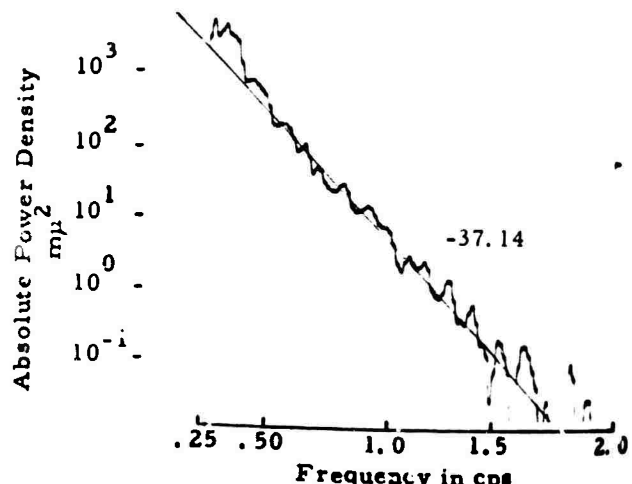

MUN 18 JAN.
SPN 25 K

A

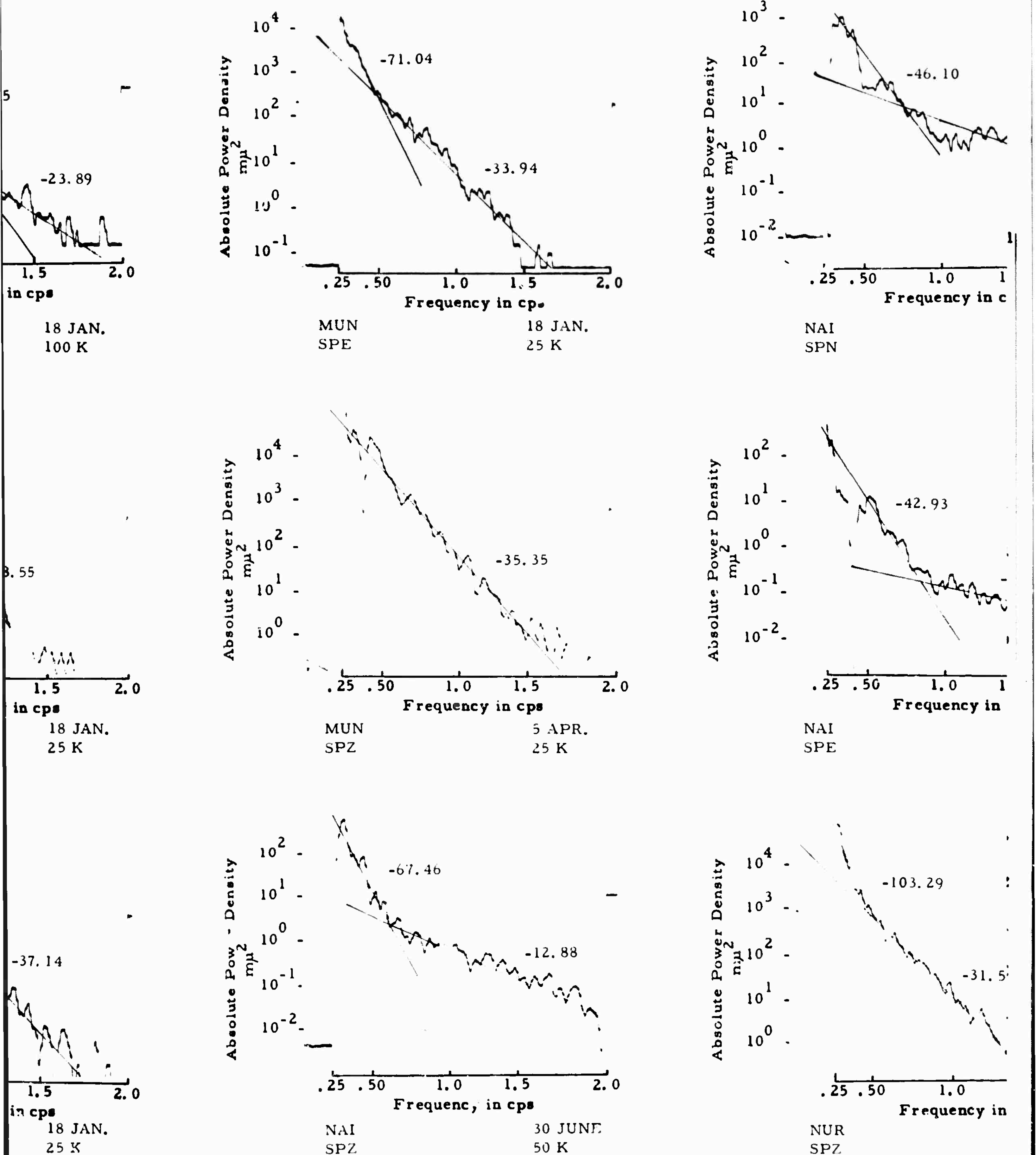
-23.89
1.5
2.0
in cps
18 JAN.
100 K
Absolute Power Density
$m\mu^2$
10^4
10^3
10^2
10^1
10^0
10^{-1}
-71.04
-33.94
.25
.50
1.0
1.5
2.0
Frequency in cps
MUN
SPE
18 JAN.
25 K
Absolute Power Density
$m\mu^2$
10^3
10^2
10^1
10^0
10^{-1}
10^{-2}
-46.10
.25
.50
1.0
NAI
SPN
1.5
2.0
in cps
18 JAN.
25 K
Absolute Power Density
$m\mu^2$
10^4
10^3
10^2
10^1
10^0
-35.35
.25
.50
1.0
1.5
2.0
Frequency in cps
MUN
SPZ
5 APR.
25 K
Absolute Power Density
$m\mu^2$
10^2
10^1
10^0
10^{-1}
10^{-2}
-42.93
.25
.50
1.0
Frequency in
NAI
SPE
-37.14
1.5
2.0
in cps
18 JAN.
25 K
Absolute Pow - Density
$m\mu^2$
10^2
10^1
10^0
10^{-1}
10^{-2}
-67.46
-12.88
.25
.50
1.0
1.5
2.0
Frequency in cps
NAI
SPZ
30 JUNE
50 K
Absolute Power Density
$m\mu^2$
10^4
10^3
10^2
10^1
10^0
-103.29
.25
.50
1.0
Frequency in
NUR
SPZ

b

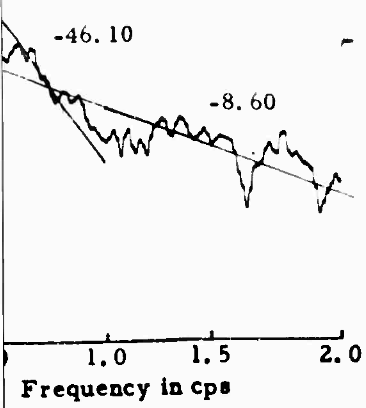

30 JUNE
100 K

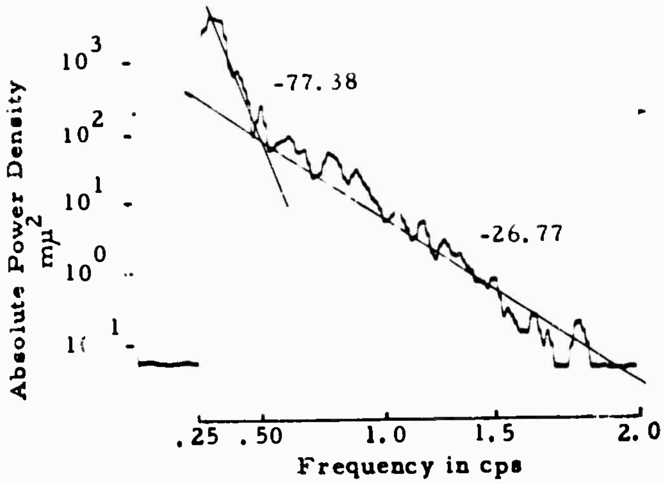

NUR
SPN

15 JAN.
25 K

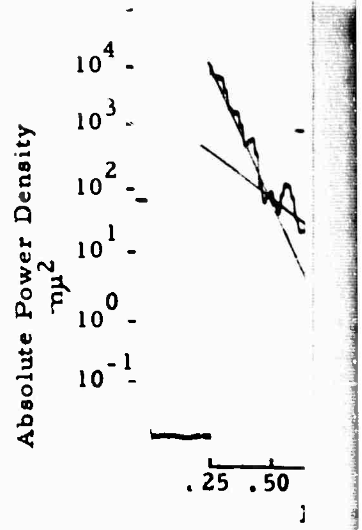

NUR
SPE

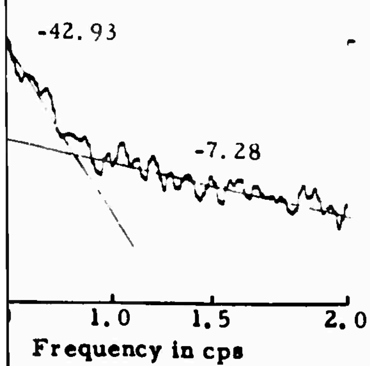

30 JUNE
100 K

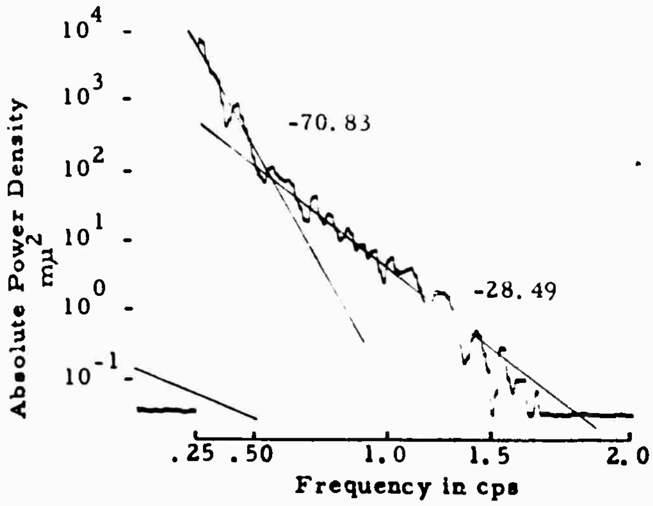

NUR
SPE

15 JAN.
25 K

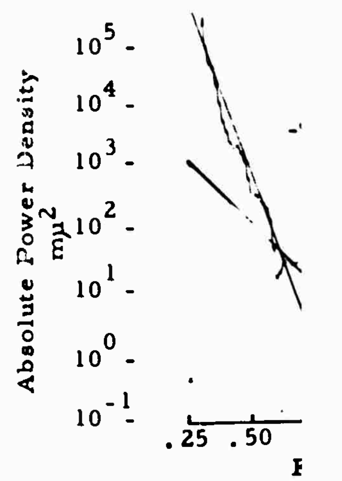

NUR
SPZ

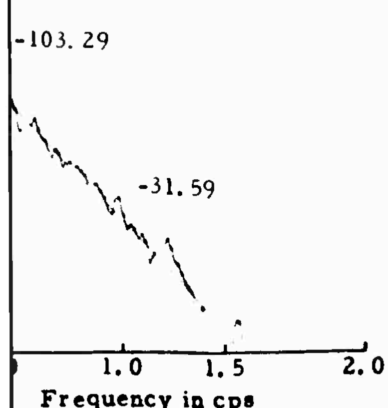

15 JAN.
25 K

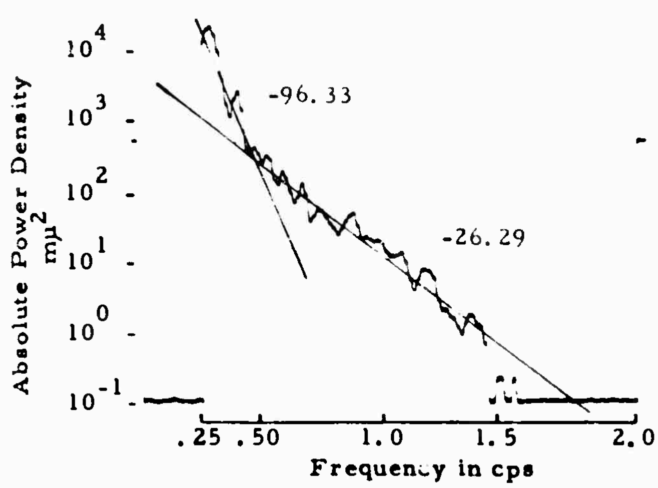

NUR
SPN

15 JAN.
25 K

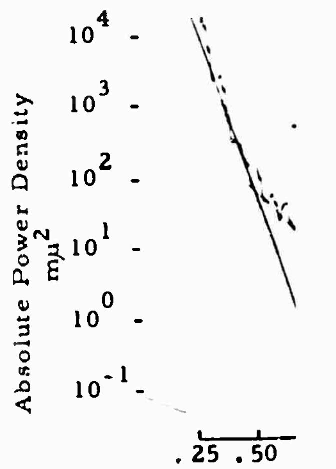

NUR
SPN

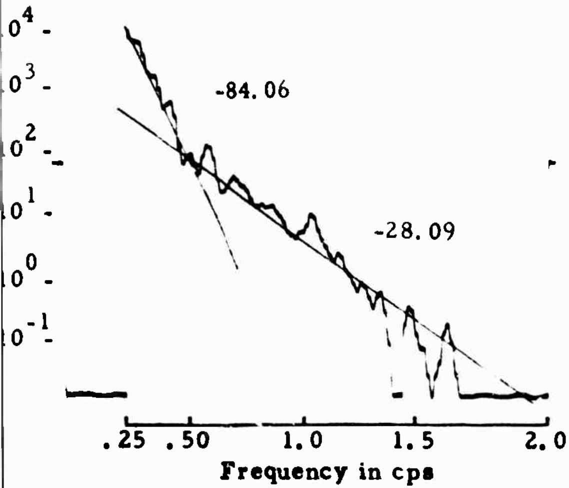

NUR 15 JAN.
SPE 25 K

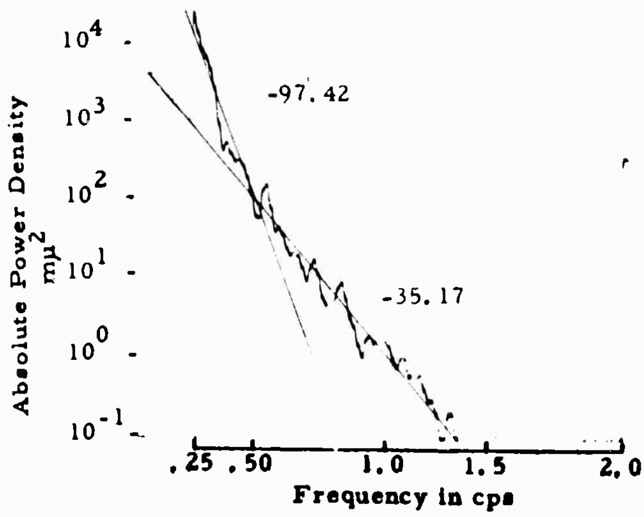

NUR 19 APR.
SPE 25 K

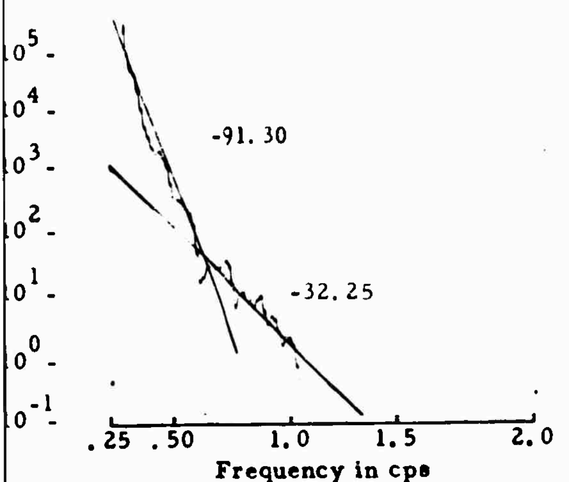

NUR 19 APR.
SPZ 25 K

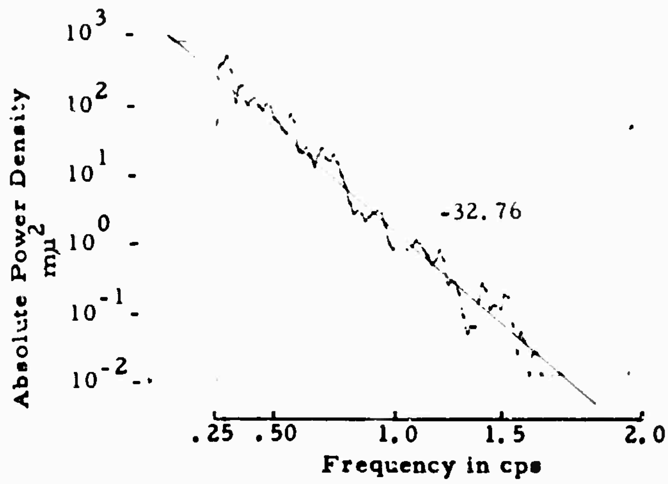

PLM 4 JAN.
SPZ 50 K

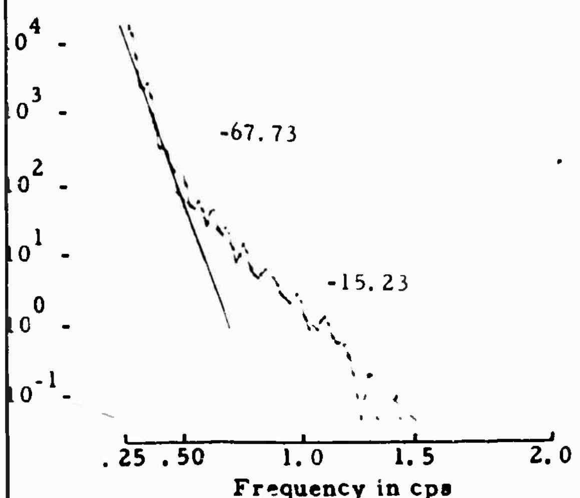

NUR 19 APR.
SPN 25 K

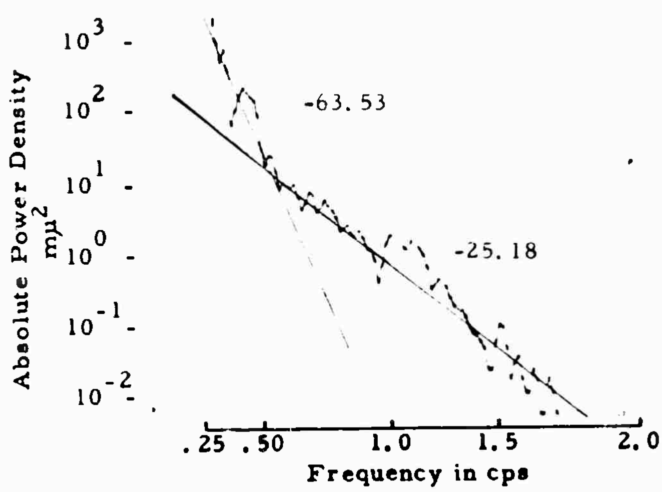

PMG 15 JAN.
SPZ 50 K

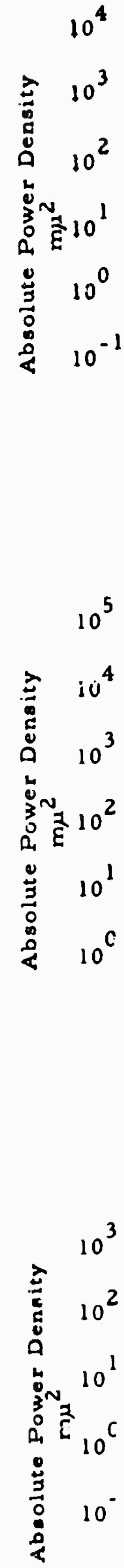

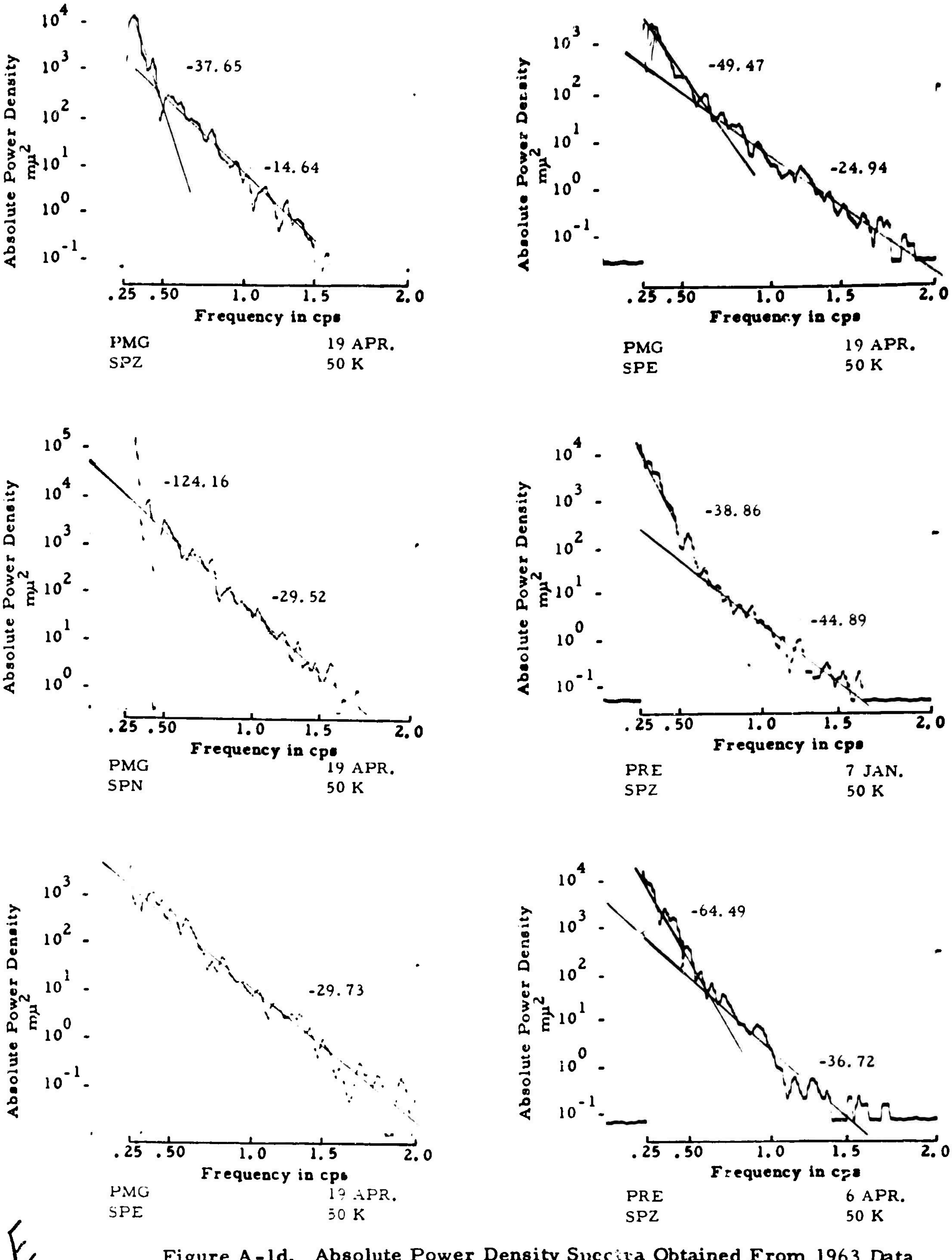

E

Figure A-1d. Absolute Power Density Spectra Obtained From 1963 Data

TABLE A-2e

ABSOLUTE POWER DENSITY SPECTRA LOCATED IN FIGURE A-1e

STATION	DATE	COMPONENT	GAIN(K)
PTO	15 April	SPZ	25
QUE	24 January	SPZ	200
QUE	24 January	SPZ	200
SCP	29 April	SPZ	100
SEO	18 March	SPZ	100
SEO	18 March	SPN	100
SEO	18 March	SPE	100
SEO	16 April	SPZ	100
SEO	16 April	SPN	100
SEO	16 April	SPE	100
SEO	6 June	SPZ	100
SEO	6 June	SPN	100
SEO	6 June	SPE	100
SHL	29 April	SPZ	200
SPA	10 January	SPZ	50
SPA	7 April	SPZ	100
SPA	7 June	SPZ	100
SPA	7 June	SPN	100
SPA	7 June	SPE	100
TOL	15 January	SPZ	50
TOL	15 January	SPN	25
TOL	15 January	SPE	25
TOL	2 April	SPZ	25
TOL	2 April	SPN	25
TOL	2 April	SPE	25
WES	5 January	SPZ	50
WIN	4 January	SPZ	100

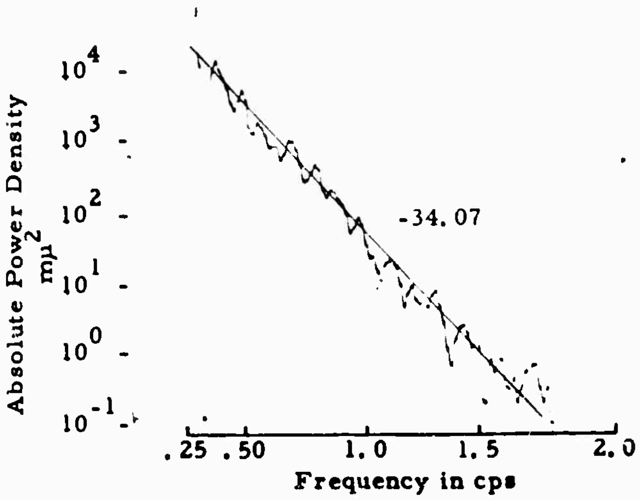

PTO 15 APR.
SPZ 25 K

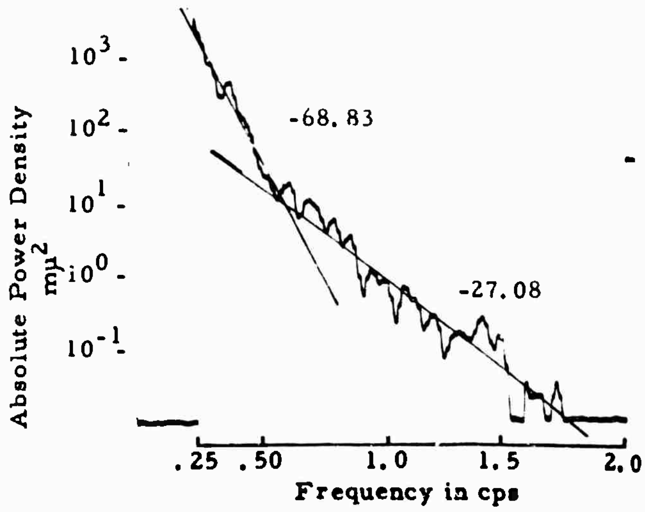

SCP 29 APR.
SPZ 100 K

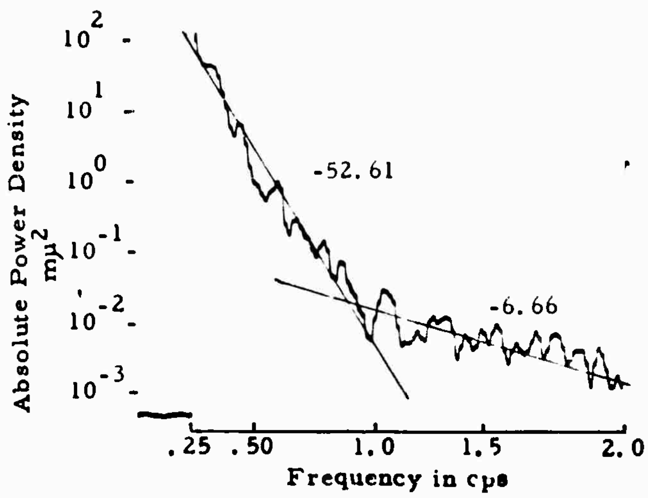

QUE 24 JAN.
SPZ 200 K

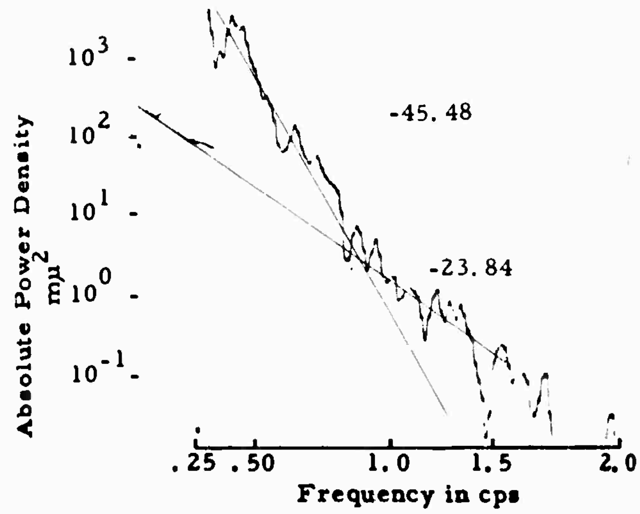

SEO 18 MAR.
SPZ 100 K

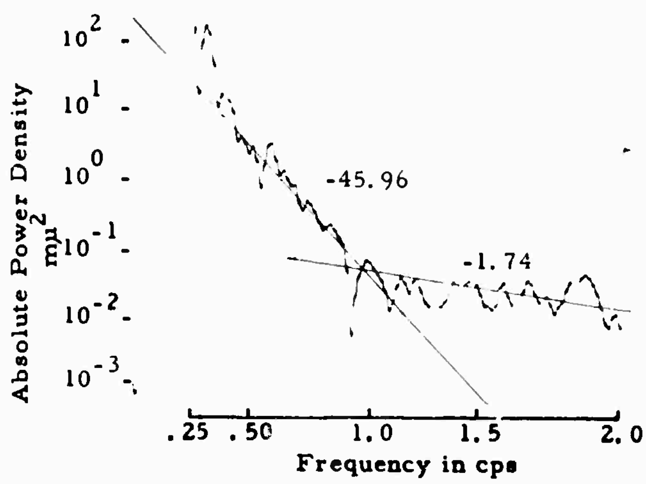

QUE 24 JAN.
SPZ 200 K

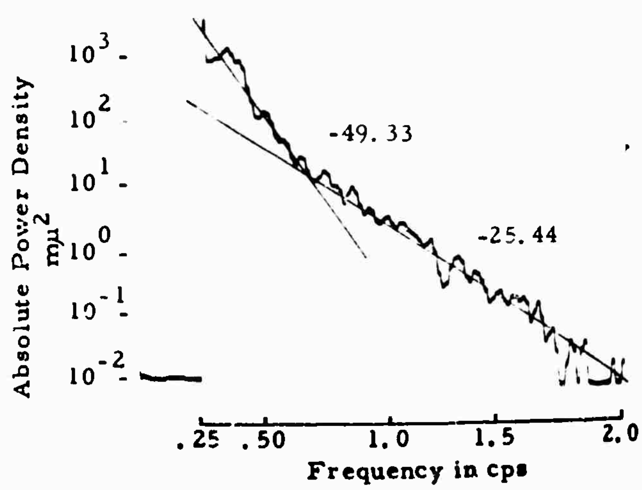

SEO 18 MAR.
SPN 100 K

A

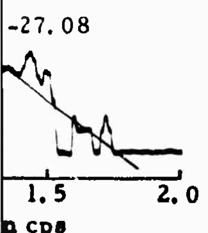

29 APR.
100 K

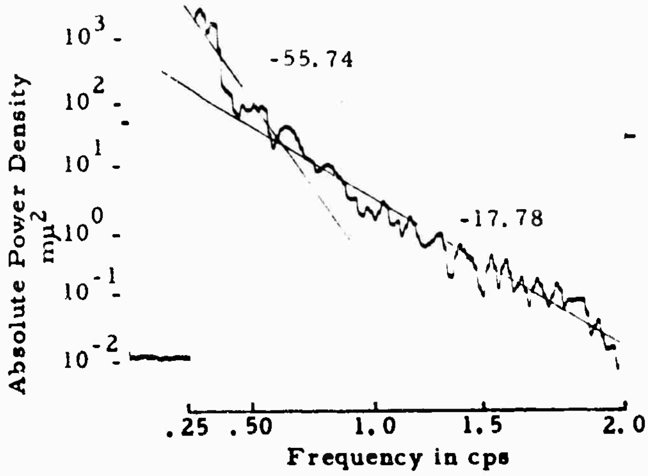

SEO
SPE

18 MAR.
100 K

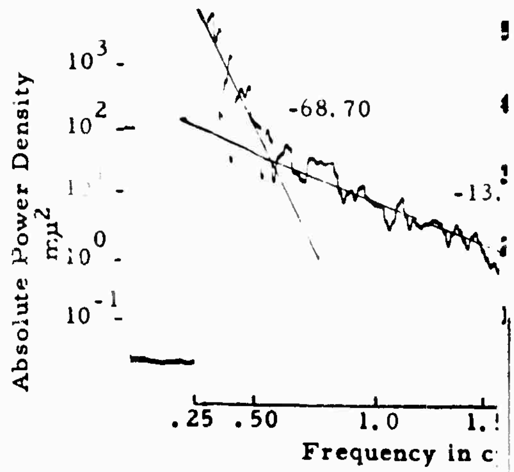

SEO
SPE

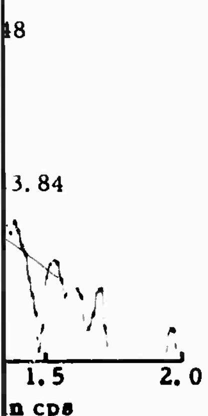

18 MAR.
100 K

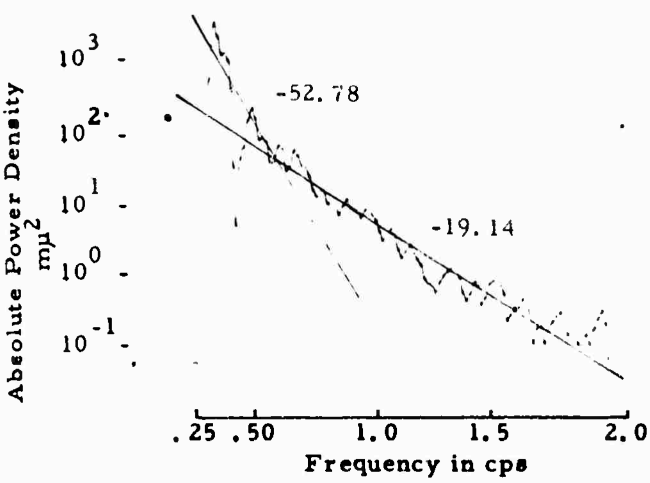

SEO
SPZ

16 APR.
100 K

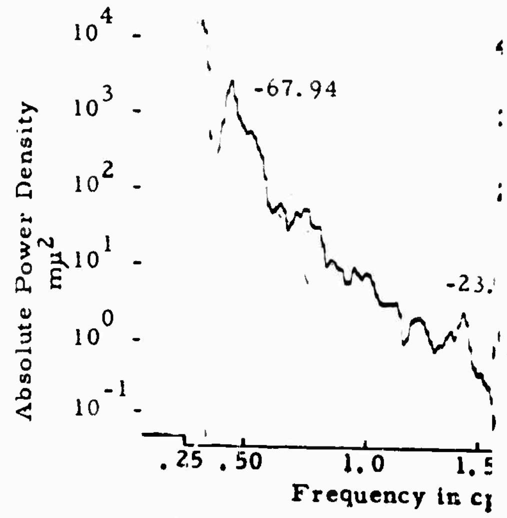

SEO
SPZ

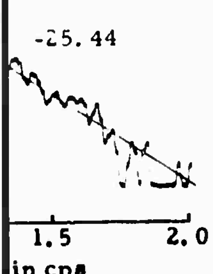

18 MAR.
100 K

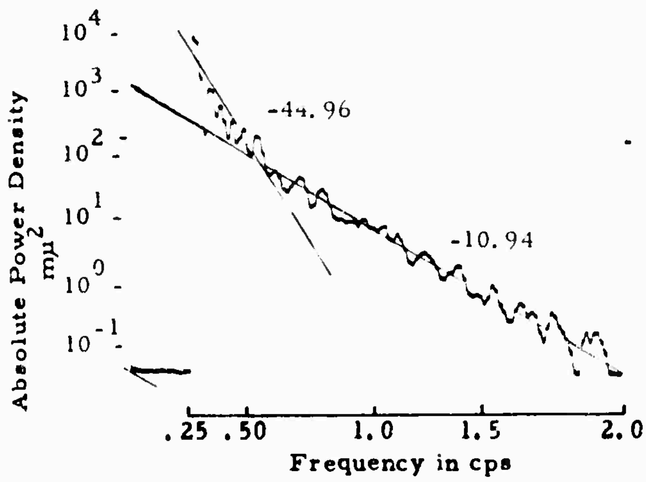

SEO
SPN

16 APR.
100 K

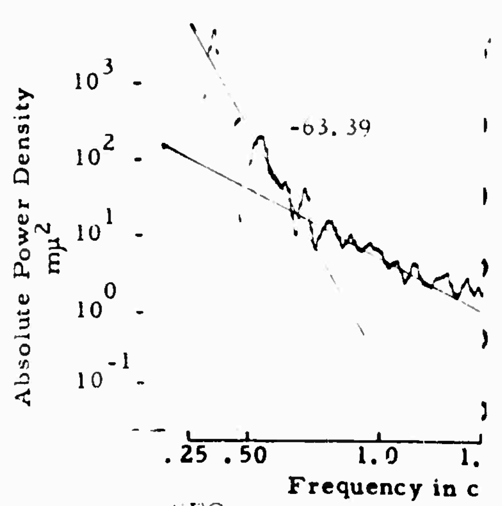

SEO
SPN

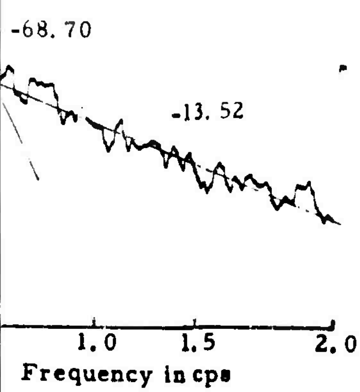

16 APR.
100 K

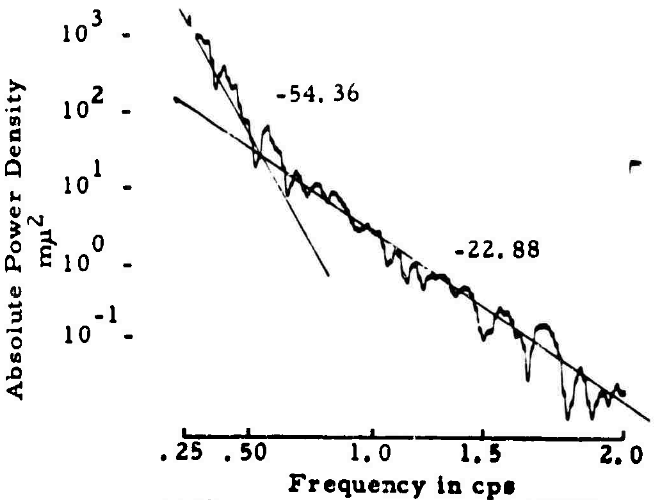

SEO
SPE

6 JUNE
100 K

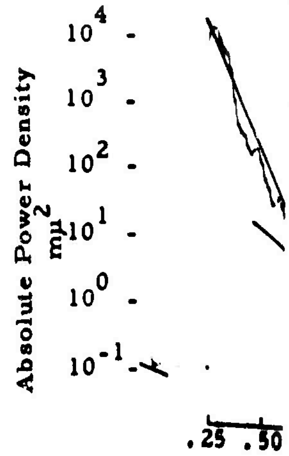

SPA
SPZ

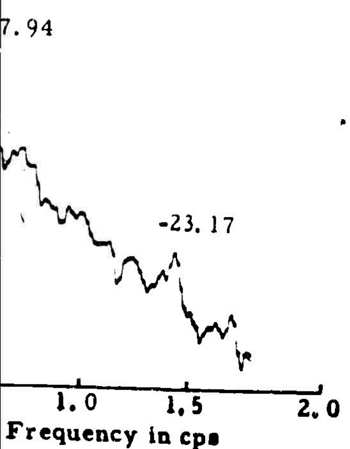

6 JUNE
100 K

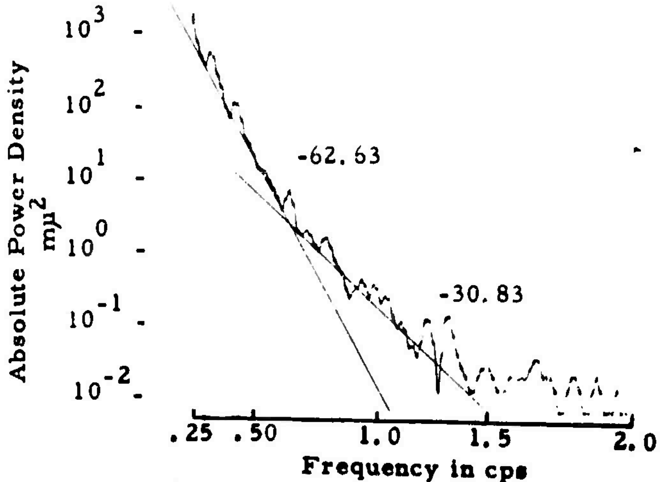

SHL
SPZ

29 APR.
200 K

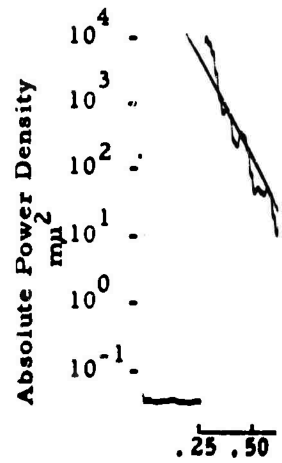

SPA
SPZ

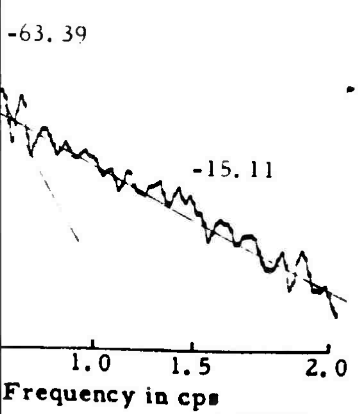

6 JUNE
100 K

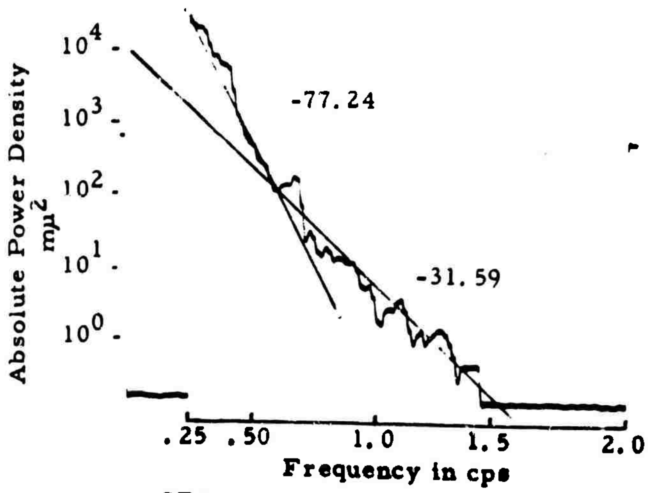

SPA
SPZ

10 JAN.
50 K

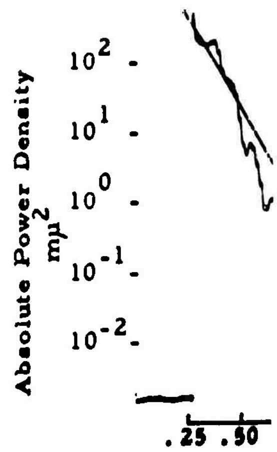

SPA
SPN

e

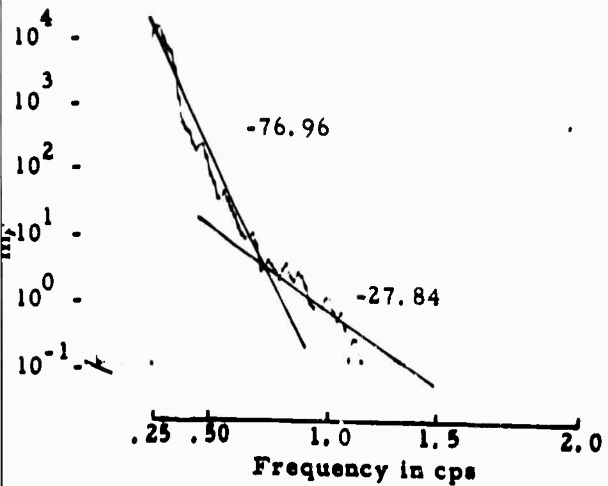

SPA 7 APR.
SPZ 100 K

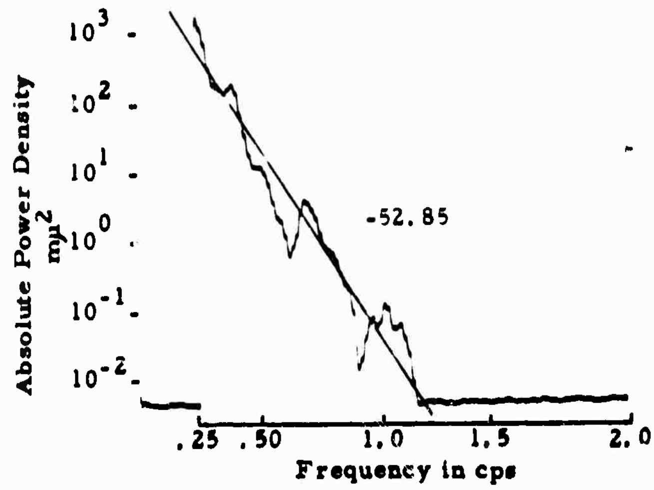

SPA 7 JUNE
SPE 100 K

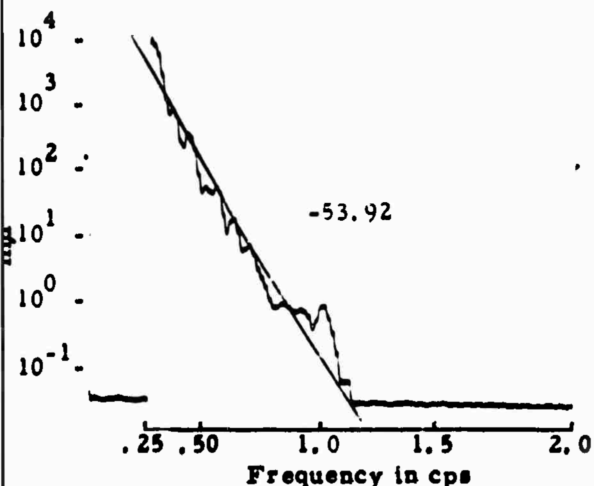

SPA 7 JUNE
SPZ 100 K

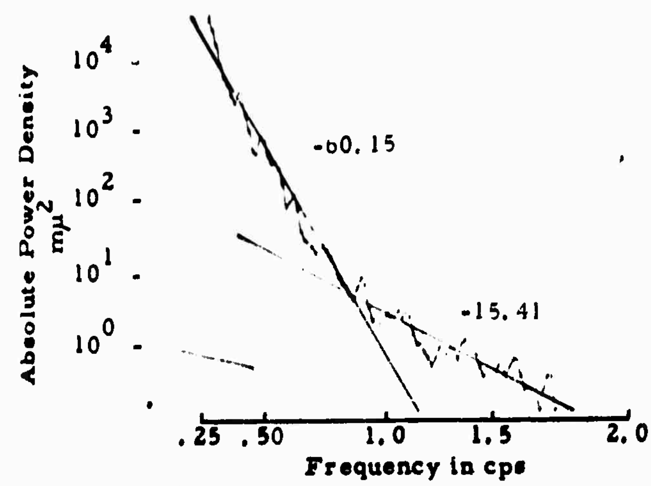

TOL 15 JAN.
SPZ 50 K

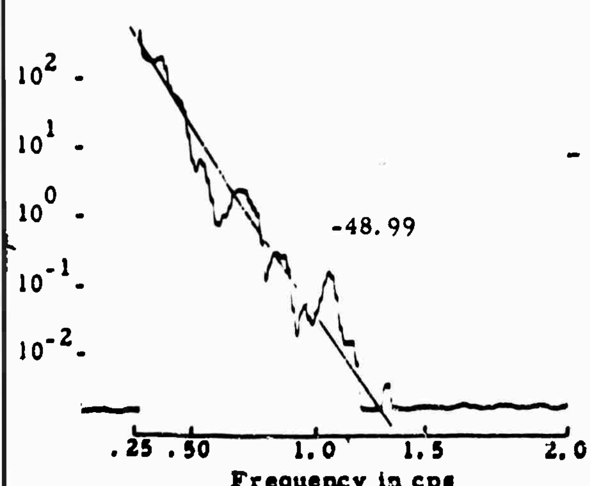

SPA 7 JUNE
SPN 100 K

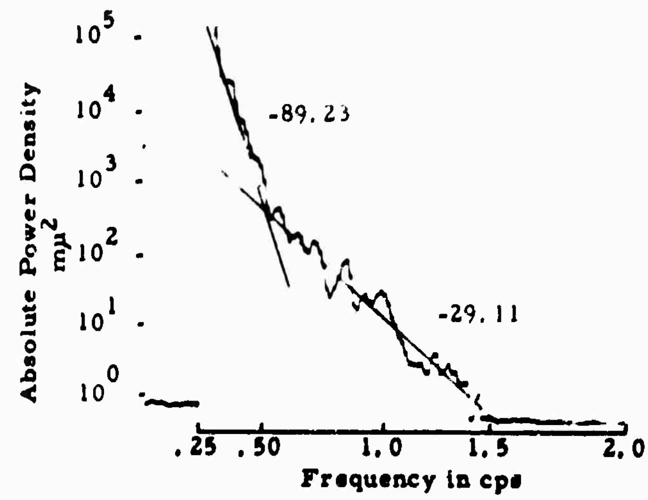

TOL 15 JAN.
SPN 25 K

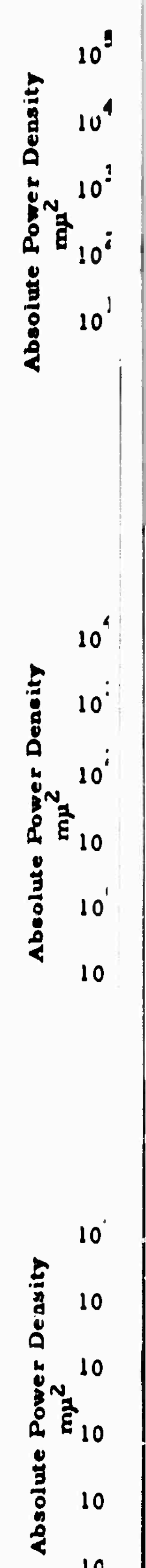

D

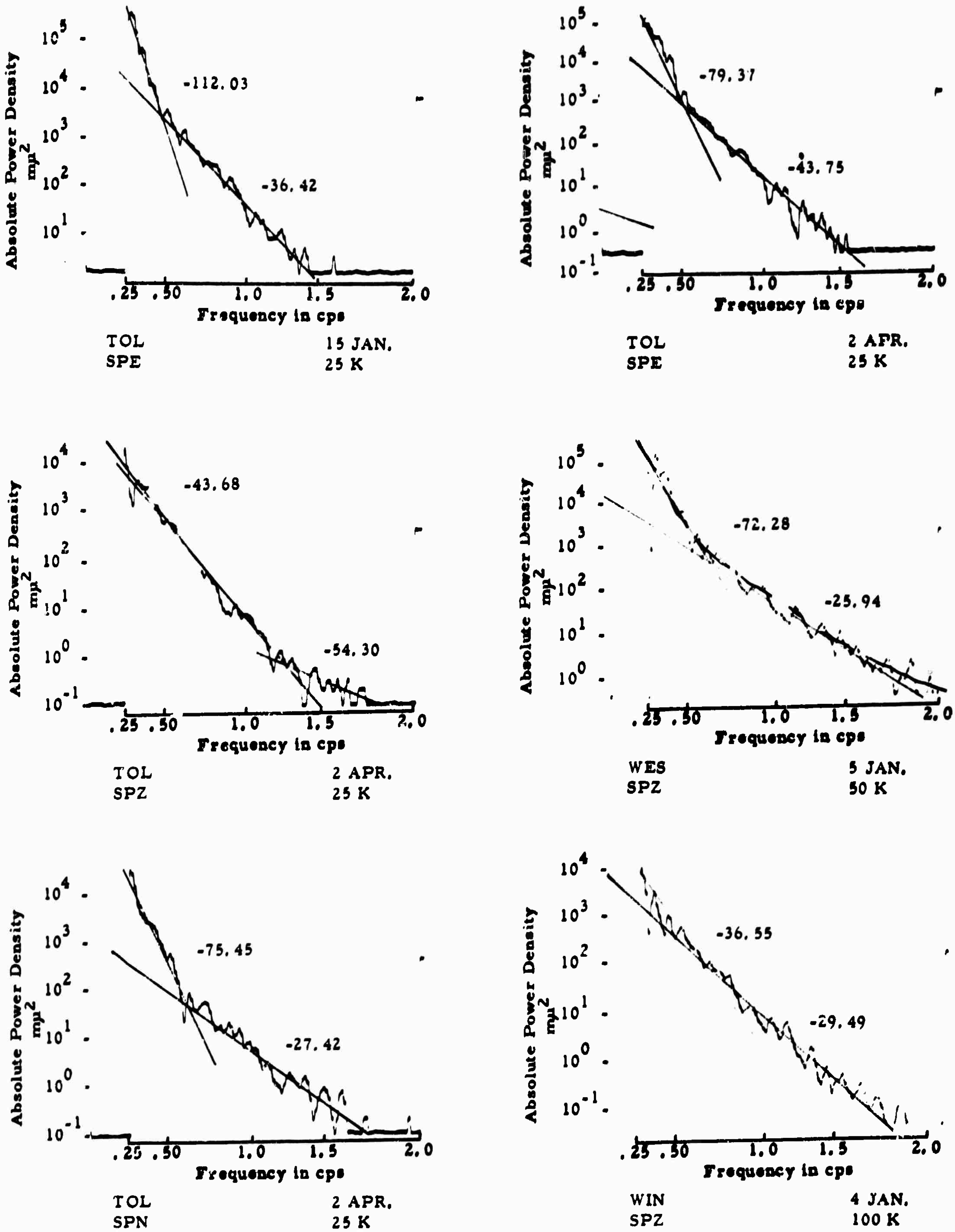

Figure A-1e. Absolute Power Density Spectra Obtained From 1963 Data

E

TABLE A-2f

ABSOLUTE POWER DENSITY SPECTRA LOCATED IN FIGURE A-1f

STATION	DATE	COMPONENT	GAIN(K)
VAL	15 January	SPZ	12.5
VAL	15 January	SPN	12.5
VAL	15 January	SPE	12.5
VAL	18 January	SPZ	12.5
VAL	7 February	SPZ	12.5
VAL	7 February	SPN	12.5
VAL	7 February	SPE	12.5
VAL	1 March	SPZ	12.5
VAL	1 March	SPN	12.5
VAL	1 March	SPE	12.5
VAL	2 April	SPZ	12.5
VAL	3 April	SPZ	12.5
VAL	3 April	SPN	12.5
VAL	3 April	SPE	12.5
VAL	19 May	SPZ	12.5
VAL	19 May	SPN	12.5
VAL	19 May	SPE	12.5
VAL	6 June	SPZ	12.5
VAL	6 June	SPN	12.5
VAL	6 June	SPE	12.5

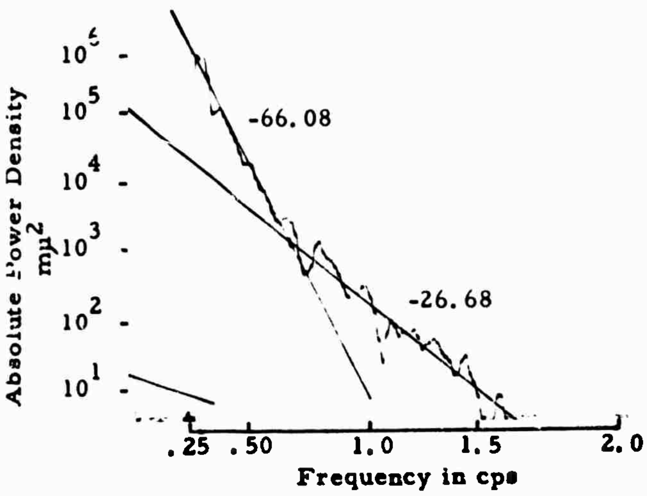

VAL 15 JAN.
SPZ 12.5 K

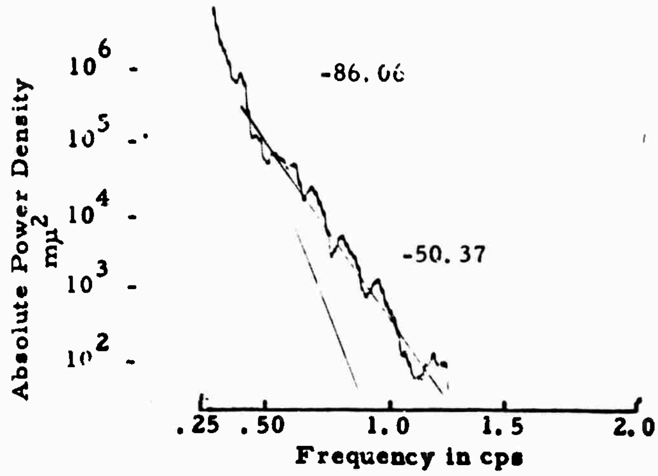

VAL 18 JAN.
SPZ 12.5 K

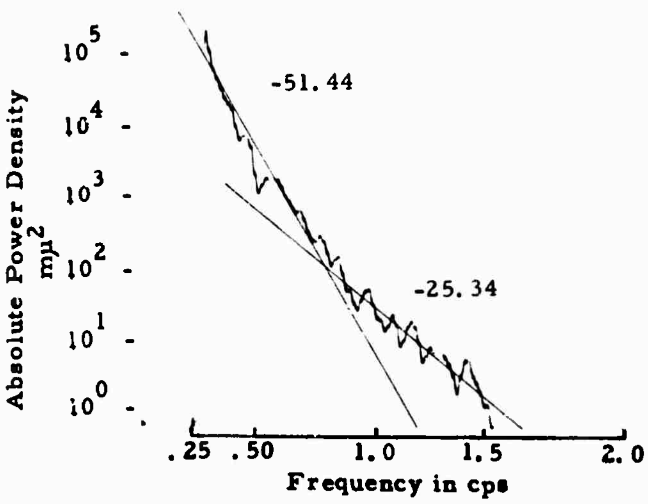

VAL 15 JAN.
SPN 12.5 K

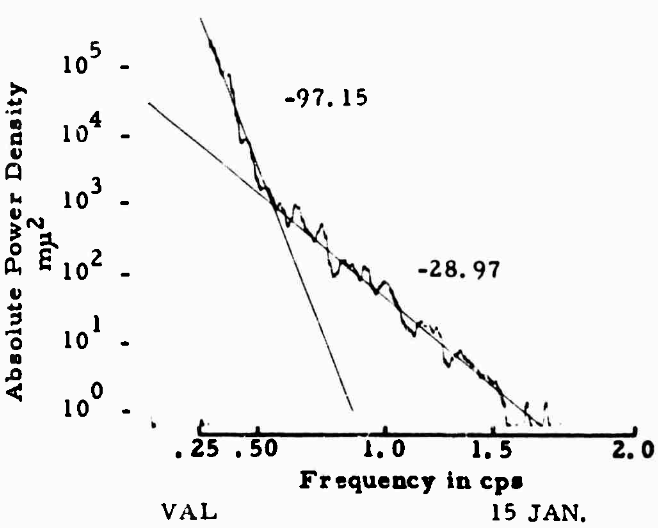

VAL 15 JAN.
SPE 12.5 K

A

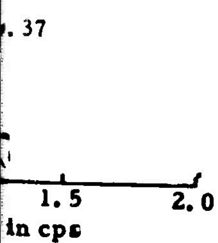

18 JAN.
12.5 K

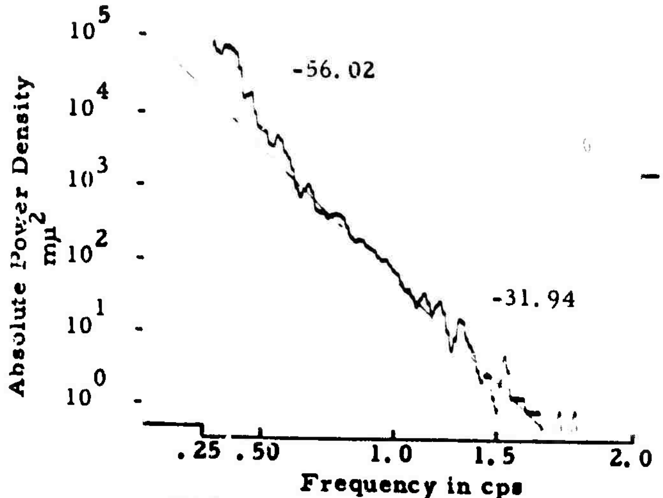

VAL
SPZ

7 FEB.
12.5 K

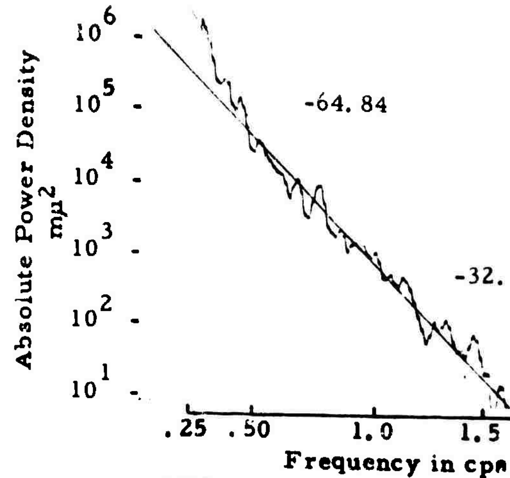

VAL
SPZ

1
12

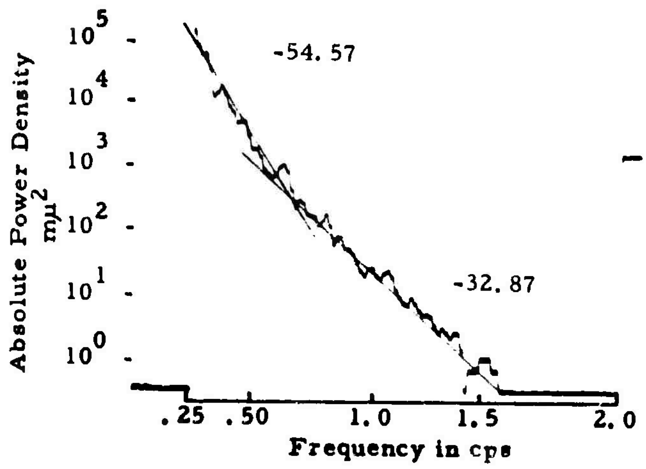

VAL
SPN

7 FEB.
2.5 K

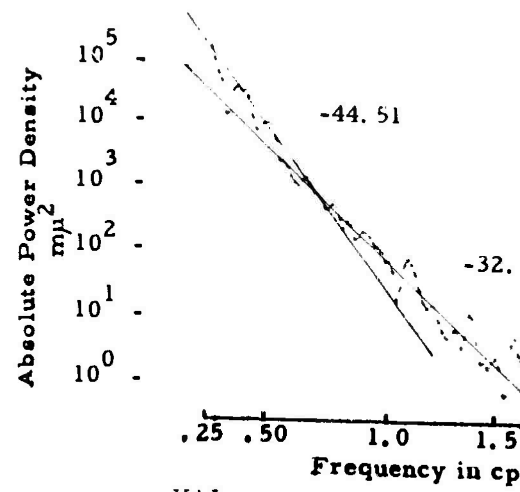

VAL
SPN

1
12

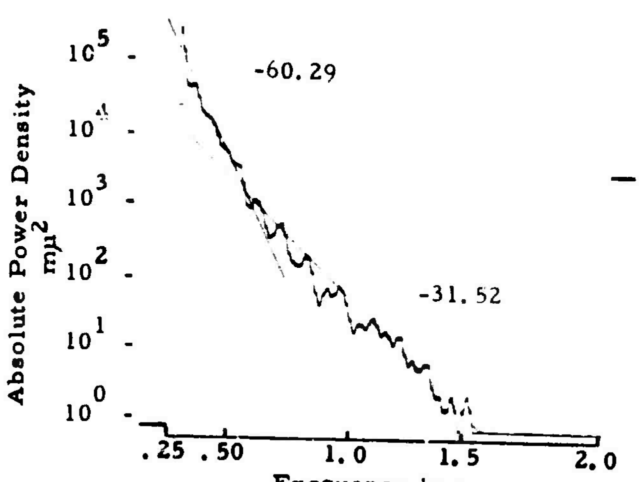

VAL
SPE

7 FEB.
12.5 K

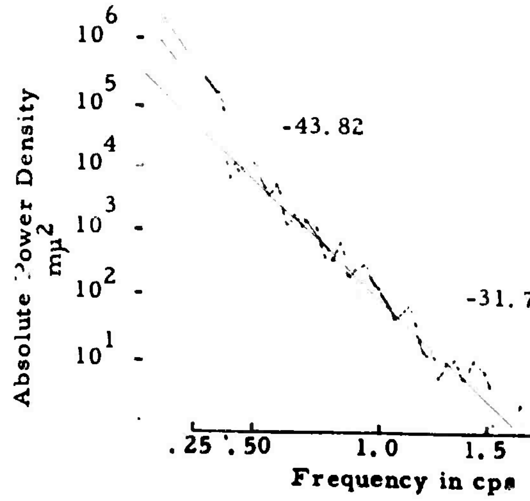

VAL
SPE

1
12

B

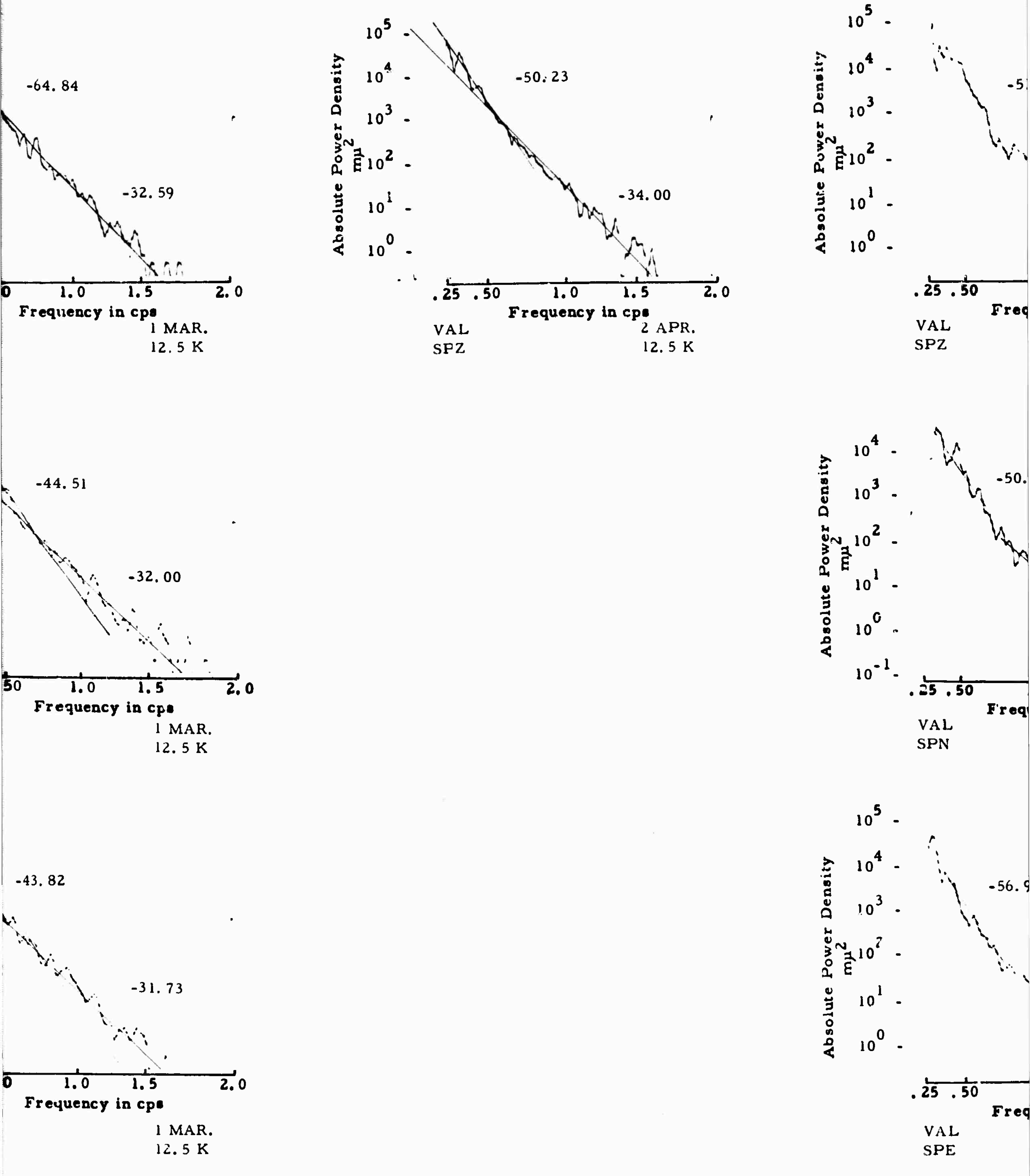

-64.84
-32.59
1.0 1.5 2.0
Frequency in cps
1 MAR.
12.5 K
Absolute Power Density
$m\mu^2$
10^5 10^4 10^3 10^2 10^1 10^0
-50.23
-34.00
.25 .50 1.0 1.5 2.0
Frequency in cps
VAL
SPZ
2 APR.
12.5 K
Absolute Power Density
$m\mu^2$
10^5 10^4 10^3 10^2 10^1 10^0
.25 .50
VAL
SPZ
-44.51
-32.00
1.0 1.5 2.0
Frequency in cps
1 MAR.
12.5 K
Absolute Power Density
$m\mu^2$
10^4 10^3 10^2 10^1 10^0 10^{-1}
.25 .50
VAL
SPN
-43.82
-31.73
1.0 1.5 2.0
Frequency in cps
1 MAR.
12.5 K
Absolute Power Density
$m\mu^2$
10^5 10^4 10^3 10^2 10^1 10^0
.25 .50
VAL
SPE

C

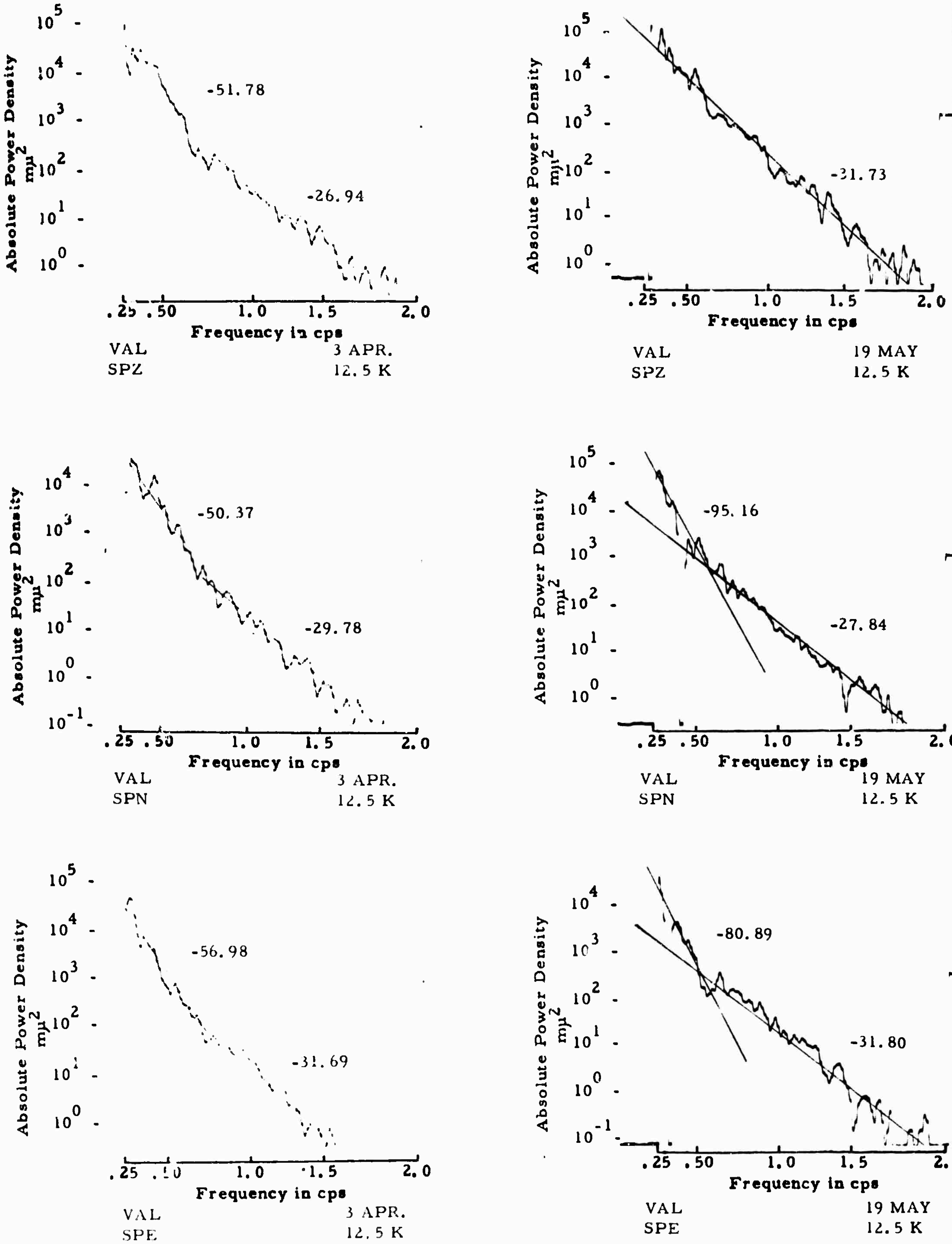

Figure A-1f. Absolute Pow

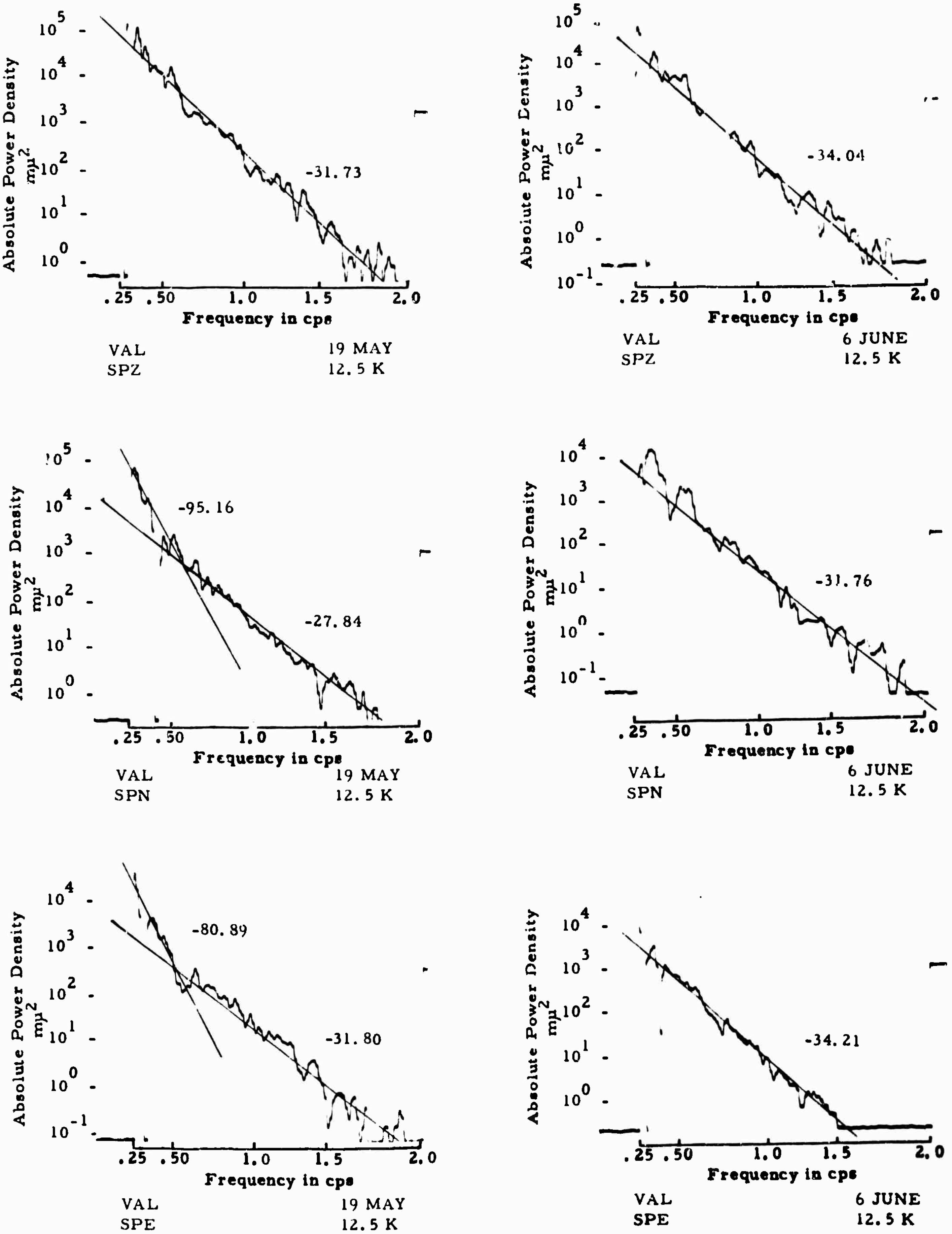

Figure A-1f. Absolute Power Density Spectra Obtained From 1963 Data

E

APPENDIX B

NOISE MAPS

APPENDIX B

NOISE MAPS

This appendix contains the noise maps for nine months in 1963. The short period maps (0.5 - 2.0 sec) precede the long period maps (3.0 - 8.0 sec) for each month so that comparison may be more easily made. These maps comprise Figures B-1 through B-18.

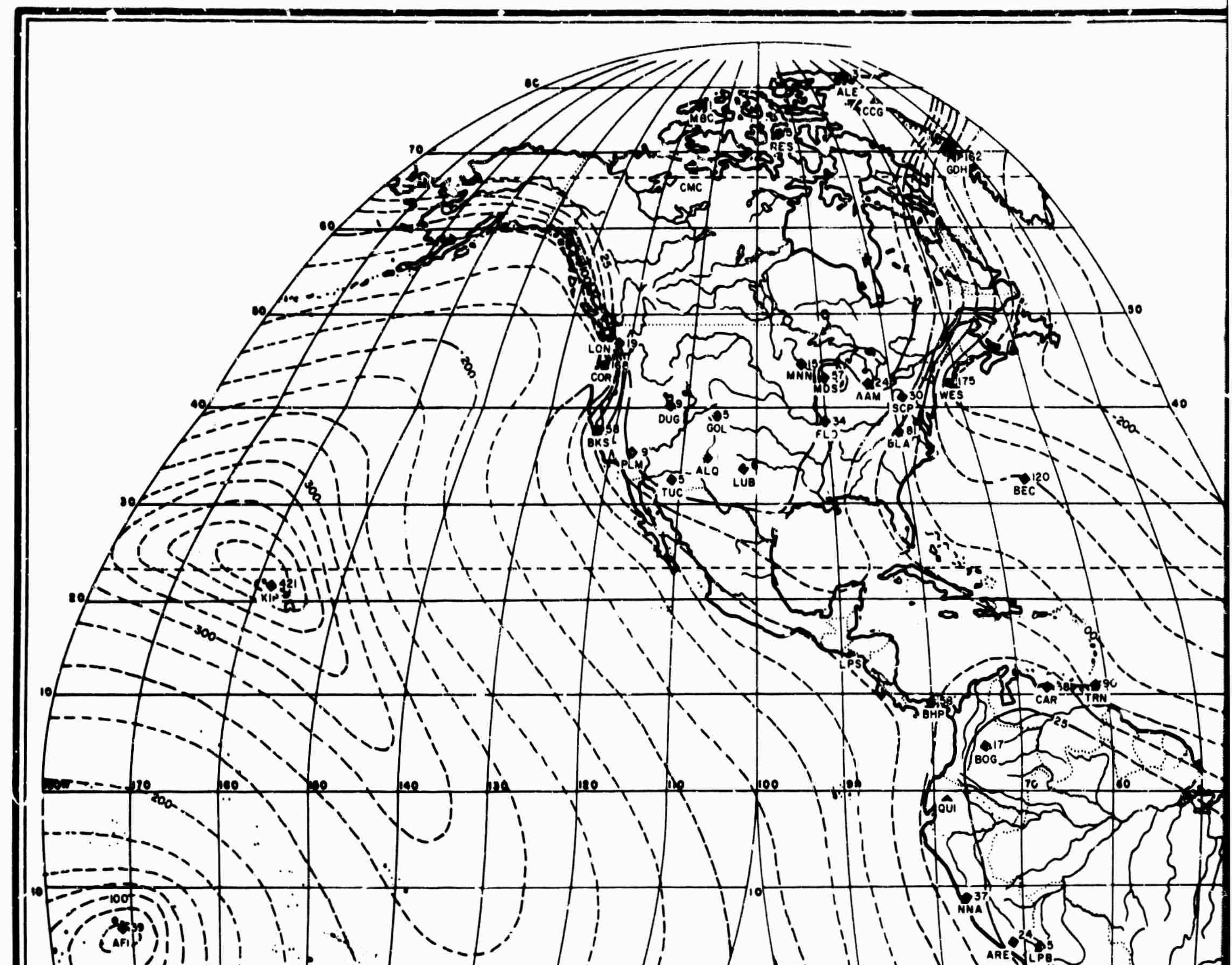
ALE
CCG
MBC
RES
GDH
CMC
LON
COR
DUG
GOL
MNN
MDS
AAM
SCP
WES
BLA
BKS
PLM
ALQ
LUB
TUC
BEC
KIP
LPS
CAR
TRN
BHP
BOG
QUI
NNA
ARE
LPB
ANT
AFI

A

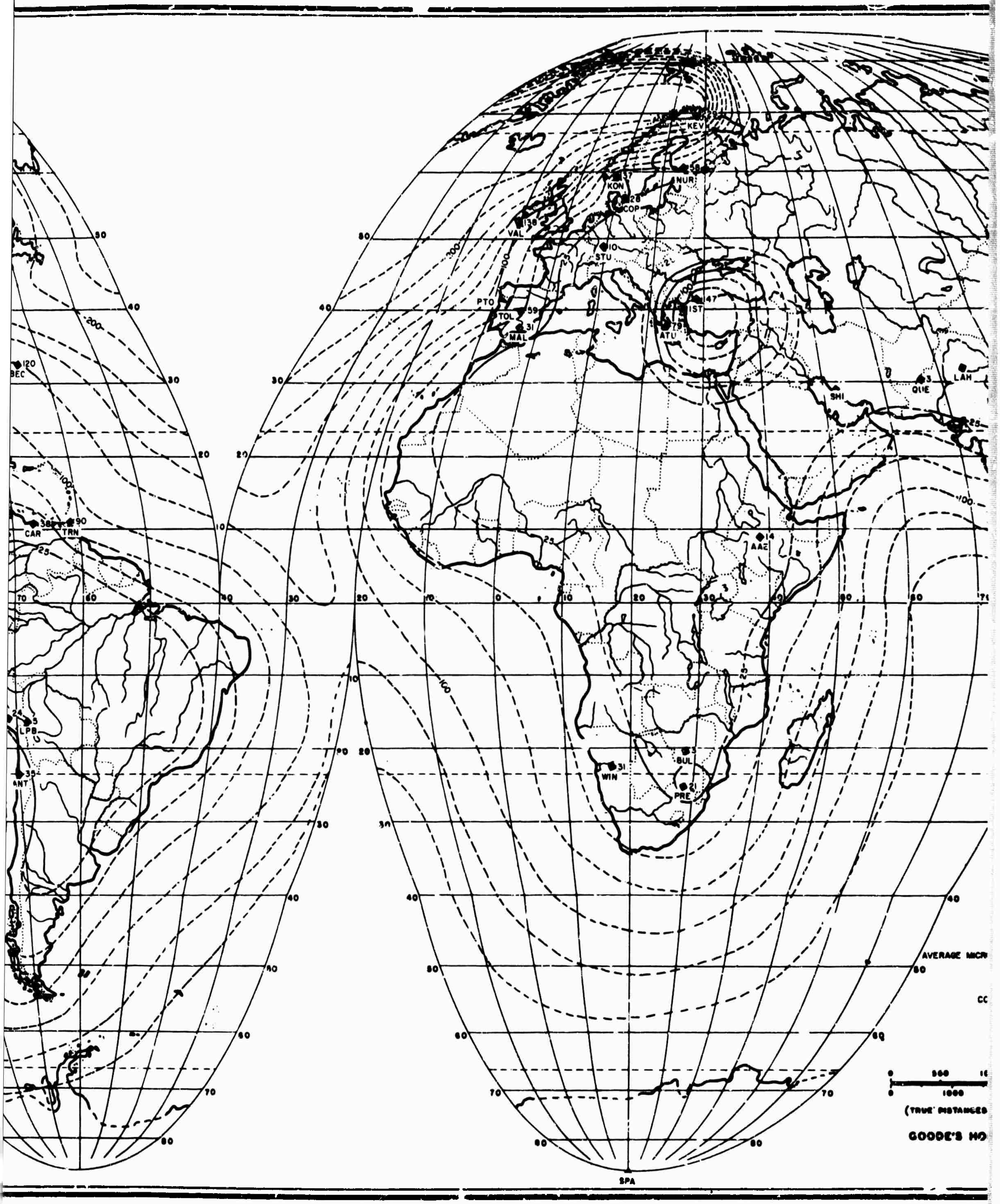
KEV
NUR
KON
COP
VAL
STU
PTO
TOL
MAL
IST
ATU
SHI
QUE
LAH
AAE
BUL
WIN
PRE
SPA
BEC
CAR
TRN
LPB
ANT
AVERAGE MICR
GOODE'S HO

Figu

B

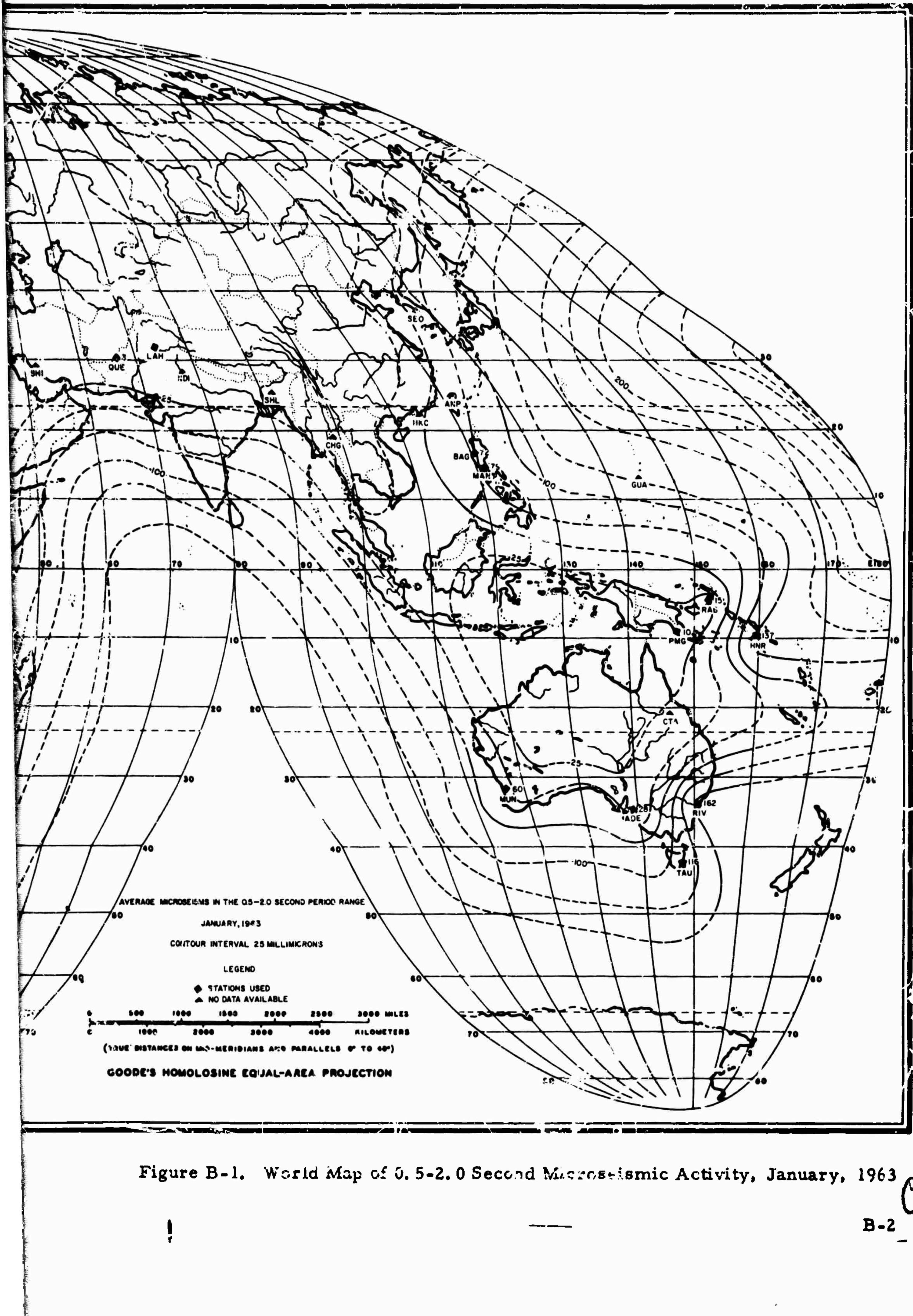

Figure B-1. World Map of 0.5-2.0 Second Macroseismic Activity, January, 1963

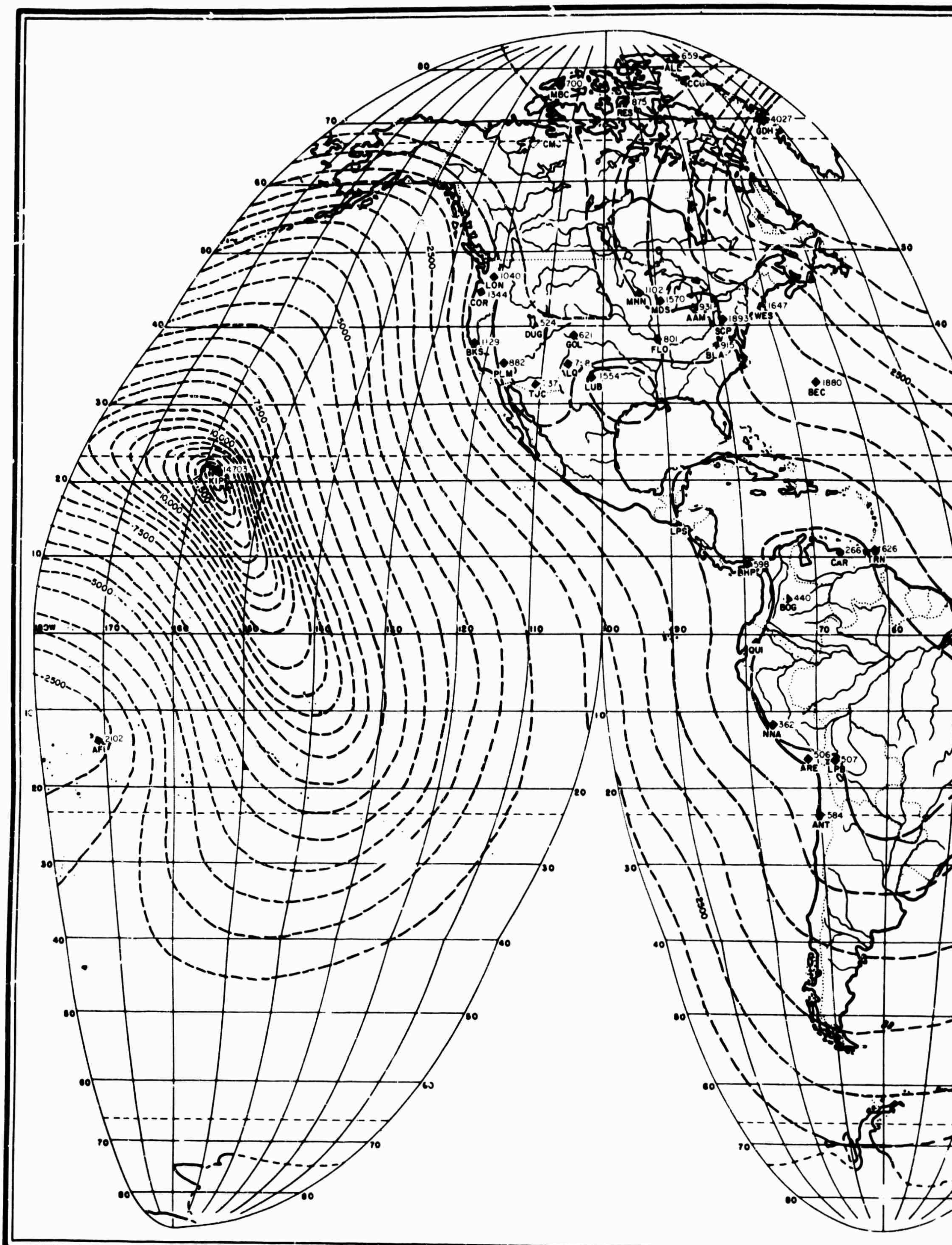
ALE 659
CCU
MBC 700
RES 875
GDH 4027
CMJ
LON 1040
COR 1344
MNN 1102
MDS 1570
AAM 931
SCP 1893
WES 1647
DUG 524
GOL 621
BKS 1129
FLO 801
SLA 915
PLM 882
LUB 1554
TJC
BEC 1880
KIP 14703
LPS
CAR 266
TRN 626
BHP 598
BOG 440
QUI
NNA 362
ARE 506
LPB 507
ANT 584
AFI 2102
2500
5000
7500
10,000

A

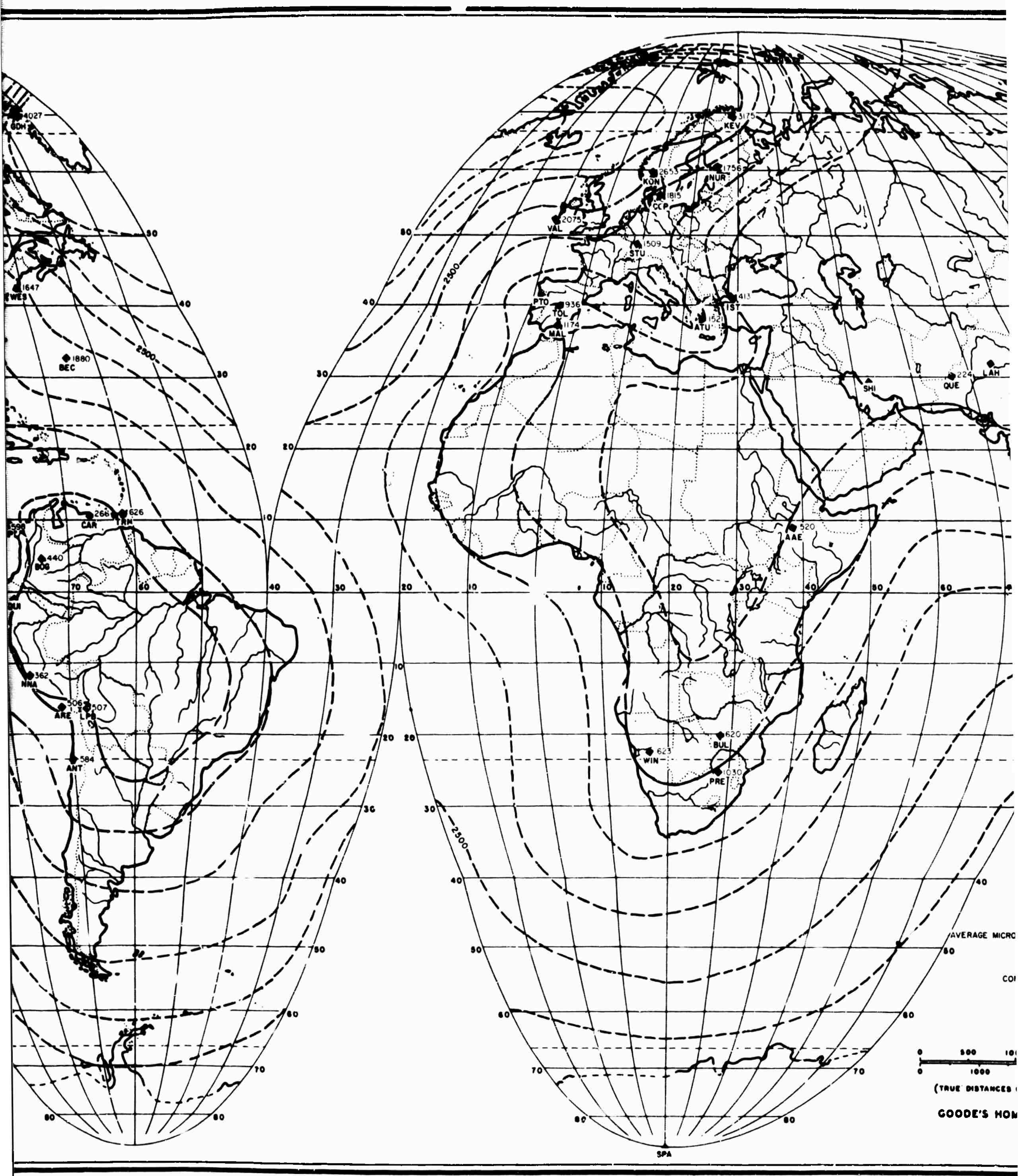
4027 GDH
1647 WES
1880 BEC
2500
266 CAR
626 TRN
440 BOG
362 NNA
506 ARE
507 LPB
584 ANT
3175 KEV
2653 KON
1756 NUR
1815 CCP
2075 VAL
1509 STU
PTO
936 TOL
1174 MAL
1413 IST
1521 ATU
SHI
224 QUE
LAH
520 AAE
620 BUL
623 WIN
1030 PRE
SPA
500
1000

b

Figure

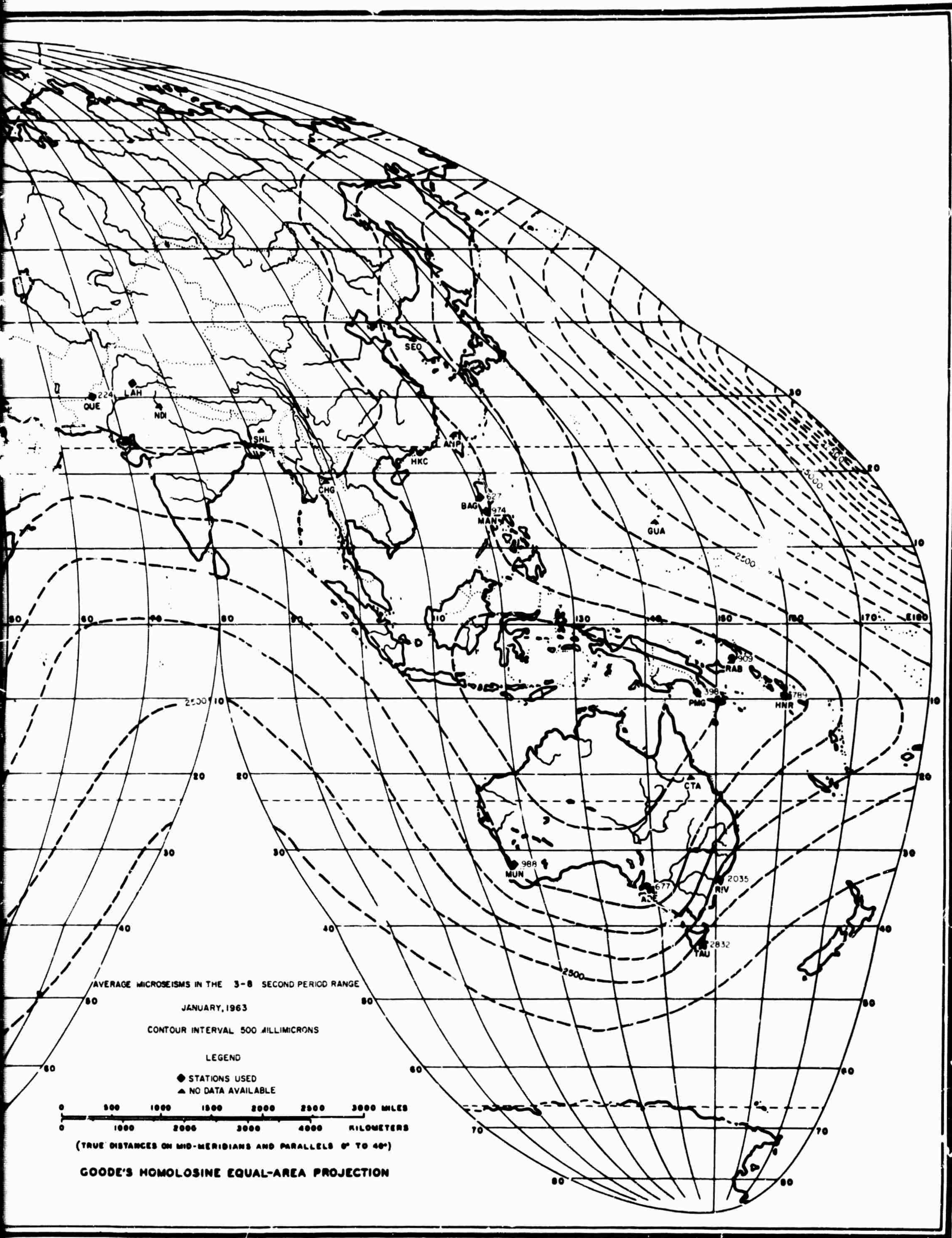

Figure B-2. World Map of 3.0-8.0 Second Microseismic Activity, January, 1963

C

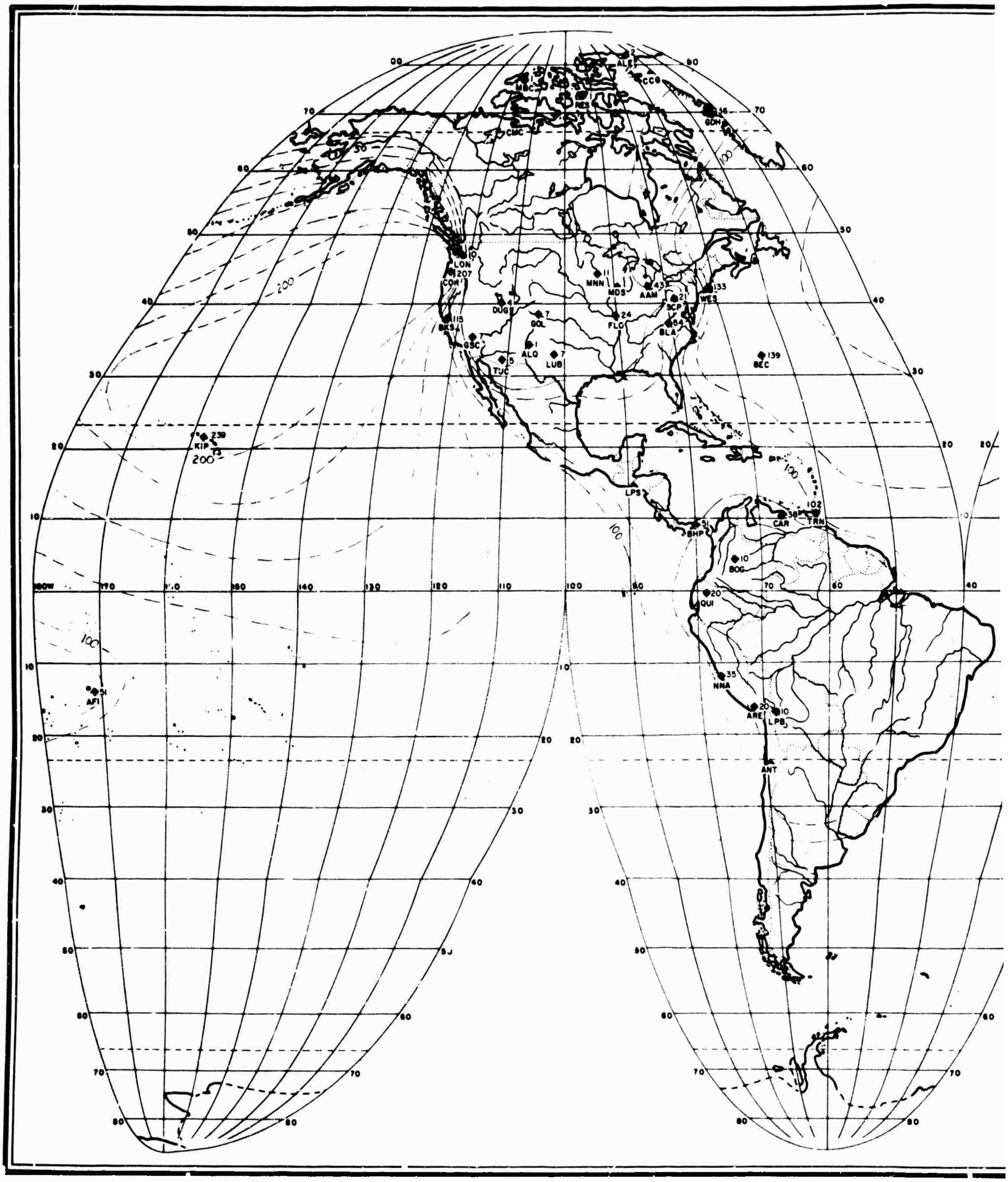

ALE 2
CCG
MBC
RES
CMC
GDH 36
LON 10
COR 207
MNN 11
MDS
AAM 43
SCP 21
WES 133
DUG
GOL 7
FLO 24
BLA 84
BKS 115
GSC
ALQ 1
LUB 7
TUC 5
BEC 139
KIP 239
T3
LPS
BHP 51
CAR 38
TRN 102
BOG 10
QUI 20
NNA 35
ARE 20
LPB 10
ANT
AFI 51
200
100

A

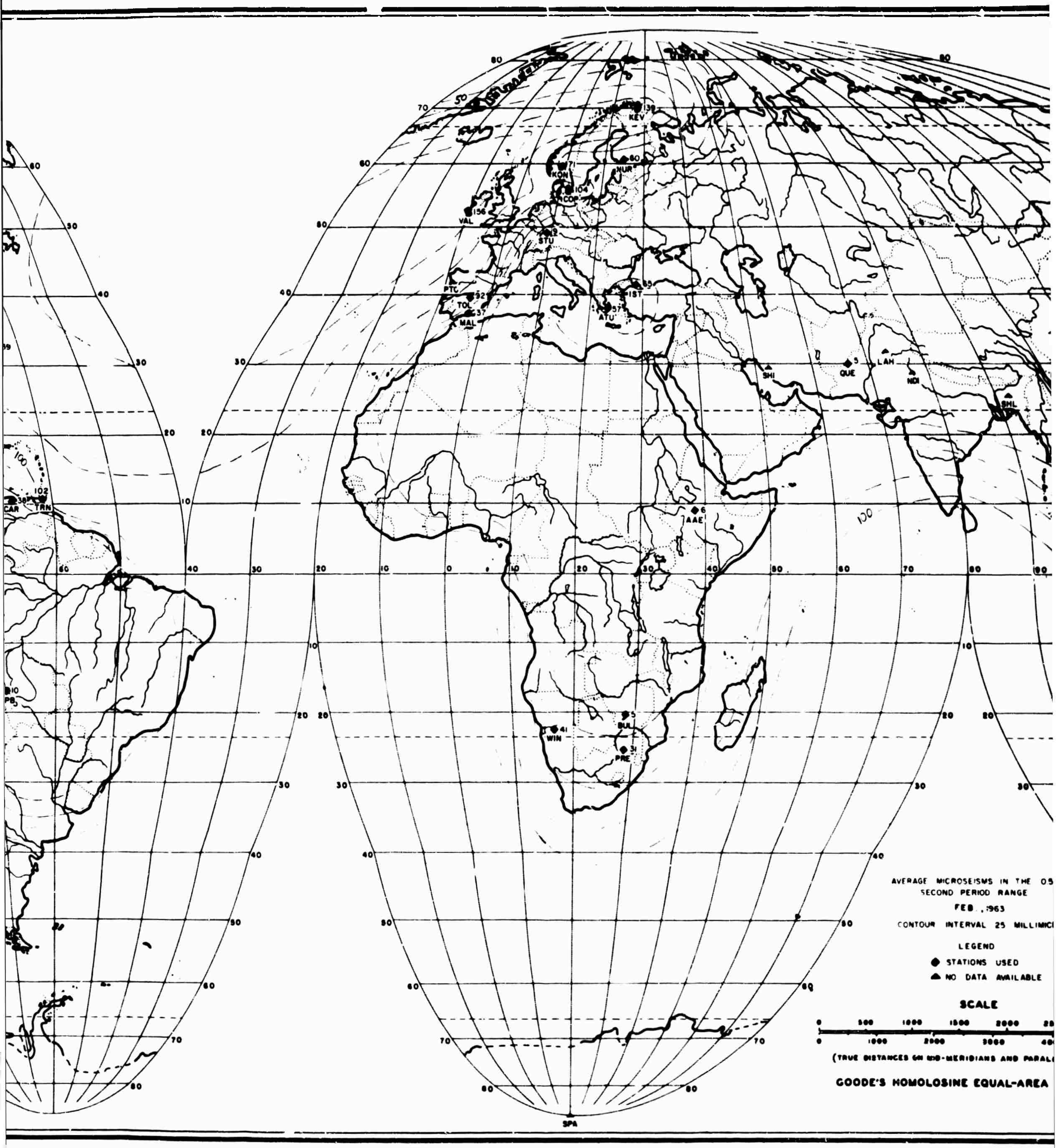

Figure B-3. World Map

B

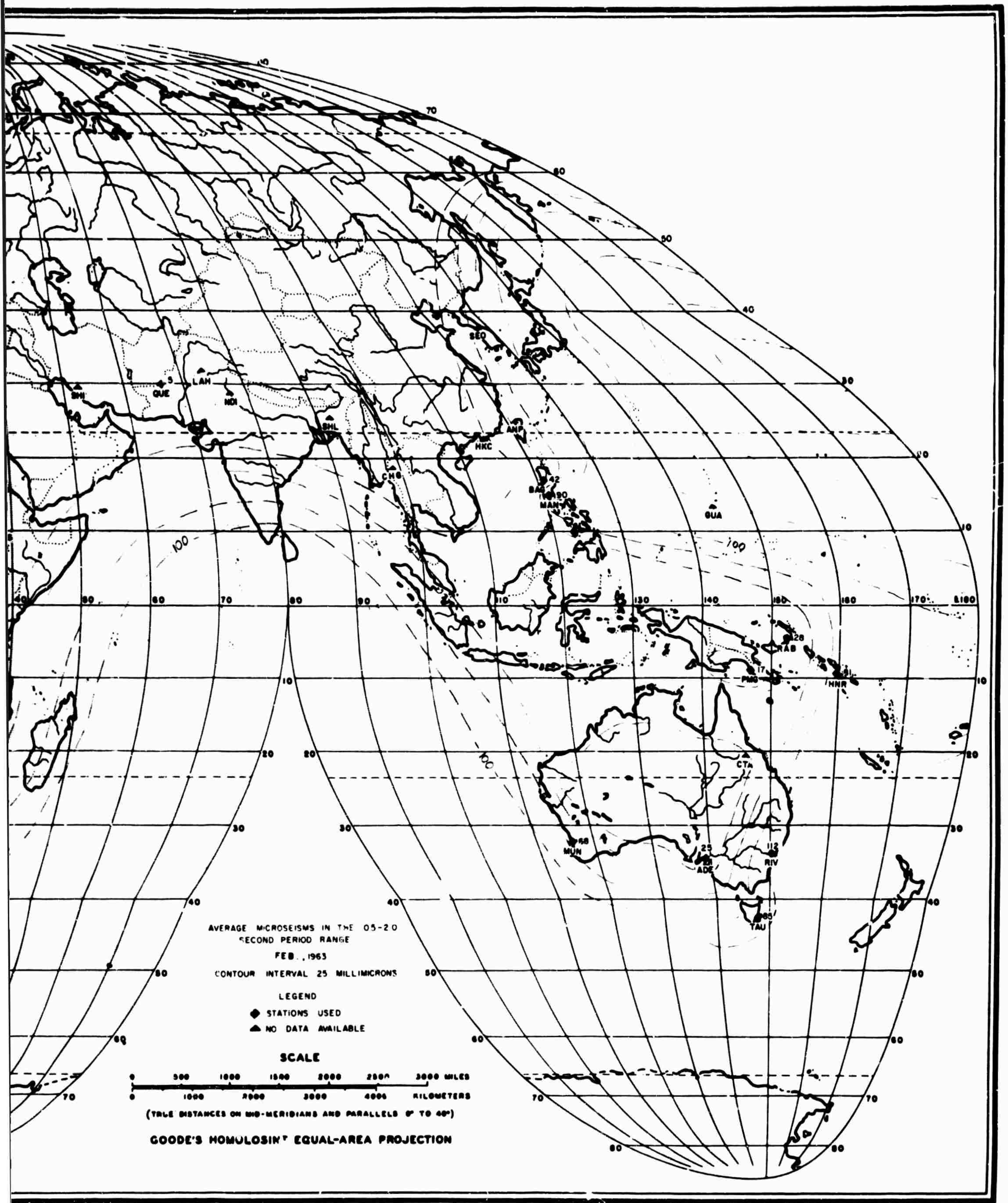

Figure B-3. World Map of 0.5-2.0 Second Microseismic Activity, February, 1963

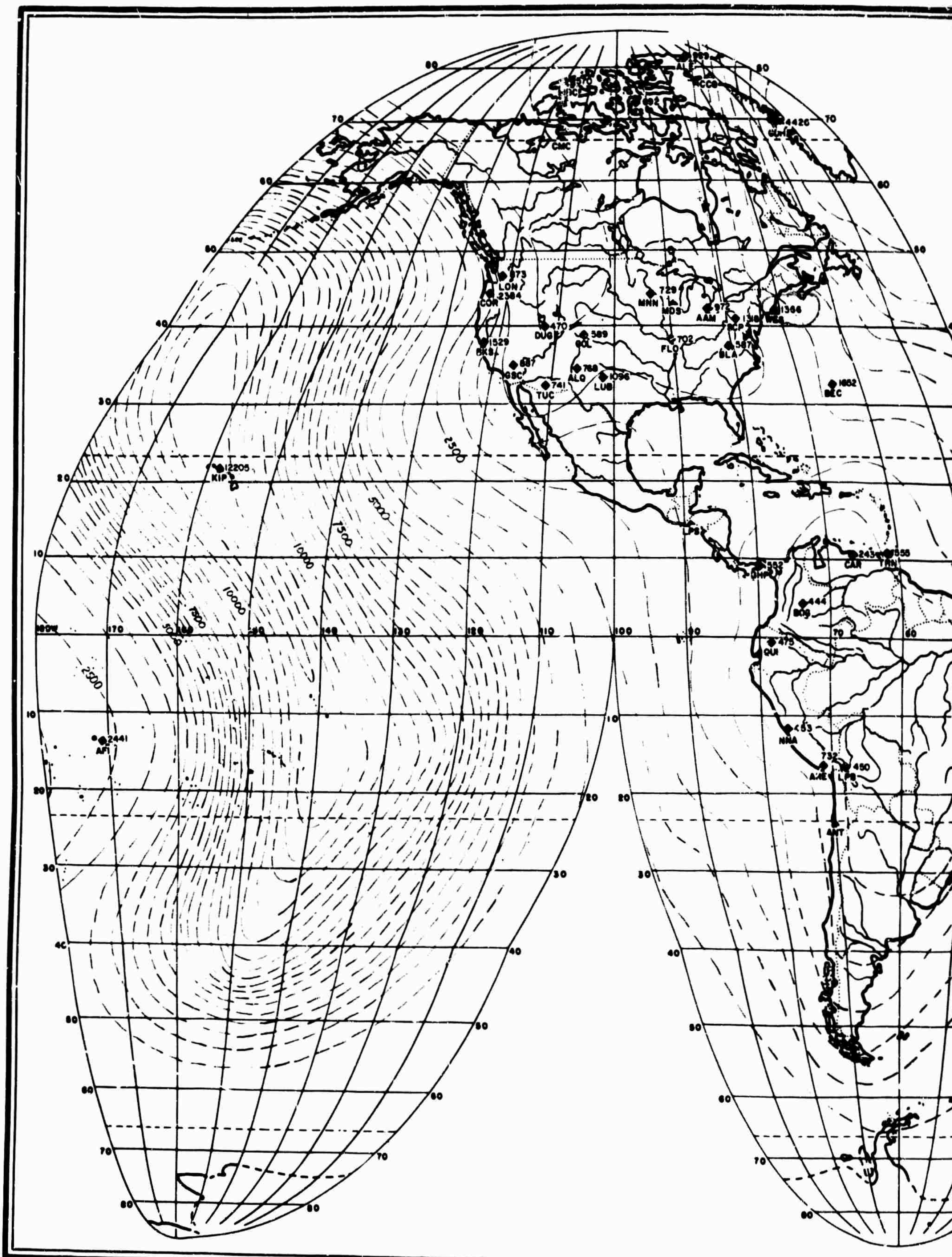

180W
2384
COR
LON
729
MNN
MDS
AAM
702
FLO
587
BLA
1366
470
589
1529
BKS
GSC
788
ALQ
1096
LUB
741
TUC
1662
BEC
12205
KIP
2441
AFI
2500
5000
7500
10000
CAR
TRN
444
BOG
475
QUI
NNA
732
450
ANT
4426
CMC

A

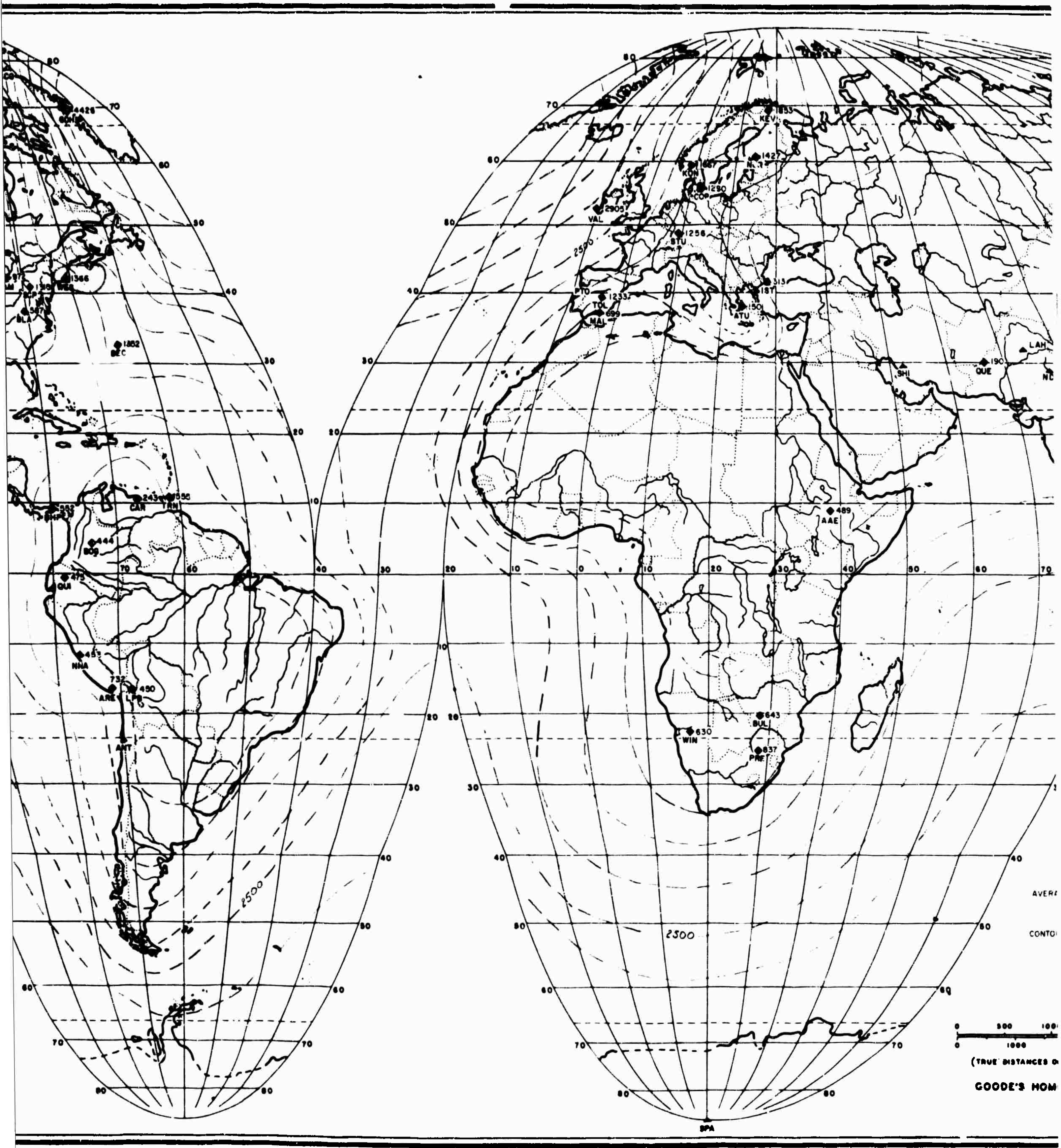

4426
1366
1852
BEC
243
CAN
556
TAN
444
BOG
473
QUI
453
NNA
732
ARE
450
LPB
ANT
2500
1853
KEV
1427
KON
1290
COP
2905
VAL
1256
STU
PTO
1233
TOL
699
MAL
313
IST
150
ATU
SHI
LAH
190
QUE
489
AAE
643
BUL
630
WIN
837
PRE
SPA
(TRUE DISTANCES

Figure B-4.

b

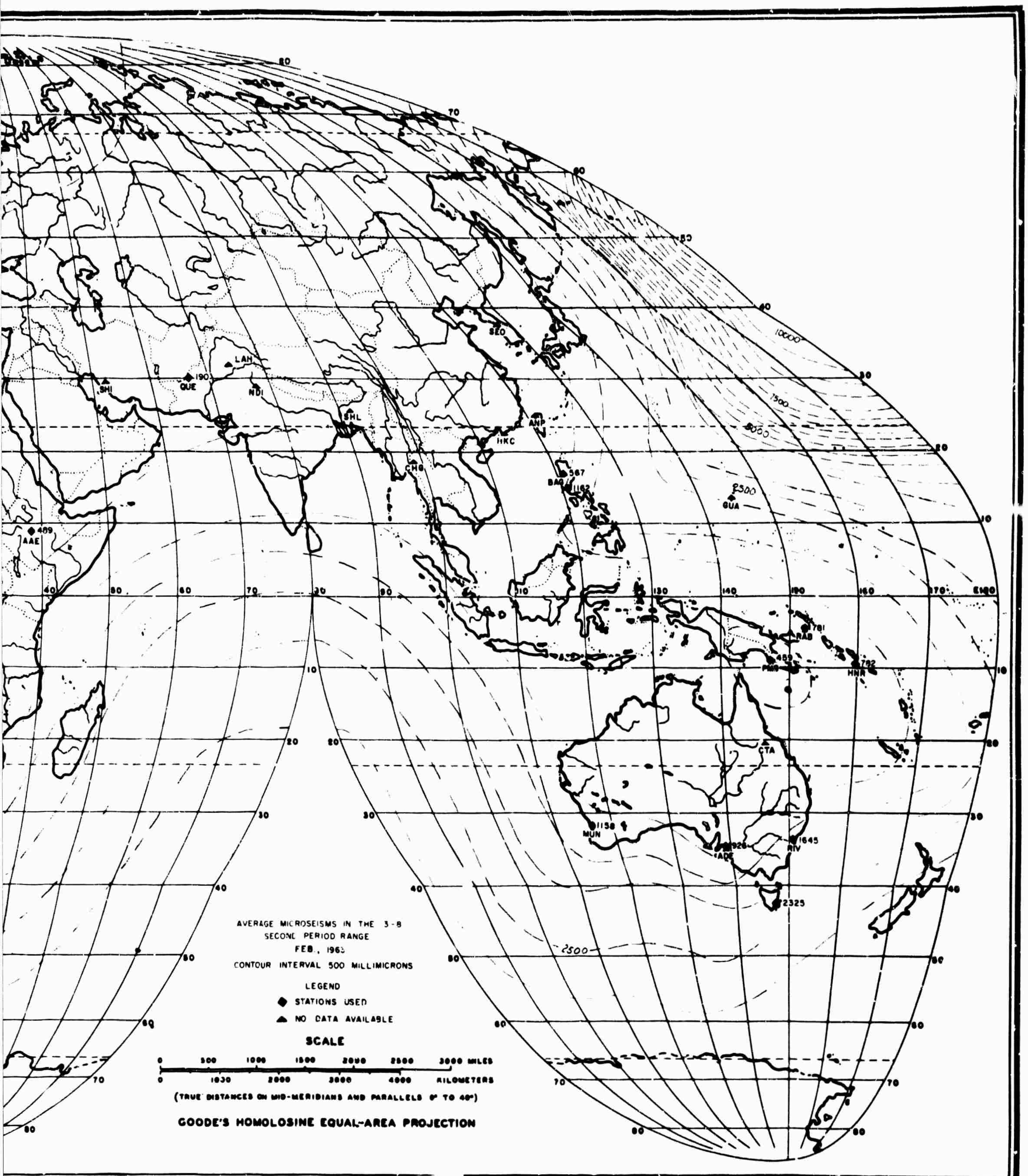

Figure B-4. World Map of 3.0-8.0 Second Microseismic Activity, February, 1963

C

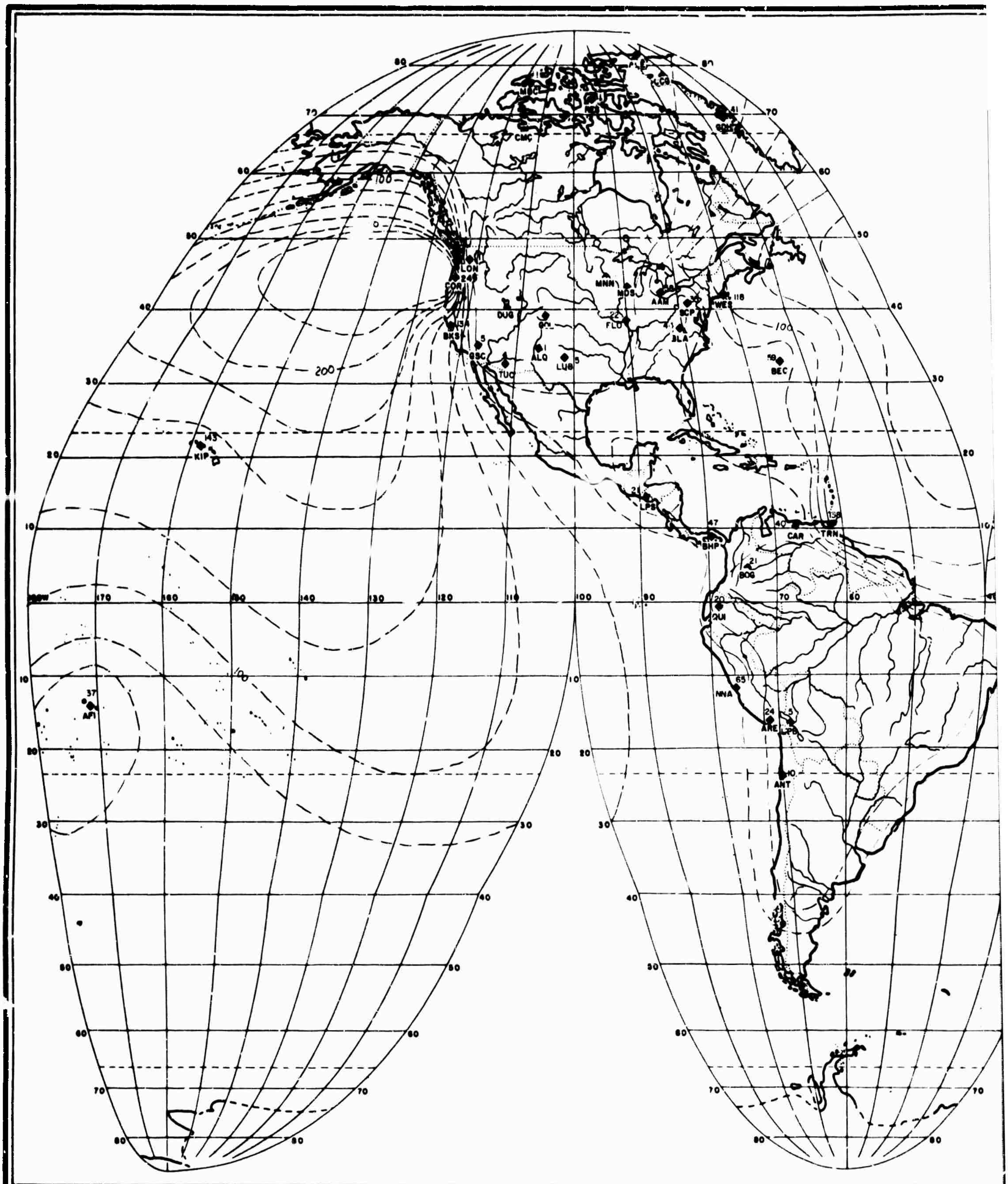

CMC
LON
COR
BKS
GSC
TUC
DUG
ALQ
LUB
MNN
MOS
FLO
AAM
SCP
WES
BLA
BEC
KIP
AFI
LPS
BHP
CAR
TRN
BOG
QUI
NNA
ARE
LPB
ANT

A

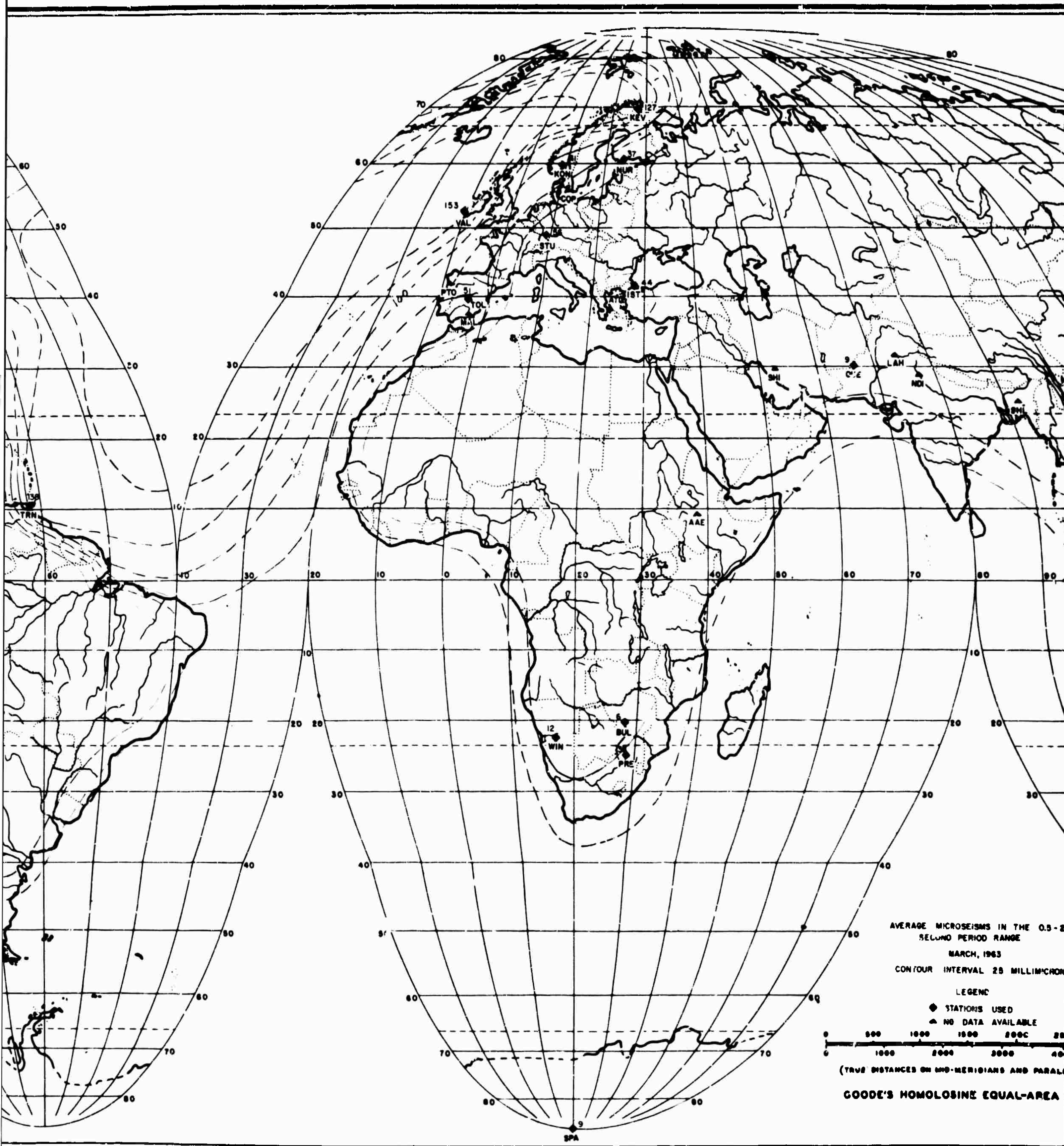

Figure B-5. World Ma

B

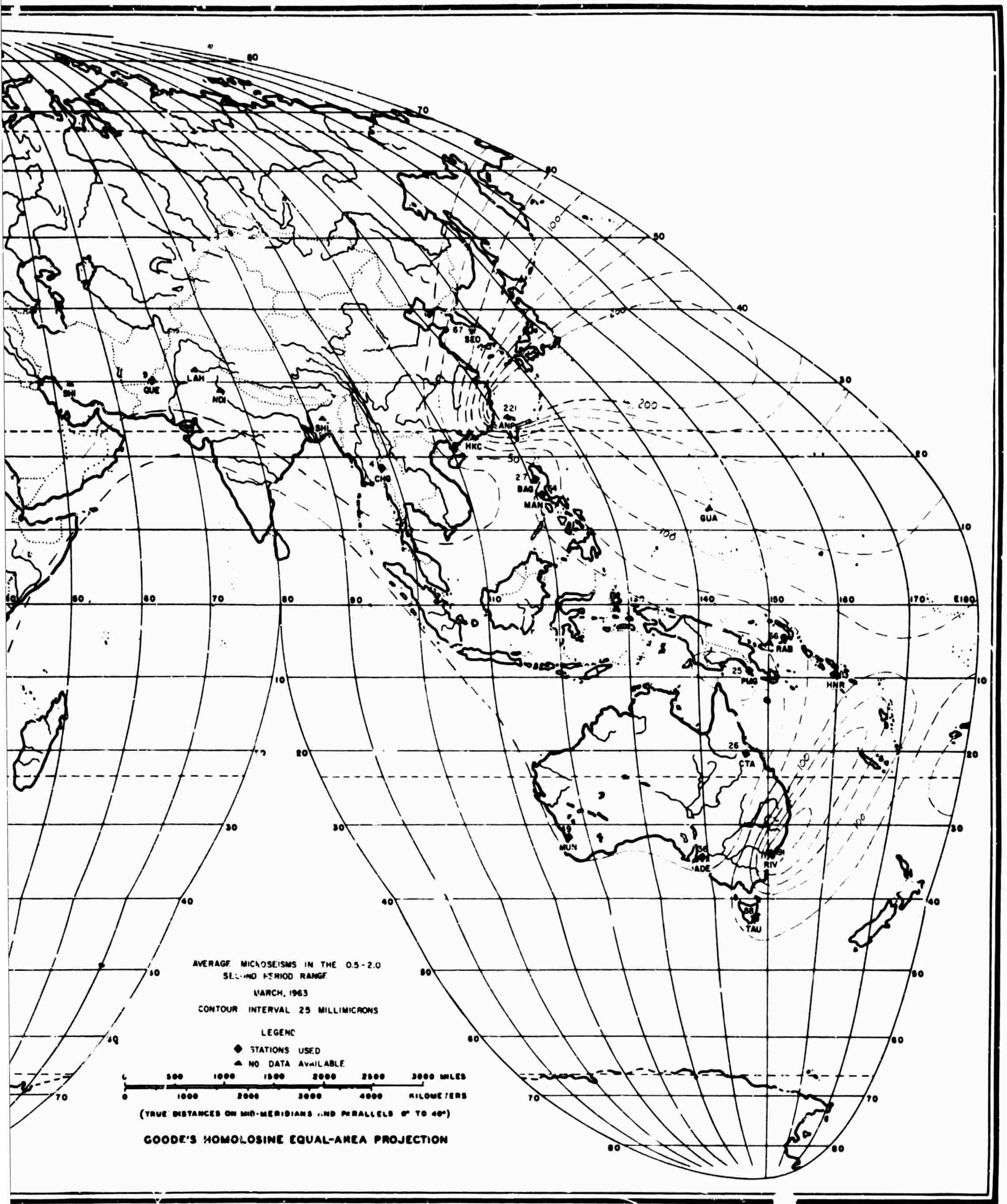

Figure B-5. World Map of 0.5-2.0 Second Microseismic Activity, March, 1963

C

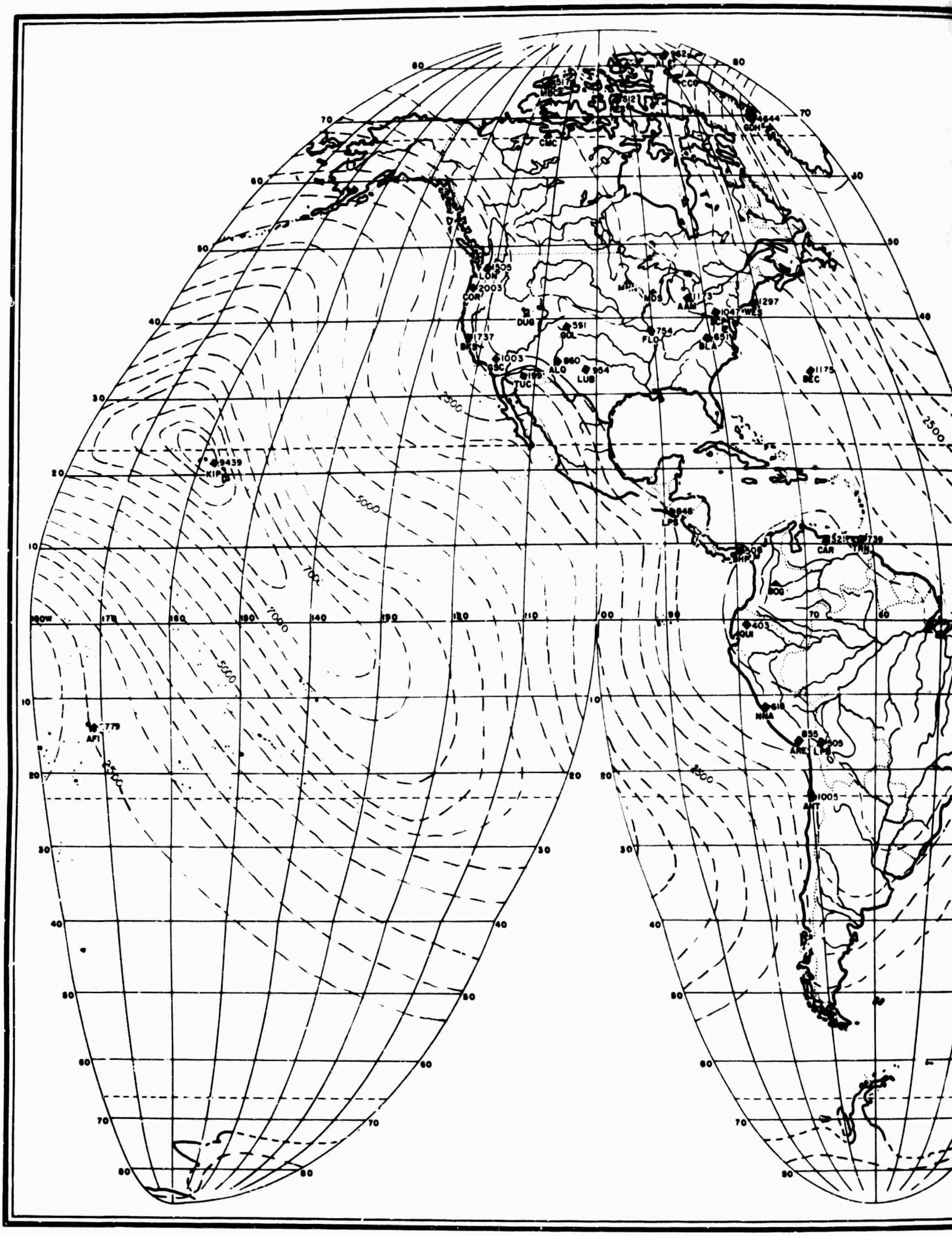
LON
COR
2003
DUG
591
GOL
1737
1003
SSC
860
ALQ
954
LUB
TUC
754
FLO
MDS
AAM
1297
WES
BLA
1175
BEC
4644
GDH
CMC
9439
KIP
779
AFI
848
LPS
CAR
BOG
403
QUI
NHA
855
ARE
1005
ANT
2500
5000
7000

A

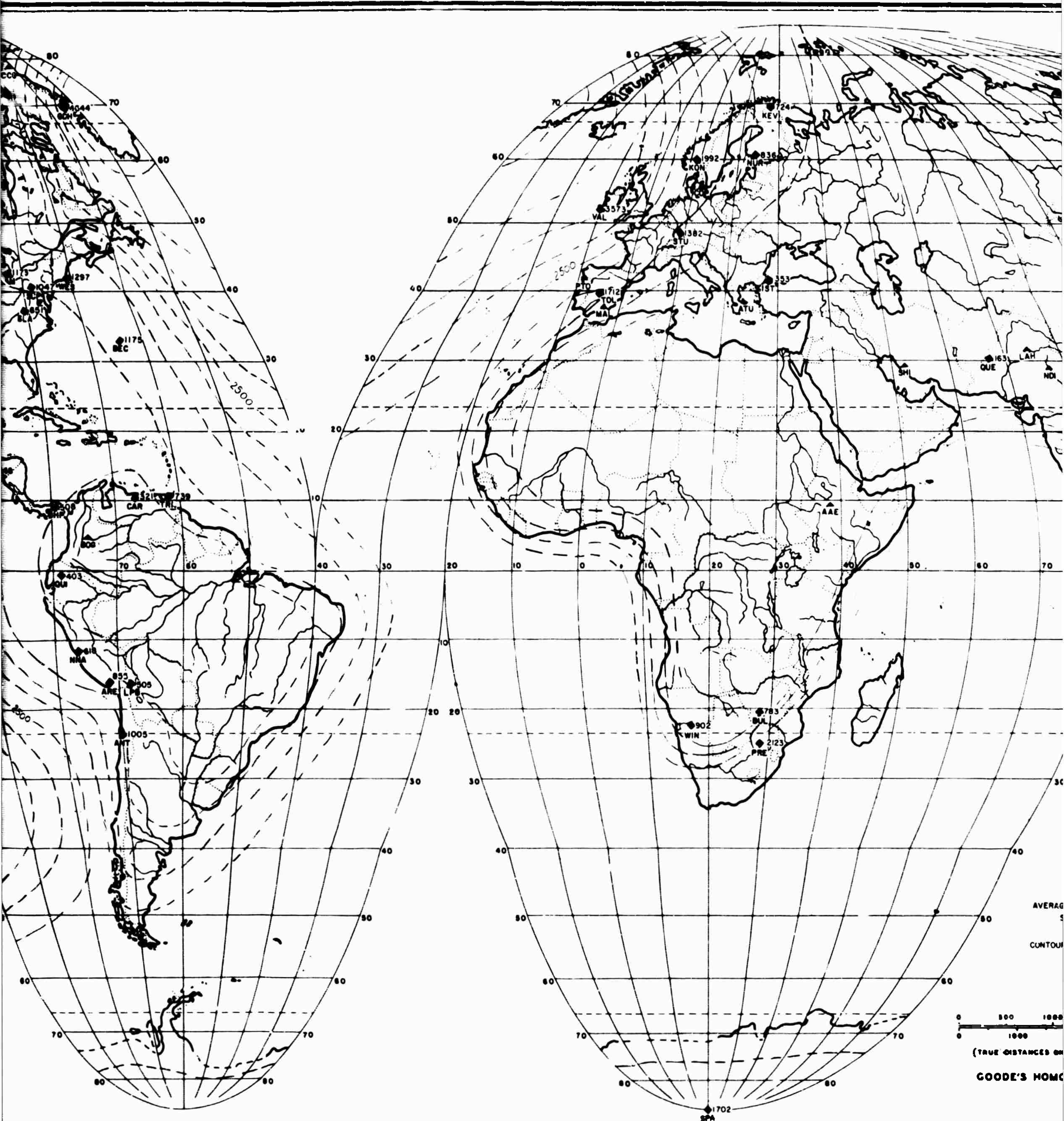
1044
SCH
1297
WES
1047
BLA
1175
BEC
CAR
1739
TRI
BOG
403
QUI
NNA
ARE
LPB
1005
ANT
1724
KEV
1992
KON
836
NUR
3573
VAL
1382
STU
PTO
1712
TOL
MA
IST
ATU
QUE
LAH
NDI
SHI
AAE
783
BUL
902
WIN
2123
PRE
1702
SPA
2500
AVERAG
CONTOU
(TRUE DISTANCES ON
GOODE'S HOMO

Figure B-

B

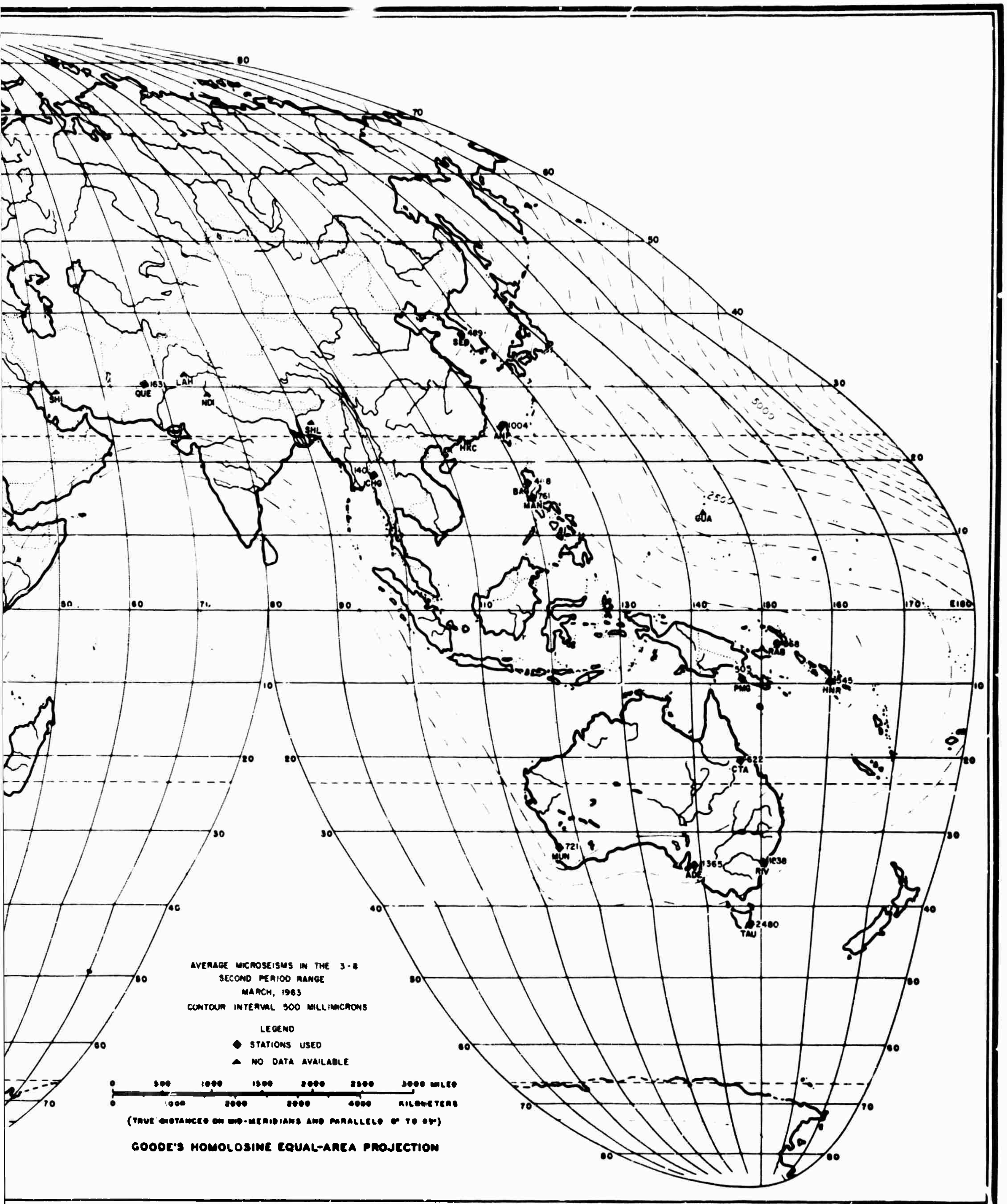

Figure B-6. World Map of 3.0-8.0 Second Microseismic Activity, March, 1963

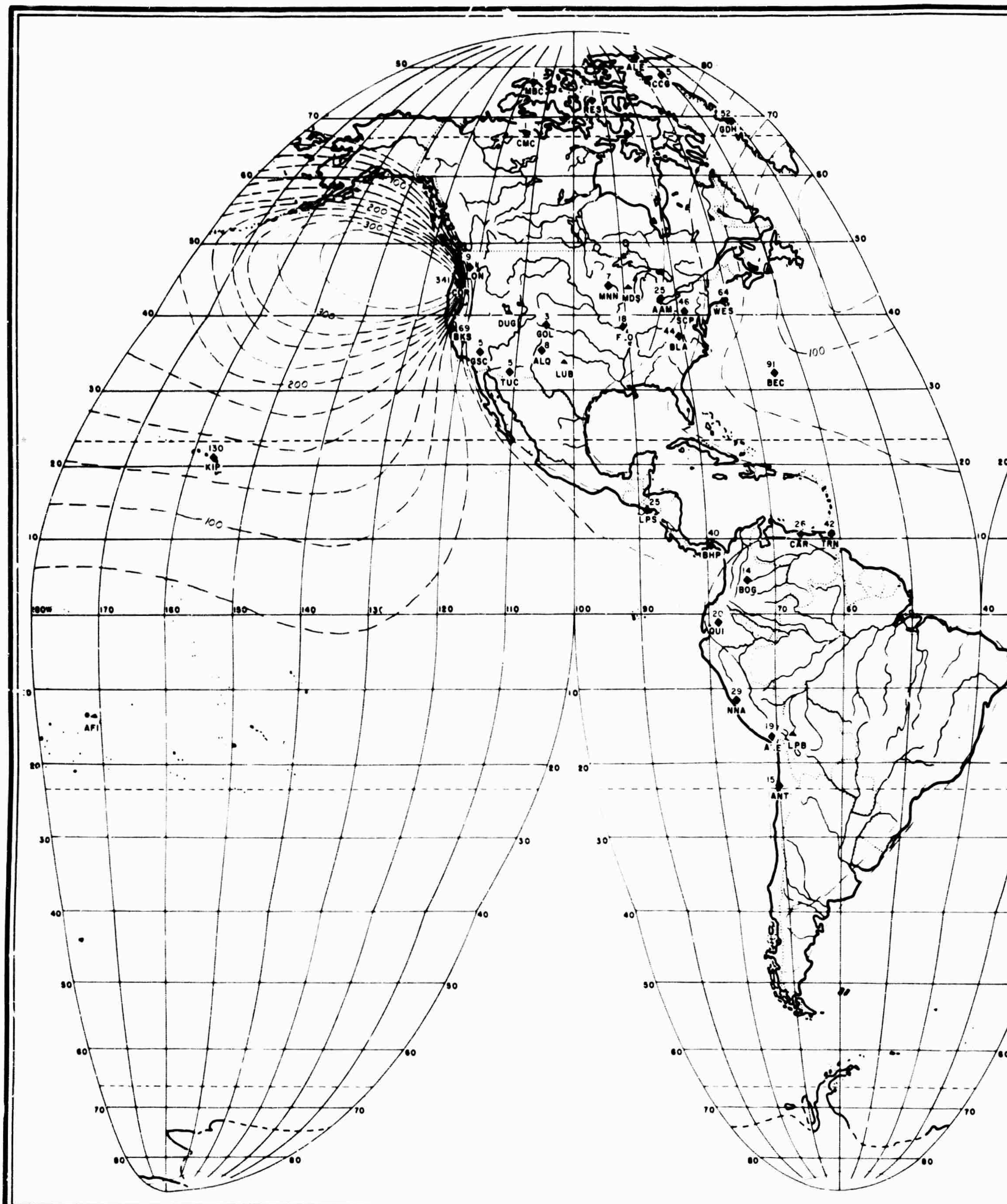

ALE
CCG
MBC
CMC
GDH
ON
COR
MNN
MDS
AAM
SCP
WES
DUG
GOL
ALQ
LUB
BKS
GSC
TUC
BEC
KIP
LPS
BHP
CAR
TRN
BOG
QUI
NNA
LPB
ANT
AFI
100
200
300

A

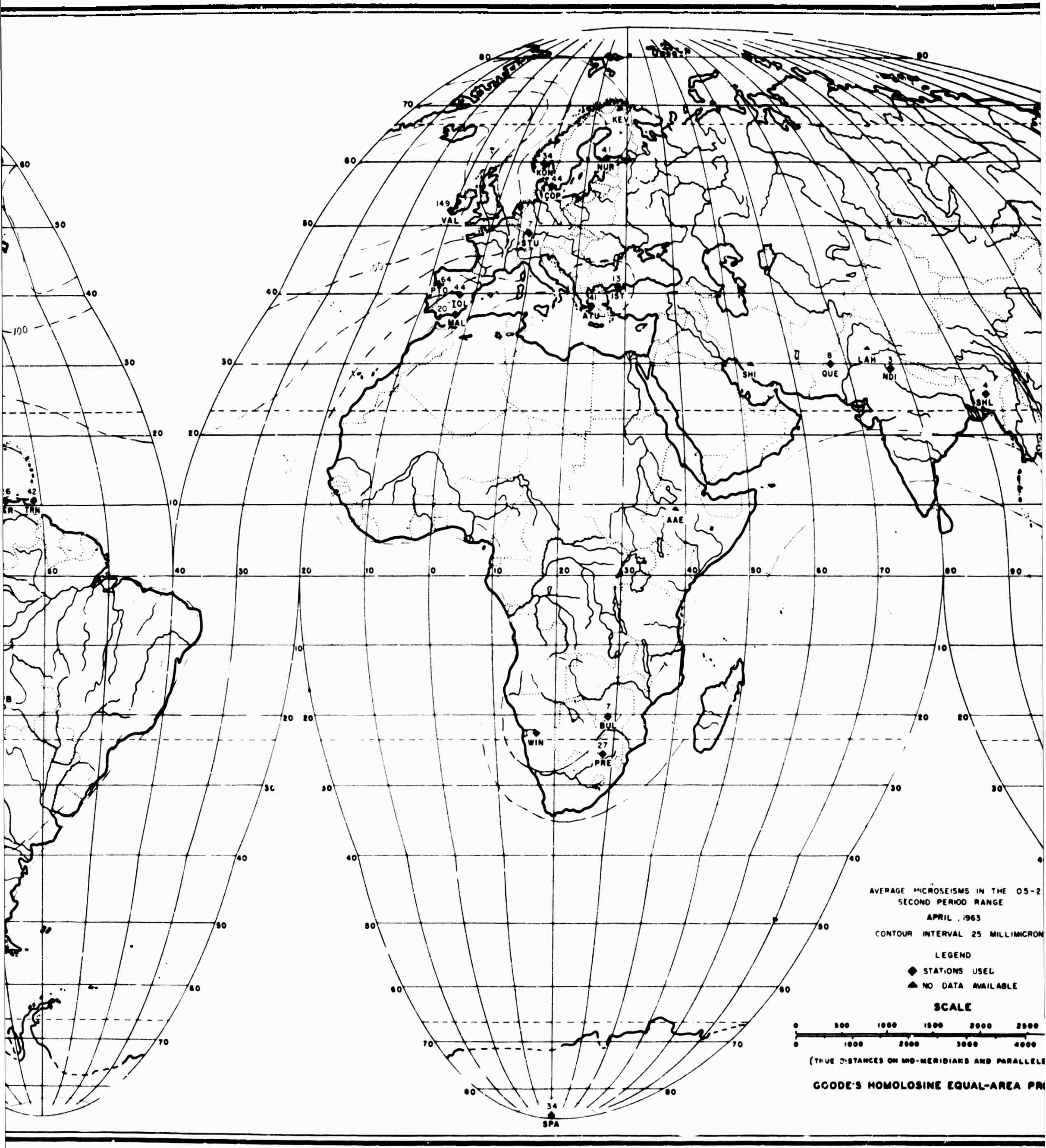

Figure B-7. World Map o

B

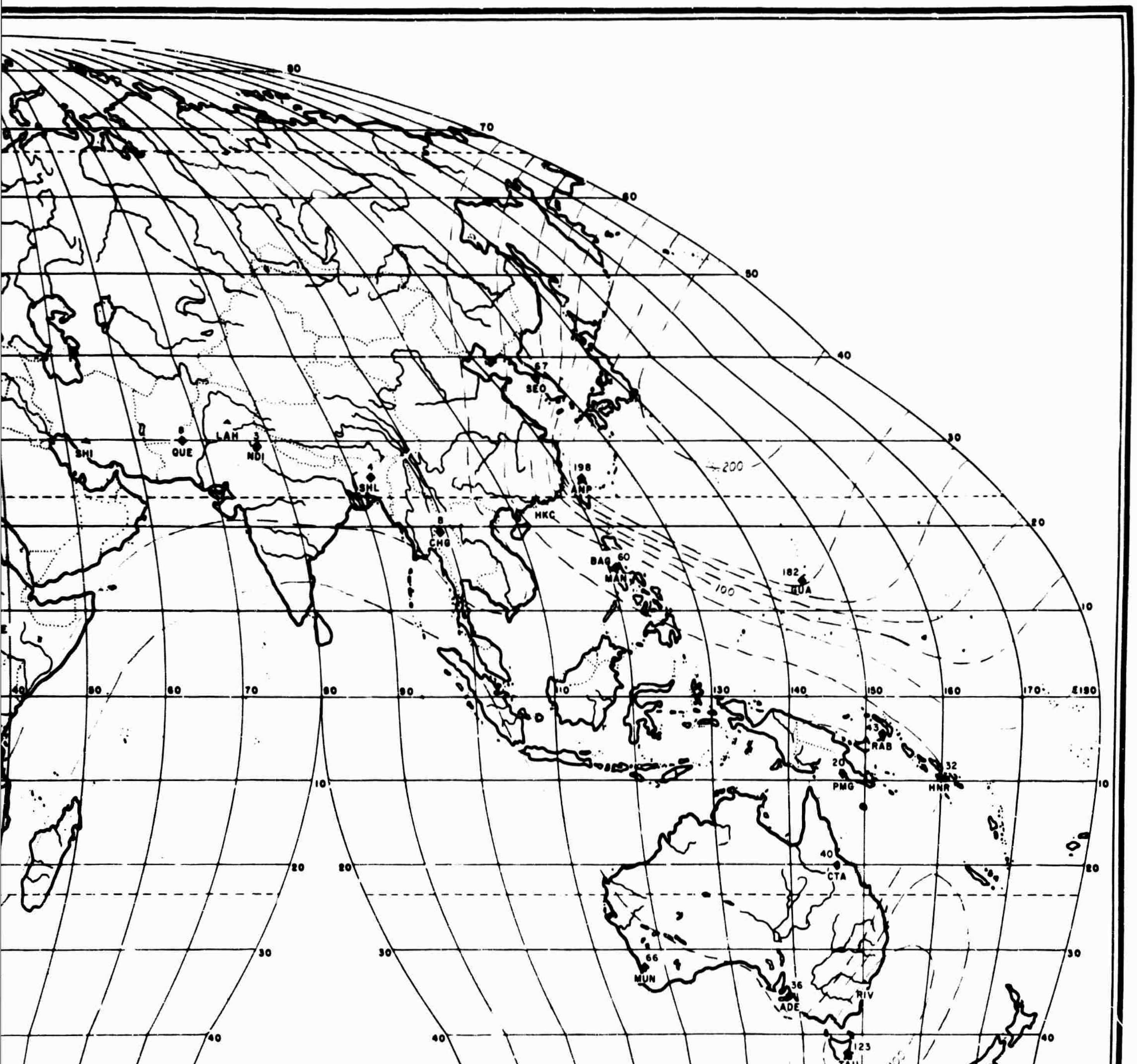

Figure B-7. World Map of 0.5-2.0 Second Microseismic Activity, April, 1963

C

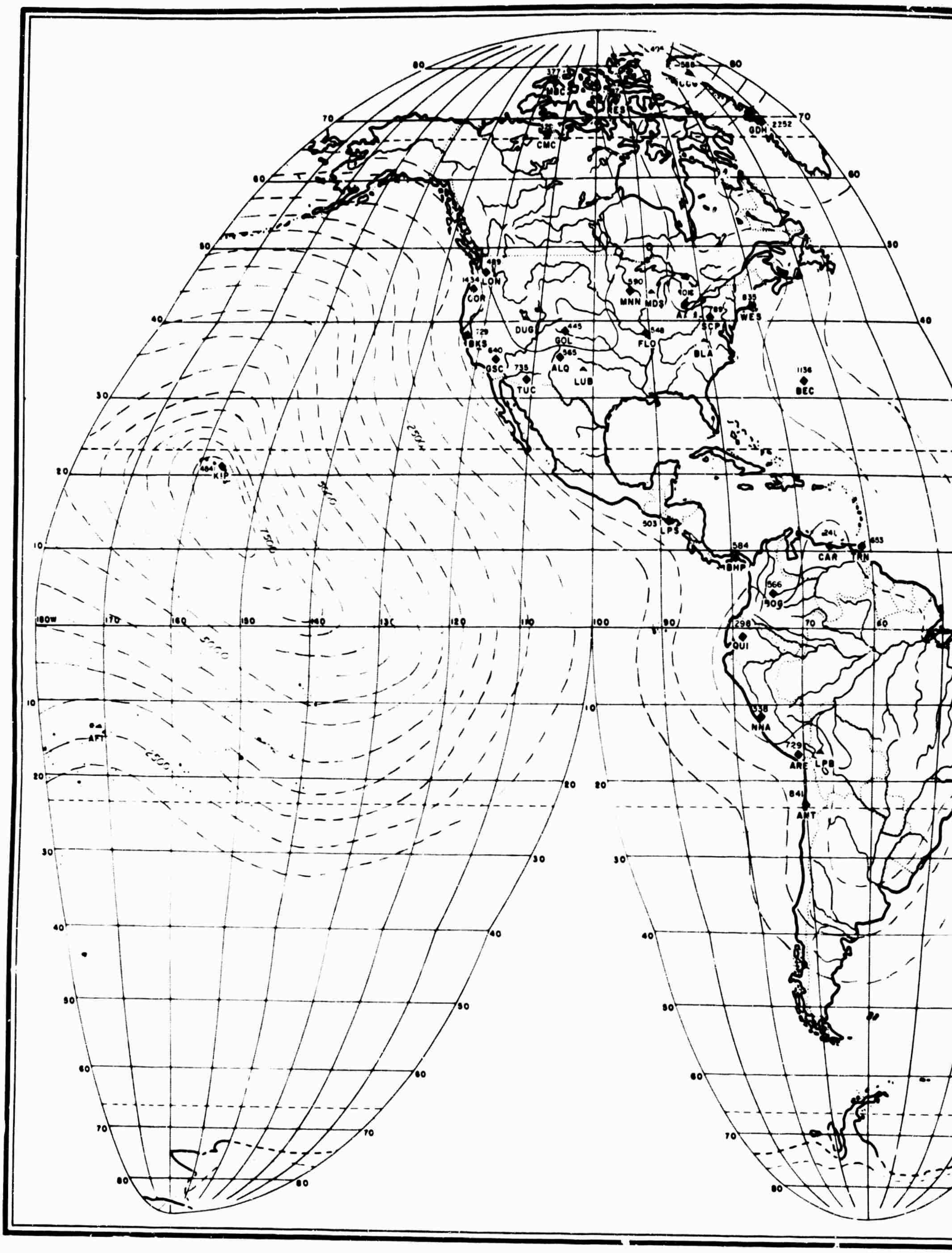

CMC
LON
COR
MNN
MDS
WES
SCP
DUG
GOL
FLO
BKS
BLA
ALQ
LUB
GSC
TUC
BEC
KIP
LPS
BHP
CAR
TRN
QUI
NNA
ARE
LPB
ANT
AFT
GDH

A

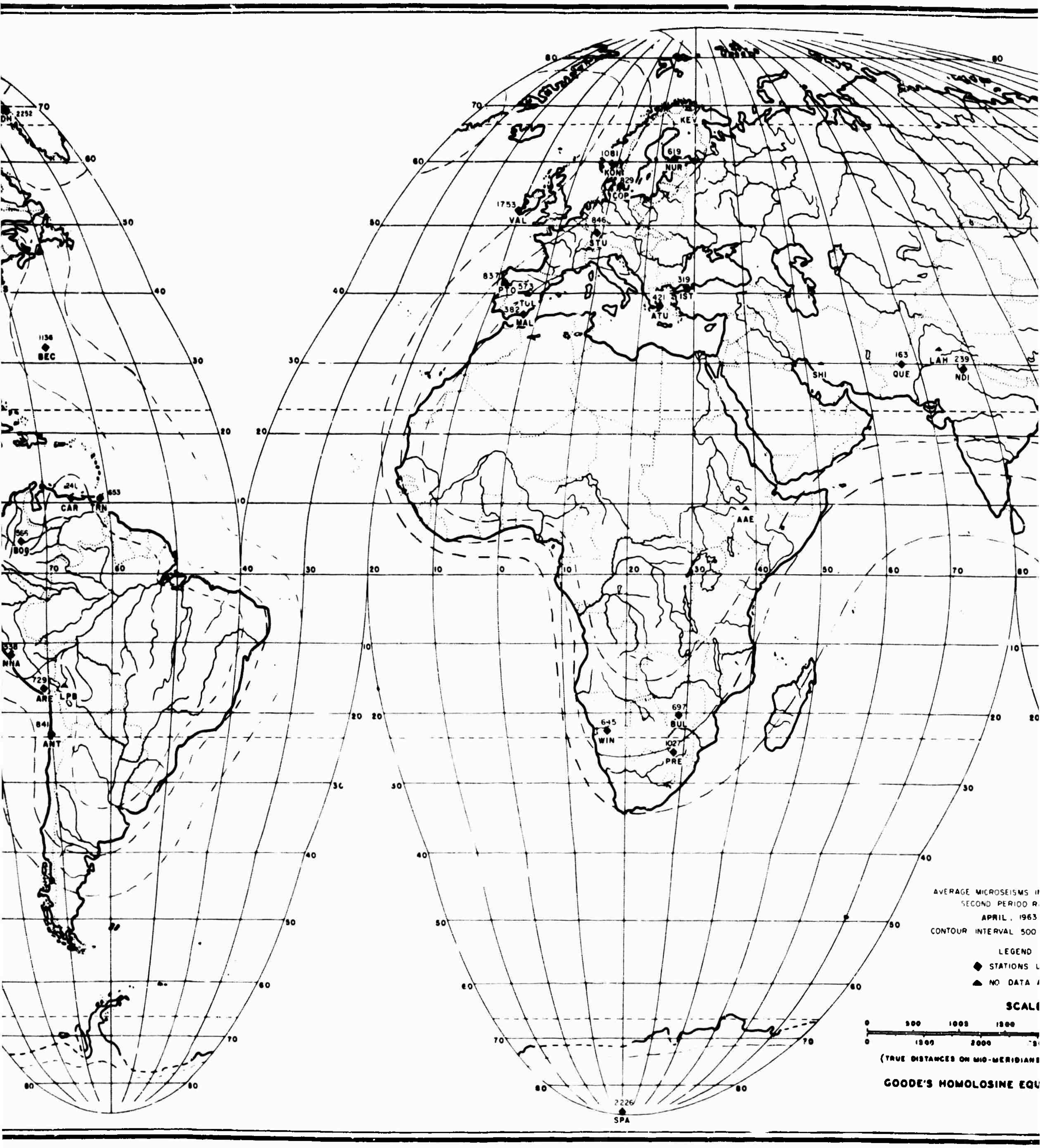

Figure B-8. Wor

b

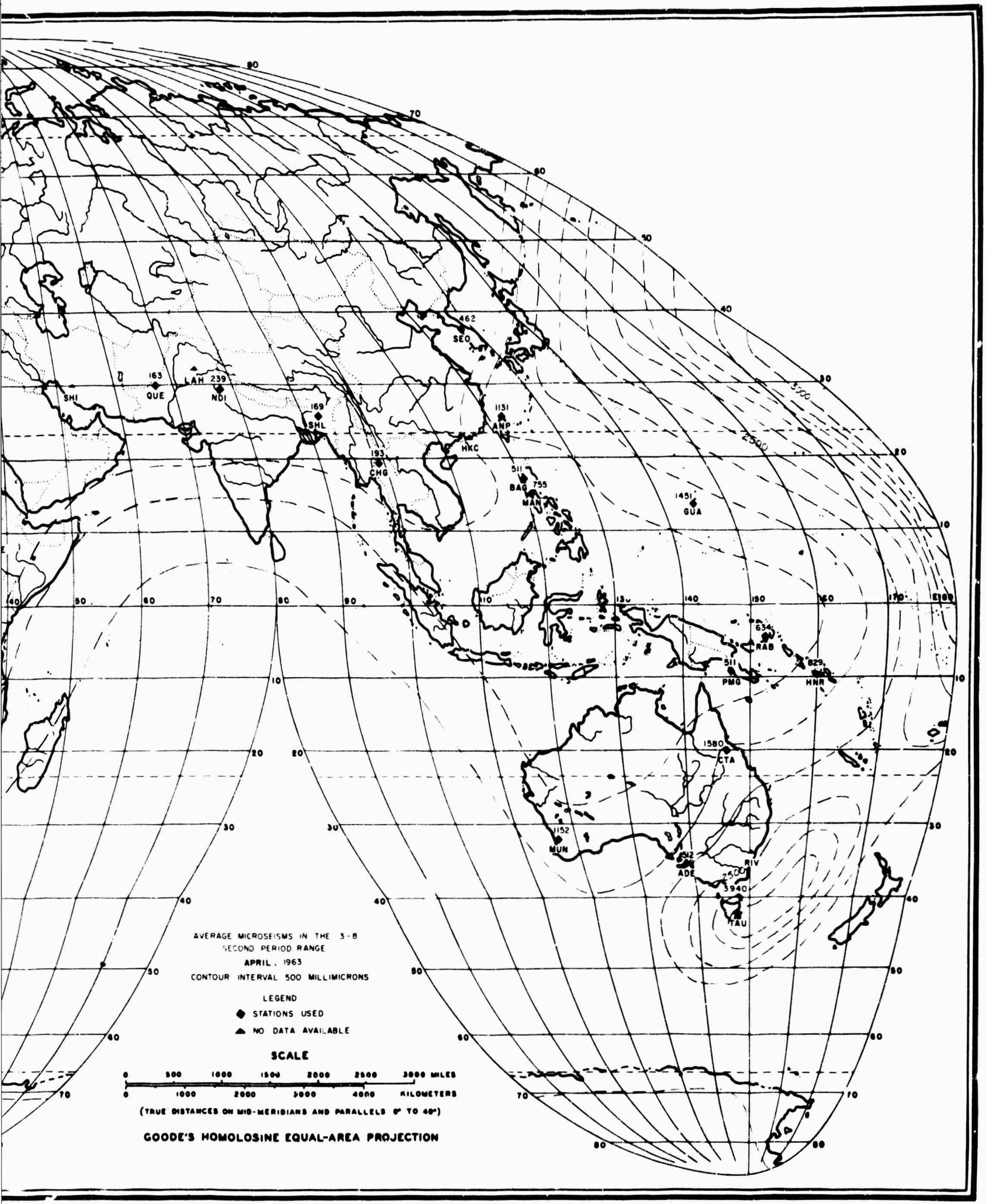

Figure B-8. World Map of 3.0-8.0 Second Microseismic Activitv, April, 1963

C

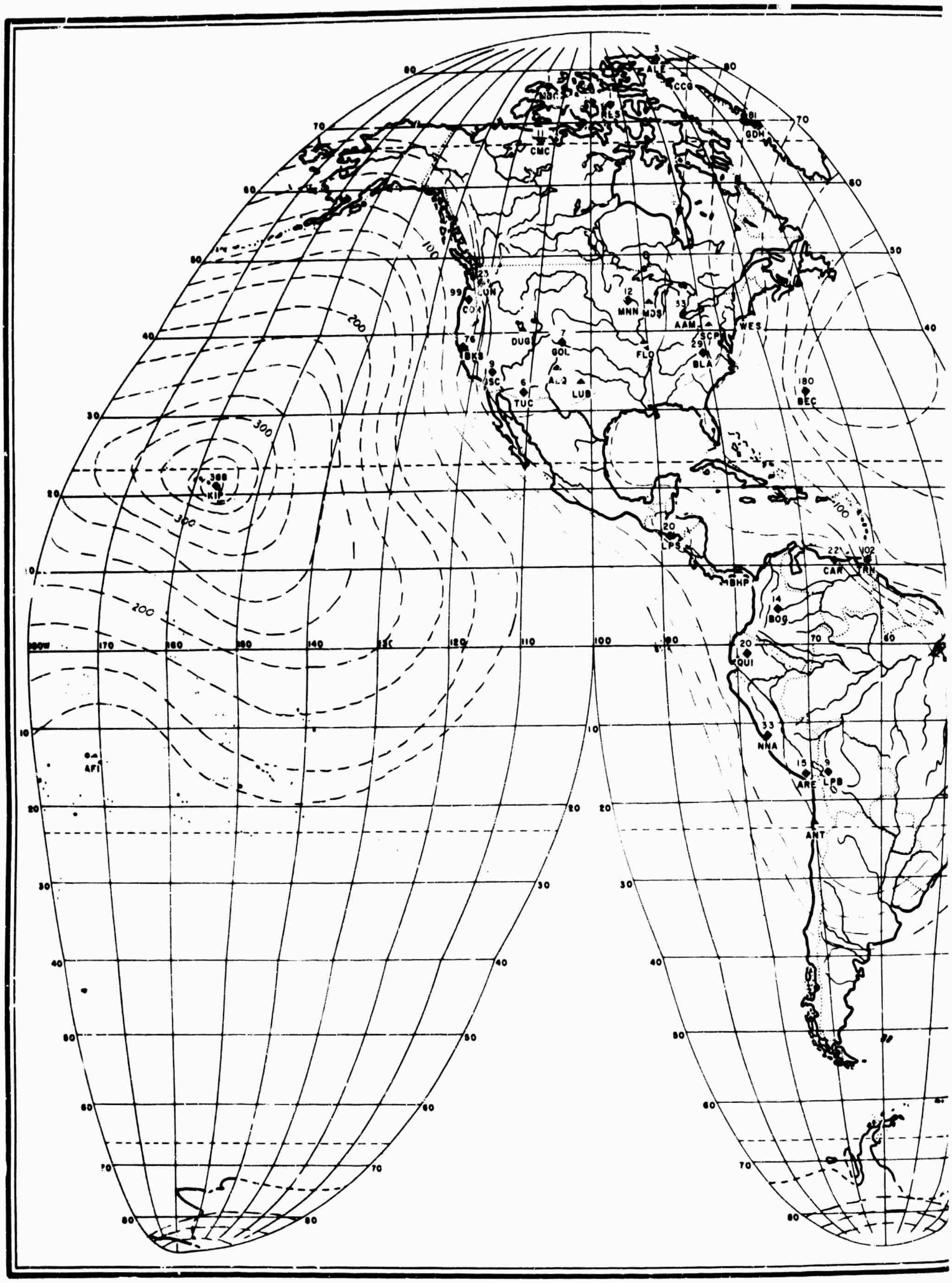

ALE
CCG
GDH
CMC
MNN
MDS
AAM
WES
SCP
BLA
FLO
DUG
GOL
LUB
TUC
BKS
COX
BEC
KIP
LPS
BHP
CAR
TRN
BOG
QUI
NNA
ARE
LPB
ANT
AFI
100
200
300

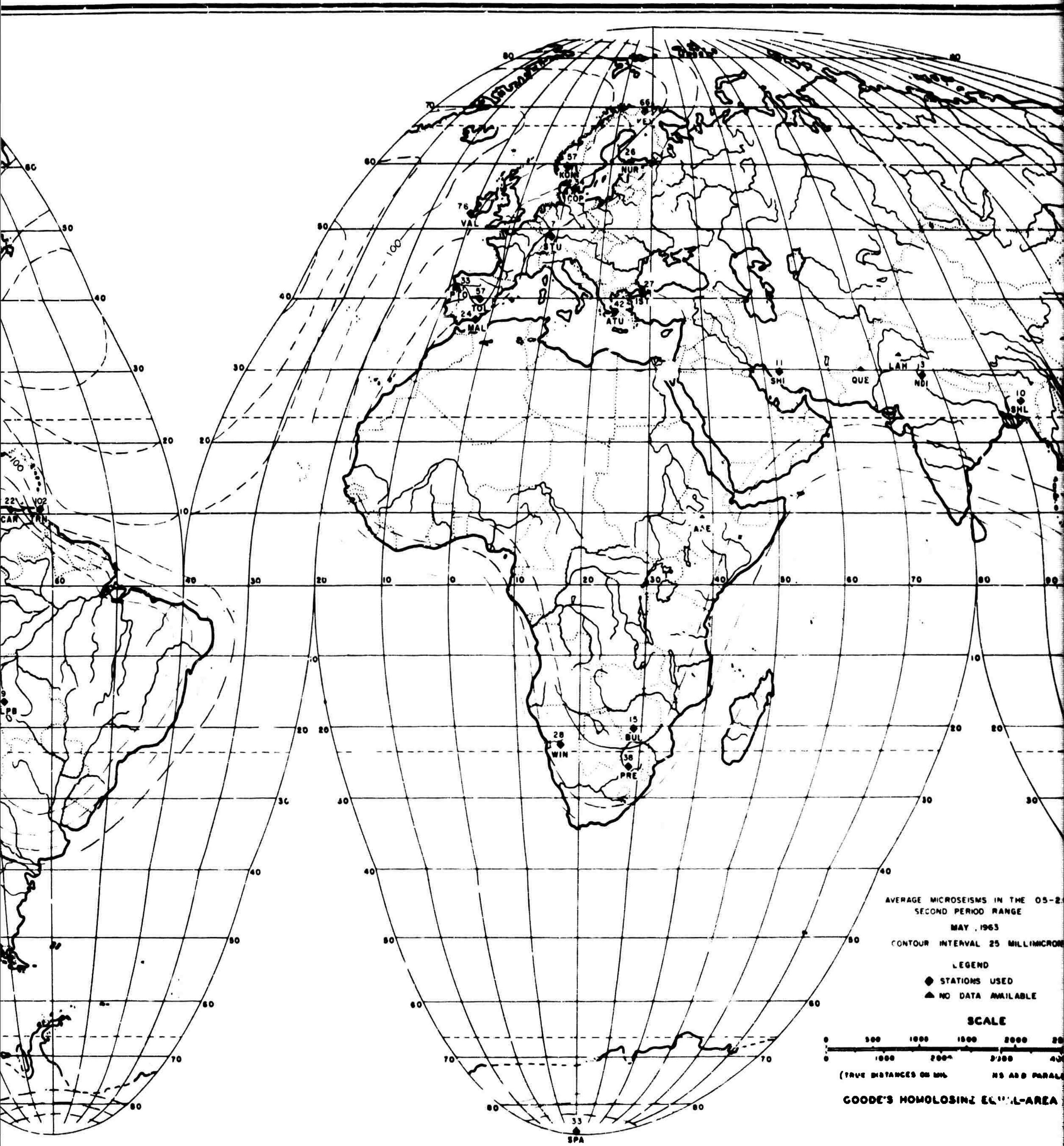

Figure B-9. World Ma

B

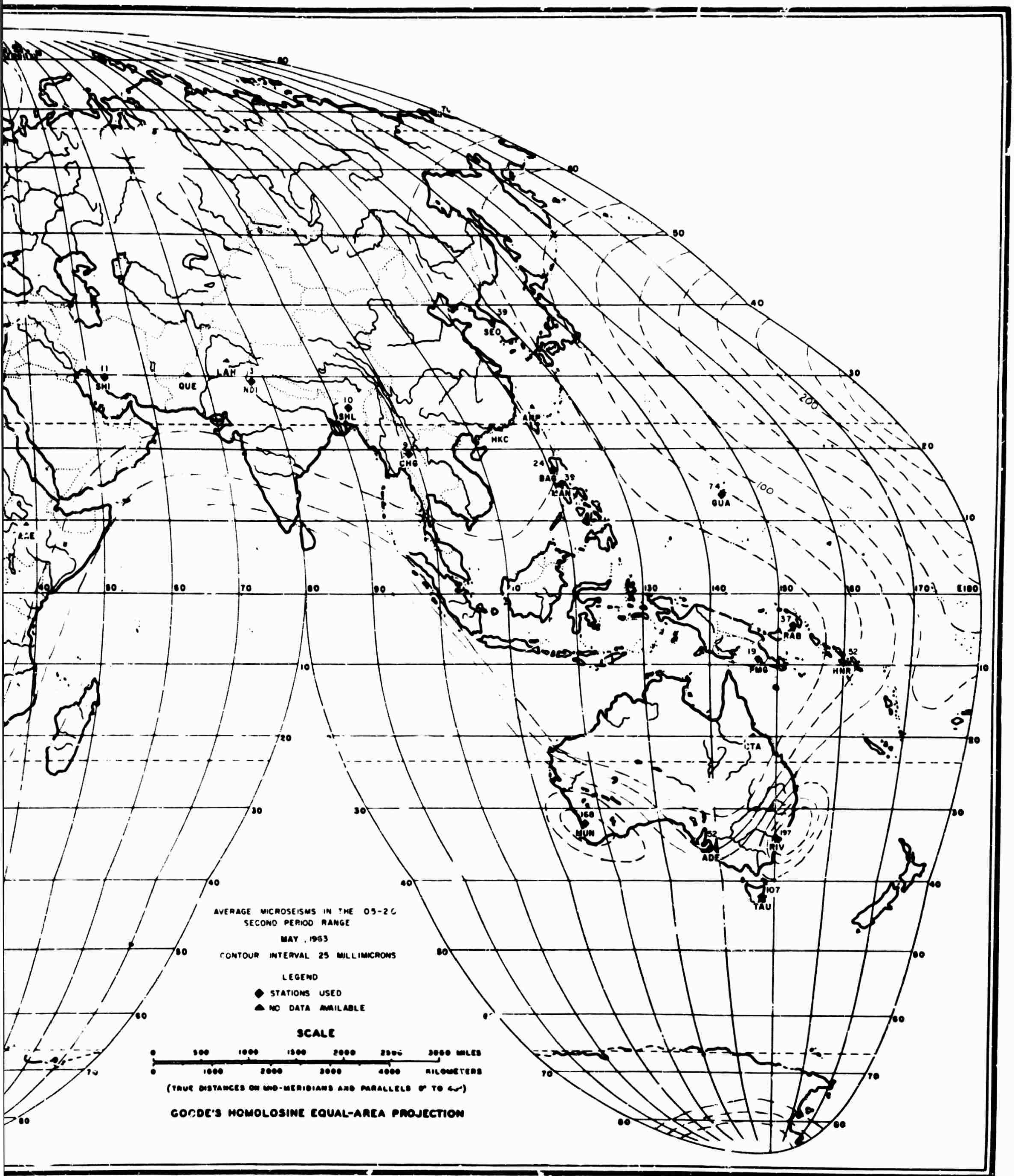

Figure B-9. World Map of 0.5-2.0 Second Microseismic Activity, May, 1963

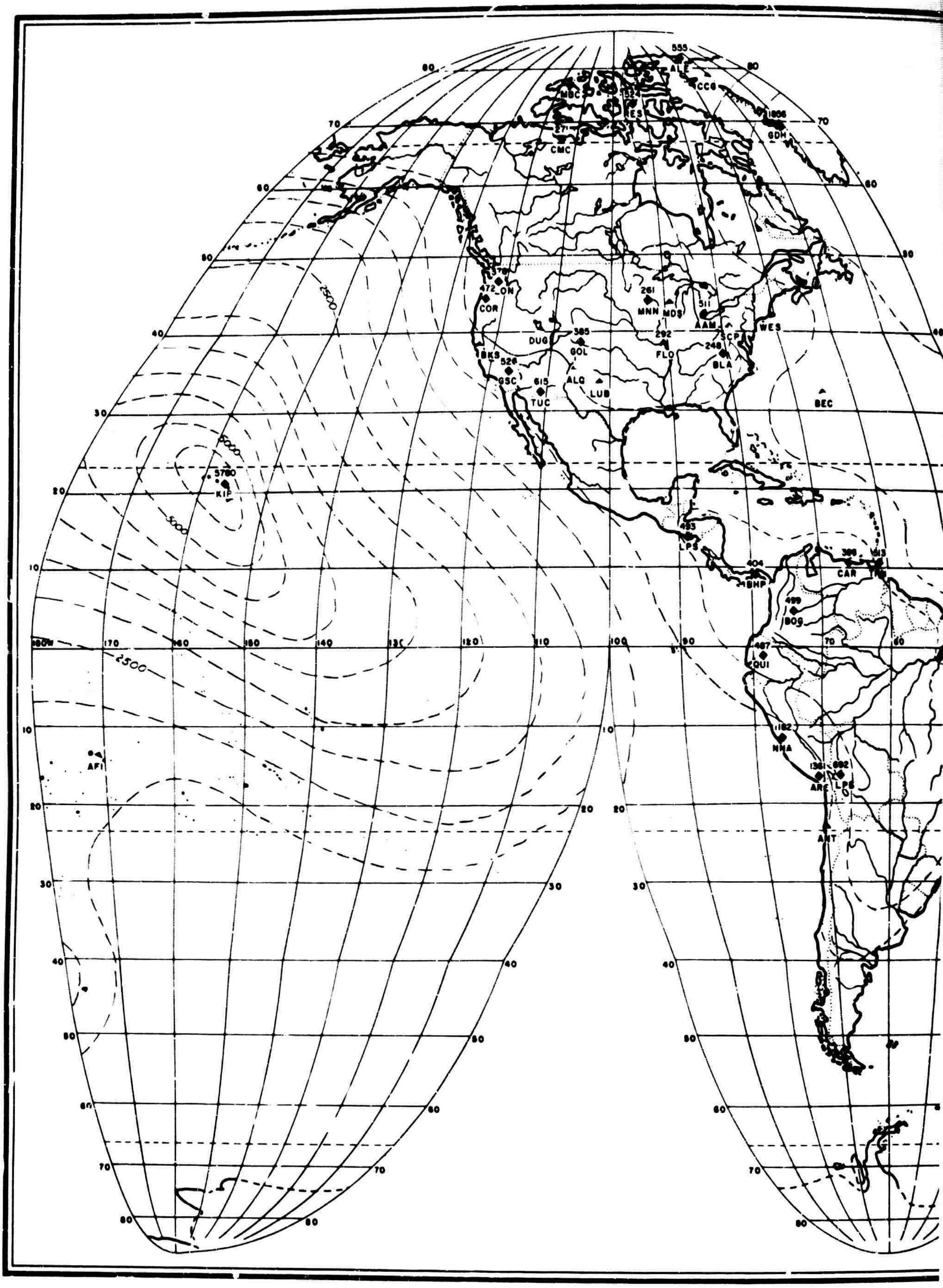
555
ALE
MBC
524
RES
CCG
1866
GDH
271
CMC
379
ON
472
COR
261
MNN
MDS
511
AAM
385
DUG
GOL
292
FLO
SCP
248
BLA
WES
BKS
526
GSC
615
TUC
ALQ
LUB
BEC
5760
KIP
2500
5000
493
LPS
404
BHP
CAR
499
BOG
487
QUI
AFI
1182
NNA
1361
ARE
LPB
ANT
180W

A

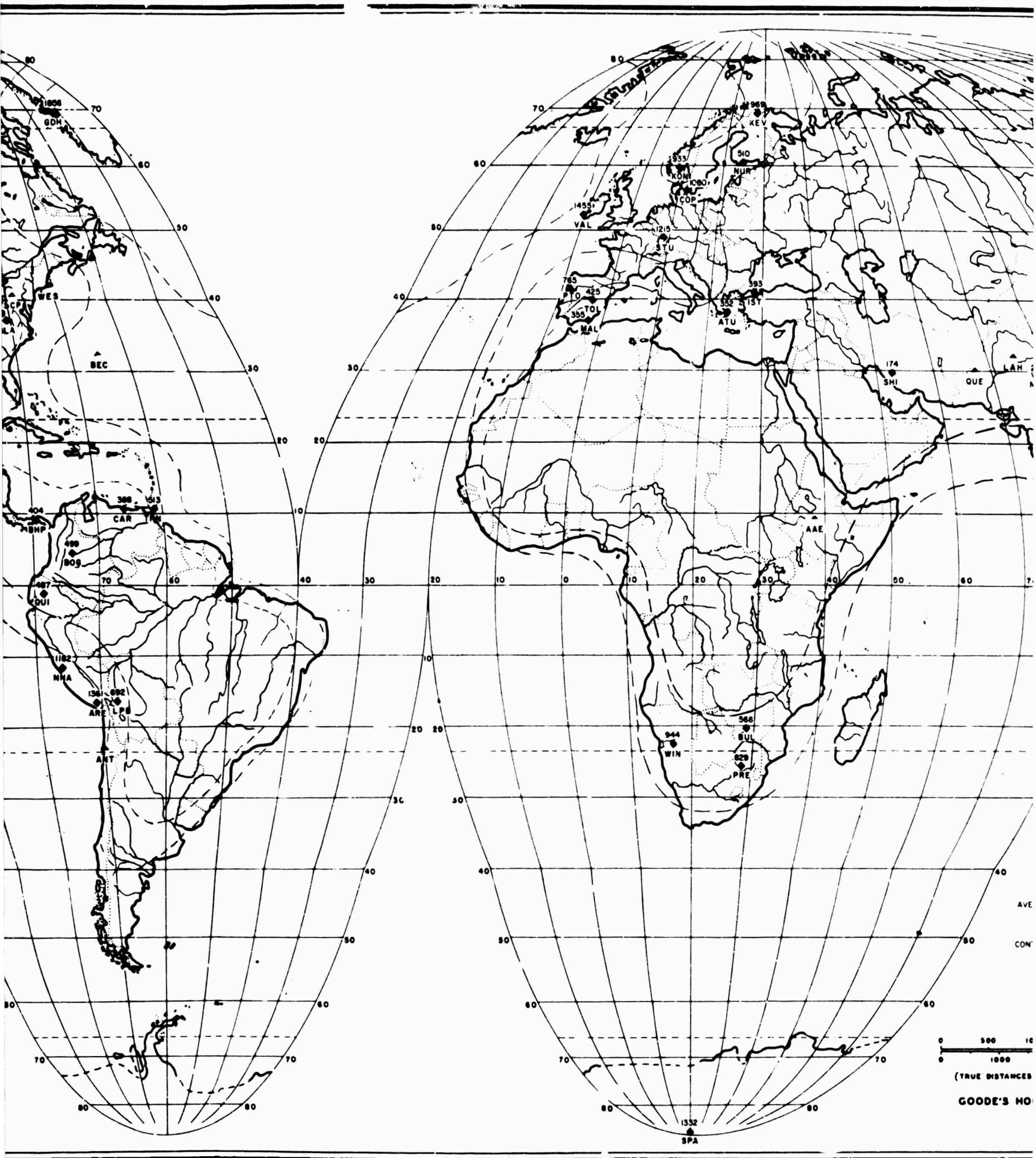
1656
GDH
WES
BEC
388
CAR
1513
TRN
404
BHP
499
BOG
1487
QUI
1182
NNA
1361
ARE
692
LPB
ANT
1969
KEV
1933
KON
510
NUR
1080
COP
1455
VAL
1215
STU
765
PTO
425
TOL
355
MAL
593
IST
552
ATU
174
SHI
QUE
LAH
AAE
944
WIN
568
BUL
829
PRE
1332
SPA
AVE
CON
(TRUE DISTANCES
GOODE'S HO

Figure B-

b

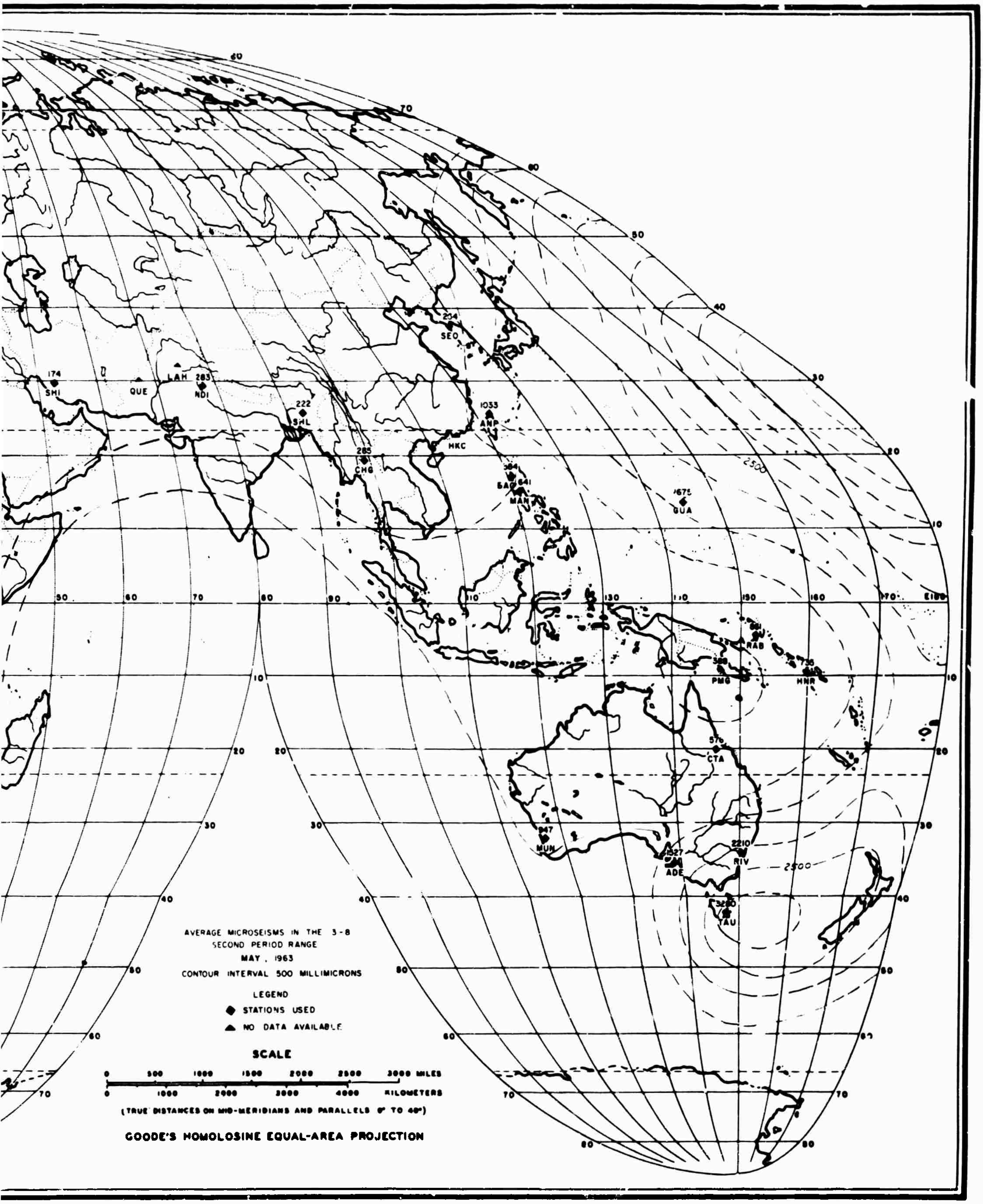

Figure B-10. World Map of 3.0-8.0 Second Microseismic Activity, May, 1963

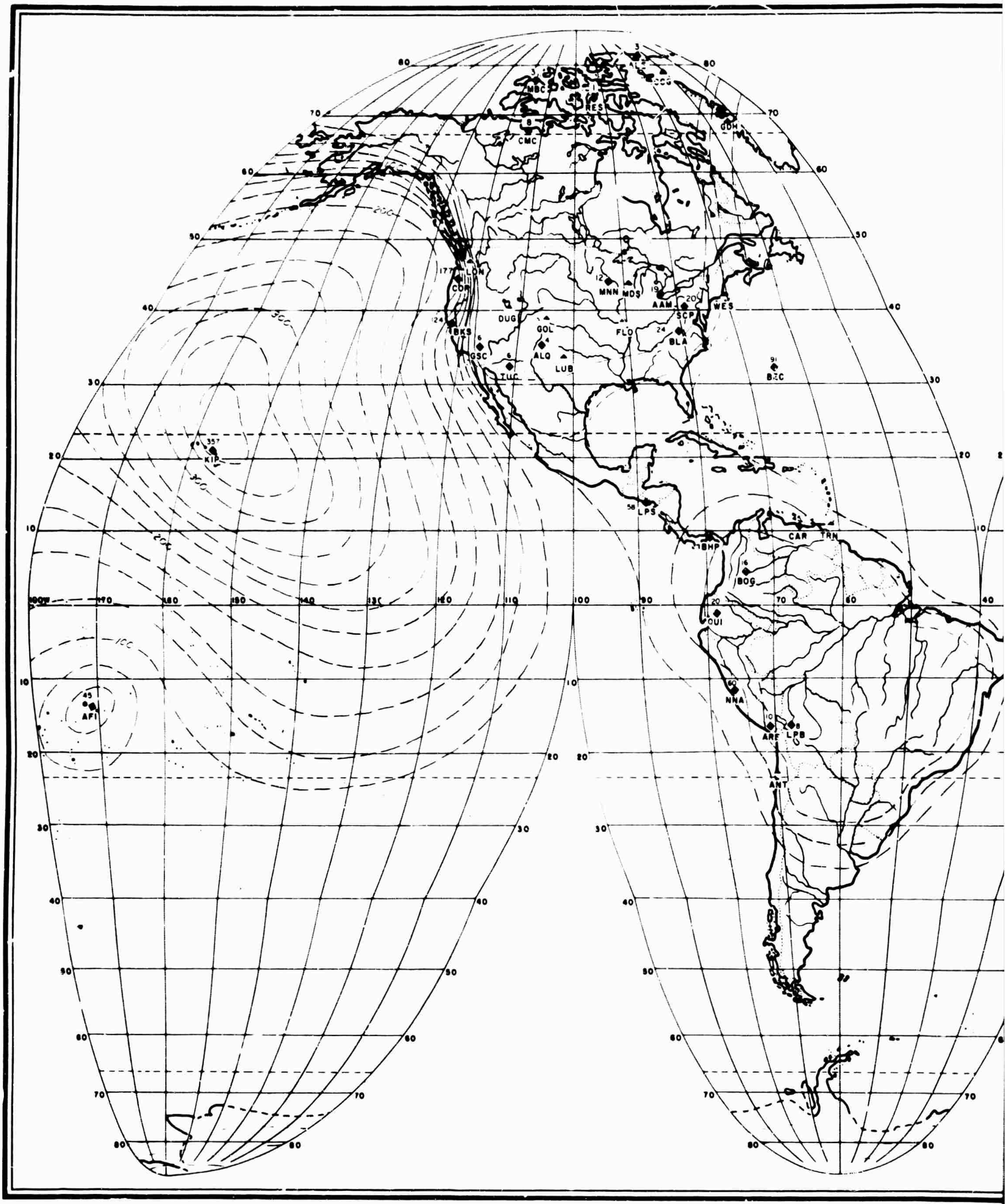
ALE
MBC
RES
GDH
CMC
LON
COR
MNN
MDS
AAM
SCP
WES
BKS
DUG
GOL
FLO
BLA
GSC
ALQ
LUB
TUC
BEC
KIP
LPS
BHP
CAR
TRN
BOG
QUI
NNA
ARE
LPB
ANT
AFI

A

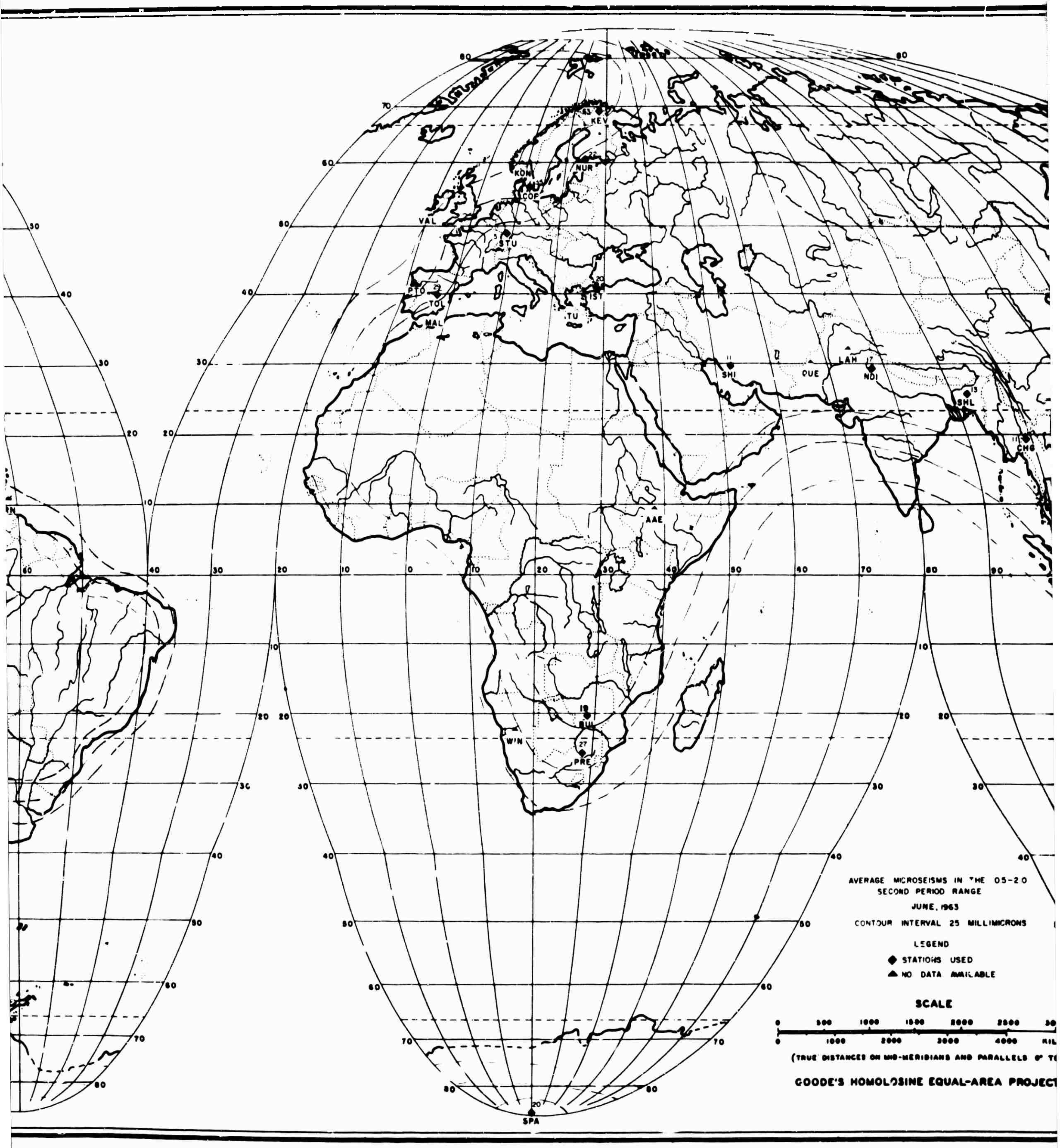

Figure B-11. World Map of (

B

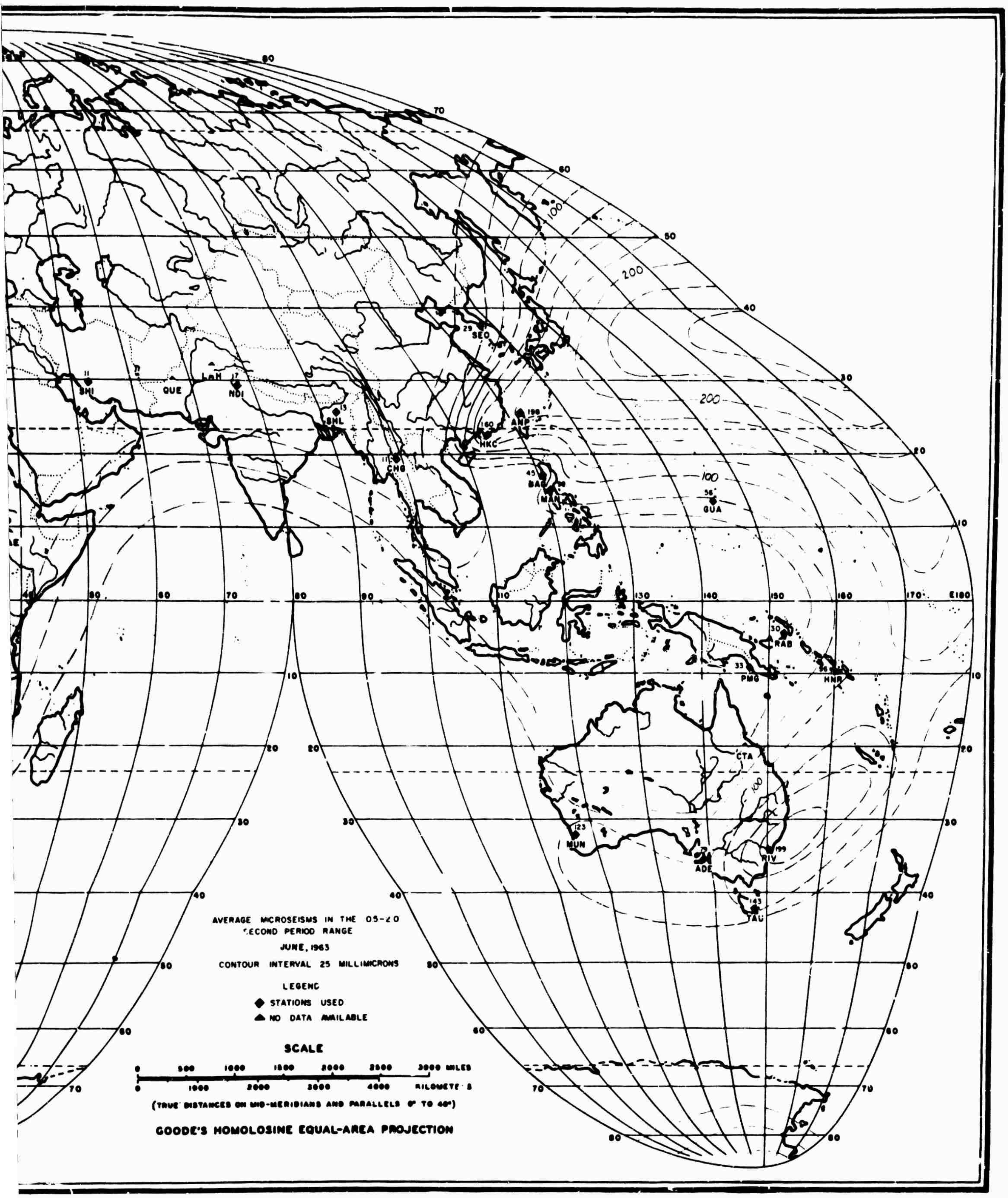

Figure B-11. World Map of 0.5-2.0 Second Microseismic Activity, June, 1963

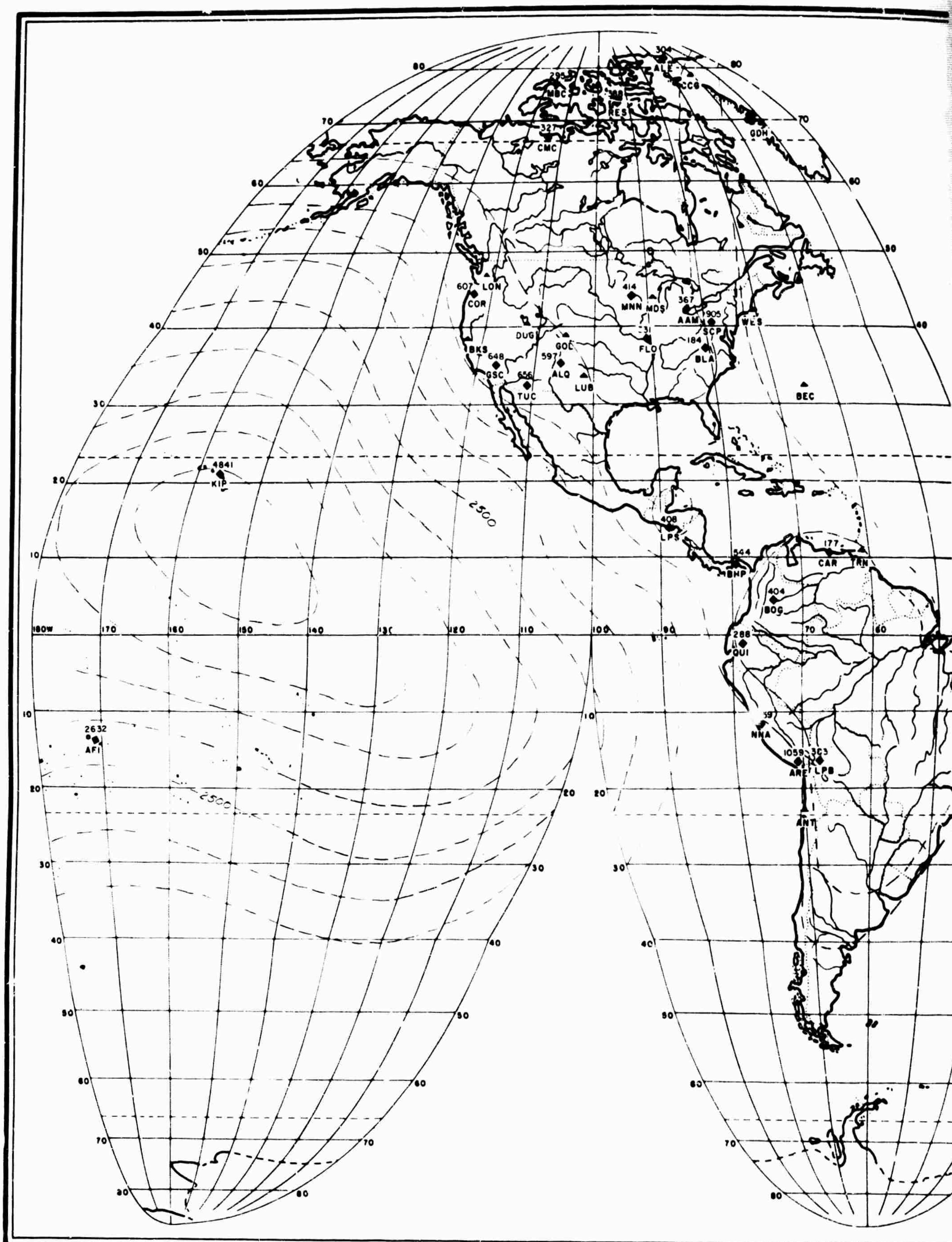
304
ALE
295
MBC
RES
GDH
327
CMC
607
LON
COR
414
MNN
MDS
367
AAM
905
SCP
WES
DUG
GOL
FLO
184
BLA
BKS
648
GSC
597
ALQ
656
TUC
LUB
BEC
4841
KIP
2500
408
LPS
544
BHP
177
CAR
TRN
404
BOG
288
QUI
NNA
1059
ARE
LPB
ANT
2632
AFI
2500

A

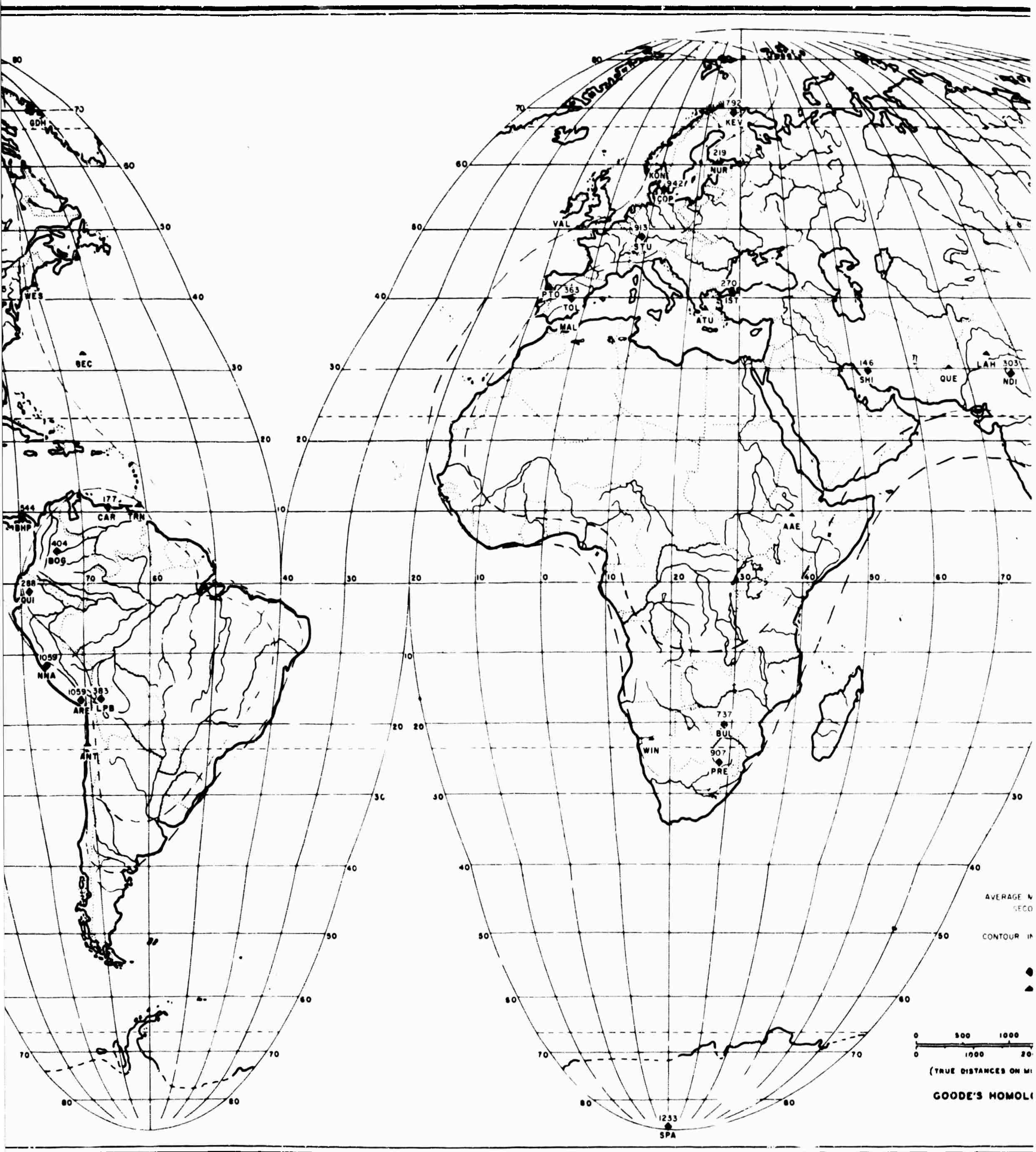
GDH
WES
BEC
177
CAR
TRN
544
BHP
404
BOG
288
QUI
1059
NHA
1059
ARE
383
LPB
ANT
792
KEV
219
NUR
KON
942
COP
VAL
913
STU
PTO
363
TOL
MAL
270
IST
ATU
146
SHI
QUE
LAH
303
NDI
AAE
737
BUL
WIN
907
PRE
1233
SPA
AVERAGE M
SECO
CONTOUR IN
(TRUE DISTANCES ON M
GOODE'S HOMOL

Figure B-12.

B

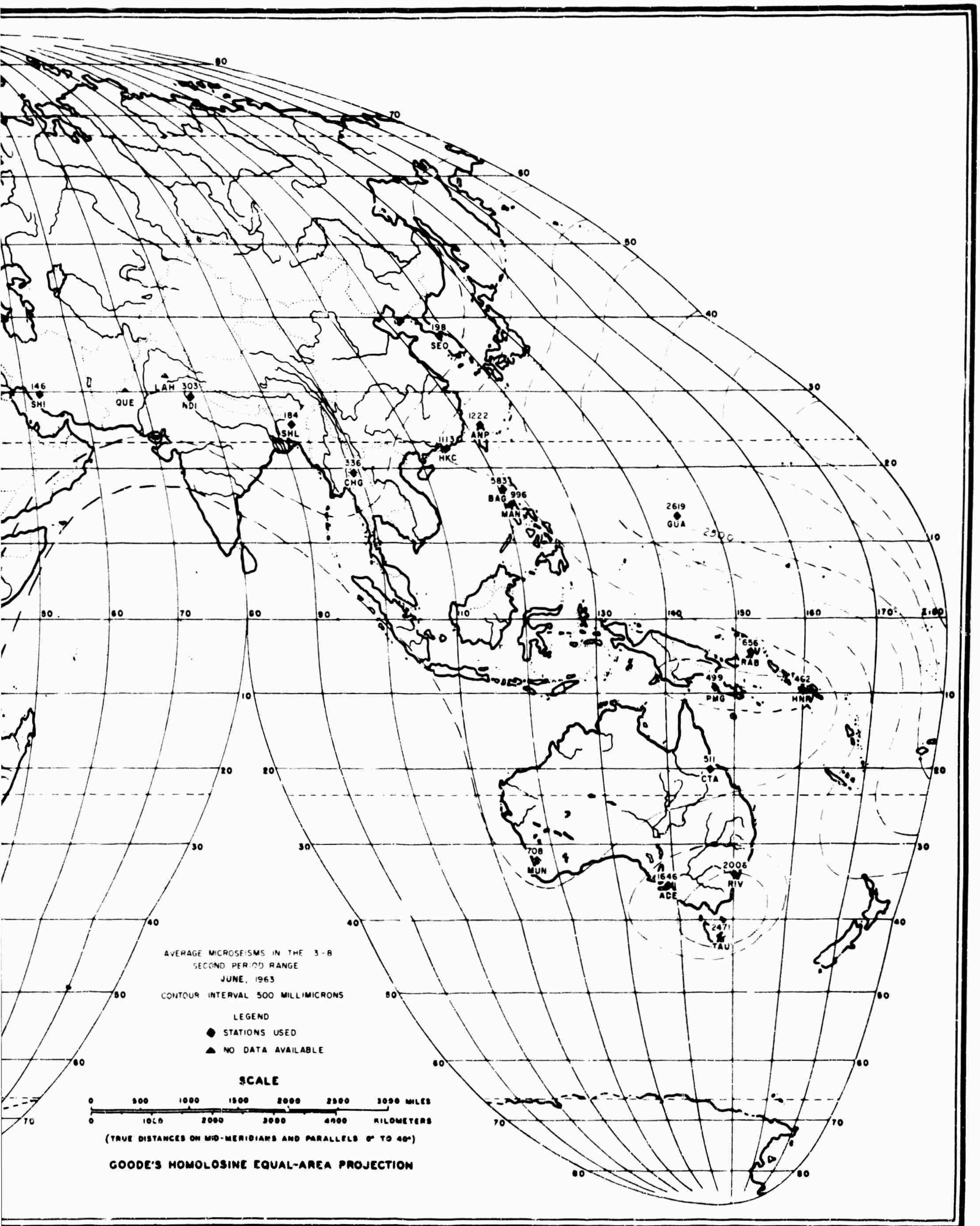

Figure B-12. World Map of 3.0-8.0 Second Microseismic Activity, June, 1963

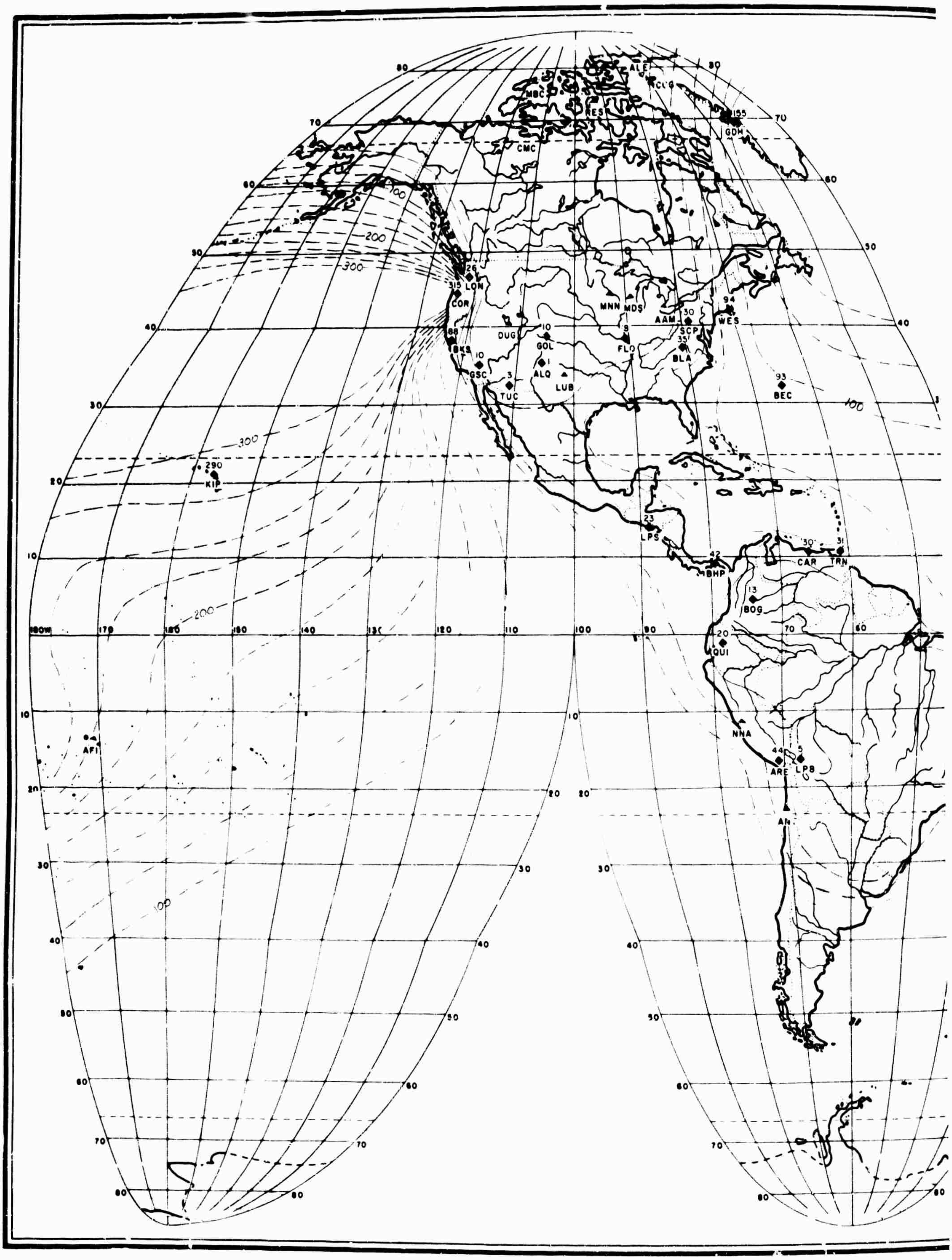

ALE
MBC
RES
GDH
155
CMC
26
LON
315
COR
88
BKS
10
GSC
DUG
10
GOL
1
ALQ
3
TUC
LUB
MNN
MDS
8
FLO
AAM
30
SCP
35
BLA
94
WES
93
BEC
290
KIP
AFI
23
LPS
42
BHP
30
CAR
31
TRN
13
BOG
20
QUI
NNA
44
ARE
5
LPB
100
200
300

A

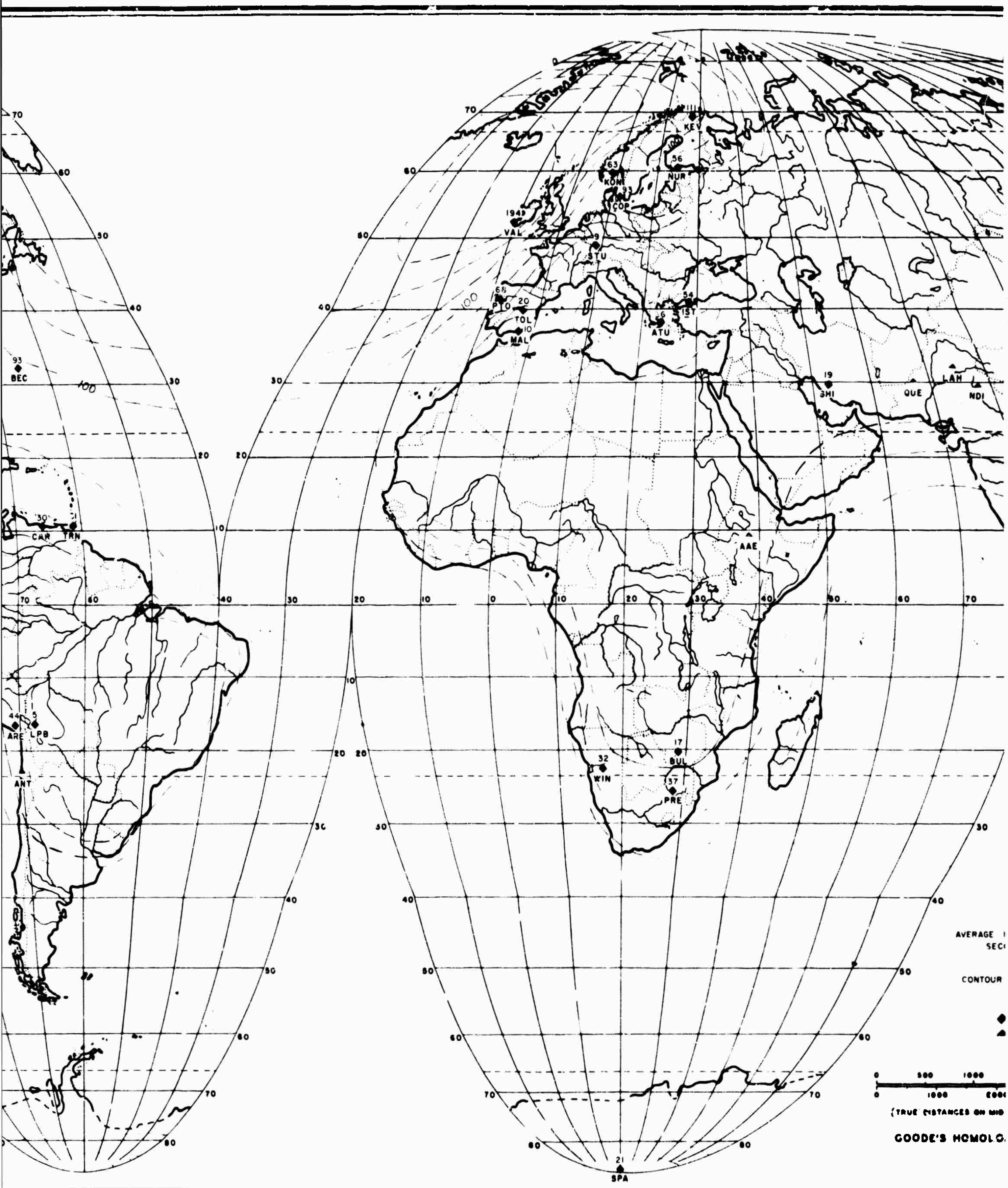
KEV
KON
NUR
COP
VAL
STU
PTO
TOL
MAL
IST
ATU
SHI
QUE
LAH
NDI
AAE
BUL
WIN
PRE
SPA
BEC
CAR
TRN
ARE
LPB
ANT
AVERAGE
CONTOUR
0 500 1000
GOODE'S HOMOLO

Figure B-13.

B

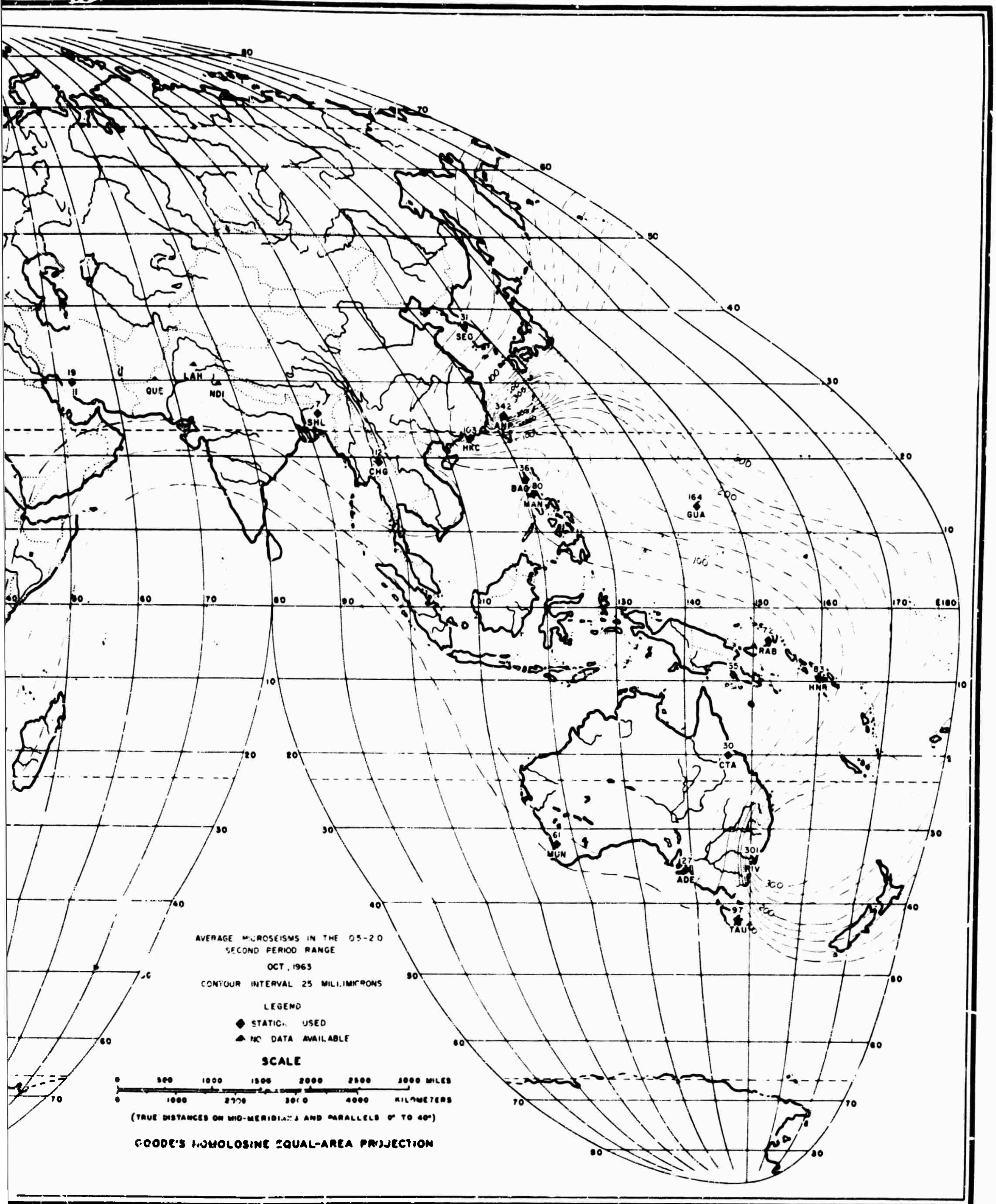

Figure B-13. World Map of 0.5-2.0 Second Microseismic Activity, October, 1963

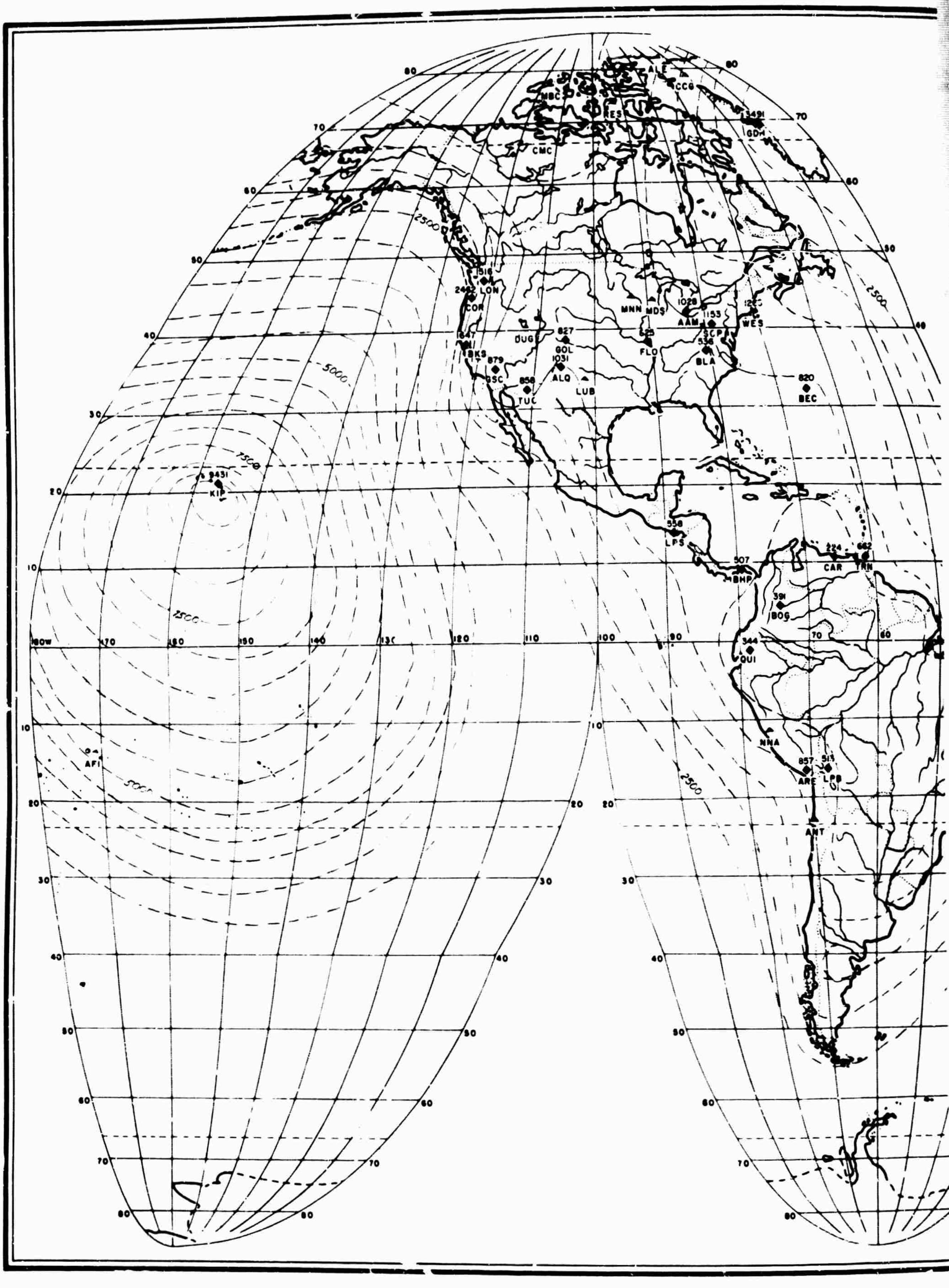

ALE
CCG
GDH
MBC
RES
CMC
1516
LON
COR
BKS
879
SSC
858
TUC
DUG
827
GOL
1031
ALQ
LUB
MNN
MDS
1029
AAM
1153
SCP
WES
FLO
536
BLA
820
BEC
KIP
AFI
556
LPS
507
BHP
224
CAR
662
TRN
391
BOG
344
QUI
NNA
857
ARE
LPB
ANT
2500
5000
7500

A

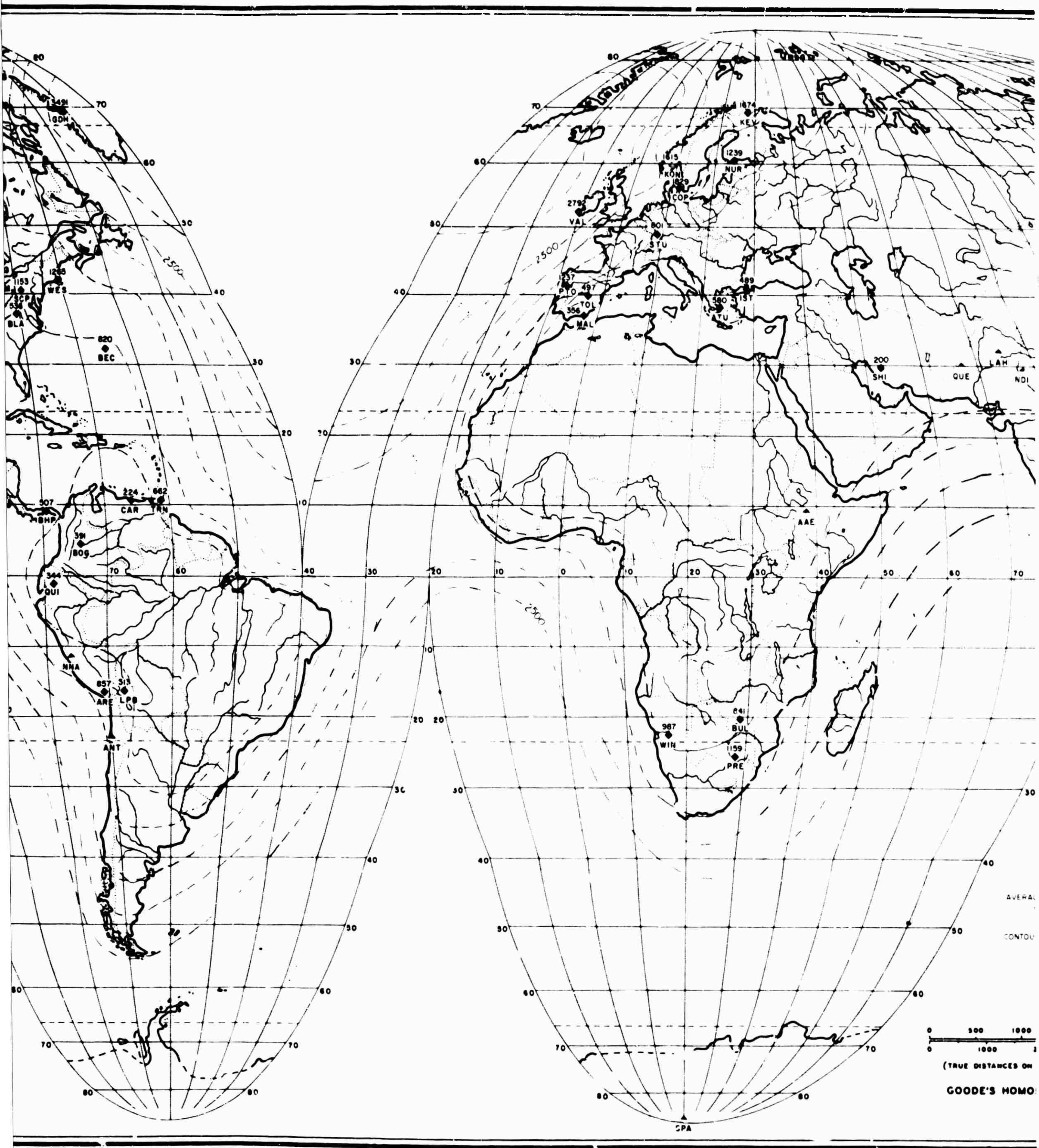
1874
KEV
1239
NUR
1615
KON
1629
COP
2792
VAL
801
STU
2500
1257
PTO
497
TOL
356
MAL
489
IST
560
ATU
200
SHI
QUE
LAH
NDI
AAE
841
BUL
987
WIN
1159
PRE
SPA
3491
GDH
1153
SCP
1265
WES
BLA
820
BEC
507
BHP
224
CAR
662
TRN
391
BOG
344
QUI
NNA
857
ARE
313
LPB
ANT
AVERA
CONTOU
(TRUE DISTANCES ON
GOODE'S HOMO

Figure B-14

b

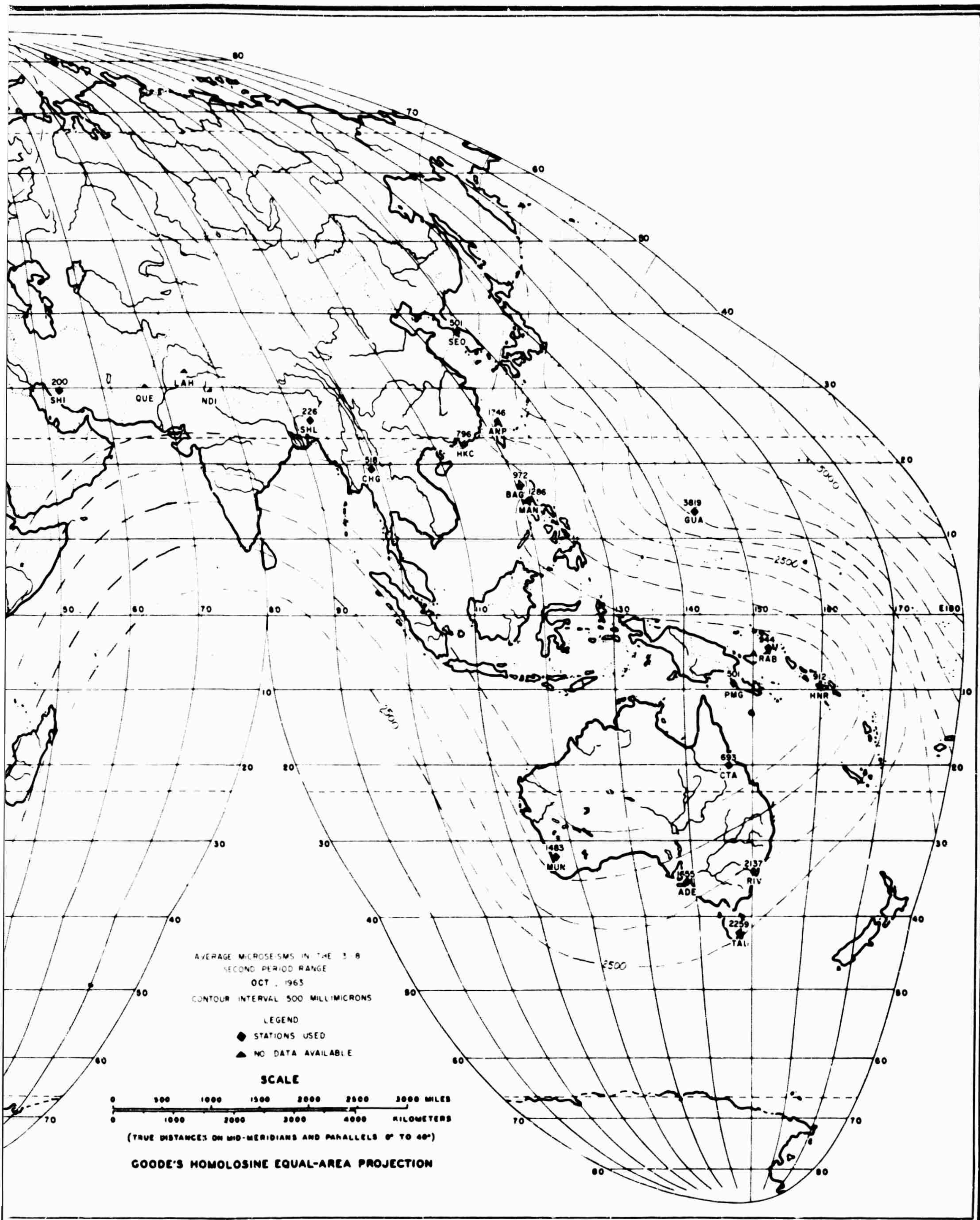

Figure B-14. World Map of 3.0-8.0 Second Microseismic Activity, October, 1963

C

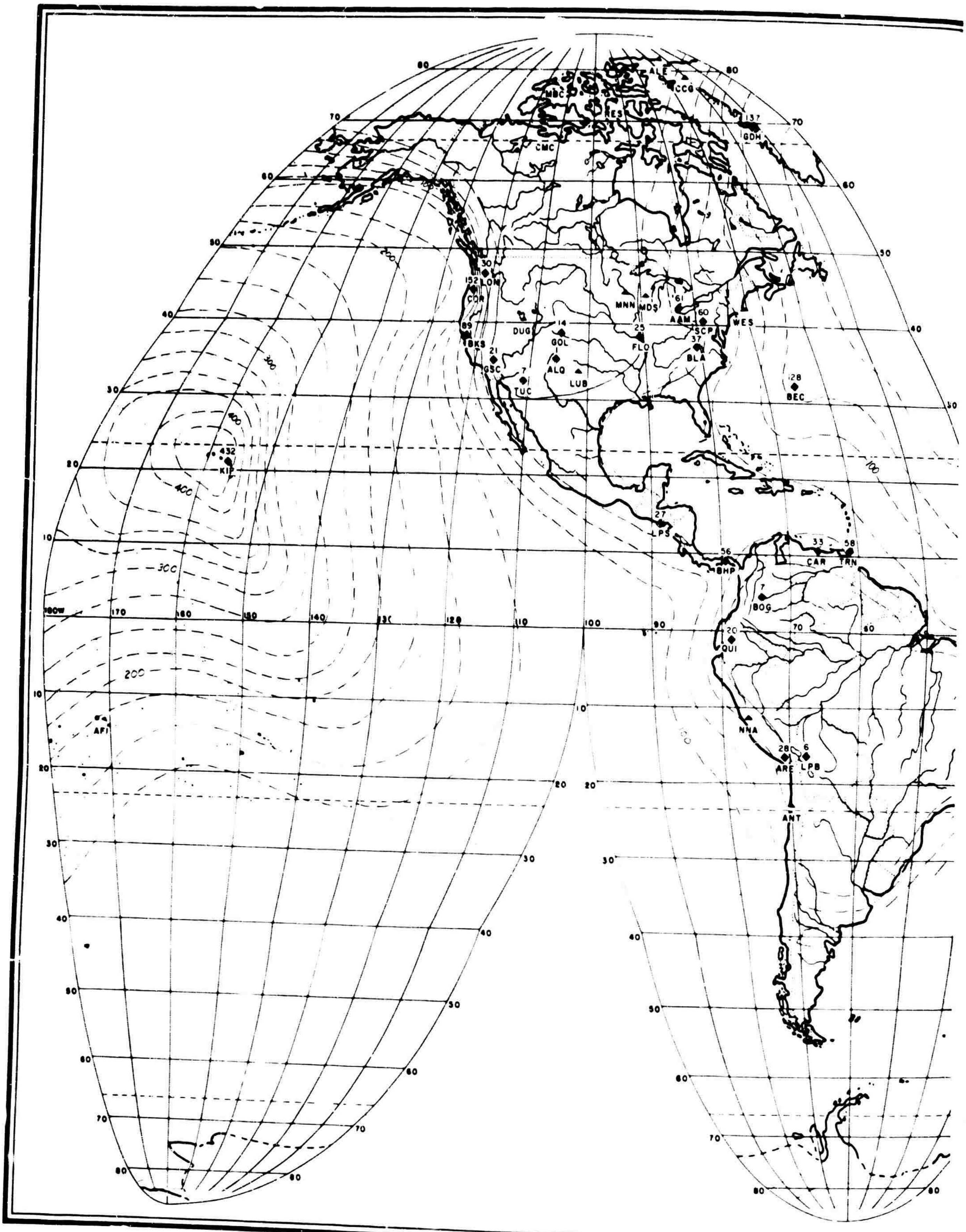
ALE
CCG
MBC
RES
137
GDH
CMC
30
LOM
152
COR
89
BKS
21
GSC
DUG
14
GOL
ALQ
LUB
7
TUC
MNN
MDS
25
FLO
61
AAM
60
SCP
37
BLA
WES
128
BEC
432
KIP
27
LPS
56
BHP
33
CAR
58
TRN
7
BOG
20
QUI
NNA
28
ARE
6
LPB
ANT
AFI
200
300
400
100
180W
170
160
150
140
120
110
100
90
70
60

A

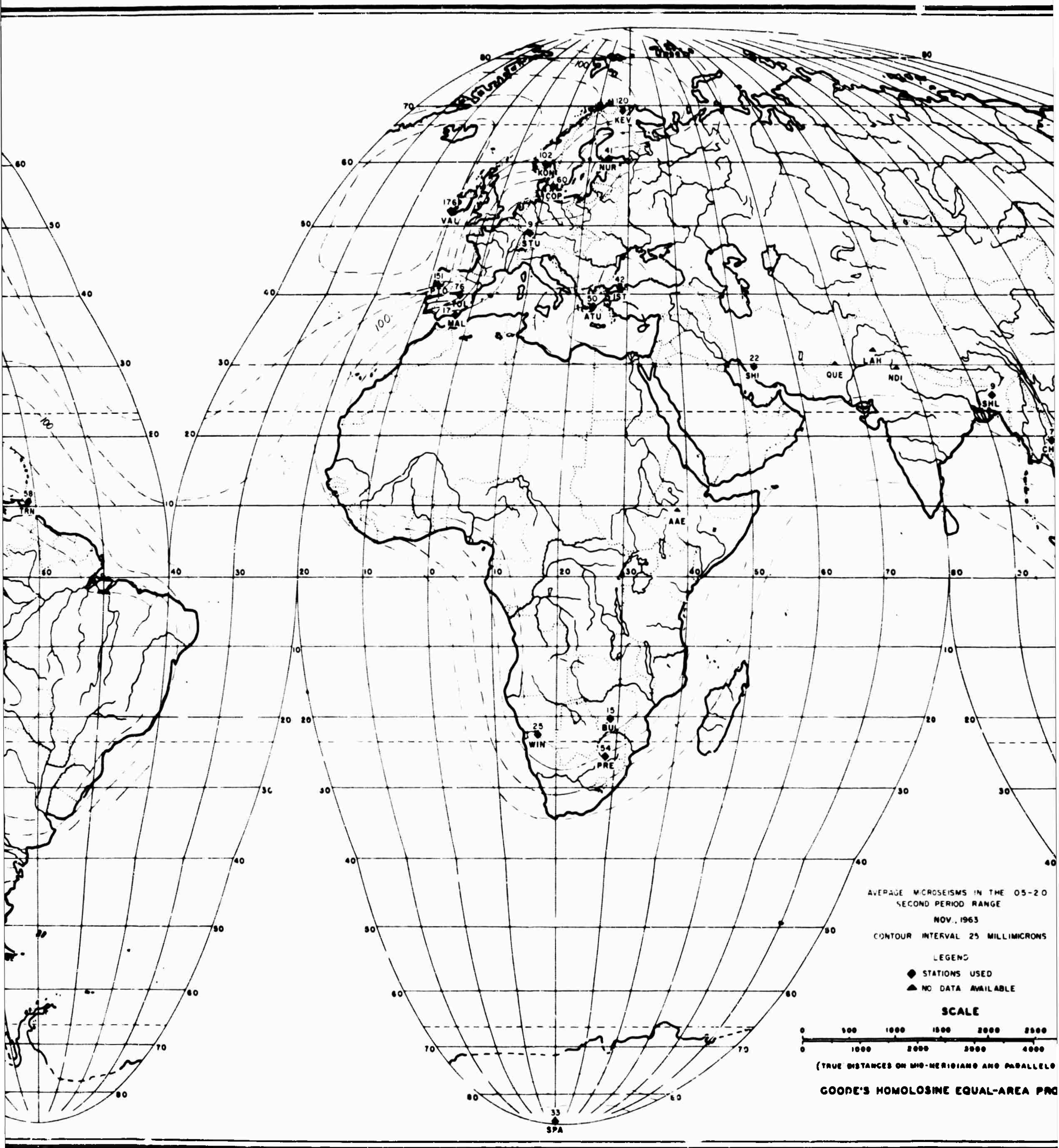

Figure B-15. World Map of (

B

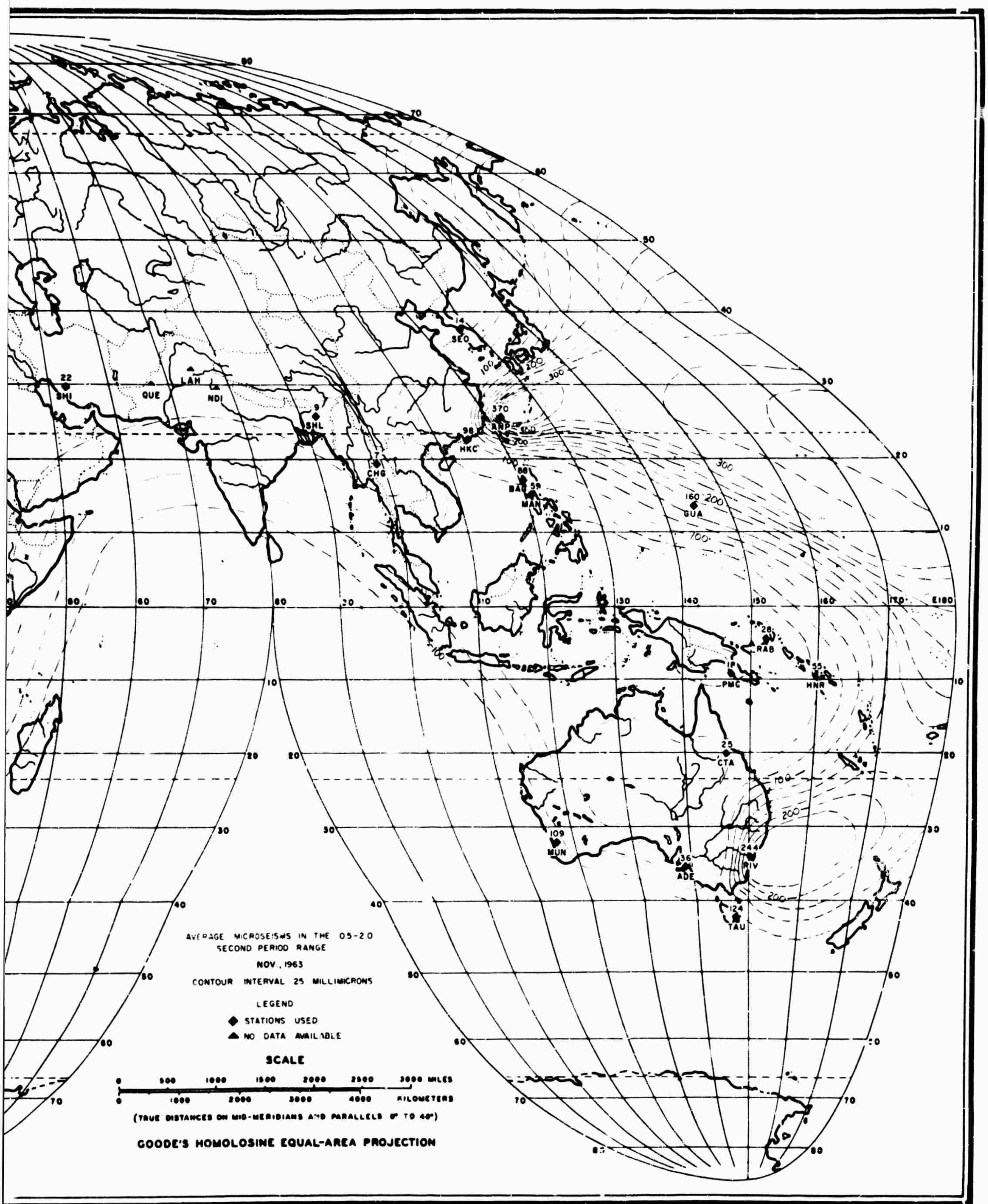

Figure B-15. World Map of 0.5-2.0 Second Microseismic Activity, November, 1963

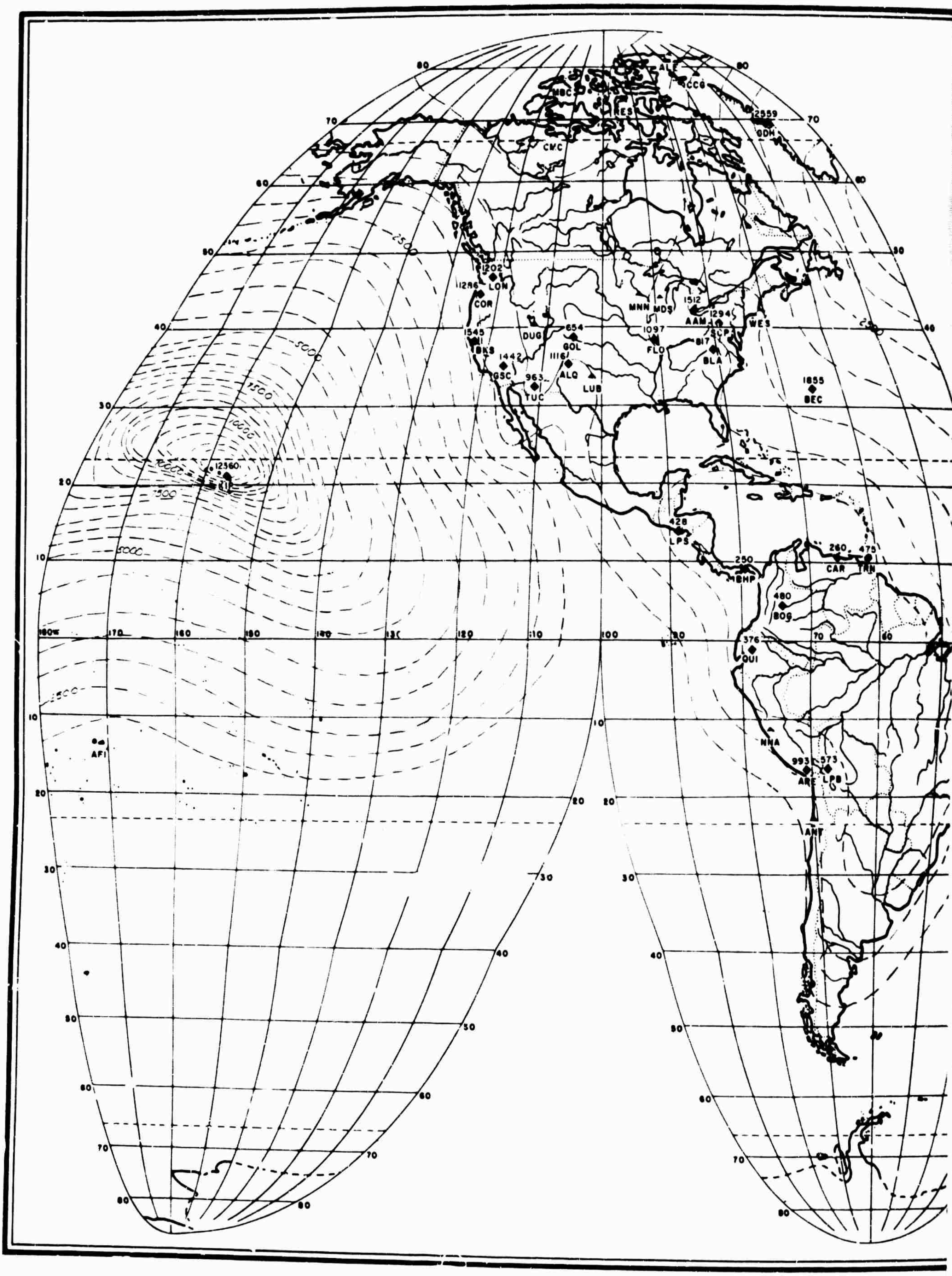

ALE
CCG
MBC
RES
CMC
2559
ODH
1202
LON
1286
COR
1545
BKS
DUG
654
GOL
1442
GSC
963
TUC
1116
ALQ
LUB
MNN
MDS
1512
AAM
1294
SCP
WES
1097
FLO
817
BLA
1855
BEC
12560
428
LPS
250
BHP
260
CAR
475
TRN
480
BOG
376
QUI
NNA
993
ARE
573
LPB
ANT
AFI
2500
5000
7500
10000

A

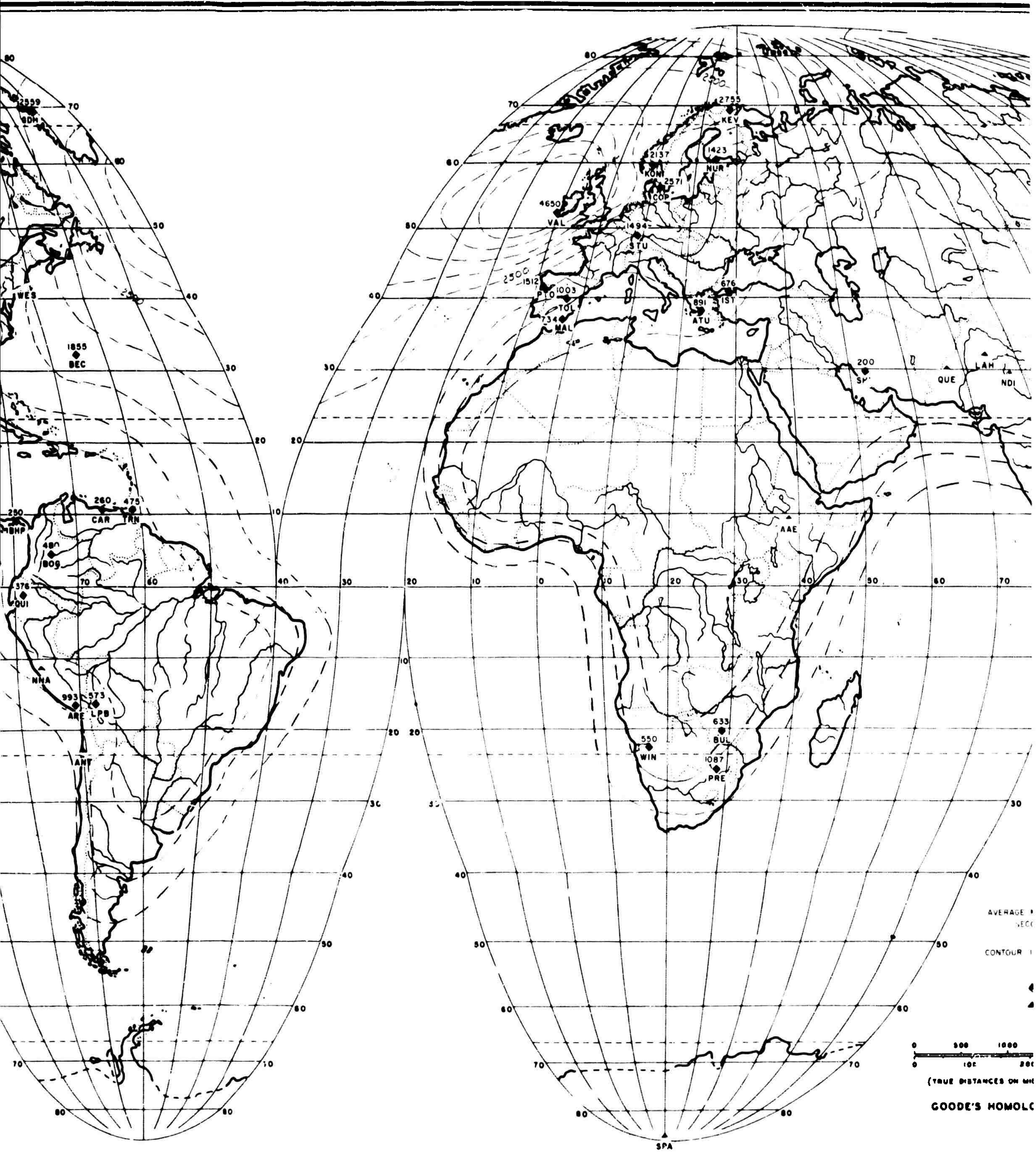

Figure B-16. V

b

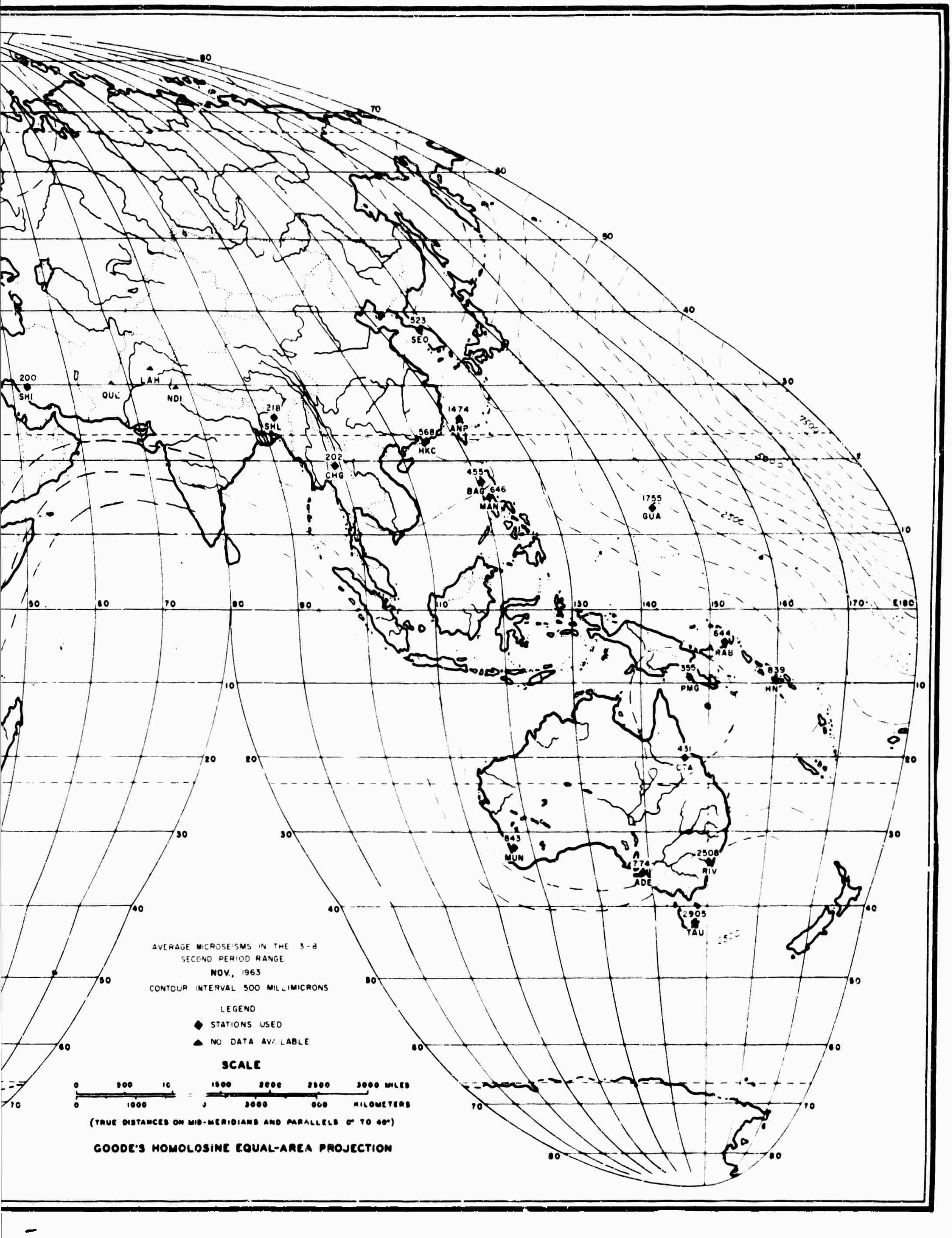

Figure B-16. World Map of 3.0-8.0 Second Microseismic Activity, November, 1963

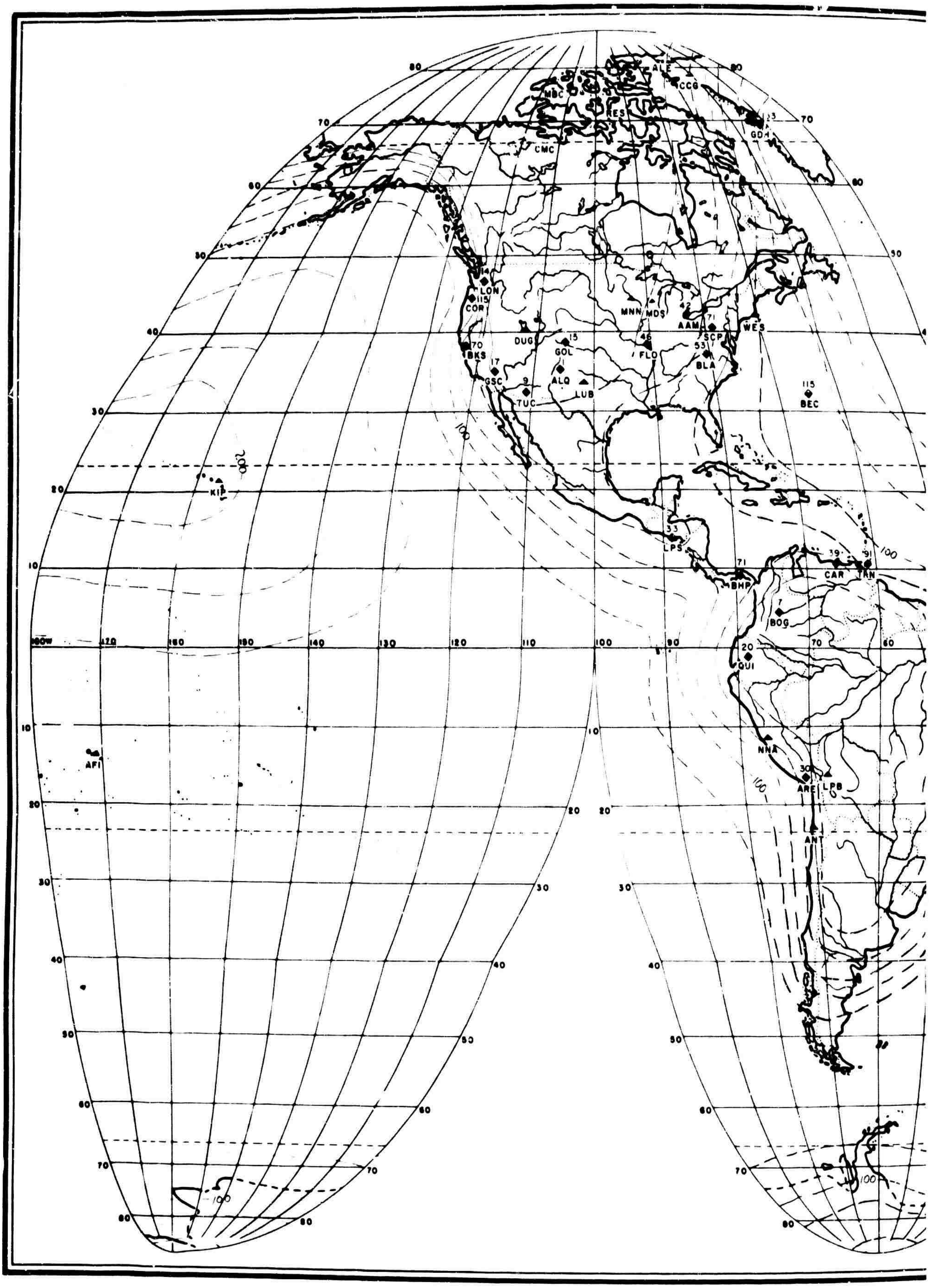

ALE
CCG
MBC
RES
GDH
CMC
LON
COR
MNN
MDS
AAM
WES
SCP
DUG
GOL
FLO
BKS
BLA
GSC
ALQ
TUC
LUB
BEC
KIP
LPS
CAR
TRN
BHP
BOG
QUI
NNA
ARE
LPB
ANT
AFI

A

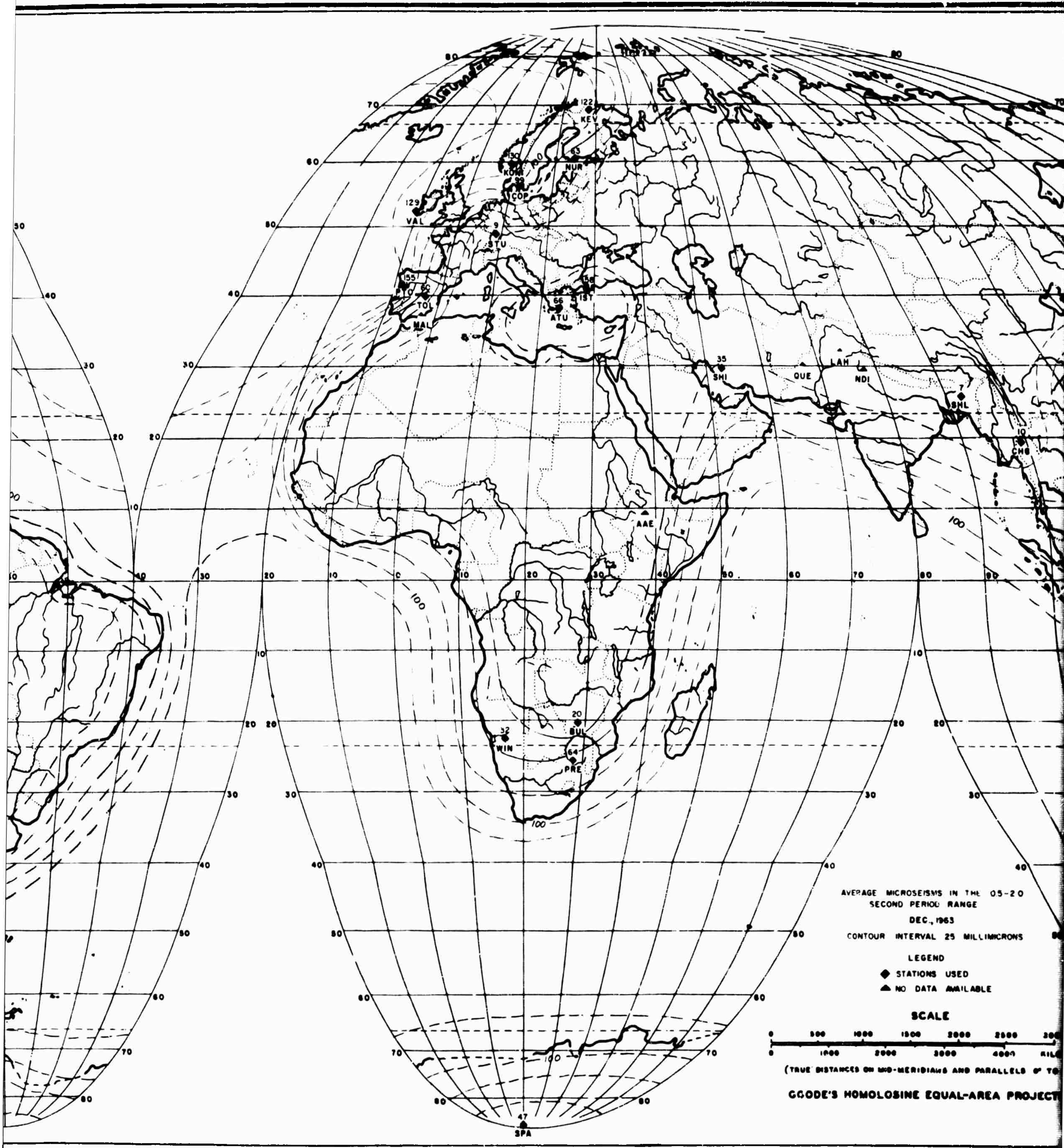

Figure B-17. World Map of 0.5

B

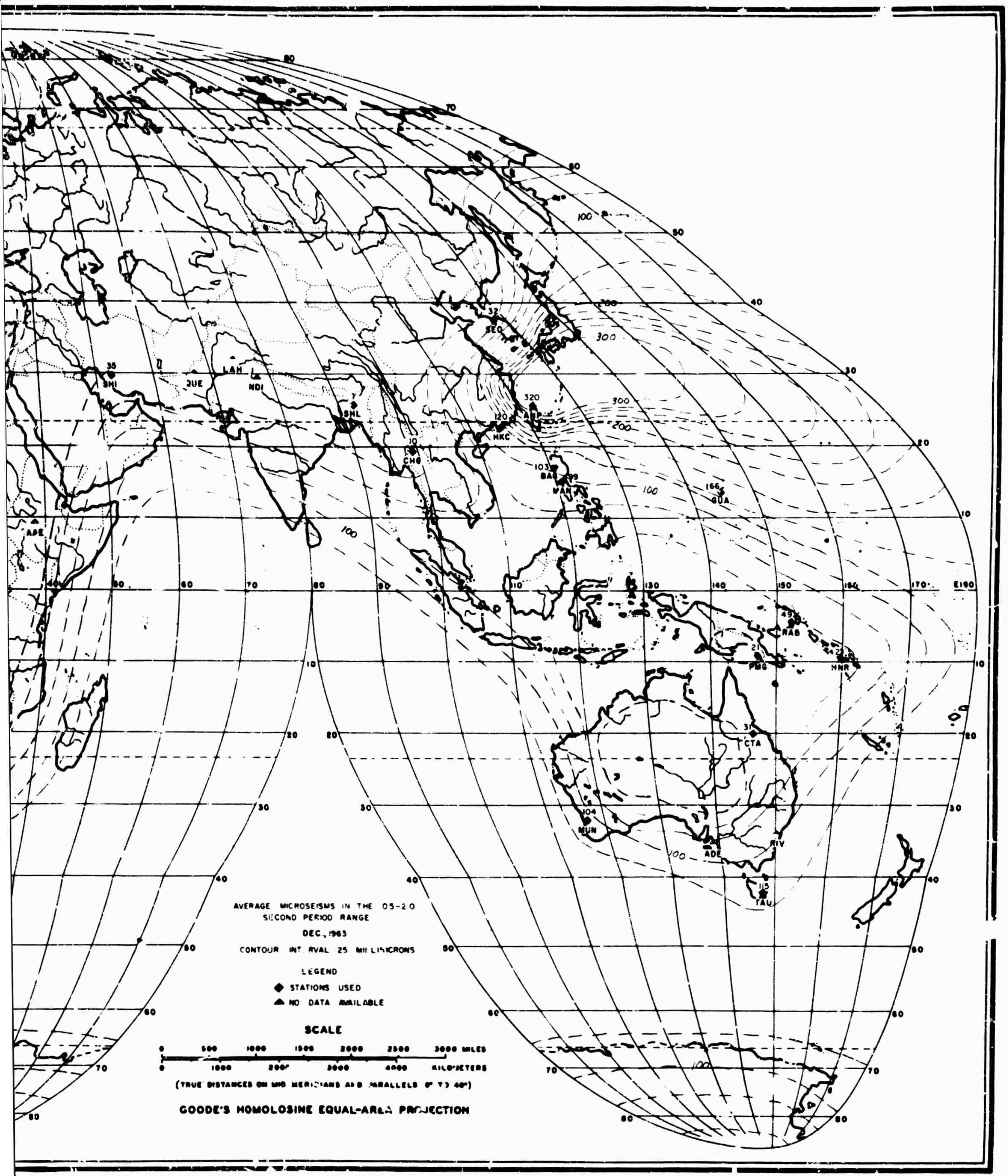

Figure B-17. World Map of 0.5-2.0 Second Microseismic Activity, December, 1963

C

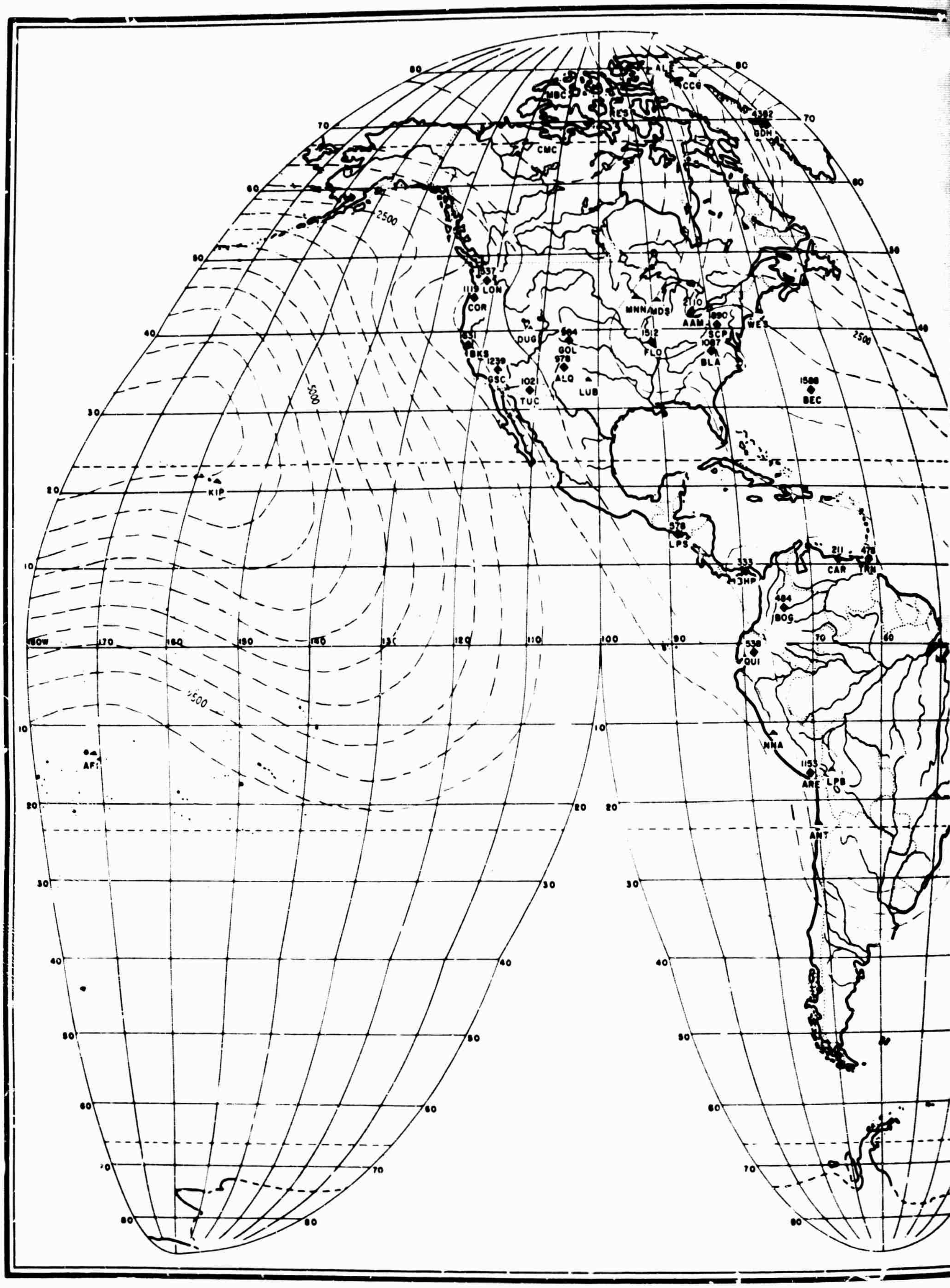
MBC
CCG
4382
GDH
CMC
2500
537
LON
1119
COR
631
BKS
1239
GSC
DUG
594
GOL
976
ALQ
1021
TUC
LUB
MNN
MDS
2110
890
AAM
WES
SCP
1512
FLO
1097
BLA
1586
BEC
5000
KIP
578
LPS
211
CAR
476
TRN
484
BOG
538
QUI
NNA
1153
ARE
LPB
ANT

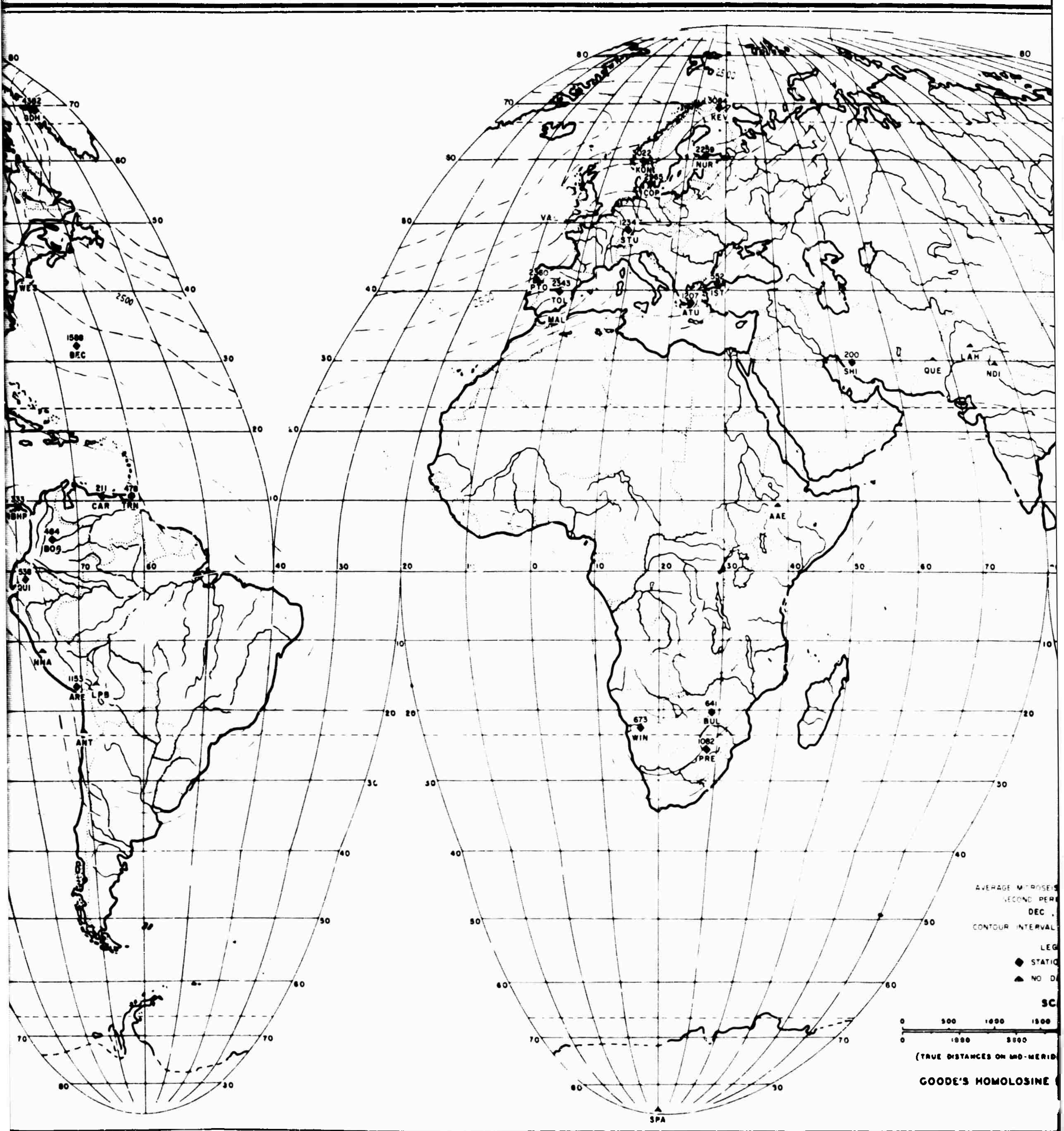

Figure B-18. Wor

B

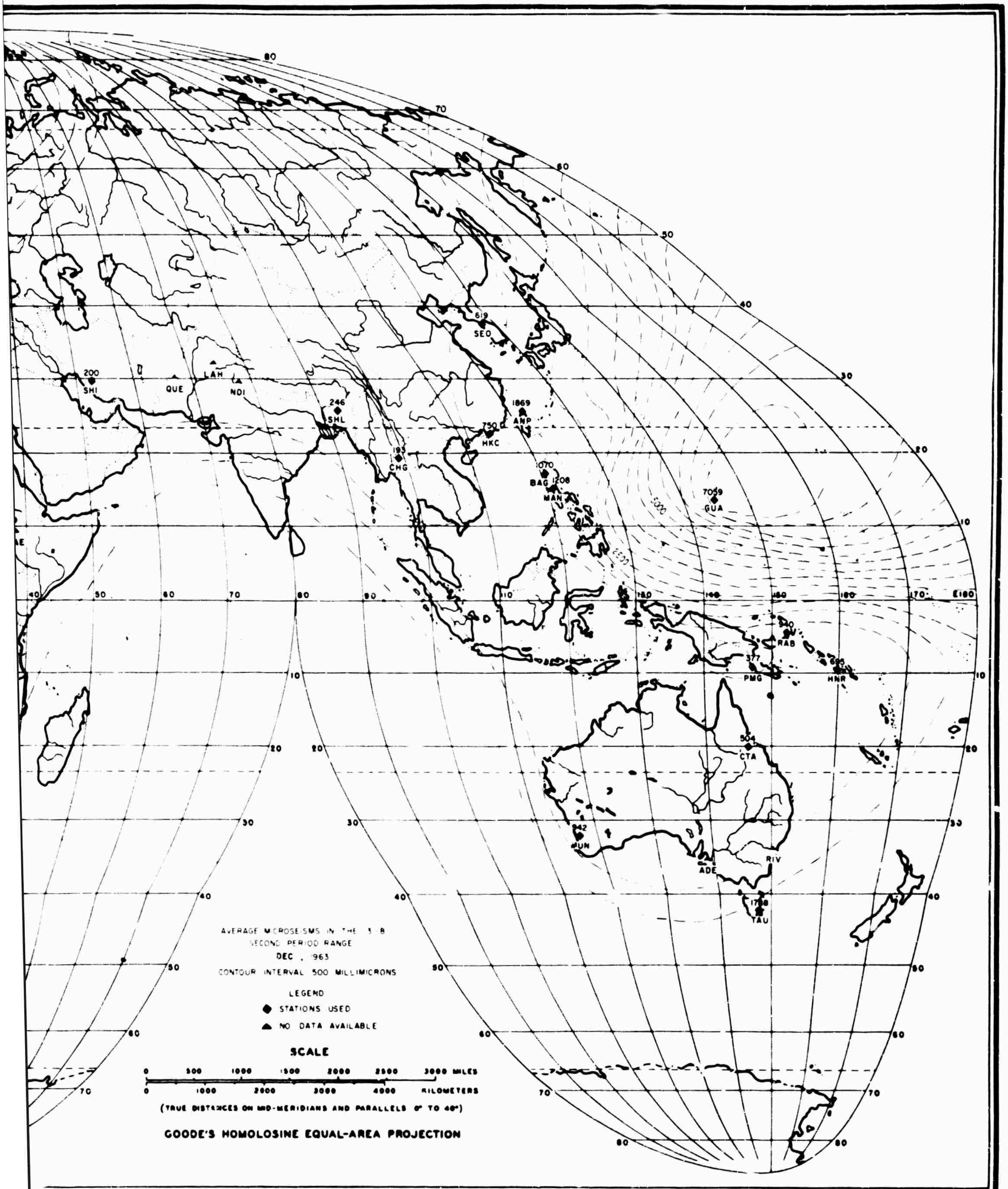

Figure B-18. World Map of 3.0-8.0 Second Microseismic Activity, December, 1963

C

REFERENCES

Benndorf, H., 1910, Uber die mikroseismischen bewegungen: Sonderabdruck Aus Geologische Rundschau, v. 1, p. 183-186.

Bradford, J. C., Weather seismic noise correlation study: Semiannual Report 1 June 1963 to 30 Nov. 1963, Contract AF 19(628)-230, United Electrodynamics, Inc., Alexandria, Va.

Bradner, Hugh, 1964, Seismic measurements on the ocean bottom: Science, v. 146, 9 Oct.

Caloi, Pietro, 1950, Due caratteristic tipi di microseismi: Annali Di Geofisica, v. 3, p. 303-314.

Carder, Dean S., 1951, The continent and ocean floor as transmitting media of microseisms (ABS): Earthquake Notes, v. 22, n. 3, p. 26.

Ewing, M. and Frank Press, 1952, Propagation of elastic waves in the ocean with reference to microseisms: Pontificiae Acadamiae Scientiarvm Scripta Varia, n. 12, p. 121-127.

Ewing, Maurice and William L. Dunn, 1952, Studies of microseisms from selected areas: Pontificiae Academiae Scientiarvm Scripta Vara, n. 12, p. 351-360.

Gutenberg, B., 1931, Microseisms in North America: Bull. Seis. Soc. Am., v. 21, p. 1-24, 1940.

Iyer, H. M., 1964, The history and science of microseisms: A VESIAC State of the Art Report No. 4410-64-X, Apr.

Iyer, H. M., 1964, Worldwide microseismic study: Nature magazine, v. 194 (June).

Ramirez, J. E., 1940, An experimental investigation of the nature and origin of microseisms at St. Louis, Missouri: Bull. Seis. Soc. Am., v. 30, p. 35-84, 139-178.

Texas Instruments Incorporated, 1962: Semiannual Tech. Rept. No. III, Contract AF 19(604)-8517, 31 Oct.

Vinnik, L. P. and N. M. Pruchkina, 1964, A study of the structure of short period microseisms: Bull. (Izv.) Acad. of Sci., USSR, Geophys. Ser. n. 5. May, p. 412-419.

UNCLASSIFIED
Security Classification

DOCUMENT CONTROL DATA - R&D

(Security classification of title, body of abstract and indexing annotation must be entered when the overall report is classified)

1. ORIGINATING ACTIVITY *(Corporate author)*
Texas Instruments Incorporated
6000 Lemon Avenue
Dallas, Texas 75222

2a. REPORT SECURITY CLASSIFICATION
Unclassified

2b. GROUP

3. REPORT TITLE
NOISE STUDY

4. DESCRIPTIVE NOTES *(Type of report and inclusive dates)*
Scientific. Interim.

5. AUTHOR(S) *(Last name, first name, initial)*
Hair, George D.; Funk, James H.; and Research Staff

6. REPORT DATE
15 November 1964

7a. TOTAL NO. OF PAGES
51

7b. NO. OF REFS
13

8a. CONTRACT OR GRANT NO. ARPA Order No. 292
AF19(604)-8517

b. PROJECT AND TASK NO.
8652-07

c. DOD ELEMENT
6250601R

d. DOD SUBELEMENT

9a. ORIGINATOR'S REPORT NUMBER(S)
Special Report No. X

9b. OTHER REPORT NO(S) *(Any other numbers that may be assigned this report)*
None

10. AVAILABILITY/LIMITATION NOTICES
1 - Distribution of this document is unlimited. It may be released to the Clearinghouse, Department of Commerce, for sale to the general public.

11. SUPPLEMENTARY NOTES
This research was supported by the Advanced Research Projects Agency

12. SPONSORING MILITARY ACTIVITY
Air Force Cambridge Research Laboratories (CRJ), L.G.Hanscom Field
Bedford, Massachusetts 01730

13. ABSTRACT
Worldwide seismic noise levels and characteristics for 1963 are discussed. Data for evaluation includes absolute power density spectra and contour maps of average worldwide microseismic activity.

Relative power density spectra were computed from 1963 data from Worldwide Standard Stations. Slopes of the least-mean-square line through the power density points were computed and a pattern of slope changes appeared at a frequency of 1.0 cps. A uniform worldwide pattern of slopes was observed between 1 cps and 2 cps. This suggests two separate sources generating microseisms above and below 1 cps, respectively, and that the spectra above 1 cps are independent of storms, fronts, etc.

The spectra for frequencies less than 1.0 cps show greater seasonal variations. These were concluded to be mostly meteorological in origin.

Monthly contour maps of average noise show that noise is seasonally variable and that it is attenuated at continental structures.

DD FORM 1 JAN 64 1473

UNCLASSIFIED
Security Classification

14. KEY WORDS	LINK A		LINK B		LINK C	
	ROLE	WT	ROLE	WT	ROLE	WT
Worldwide seismic noise, 1963 noise levels, power density spectra.						

INSTRUCTIONS

1. ORIGINATING ACTIVITY: Enter the name and address of the contractor, subcontractor, grantee, Department of Defense activity or other organization *(corporate author)* issuing the report.

2a. REPORT SECURITY CLASSIFICATION: Enter the overall security classification of the report. Indicate whether "Restricted Data" is included. Marking is to be in accordance with appropriate security regulations.

2b. GROUP: Automatic downgrading is specified in DoD Directive 5200.10 and Armed Forces Industrial Manual. Enter the group number. Also, when applicable, show that optional markings have been used for Group 3 and Group 4 as authorized.

3. REPORT TITLE: Enter the complete report title in all capital letters. Titles in all cases should be unclassified. If a meaningful title cannot be selected without classification, show title classification in all capitals in parenthesis immediately following the title.

4. DESCRIPTIVE NOTES: If appropriate, enter the type of report, e.g., interim, progress, summary, annual, or final. Give the inclusive dates when a specific reporting period is covered.

5. AUTHOR(S): Enter the name(s) of author(s) as shown on or in the report. Enter last name, first name, middle initial. If military, show rank and branch of service. The name of the principal author is an absolute minimum requirement.

6. REPORT DATE: Enter the date of the report as day, month, year, or month, year. If more than one date appears on the report, use date of publication.

7a. TOTAL NUMBER OF PAGES: The total page count should follow normal pagination procedures, i.e., enter the number of pages containing information.

7b. NUMBER OF REFERENCES: Enter the total number of references cited in the report.

8a. CONTRACT OR GRANT NUMBER: If appropriate, enter the applicable number of the contract or grant under which the report was written.

8b, 8c, & 8d. PROJECT NUMBER: Enter the appropriate military department identification, such as project number, subproject number, system numbers, task number, etc.

9a. ORIGINATOR'S REPORT NUMBER(S): Enter the official report number by which the document will be identified and controlled by the originating activity. This number must be unique to this report.

9b. OTHER REPORT NUMBER(S): If the report has been assigned any other report numbers *(either by the originator or by the sponsor)*, also enter this number(s).

10. AVAILABILITY/LIMITATION NOTICES: Enter any limitations on further dissemination of the report, other than those imposed by security classification, using standard statements such as:

(1) "Qualified requesters may obtain copies of this report from DDC."

(2) "Foreign announcement and dissemination of this report by DDC is not authorized."

(3) "U. S. Government agencies may obtain copies of this report directly from DDC. Other qualified DDC users shall request through ______________________."

(4) "U. S. military agencies may obtain copies of this report directly from DDC. Other qualified users shall request through ______________________."

(5) "All distribution of this report is controlled. Qualified DDC users shall request through ______________________."

If the report has been furnished to the Office of Technical Services, Department of Commerce, for sale to the public, indicate this fact and enter the price, if known.

11. SUPPLEMENTARY NOTES: Use for additional explanatory notes.

12. SPONSORING MILITARY ACTIVITY: Enter the name of the departmental project office or laboratory sponsoring *(paying for)* the research and development. Include address.

13. ABSTRACT: Enter an abstract giving a brief and factual summary of the document indicative of the report, even though it may also appear elsewhere in the body of the technical report. If additional space is required, a continuation sheet shall be attached.

It is highly desirable that the abstract of classified reports be unclassified. Each paragraph of the abstract shall end with an indication of the military security classification of the information in the paragraph, represented as *(TS)*, *(S)*, *(C)*, or *(U)*.

There is no limitation on the length of the abstract. However, the suggested length is from 150 to 225 words.

14. KEY WORDS: Key words are technically meaningful terms or short phrases that characterize a report and may be used as index entries for cataloging the report. Key words must be selected so that no security classification is required. Identifiers, such as equipment model designation, trade name, military project code name, geographic location, may be used as key words but will be followed by an indication of technical context. The assignment of links, rules, and weights is optional.